IDŐJÁRÁS

QUARTERLY JOURNAL
OF THE HUNGARIAN METEOROLOGICAL SERVICE

CONTENTS

****

http://www.met.hu/firat/ido-e.html

VOL. 105 * NO. 1 * JANUARY–MARCH 2001

IDŐJÁRÁS

Quarterly Journal of the Hungarian Meteorological Service

Editorial Office: P.O. Box 39, H-1675 Budapest, Hungary or
Gilice tér 39, H-1181 Budapest, Hungary
E-mail: prager.t@met.hu or *antal.e@met.hu*
Fax: (36-1) 346-4809

Subscription by

mail: IDŐJÁRÁS, P.O. Box 39, H-1675 Budapest, Hungary
E-mail: prager.t@met.hu or *antal.e@met.hu*; *Fax: (36-1) 346-4809*

IDŐJÁRÁS

Quarterly Journal of the Hungarian Meteorological Service
Vol. 105, No. 1, January–March 2001, pp. 1–17

Regional climate change in Hungary: a survey and a stochastic downscaling method

Judit Bartholy, István Matyasovszky and **Tamás Weidinger**

Department of Meteorology, Eötvös Loránd University,
H-1518 Budapest, P.O. Box 32, Hungary; E-mail: bari@ludens.elte.hu

(Manuscript received 2 June 2000; in final form 27 December 2000)

Abstract—The first part of this review paper summarizes the changes in Hungarian temperature and precipitation series during this century. Then, some possible hydrological, agricultural and ecological consequences of a future climate change are outlined, obtained after using empirical downscaling techniques developed for estimation of local effects of a global climate change. Finally, local temperature and precipitation changes corresponding to the doubling of the concentration of atmospheric greenhouse gases obtained with a stochastic downscaling method are presented. Climate of Hungary has become warmer and dryer during this century. The global climate change expected under increasing concentration of atmospheric greenhouse gases further contributes to this tendency.

Key-words: regional climate change, downscaling, stochastic model, temperature, precipitation.

1. Introduction

A presumably global climate change due to the increasing concentration of atmospheric greenhouse gases is an important issue for many reasons. Local consequences of this global change may be quite variable over different regions of even a relatively small area.

In order to simulate climates, atmospheric and coupled atmosphere-ocean general circulation models (GCMs) are widely used. A standard method to assess the change of climate mainly on the atmospheric GCMs (AGCM) is to run such a model under atmospheric CO_2 concentration before the industrial revolution ($1\times CO_2$ case) and, then, run it again under doubled CO_2 content ($2\times CO_2$ case). For coupled models a modified version of the $2\times CO_2$ experiment is to run the ocean-atmosphere model from the present or previous climate under continuously increasing CO_2 concentration, until it reaches the doubling level. This non-equilibrium, but more realistic state (say 10 years averages) is

compared to initial state. However, due to the relatively low horizontal resolution (a few hundred kilometers for the coupled and about one hundred for the equilibrium AGCMs) and quite simple parameterizations of these models (atmosphere-surface feedbacks, radiative processes, cloud and precipitation forming, etc.), the results for small areas, such as the Carpathian Basin, are considerably uncertain. There is a need, therefore, to "downscale" the large-scale output of GCMs to smaller scales.

There are three main types of downscaling approaches (*Giorgi* and *Mearns*, 1991). The basis of empirical techniques is a quite strong assumption that similar large-scale climate changes have similar local consequences independent of the factors causing the global change. This hypothesis motivates the use of temporal or spatial analogies (*Mika*, 1992; *Rácz*, 1999).

Another type of downscaling methods include meso-scale numerical modeling. Meso-scale models use GCM outputs as initial and boundary conditions (*Giorgi et al.*, 1992; *Marinucci et al.*, 1995; *McGregor*, 1997). This technique requires substantial effort in terms of modeling and computer programming and no satisfactory long simulation is available to assess extremes. These difficulties, among others, may motivate the use of stochastic downscaling procedures which appear to be specific combinations of the previous two techniques.

Stochastic downscaling methods have two key elements. The first element includes large-scale circulation of the atmosphere and the second element represents a linkage between local surface variables and large-scale circulation. The linkage is expressed by a stochastic model using an observational data series. Then, this model may be utilized with GCM outputs characterizing atmospheric circulation (*Bogárdi et al.*, 1993; *Bartholy et al.*, 1995a; *Giorgi et al.*, 1999).

Examination of local effects of climate change started at the end of eighties in Hungary. Climate change scenarios have been created for Hungary by *Mika* (1988, 1991, 1992) using an empirical downscaling method and, later, for smaller and sensitive regions of the country, namely for the watershed of Balaton-Sió and the Great Hungarian Plain (*Fig. 1*) by *Bartholy et al.* (1995b), *Bartholy* and *Matyasovszky* (1998) based on a stochastic downscaling technique. Causes and magnitude of climate change, as well as its hydrological, agricultural, forestrial and energetic consequences were evaluated (*Faragó et al.*, 1990, 1991; *Faragó*, 1998). Recently, transformation of the land of the Great Hungarian Plain is analyzed as a consequence of changing climate (*Mika et al.*, 1995; *Kertész et al.*, 1999).

The first part of the present review paper summarizes trend analyzes of the long time series of annual mean temperature and annual precipitation amount. Then, major results obtained from an empirical downscaling technique are presented. In the next section, a stochastic downscaling method and its results are discussed. Finally, a brief section for summary is provided.

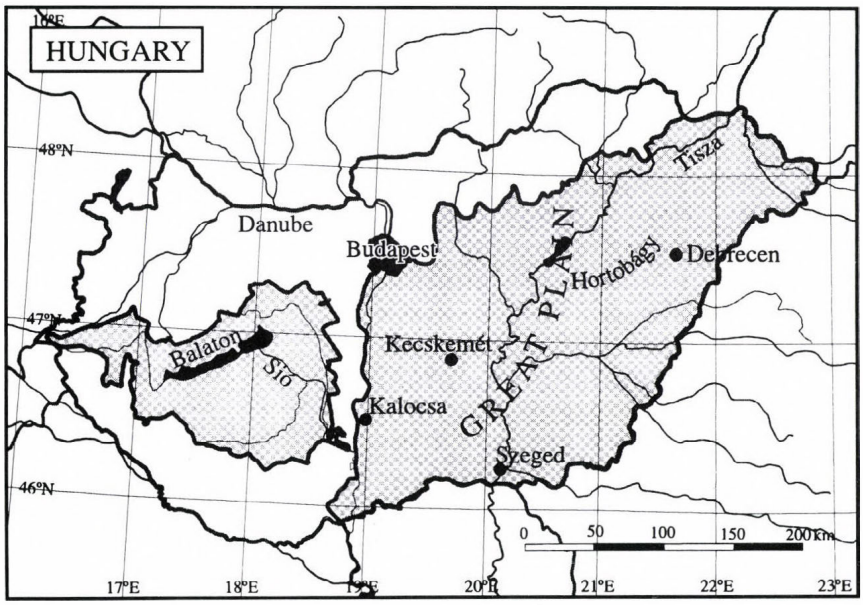

Fig. 1. The two sensitive regions of Hungary selected for the stochastic downscaling model.

2. Trends of temperature and precipitation in Hungary

Hungary is located in the middle of Carpathian Basin (Fig. 1) with a climate formed by oceanic, continental and slightly Mediterranean influences. Spatial distribution of temperature is principally driven by latitude. Maximum values (11–11.5 °C) are found in the southeastern margins of the country, but hilly northern regions have only 8–9 °C annual mean temperatures. The coldest month is January with –1– –4 °C mean temperatures, while the warmest period can be identified by month July, when the mean temperature is between 18–22 °C.

The mean annual precipitation amount is about 550–600 mm. Maximum values (800–900 mm) appear at the southwestern margins of the country; the lowest amounts (below 500 mm) are measured in Hortobágy (see Fig. 1) and in southeast of the country. Precipitation also has a characteristic annual cycle. Largest amounts are detected at the beginning of summer (June), the smallest ones in the second part of winter. In the southwestern region, there is a small second maximum of precipitation amounts due to Mediterranean effects in the period October-November. Precipitation is a highly variable meteorological element in Hungary as in many areas of the Earth. The ever observed wettest years gain three times more precipitation than the driest ones, and each month may suffer total shortage of precipitation (*Péczely*, 1981).

Molnár and *Mika* (1997) performed a linear trend analysis of temperature and precipitation for 16 locations in Hungary using homogenized time series for the period from 1881 to 1990. The methodology of homogenization is described by *Szentimrey* (1995, 1996). Each station exhibits a warming tendency at least at a 5% significance level with an average rate of 1 °C/100 year. Variation of the rate of increasing temperature is quite small and is in good agreement with other results for Central Europe (*Brazdil*, 1992; *Böhm*, 1992).

Daily maximum and minimum temperatures have also been examined for five locations in Hungary for this century. *Iványi* (1995) and *Domonkos* (1998) concluded that these data are characterized by decadal fluctuations rather than long-term changes.

Precipitation shows a negative trend, which is statistically significant at a 5% level for 10 stations. The average rate of the change is –90 mm/100 year with a largest value of –230 mm/100 year and a smallest one of –27 mm/100 year. A previous work (*Koflanovits-Adámy* and *Szentimrey*, 1986) performed for 84 stations in the Carpathian Basin for the period from 1901 to 1984 resulted in similar results. Aridification of this region is confirmed by *Bartholy* and *Pongrácz* (1998). *Tar* (1992) and *Molnár* (1996a; 1996b; 1996c) analyzed the frequency of years warmer or colder than average as well as dryer or wetter years as compared to the average. They found a statistically significant increasing trend of warm and dry years.

3. Effects of climate change in Hungary obtained from empirical downscaling methods

Climate change analyses generally concentrate on temperature and precipitation, and the performance of several other meteorological elements can be estimated using the changes of the two above parameters. An estimation of the climate for Hungary or for the total Carpathian Basin under changing global climate was performed by *Mika* (1988, 1991, 1992) and *Molnár* and *Mika* (1997) using: (i) a statistical relationship between local meteorological elements and Northern Hemisphere temperature and ocean-continent temperature contrast; (ii) paleoclimatological analogies; (iii) a simple regional energy balance model. Results for changes of regional climate as a function of the change of average hemisphere temperature are summarized in *Table 1*. As it is expected, the largest the hemisphere temperature change, the largest the local response. However, behavior of precipitation is non-linear. A small global warming (0.5–1 °C) results in a considerable dryer climate, but a 4 °C warmer Northern Hemisphere yields much wetter local climate. Also, wide range of estimated changes indicates high uncertainty. A moderate global warming

entails a 20% increase of sunshine duration and the average duration of drought periods from the actual value of 1.4 month/year to 2 month/year.

Table 1. Expected changes of temperature and precipitation in Hungary, in connection with different values of hemispheric temperature changes after *Molnár* and *Mika* (1997). Calculation of the annual mean temperature changes is added by the authors. (Intervals indicate high uncertainty.)

Hemispheric temperature change ΔT, [°C]	**+0.5**	**+1**	**+2**	**+4**
Temperature change for Hungary, summer*	+0.6	+0.8	+1.5	+3
Temperature change for Hungary, winter*	+0.1; +0.5	+1 ; +2.5	+3	+6
Temperature change for Hungary, year	+0.3; +0.6	+0.9; +1.6	+2; +2.5	+4; +5
Precipitation change for Hungary, year, [mm]	–30	–20; –100	+ or 0	+40; +400
Geographical analogy	within HU; Voyvodina, YU Zhil-valley, RO; Plovdiv, BG	Varna, BG	Burgas, BG Yalta, UKR	Firenze, I; Washington, U.S.A.

* The +0.5°C column refers to the summer and winter half years.

These changes of temperature and precipitation can produce several ecological, agricultural and economical problems. Ecological effects include —for instance—drought, drying of upper layer of soils, sinking of ground water level, which arise problems of demand for increasing irrigation and, thus for more reservoirs. Such possible dangers especially affect large lowland areas between the Danube-Tisza Interfluve, where sinking of the ground water level has started in the middle of seventies (*Kertész et al.*, 1999) and partly recovered just in the recent normal and wet years.

As a consequence of change of climate and soil conditions it is important to evaluate crop outlooks. For instance, crop of maize and wheat was examined and a 10–20% decrease was obtained, which, however, can be partly compensated by the increasing atmospheric CO_2 concentration, milder winters and modest denitrification due to the dryer climate (*Bacsi* and *Hunkár*, 1994; *Harnos*, 1998; *Kovács* and *Dunkel*, 1998). Relationship between climate change and possibilities of plant migration was analyzed by *Mátyás* (1997) and *Kovács et al.* (1998).

4. Local effects of climate change in Hungary obtained from a stochastic downscaling model

Stochastic downscaling methods are based on the fact that there exists a considerable stochastic relationship between large-scale atmospheric circulation and meteorological, hydrological (hydrometeorological) variables. Frequently, the large-scale circulation pattern (CP) is classified and every day is assigned to one of daily CP types. The relationship is estimated from observed data and then is used with large-scale circulation available from GCM output for present climate ($1\times CO_2$) and $2\times CO_2$ cases. Thus, an estimation can be obtained for local hydrometeorological parameters under a new, such as $2\times CO_2$ climate (*Bogárdi et al.*, 1993). Such a methodology is based on two assumptions. The first part assumes that the GCM-produced CP types may be considered the same as the types obtained from observed data. This part of the hypothesis can be verified. The other part of the hypothesis assumes that if observed data reflect a linkage between daily CP types and daily local hydrometeorological factors, this linkage will remain in a climate change situation. This part of the hypothesis cannot be checked with statistical means and probably is not fully valid because of the direct change of the radiation balance and the corresponding surface-biosphere-atmosphere feedbacks. These latter interactions, however, are known relatively inaccurately and it is difficult, even if at all possible, to predict how such a linkage may change. Changes of the radiative balance could, however, be estimated by a locally adjusted radiative-convective model (*Práger* and *Kovács*, 1988). Without these effects, the results of downscaling represent a partial approach of the full (i.e., radiative plus advective) change of the thermal variables.

The methodology consists of three main parts. First, a system of large-scale circulation patterns is defined using the spatial distribution of either sea level air pressure, or middle tropospheric pressure heights. One of the main approaches to classify such spatial variables includes subjective classifications when meteorological experience is applied. These classifications are subjective because they reflect the attitudes of meteorologists, but are objective in the sense that are based on the physical behavior of the atmosphere. For instance, the so-called Hess-Brezowsky system of circulation types (*Hess* and *Brezowsky*, 1969) is frequently used in Europe for many purposes. Another classification approach consists of objective classification methods. Objectivity means here that a given algorithm automates the data processing, although the choice and application of a given algorithm is subjective. This type of classification is generally based on different versions of clustering (*Wilson et al.*, 1992), fuzzy clustering (*Bárdossy et al.*, 1995), classification using neural networks (*Muster et al.*, 1994), or other techniques (*Breinman et al.*, 1984).

In the second step of the methodology a stochastic model is developed to describe the behavior of hydrometeorological variables as conditioned on circulation types. In order to reproduce the space-time statistical structure of local hydrometeorological variables, a suitable model should be chosen. Autoregressive processes represent a well-developed and commonly used tool to model time series. They have been developed principally for Gaussian processes, but climatic factors do not usually follow a Gaussian distribution. Therefore, it is desirable to construct a transformation establishing a relationship between the distribution of a local climatic factor and a normal distribution.

Let the vector $\mathbf{Z}(t) = (\mathbf{Z}(t,u_1), \mathbf{Z}(t,u_2), \ldots, \mathbf{Z}(t,u_K))$ represent a daily climatic variable at locations $u_1, u_2, \ldots, u_K$ and time t and let $\mathbf{W}(t)$ be a K-dimensional normal random vector at time t. We suppose for simplicity that each component of the vector $\mathbf{W}(t)$ has zero mean and unit variance. For a fixed CP type and time t, any component Z of $\mathbf{Z}(t)$ can be related to the corresponding component W of $\mathbf{W}(t)$ prescribing that

$$P(Z<z) = F(z) = p, \tag{1}$$
$$P(W<w) = \Phi(w) = p, \tag{2}$$

where Φ is the standard normal distribution function and p is any value satisfying $0 < p < 1$ for temperature and $p_0 < p < 1$ for precipitation, p_0 being the probability of precipitation occurrence. Thus:

$$Z = F^{-1}(\Phi(W)). \tag{3}$$

Estimating $F(z)$ is a simple task for temperature, since the temperature is distributed nearly normally. For the purpose *Matyasovszky et al.* (1994a) used binormal distributions (*Tóth* and *Szentimrey*, 1990). Precipitation, however, represents a much more complicated task. Namely, the probability distribution function of daily precipitation can not be considered as continuous due to dry days, i.e., $F(z)$ has a form:

$$F(z) = \begin{cases} 0, & z < 0 \\ (1-p_0) + p_0 H(z), & z \geq 0 \end{cases},$$

where H is the probability distribution function of daily precipitation amount on wet days. In order to model $F(z)$, *Bárdossy* and *Plate* (1992) proposed a power transformed truncated normal distribution which, however, does not work under the climate of Hungary. Therefore, *Matyasovszky et al.* (1993) developed a non-parametric technique to estimate distribution function of daily precipitation.

The time dependency of $\mathbf{W}(t)$ is described using first order autoregressive ($AR(1)$) processes. The transformation of the random vector $\mathbf{Z}(t)$ into the normal vector $\mathbf{W}(t)$ depends on the climatic variable under consideration. The process $\mathbf{W}(t)$ is described by the following multivariate $AR(1)$ process when CP type j occurs at time t:

$$\mathbf{W}(t) = \mathbf{B}_j \mathbf{W}(t-1) + \mathbf{C}_j \mathbf{U}(t) . \tag{4}$$

Using the so-called Yule-Walker equations, the matrices $\mathbf{B}_j$ and $\mathbf{C}_j$ can be calculated as

$$\mathbf{B}_j = \mathbf{G}_{1j}\mathbf{G}_{0j}^{-1}, \tag{5}$$

$$\mathbf{C}_j\mathbf{C}_j^{T} = \mathbf{G}_{0j} - \mathbf{G}_{1j}\,\mathbf{G}_{0j}^{-1}\mathbf{G}_{1j}^{T} \tag{6}$$

and $\boldsymbol{G}_{0j}$, $\boldsymbol{G}_{1j}$ are the covariance matrices of $\mathbf{W}(t)$ for lags 0 and 1 and CP type j, respectively. $\mathbf{U}(t)$ represents a K-dimensional standard normal vector which consists of K standard normal uncorrelated random variables. The matrices $\mathbf{G}_{0j}$, $\mathbf{G}_{1j}$ can directly be estimated from observed data in the case of temperature due to its nearly normality. However, these matrices can only be estimated indirectly when precipitation is in question. Indicator series defined by precipitation quantiles are used to estimate the correlations among the indicator series; the required correlations can then be calculated from the indicator series correlations. The indicator series $I_Z(t,u_k)$ is defined for any q, $1-p_{0k} < q < 1$ as

$$I_Z(t,u_k) = 1, \quad Z(t,u_k) \geq z_{qk}, \tag{7}$$

$$I_Z(t,u_k) = 0, \quad Z(t,u_k) < z_{qk}, \tag{8}$$

where z_{qk} is the qth quantile of precipitation at location u_k. Indicator series $I_W(t,u_k)$ of W and $I_Z(t,u_k)$ are the same due to the transformation between Z and W. The required correlation $g(i,k)$, the (i,k)th element of $\mathbf{G}_0$, is related to the correlation of the indicator series $g^{(q)}(i,k)$ through the relationship (*Abramowitz* and *Stegun,* 1965, p. 128)

$$g^{(q)}(i,k) = \frac{1}{2\pi(1-q)q} \int_0^{\sin^{-1}(g(i,k))} \exp\left(-\frac{w_q}{1+\sin(s)}\right) ds , \tag{9}$$

where w_q is the qth quantile of standard normal distribution. This equation can be solved for $g(i,k)$ using a numerical algorithm. The elements of $\mathbf{G}_1$ are derived in a similar way.

In the final step, statistical characteristics of four time series are compared and thus a local climate change estimation is obtained. The four time series consists of observed data, simulated data corresponding to present climate, and simulated data corresponding to both GCM-generated $1\times CO_2$ and $2\times CO_2$ climates. Simulated data are obtained by the stochastic model with either observed circulation types or circulation types generated by a GCM.

The authors developed and applied such a model to two sensitive regions of the Carpathian Basin (Fig. 1), namely for the watershed of Balaton-Sió (*Bartholy et al.*, 1995b; *Weidinger et al.*, 1994; *Weidinger et al.*, 1995) and the Great Hungarian Plain (*Bartholy* and *Matyasovszky*, 1998) and to several other areas, such as to dry continental climate of Nebraska (*Matyasovszky et al.*, 1993; 1994b), dry subtropics of Arizona (*Bartholy* and *Duckstein*, 1994), the Mediterranean climate of Greece (*Matyasovszky et al.*, 1995) and to Alpine region in Austria (*Nachtnebel et al.*, 1996). Computations were carried out using ECHAM, a coupled GCM developed by Max Planck Institute for Meteorology, Hamburg, Germany (*Cubash et al.*, 1991), and a GCM of Canadian Climate Centre (CCC), Victoria, Canada (*Boer et al.*, 1984). ECHAM shows a 1.5 °C global warming at reaching the non-equilibrium $2\times CO_2$ concentration, while CCC, which does not have a coupled ocean model predicts 3.5 °C global equilibrium temperature increase (*Boer et al.*, 1984). Results presented in *Fig. 2* are based on ECHAM model.

Expected temperatures under $2\times CO_2$ climate have no considerable spatial variability in the Great Hungarian Plain (*Fig. 3*). Each season exhibits a statistically significant positive trend, which is, however, only 0.1–0.5 °C except for autumn where the increase of temperature exceeds 1.5 °C (*Bartholy* and *Matyasovszky*, 1998). Thus the annual mean temperature change is about +0.7 °C, which is considerably smaller than the global warming 1.5 °C produced by the ECHAM, and corresponding values in Table 1 (after *Molnár* and *Mika*, 1997). *Fig. 4*, showing the probability density function of daily mean temperature in Kecskemét for October, demonstrates that not only the means but also the standard deviations will change under the non-equilibrium $2\times CO_2$ climate. Decreasing tendency of standard deviations implies a less variability of temperature.

Evaluation of precipitation is a much more complicated task since it has a spatio-temporal intermittence (*Bogárdi et al.*, 1993). Therefore, it is necessary to analyze both the probability of precipitation occurrence and the amount of precipitation during a wet period. Another important characteristic is the probability distribution of wet and dry day durations. A major experience of our examination is that frequency of precipitation occurrence becomes smaller,

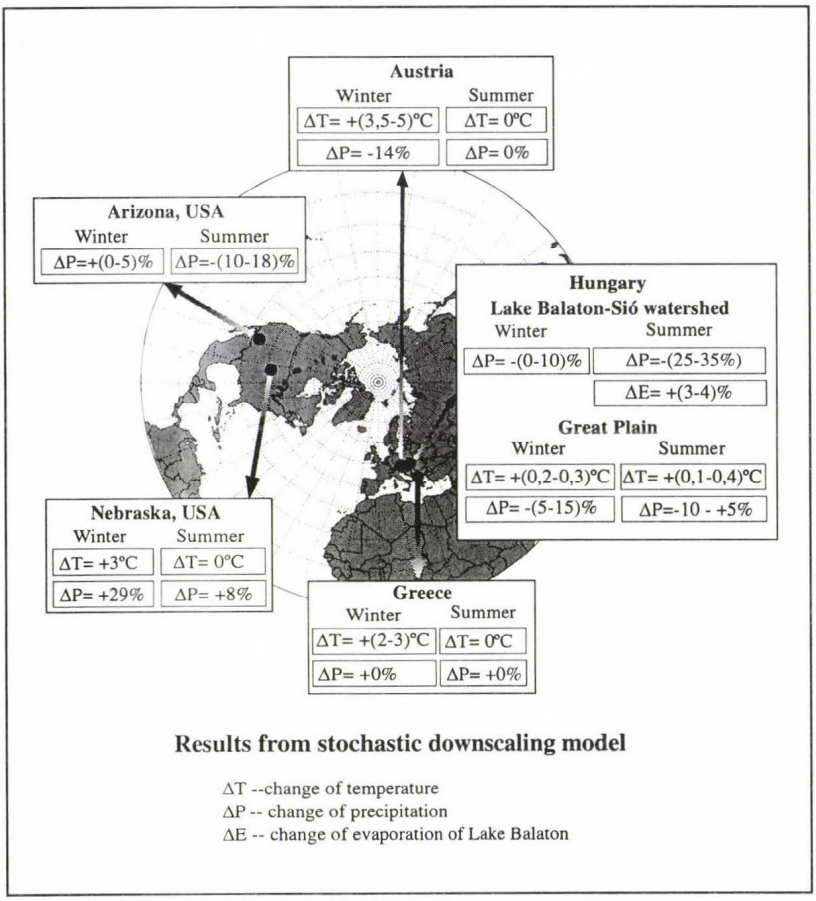

Fig. 2. Regional climate change results from the stochastic downscaling model in different regions of the Northern Hemisphere.

while the amount of precipitation in wet periods seems larger or at least not smaller. This indicates a precipitation climate that is more variable in time (*Matyasovszky et al.*, 1993; *Matyasovszky et al.*, 1995; *Nachtnebel et al.*, 1996). On the other hand, the change of precipitation amounts shows slight spatial differences in the Great Hungarian Plain (*Bartholy* and *Matyasovszky*, 1998). In summer (*Fig. 5*), precipitation amount slightly decreases with a rate of +5 – –10%, while the winter has a more characteristic decreasing tendency by –5 – –15%. Summarizing each season, the change of annual precipitation is slightly below 10%.

The same analysis was carried out for the watershed Balaton-Sió by using 28 precipitation stations (*Bartholy et al.*, 1995). Both the frequency and the

amount of precipitation in wet days decrease substantially in summer. Spatial distribution of precipitation is slightly more complicated in winter. Frequency of precipitation occurrence is surely decreasing, but the amount on wet days is decreasing (increasing) over a larger northern (a smaller southern) part of the area, respectively. Finally, the precipitation amount appears to have a 25–35% decrease in summer, while the winter will probably have only a slightly dryer (0–10% decrease) climate.

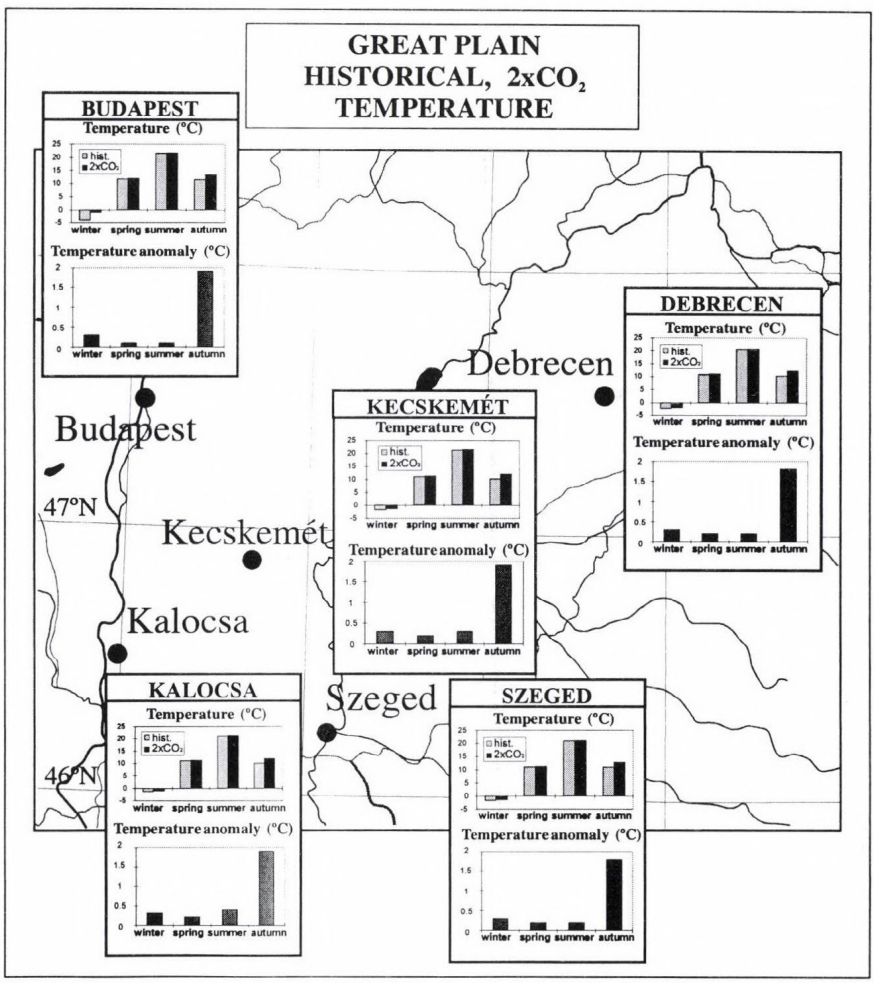

Fig. 3. Expected changes of temperature for selected stations in the Great Hungarian Plain obtained from a stochastic downscaling technique with doubled atmospheric CO_2 concentration.

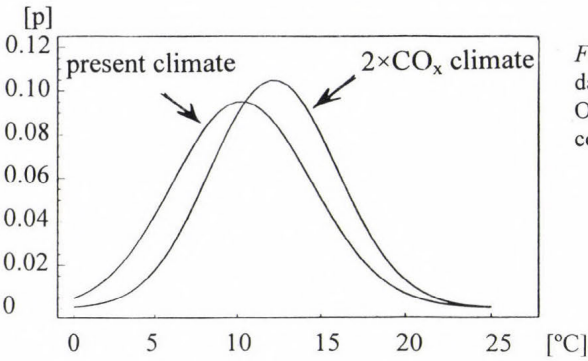

Fig. 4. Probability density functions of daily mean temperature in Kecskemét for October under present and 2×CO_2 climate conditions.

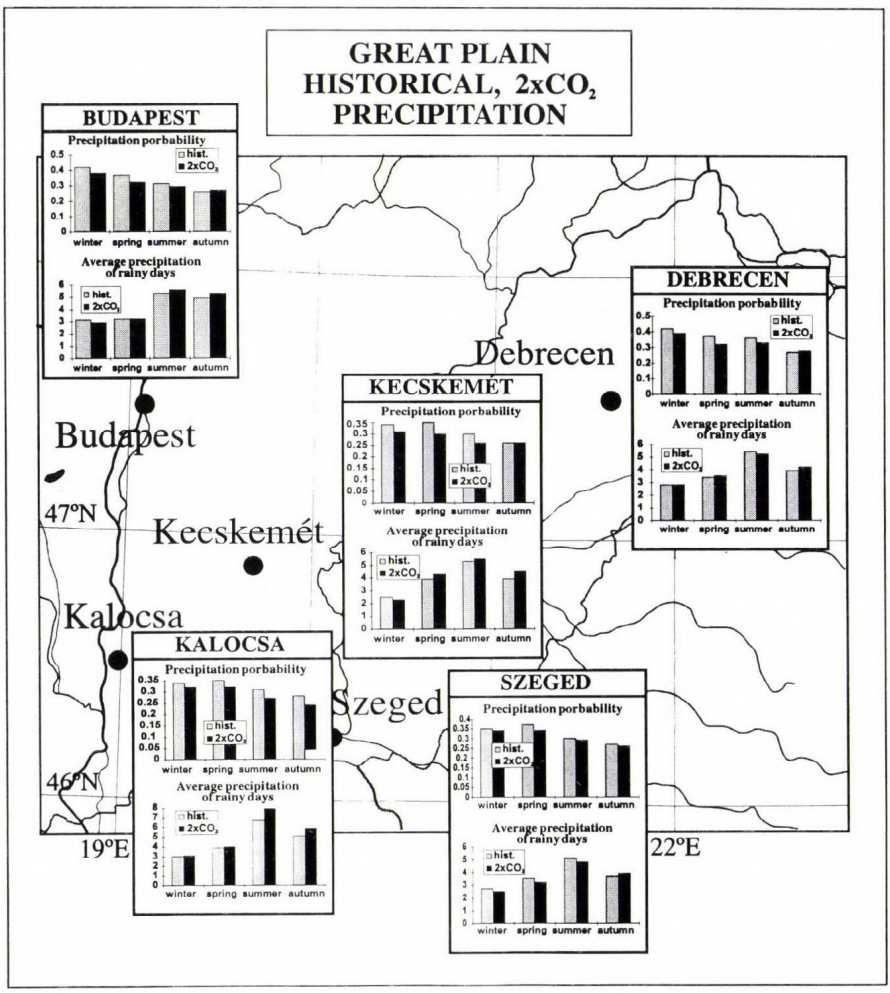

Fig. 5. Expected changes of precipitation for selected stations in the Great Hungarian Plain obtained from a stochastic downscaling technique with doubled atmospheric CO_2 concentration.

Smaller changes of precipitation were obtained for the Great Hungarian Plain, suggesting that smaller differences can be expected within the region in case of a dryer regional climate (*Table 2*).

Table 2. Expected changes of temperature [°C] and precipitation [mm] in Hungary, obtained with a stochastic downscaling technique for doubled atmospheric CO_2 concentration

Hemispheric temperature change ΔT, [°C]	**+1.5**
Temperature change for the Great Hungarian Plain, summer	+0.2 ; +0.3
Temperature change for the Great Hungarian Plain, winter	+0.1 ; +0.4
Temperature change for the Great Hungarian Plain, year	~ +0.7
Precipitation change for the Great Hungarian Plain, summer [mm]	–20 ; +5
Precipitation change for the Great Hungarian Plain, winter	–20 ; –5
Precipitation change for the Great Hungarian Plain, year	–40 ; +10
Precipitation change for Lake Balaton-Sió watershed in Hungary, summer	–75 ; –35
Precipitation change for Lake Balaton-Sió watershed in Hungary, winter	–15 ; 0

A modified version of our stochastic downscaling methodology was also applied for assessing evaporation of Lake Balaton under $2\times CO_2$ climate. The lake evaporation was estimated by adjusting pan evaporation measurements of surrounding locations (*Weidinger et al.*, 1995). Calculations performed for summer months indicate only a 3–4% increase of evaporation, which is in a good agreement with the slight warming obtained for this season.

5. Summary

Main conclusions of the linear trend analysis for time series of homogenized annual mean temperature and annual precipitation amount in Hungary are summarized in the following few sentences. An increasing trend of annual mean temperature is statistically significant at least at a 95% level and reaches 1 °C/100 year. A decreasing trend of annual precipitation amount is statistically significant at least at a 95% level and reaches 90 mm/100 year. As a consequence of the above two facts, a clear aridification proceded during the 20th century. This tendency will probably be strengthened by the increasing concentration of atmospheric greenhouse gases.

Our stochastic downscaling method for a doubled CO_2 concentration for two sensitive climate regions of Hungary (the Balaton-Sió watershed and the Great Hungarian Plain) has resulted in:

(i) The 0.7 °C increase of annual mean temperature obtained with a stochastic downscaling method under a 1.5 °C global warming (from the ECHAM model) is considerably smaller than the previous estimations. One of the reasons might be the lack of direct radiation effects on temperature, not considered by the method.

(ii) Anticipated temperature changes in Hungary are substantially smaller than changes estimated for other regions of Earth located nearly at the same latitudes as Hungary, given in Section 4. This difference, however, can not be connected to the lack of radiation processes.

(iii) The frequency of wet days is estimated as decreasing for future, while precipitation amount on wet days is expected to be quite variable.

(iv) Future precipitation deficit over the Balaton-Sió watershed seems remarkably greater than in the Great Hungarian Plain. The scale of our climate change scenarios for precipitation is similar to a previous estimation using an empirical downscaling method, but the results obtained for different regions point out the necessity of distinction even within small areas.

Acknowledgements —Research leading to this paper was supported by Finance for High Education and Investigation Projects FKFP-0193, Hungarian Scientific Funds OTKA-T026629, OTKA-T025803 and János Bólyai Research Scholarship. Authors are very grateful for *János Mika* from Hungarian Meteorological Service and two anonymous reviewers for their helpful comments.

References

Abramowitz, M. and *Stegun, I.*, 1965: *Handbook of Mathematical Functions.* Dover Mineola, N. Y.

Bacsi, Zs. and *Hunkár, M.*, 1994: Assessment of the impacts of climate change on yields of winter wheat and maize, using crop models. *Időjárás 98*, 119-134.

Bartholy, J. and *Duckstein, L.*, 1994: Comparing and extending the CCC and MPI GCM outputs from western USA for global change studies. *Annales Gepohysicae, Supplement II. to Vol. 12*, C355.

Bartholy, J., Barcza, Z. and *Matyasovszky I.*, 1995a: Large-scale changes – regional consequences. Methodological study on regional climate change predictions. *Annales Geophysicae, Supplement II. to Vol. 13*, C333.

Bartholy, J., Bogárdi, I. and *Matyasovszky, I.*, 1995b: Effect of climate change on regional precipitation in Lake Balaton watershed. *Theor. Appl. Climatol. 51*, 237-250.

Bartholy, J. and *Matyasovszky, I*, 1998: Effect of climate change on temperature and precipitation in the Carpathian Basin. In *Climate Change and Consequences* (in Hungarian) (ed.: *Dunkel, Z.*). *Meteorological Scientific Days '97*, November 20-21, 1997, Hungarian Meteorological Service, Budapest, 117-125.

Bartholy, J. and *Pongrácz, R.*, 1998: The differing trends of the Hungarian precipitation time series, areal and decadal changes of extreme precipitation (in Hungarian). In *Proc. of IIth Conference of Forest and Climate* (eds.: *Tar, K.* and *Szilágyi, K.*) Sopron, June 4-6, 1997, Kossuth University Press, Debrecen, 62-66.

Bárdossy, A. and *Plate, E.*, 1992: Space-time model for daily rainfall using atmospheric circulation patterns. *Water Resour. Res. 28*, 1247-1260.

Bárdossy, A., Duckstein, L. and *Bogárdi, I.*, 1995: Fuzzy rule-based classification of circulation patterns for precipitation events. *Int. J. Climatol. 15*, 1087-1097.

Boer, G.J., McFarlane, N.A. and *Laprise, R.*, 1984: The climatology of the Canadian Climate Centre General Circulation Model as obtained from a five-year simulation. *Atmos. Ocean 22*, 432-437.

Bogárdi, I., Matyasovszky, I., Bárdossy, A. and *Duckstein, L.*, 1993: Application of a space-time stochastic model for daily precipitation using atmospheric circulation patterns. *J. Geophys. Res. 98(D9)*, 16,653-16,667.

Böhm, R., 1992: Lufttemperaturschwankungen in Österreich seit 1775. *Österreichische Beiträge zu Meteorologie und Geophysik, Heft. 96.*

Brázdil, R., 1992: Reconstruction of the climate of Bohemia and Moravia in the last millennium – problems of data and methodology. *European climate reconstructed from documentary data: methods and results (*ed.: *Frenzel, B.)*, 75-86.

Breinman, L., Friedman, J.H., Olshen, A. and *Stone, J.C.*, 1984: *Classification and Regression Trees.* Wadsworth and Brooks, Monterey, Calif.

Cubash, U., Hasselmann, K.-Hock, H., Maier-Reimer, E.-Mikolajewicz and *U.-Santer, B.D.*, 1991: *Time-dependent greenhouse warming computations with a coupled ocean-atmosphere model.* Max Planck Inst. Meteorolol., 67.

Domonkos, P., 1998: Statistical characteristics of extreme temperature anomaly groups in Hungary. *Theor. Appl. Climatol. 59*, 165-180.

Faragó, T., Iványi, Zs. and *Szalai, S.* (eds.), 1990: Climate variability and change – I. Causes, processes, regional impacts with special emphasis on the socio-economic impacts and the tasks related to the international cooperation (in Hungarian). *Hungarian Ministry for Environment and Regional Policy, Hungarian Meteorological Service*, Budapest, 100 p.

Faragó, T., Iványi, Zs. and *Szalai, S.* (eds.), 1991: Climate variability and change – II. Changes in composition of atmosphere and in the climatic characteristics, detection, modelling, scenarios and impacts of the regional changes. Summary (in Hungarian). *Hungarian Ministry for Environment and Regional Policy, Hungarian Meteorological Service*, Budapest, 31 p.

Faragó, T. (ed.), 1998: Stabilisation of the greenhouse gas emissions: The Kyoto Protocol. Adoption of the Kyoto Protocol to the United Nations framework Convention on Climate Change and agenda in Hungary. *Hungarian Commission on Sustainable Development*, Budapest, 96 p.

Giorgi, F. and *Mearns, L.O.*, 1991: Approaches to the simulation of regional climate change: a review. *Reviews of Geophysics 29*, 191-216.

Giorgi, F., Marinucci, M.R. and *Visconti, G.*, 1992: A $2\times CO_2$ climate change scenario over Europe generated using a Limited Area Model nested in a General Circulation Model. II: Climate Change Scenario. *J. Geophys. Res. 97*, 10011-10028.

Giorgi, F., Mearns, L.O., Bogárdi, I., Matyasovszky, I. and *Palecki, M.*, 1999: Comparison of climate change scenarios generated from regional climate model experiments and empirical downscaling. Special issue on new developments and applications with the NCAR Regional Climate Model (RegCM). *J. Geophys. Res. 104(D6)*, 6603-6621.

Harnos, Zs., 1998: Expected climate tendencies and their impact on the production of some crops. In *Climate Change and Consequences* (in Hungarian) (ed.: *Dunkel, Z.*). *Meteorological Scientific Days'97*, November 20-21, 1997, Hungarian Meteorological Service, Budapest, 55-66.

Hess, P. and *Brezowsky, H.*, 1969: *Katalog der Groswetterlagen Europas.* Berichte des Deutchen Wetterdienstes Nr. 113, Bd. 15, 2. neu bearbeitete und erganzte Aufl., Offenbach a. Main, Selbstverlag des Deutschen Wetterdienstes.

Iványi, Zs., 1995: Variation of daily extreme temperatures in Hungary. *Időjárás 99*, 85-92.

Kertész, Á., Lóczy, D., Mika, J., Papp, S., Huszár, T. and *Sántha, A.*, 1999: Studies on the impact of global climate change on some environmental factors in Hungary. *Időjárás 103*, 37-65.

Koflanovits-Adámy, E. and *Szentimrey, T.*: 1986: The variations of the precipitation amounts in the Charpathian Basin during the present century (in Hungarian). *Időjárás 90*, 206-216.

Kovács, G. and *Dunkel, Z.*, 1998: : Assessment of the impacts of climate change on arable lands of Hungary for the next half century (in Hungarian). In *Climate Change and Consequences* (ed.:

Dunkel, Z.). *Meteorological Scientific Days '97*, November 20-21, 1997, Hungarian Meteorological Service, Budapest, 181-193.

Kovács-Láng, E., Kröel-Dulay, Gy., Kertész, M., Mika, J., Rédei, T., Rajkai, K., Hahn, I. and *Bartha, S.*, 1998: Change of the gap dynamics of succession in a semiarid gradient for the perennial open sandy steppe (in Hungarian). In *Climate Change and Consequences* (ed.: *Dunkel, Z.*). *Meteorological Scientific Days '97*, November 20-21, 1997, Hungarian Meteorological Service, Budapest, 43-54.

Marinucci, M.R., Giorgi, F., Beniston, M., Id, M., Chuck, P., Okamura, A. and *Bernasconi, A.*, 1995: High resolution simulations of January and July climate over the western alpine region with a nested regional modeling system. *Theor. Appl. Climatol. 51*, 119-138.

Matyasovszky, I., Bogárdi, I., Bárdossy, A. and *Duckstein, L.*, 1993: Space-time precipitation reflecting climate change. *Hydrol. Sci. J. 38*, 539-558.

Matyasovszky, I., Bogárdi, I., Bárdossy, A. and *Duckstein, L.*, 1994a: Local temperature estimation under climate change. *Theor. Appl. Climatol. 50*, 1-13.

Matyasovszky, I., Bogárdi, I. and *Duckstein, L.*, 1994b: Comparison of two general circulation models to downscale temperature and precipitation under climate change. *Water Resour. Res. 30*, 3437-3448.

Matyasovszky, I., Bogárdi, I. and *Ganoulis, J.*, 1995: Impact of global climate change on temperature and precipitation in Greece. *Appl. Math. Comp. 70*, 1-35.

Mátyás, Cs., 1997: Effects of environmental change on the productivity of tree populations. In *Perspectives of forest genetics and tree breeding in a changing world. IUFRO World Series* (ed.: *Mátyás, Cs.*), Vol. 6., Vienna, 109-121.

McGregor, J.L., 1997: Regional climate modelling. *Meteorol. Atmos. Phys. 63*, 105-117.

Mika, J., 1988: Regional features of global warming in Carpathian Basin (in Hungarian). *Időjárás 92*, 178-189.

Mika, J., 1991: Predictable impacts of a major global warming in Hungary (in Hungarian). *Időjárás 95*, 265-278.

Mika, J., 1992: Method of slices to estimate regional features of the global warming at extratropical latitudes. *Proc. of 5th Int. Meeting on Statistical Climatology*, June 22-26, 1992, Toronto, Canada , 433-436.

Mika, J., Ambrózy, P., Bartholy, J., Nemes, Cs. and *Pálvölgyi, T.*, 1995: Time variability of the climate of the Hungarian plains Alföld (in Hungarian). *Vízügyi Közlemények LXXVII*, 261-286.

Molnár, K., 1996a: Trend of precipitation amount in Hungary (in Hungarian). *Természet Világa*, Special Issue, 66-68.

Molnár, K., 1996b: Areal distribution of temperature and precipitation trends in Hungary for 110 years (1881-1990) (in Hungarian). *Földrajzi Értesítő XLV*, 23-33.

Molnár, K., 1996c: Temperature and precipitation trends for Hungary. *Proc. of 17th International Conference on Carpathian Meteorology*, October 14-18, 1996, Visegrád, Hungary, 161-166.

Molnár, K. and *Mika, J.*, 1997: Climate as a changing component of landscape: recent evidence and projections for Hungary. *Z. Geomorph. N.F.* Suppl.-Bd. 110, 185-195.

Muster, H., Bárdossy, A. and *Duckstein, L.*, 1994: Adaptive neuro-fuzzy modeling of a non-stationary hydrologic variable. *Proc. of International Symposium on Water Resources Planning in Changing World.* Karlsruhe, Germany, June 1994, II/221-230.

Nachtnebel, H.P., Hebenstreit, K., Bogárdi, I. and *Matyasovszky, I.*, 1996: Effect of climate change on the hydrology of an alpine watershed (in German). *Proc. of Internationales Symposium am 27-28. November 1995 im Europaischen Patentamt in München*, Institut für Wasserwesen, Heft 56b, 307-331.

Péczely, Gy., 1981: *Climatology* (in Hungarian). Tankönyvkiadó, Budapest, 336 p.

Práger, T. and *Kovács, E.*, 1988: Investigation of effects of atmospheric trace gaese and aerosol particles on climate with a radiative convective model (in Hugarian). *Időjárás 92*, 153-162.

Rácz, L., 1999: *Climate History of Hungary Since 16th Century: Past, Present and Future*. Centre for Regional Studies of Hungarian Academy of Sciences, Pécs, No. 28., 160 p.

Szentimrey, T., 1995: General problems of the estimation of inhomogeneities, optimal weighting of the reference stations. *Proc. of 6th International Meeting on Statistical Climatology.* 19-23 June 1995, Galway, Ireland, 62-63.

Szentimrey, T., 1996: Some statistical problems of homogenisation: break points detection, weighting of reference series. *Proc. of 13th Conference on Probability and Statistics in the Atmospheric Sciences.* 21-23 February 1996, San Francisco, California, 365-368.

Tar, K., 1992: Climate of Túrkeve (in Hungarian). *Proc. of Conference on 145 Anniversary of the Birth of Hegyfoky Kabos*. Debrecen, Túrkeve, 156-164.

Tóth, Z., and Szentimrey, T., 1990: The binormal distribution: A distribution for representing asymmetrical but normal-like weather elements. *J. Climate 3*, 128-136.

Weidinger, T., Matyasovszky, I. and *Bogárdi, I.*, 1994: The influence of atmospheric circulation on the water budget of Lake Balaton. *Meteorol. Zeitschrift, N.F. 3*, 288-296.

Weidinger, T., Matyasovszky, I., Bartholy, J. and *Bogárdi, I.*, 1995: Climate change impact on daily pan evaporation. *Meteorol. Zeitschrift, N.F. 4* , 235-245.

Wilson, L.L., Lettenmaier, D.P. and *Skyllingstad, E.*, 1992: A hierarchical stochastic model of large scale atmospheric circulation patterns and multiple station daily precipitation. *J. Geoph. Res. 97*, 2791-2809.

IDŐJÁRÁS

Quarterly Journal of the Hungarian Meteorological Service
Vol. 105, No. 1, January–March 2001, pp. 19–28

Investigation of surface-atmosphere heat exchange processes using surface and satellite measurements

Judit Kerényi[1] and **Iván Csiszár**[2]

[1]*Hungarian Meteorological Service, Satellite Research Laboratory,*
P.O. Box 39, 1675-Budapest, Hungary; E-mail: kerenyi.j@met.hu

[2]*Cooperative Institute for Research in the Atmosphere*
National Oceanic and Atmospheric Administration
National Environmental Satellite Data and Information Service
Office of Research and Applications
Camp Springs, MD, U.S.A.; E-mail: ivan.csiszar@noaa.gov

(Manuscript received 20 February 2001; in final form 27 February 2001)

Abstract—Seasonal changes in surface-atmosphere heat exchange processes were studied over diverse vegetated surfaces by the synergy of ground observations and satellite measurements over two target areas in Hungary. NOAA Advanced Very High Resolution Radiometer (AVHRR) Global Area Coverage (GAC) data and the NOAA Global Vegetation Index (GVI) weekly data set were combined with conventional ground observations from meteorological stations. Multi-year mean seasonal cycles of satellite-derived parameters were derived and compared. The temporal variation of day- and nighttime temperature difference (DNTD) proved to be directly related to that of latent heat exchange through vegetation conditions and precipitation. Sensible heat flux was characterized by the air-skin temperature difference. The observed differences over the two target areas can be attributed to differences in the dominant vegetation. Time series of DNTD, derived from daytime GVI temperature data and nighttime minimum soil temperature, exhibited significant interannual variability also.

1. Introduction

The derivation of large-scale continuous fields of surface characteristics is possible only by the use of high-or moderate spatial resolution satellite imager data. The Advanced Very High (spectral) Resolution Radiometer (AVHRR) on board the operational polar orbiting NOAA satellites provides top-of-the atmosphere measurements in five atmospheric window channels in the visible to infrared range of the radiometric spectrum. The current configuration of NOAA's Polar Orbiting Environmental Satellite System (POES), consisting of one "morning"

and one "afternoon" operational satellite, allows four views of a given target area for most of the globe. The multispectral information from AVHRR can be analysed to derive a number of surface and atmospheric parameters, many of which were not planned to be studied by this instrument during it's design.

Many of the AVHRR-derived parameters can be used to describe the thermo-physical properties of land surface and to characterize the surface energy exchange processes. The surface energy balance can be described by the following equation (see, for example, *Dunkel et al.*, 1991):

$$R_n = G + H + LE \tag{1}$$

where R_n is the net radiation flux, G is the soil heat flux, H is the (vertical) sensible heat flux and LE is the (vertical) latent heat flux. There have been numerous theoretical and empirical studies to quantify these parameters from satellite data and to produce high-resolution maps of them (*Seguin* and *Itier*, 1983; *Hurtado et al.*, 1994; *Choudhury*, 1994; *Tarpley*, 1994; *Diak et al.*, 1995; etc.). In this paper we rather focus on describing the temporal variation of satellite-derived surface parameters that are related to the above fluxes. It is thus not our goal to derive accurate quantitative estimates of all fluxes, but rather to compare the interrelation of their temporal changes over the growing season.

A combination of the visible (*VIS*) and near-IR (*NIR*) measurements of AVHRR, the Normalized Difference Vegetation Index, $NDVI = (NIR - VIS)/(NIR + VIS)$ provides information on the amount and state of vegetation cover. This parameter can be further used to derive higher-level products, such as the fraction of green vegetation or leaf area index (*Price*, 1993; *Nemani et al.*, 1996; *Gutman* and *Ignatov*, 1998; *Carlson* and *Ripley*, 1999). NDVI is also an important parameter in land cover classification schemes *(DeFries* and *Townshend*, 1994).

Surface temperature measurements from AVHRR, taken at different local times can be used for the reconstruction of the diurnal temperature cycle, and it's amplitude, the diurnal temperature range (DTR), which latter is an important surface characteristic related to thermal inertia (*Price*, 1985; *Tänczer et al.*, 1995; *Sobrino* and *Kharraz*, 1999). DTR is a good indicator of surface moisture conditions through evaporation from bare soil and evapotranspiration by vegetation, and also the long-term monitoring of land cover change from desertification, de- or reforestation, wildfires etc.

A combination of satellite-derived parameters with conventional measurements at the ground provides further opportunity for the characterization of energy fluxes near the surface. Here we used the difference between the surface skin temperature and the maximum air temperature to characterize the daily maximum sensible heat flux at the surface. In the analysis ground measurements of precipitation were also used as a control parameter to characterize surface moisture conditions. The seasonal changes of surface conditions were studied over two target areas in Hungary with different vegetation cover.

The results of such a study are sensitive to any inaccuracies of the input data and to artifacts inherent in the observational system. The orbital drift of the "afternoon" NOAA satellites introduces spurious interannual trends in observed surface reflectances (and NDVI to a smaller extent) because of the bidirectional effects due to changing solar illumination angle and also in surface temperatures, mostly because of the changing local time of observation. Imperfections in preprocessing, such as calibration and cloud screening, may introduce additional errors. Therefore a careful analysis and processing of the original satellite data is required before the detailed physical analysis.

In the remaining of this paper, Section 2 of this paper presents the data used for our analysis. The methodology and the results are discussed in Sections 3 and 4 respectively, followed by the conclusions in Section 5.

2. Data

2.1 Surface data

The surface data used in this study were measured at the meteorological stations at Szarvas (46.52°N, 20.34°E) and Keszthely (46.46°N, 17.15°E). They include daily maximum and minimum air temperatures at 2 m (T_{max}, T_{min}), the daily minimum near-ground temperature (*Radmin*, measured at 2 cm and often referred to as *radiative minimum temperature*), and daily precipitation amount. Szarvas is located in a mostly agricultural area, whereas the area around Keszthely is a mixture of forests, marshlands and croplands. The climate in Keszthely is more affected by oceanic influence, resulting in somewhat higher annual precipitation amount and smaller annual temperature variability.

2.2 Satellite data

Global Area Coverage (GAC) 4-km data are produced by sampling and averaging onboard satellite from the full 1-km resolution AVHRR measurements in five wavebands: the visible (VIS, 0.58–0.68 μm, channel 1), near-IR (NIR, 0.73–1.1 μm, channel 2), mid-infrared (3.6–3.9 μm, channel 3) and thermal infrared (IR, 10.3–11.3 and 11.5–12.5 μm, channels 4 and 5, respectively). Daytime and nighttime GAC data have been archived at NOAA/NESDIS for the two target areas since July 1993.

From the GAC raw data visible and near-IR reflectances were derived using the time-dependent post-launch calibration coefficients (*Rao* and *Chen*, 1995, 1996). The reflectances were combined into NDVI. Channel 4 and 5 brightness temperatures, T_4 and T_5, were derived from observed radiances using on-board calibration coefficients. Channel 3 reflectance (used to detect snow contamination in early spring) was calculated following the approach by *Stowe et al.* (1999) in removing the thermal component based on T_4 and T_5. Data from this dataset will hereafter referred to as GAC Target Dataset (GTD) data.

The operational NOAA Global Vegetation Index (GVI) weekly dataset (*Kidwell*, 1997) is produced from afternoon GAC observations. It is sampled first in space (one pixel out of about 16 GAC pixels on a daily basis within each gridbox of a 0.15° by 0.15° resolution Plate Carree grid) and then in time (one observation per week from the sampled daily data). The temporal compositing is done by taking observations corresponding to the maximum NIR- and VIS count difference over the seven-day period within each gridbox, ensuring the selection of the data that are least affected by clouds and aerosol. The calibration of the visible, NIR and IR data was done similarly to the GTD data. Both GTD and GVI data were screened for cloud contamination. Daytime GTD data were screened by the spatial heterogeneity technique of *Coakley* and *Bretherton* (1982) applied to visible reflectances. Residual clouds were screened out by $T_4 - T_{max}$ and visible reflectance threshold tests. Finally, outliers in visible reflectance in each 10-degree bin of satellite zenith angle were eliminated. Nighttime GTD data were screened by the Coakley and Bretherton method applied to T_4 and by a $T_4 - T_{min}$ threshold test. GVI data were screened for residual clouds by examining the departure of the weekly T_4 value from multi-year means (*Gutman et al.*, 1995).

3. Method

For compatibility between satellite observations from different years, we performed corrections for post-launch calibration errors and satellite orbital drift effects in VIS, NIR and NDVI using the parameterization by *Gutman* (1999a), which normalizes the observed reflectances to a common solar zenith angle. Similarly, brightness temperature data were also normalized to a common local observation time by the formulae of *Gutman* (1999b). NOAA-11 AVHRR data from July 1993–December 1994 were not used in this regional study because of the increasing uncertainty in the accuracy of these correction schemes for extreme observational conditions caused by the large satellite orbital drift towards the end of the satellites' lifetime.

The corrected T_4 and T_5 values in both AVHRR datasets were combined into Land Surface Temperature (T_s) using a split-window equation (*Gutman*, 1994) including the emissivity (ε) correction based on *NDVI* (*Van de Griend* and *Owe*, 1993):

$$T_s = T_4 + 2.63 \times (T_4 - T_5) + 1.274 + (T_4 + T_5)/2 \times (0.156 + 3.98 \times (T_4 - T_5)/(T_4 + T_5)) \times (1 - \varepsilon)/\varepsilon, \quad (2)$$

where $\varepsilon = 1.013 + 0.0681 \times \ln(NDVI)$.

The satellite-derived parameters were derived and averaged over 50×50 km rectangular areas around the meteorological stations in Szarvas and Keszthely.

It has been shown that the daytime and nighttime observations from the AVHRR sensor are good indicators of the diurnal temperature range (*Csiszár* and *Kerényi*, 1995) and thus the massive processing of 3-hour geostationary METEOSAT data is not necessary to characterize daily temperature variations. Note, however, that as the afternoon AVHRR observations deviate to some extent from the daily maximum temperatures, absolute values of DTR cannot be readily derived from AVHRR observations. In this paper we will use the AVHRR day-night difference (DNTD) values, which are smaller than, but well correlated with the maximum temperature range. The 10-day DNTD was derived from the cloud free daytime ($T_s(d)$) and nighttime ($T_s(n)$) surface temperature values from AVHRR only. As the daytime and nighttime GTD data were very rarely cloud free on the same day, maximum value compositing was not possible. Therefore 10-day mean DNTD was calculated from the 10-day mean $T_s(d)$ and the 10-day mean $T_s(n)$ values. Consequently, 10-day mean NDVI and the $(T_s(d)) - (T_{max})$ differences were calculated from the GTD data.

In the case of the GVI dataset, which includes only daytime observations, $T_s(n)$ was substituted by Radmin to derive DNTD. To check the applicability of this parameter we compared the Radmin values with the $T_s(n)$ values derived from GTD data for two years when both data were available. *Fig. 1* shows that the difference between the two kinds of data is within 2–3 degrees. It is also obvious that $T_s(d)$ tends to be more variable in time than $T_s(n)$ and thus DNTD is mostly driven by changes of $T_s(d)$.

4. Results

The annual variation of NDVI, DNTD and the $T_s(d) - T_{max}$ difference was derived using GTD data for the 1996–1998 period. *Fig. 2* shows the 3-year mean values of these parameters at Szarvas and Keszthely targets. Comparing the NDVI values at the two targets one can see an earlier greenup in spring at the Szarvas target with maximum NDVI in June, whereas at the Keszthely target the greenup started later, but NDVI decreased only in September. We can also see that in both targets DNTD increases at the beginning of the year. At the end of May, when vegetation has reached a certain stage of development with the corresponding evepotranspiration—NDVI is about 0.3—the DNTD increase quickly reverses, and after a few weeks it levels off at a lower value. In Szarvas, however, there is a weaker secondary maximum at the end of summer, which can be explained by the fact that solar irradiation is still high, but the vegetation cover is low.

The $T_s(d) - T_{max}$ difference closely follows the variation of DNTD. This suggests that the daytime-only GVI temperature data still hold useful information about surface heat exchange processes, which should be further examined in the future.

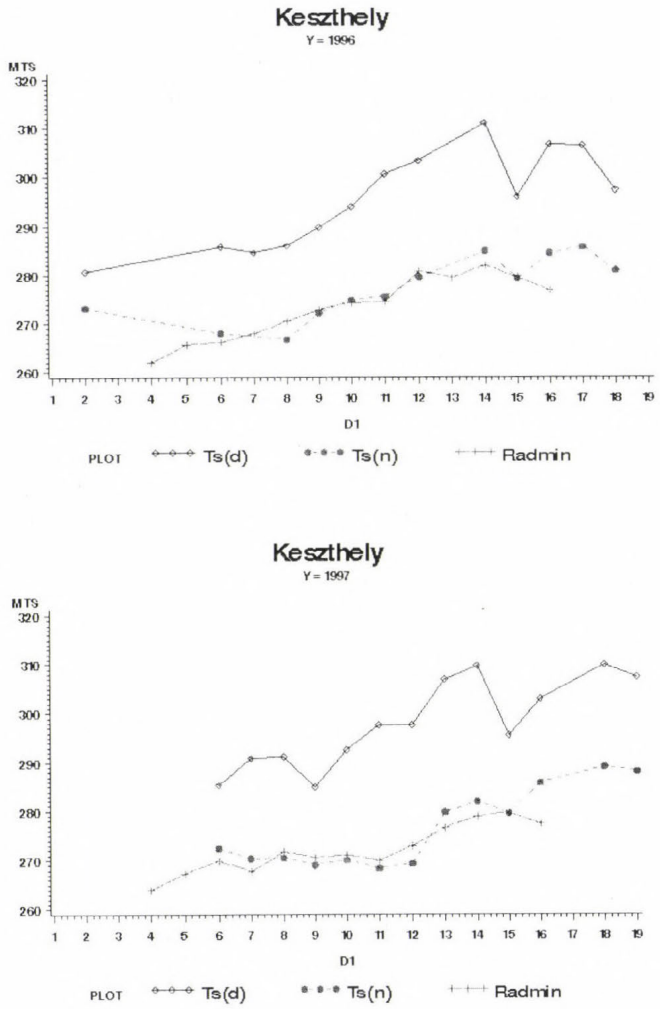

Fig. 1. Daytime ($T_s(d)$) and nighttime ($T_s(n)$) surface temperature [K] derived from GTD data and the radiation minimum temperature at the Keszthely target in 1996 and 1997. The horizontal axis denotes dekades of Julian days.

Figs. 3 and *4* show examples of temporal variation of NDVI, DNTD and precipitation in individual years over the Szarvas and Keszthely target areas respectively. Here the AVHRR data were taken from the GVI dataset for compatibility between years over a longer period. One can clearly see that DNTD is directly related to evaporation, i.e. the combined effect of soil moisture and vegetation condition. Also, to analyze DNTD in a certain months, history from the previous several months needs to be considered. In 1992 in Szarvas, the greenup started quite early, despite the low precipitation amount (probably temperature

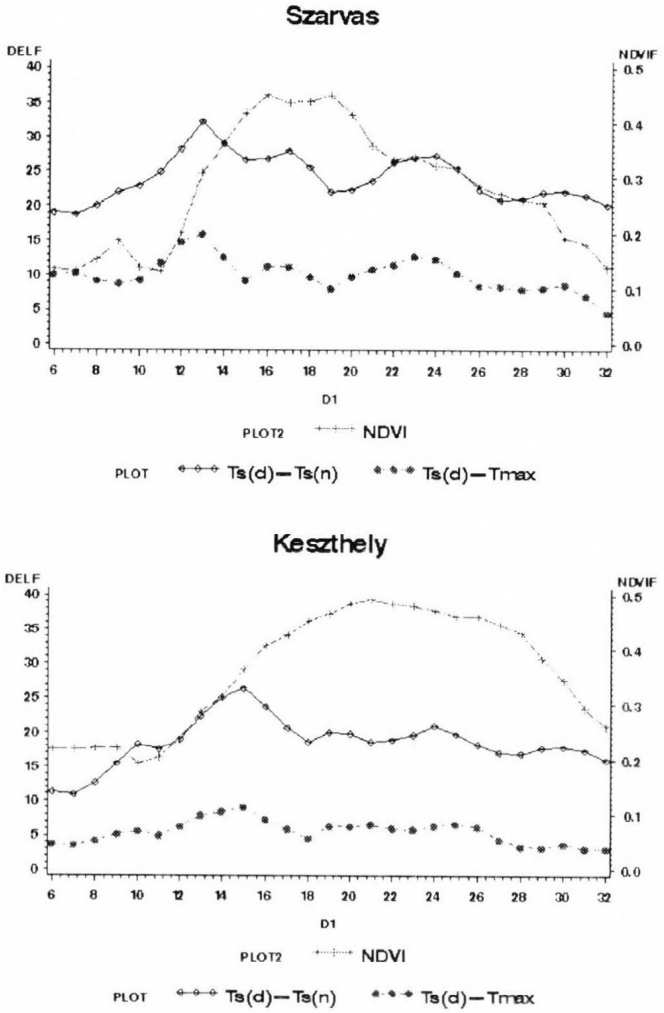

Fig. 2. The annual variation of the 3-year mean value of *NDVI*, $T_s(d) - T_s(n)$ (= *DNTD*) and $T_s(d) - T_{max}$ [K] at Szarvas and Keszthely. The horizontal axis denotes dekades of Julian days.

conditions were still favorable). However, because the soil moisture content was low, DNTD was still high until May. It decreased only in June, with increased rainfall, although the vegetation conditions were not so good because of the prolonged dry period earlier. In 1998 in Szarvas, precipitation was high in spring, but there was a delay in vegetation development, and thus evapotranspiration could not suppress the DNTD values. DNTD decreased again in June, this time because by then vegetation growth had reached the stage when evapotranspiration could efficiently use the abundant soil moisture from the previous months.

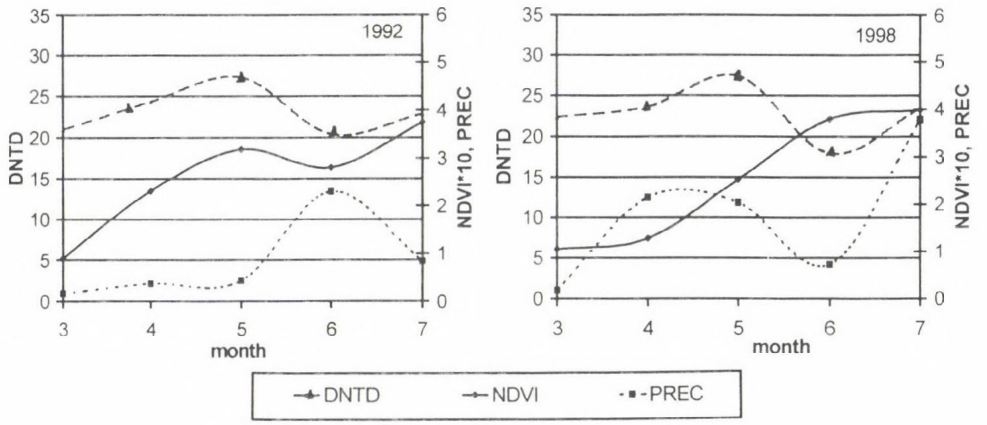

Fig. 3. The annual variation of NDVI, precipitation [mm] and DNTD [K] at Szarvas station in 1992 and 1998.

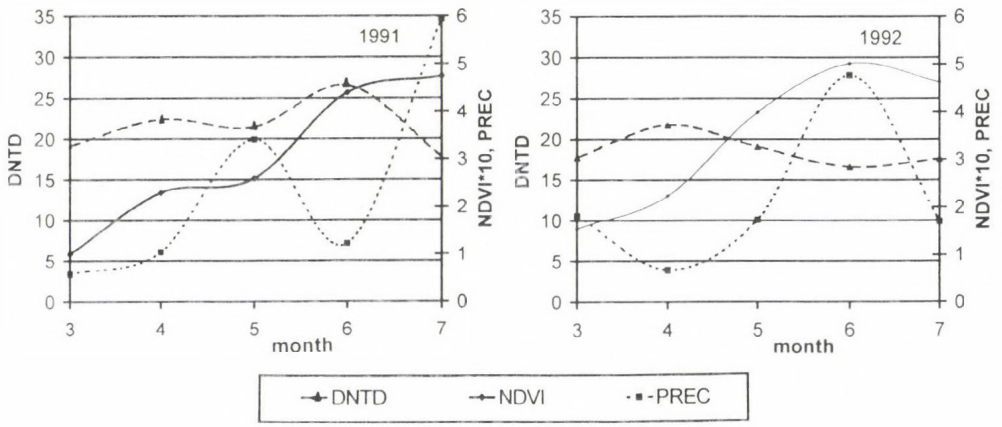

Fig. 4. The annual variation of NDVI, precipitation [mm] and DNTD [K] at Keszthely station in 1991 and 1992.

In Keszthely precipitation amount was relatively high in May 1991. It immediately shows in the temporary small decrease of DNTD. In June, with high NDVI and low precipitation, DNTD still remains high, probably much of the moisture from the May precipitation was efficiently removed from the soil in May. In 1998, the low DNTD values in May and June are the obvious results of high precipitation amount and well developed vegetation.

5. Conclusions

Results from our study have served as examples of the combination of satellite and surface data to efficiently study intra- and inter-annual changes in surface-atmosphere heat exchange processes. DNTD is a good indicator of latent heat exchange through direct evaporation from soil and evapotranspiration from vegetation. As such, it is also indirectly related to soil moisture, precipitation and vegetation condition. Both DNTD and the air-skin temperature difference (an indicator of sensible heat flux) are mostly driven by daytime temperature.

Time series of the various parameters also have shown that the surface processes can be understood only by the synergistic analysis of the different components of the surface—atmosphere system. On the other hand, the signature in the satellite-derived quantities, particularly NDVI and DNTD, is an integrated result of various current processes as well as their time history during the previous period. Analysis of separate spectral reflectances (*Gutman et al.*, 2000) or separate daytime and nighttime temperatures can thus reveal further details of the processes. For example, analysis of absolute temperature values and their anomalies is helpful in explaining vegetation conditions (*Kogan*, 1997).

Acknowledgement—This work has been supported by the US-Hungarian Science and Technology Joint Fund (No. 548) and the Hungarian Scientific Research Funds (No. T25543).

References

Carlson, T.N. and *Ripley, D.N.*, 1999: On the relation between NDVI, fractional vegetation cover and leaf area index. *Remote Sens. Environ 62*, 241-252.

Choudhury, J.B., 1994: Synergism of multispectral satellite observations for estimating regional land surface evaporation. *Remote Sens. Environ. 49*, 264-274.

Coakley, J.A. and *Bretherton, F.P.*, 1982: Cloud cover from high-resolution scanner data: Detecting and allowing for partially filled fields of view. *J. Geophys. Res. 87*, 4917-4932.

Csiszár, I. and *J.Kerényi*, J., 1995: The effect of the vegetation index on the daily variation of the active surface temperature. *Adv. Space Res. 16.*, No.10, (10)177–(10)180.

DeFries, R. and *Townshend, J.R.G.*, 1994: NDVI-derived land cover classification at global scales. *Int. J. Remote Sens. 15*, 3567-3586.

Diak, G. R., Rabin, R.M., Gallo, K. and *Neale, C.M.*, 1995: Regional-scale comparisons of vegetation and soil wetness with surface energy budget properties from satellite and in-situ observations. *Remote Sensing Reviews 12*, 355-382.

Dunkel, Z., Pásztor, K. and *Tiringer, C.*, 1991: Calculation of diurnal variation of surface temperature using a simplified energy balance model. *Időjárás 95*, 170-177.

Van de Griend, A.A. and *Owe, M.*, 1993: On the relationship between thermal emissivity and the normalized difference vegetation index for natural surfaces. *Int. J. Remote Sens. 14*, 1119-1131.

Gutman, G., 1994: Multi-annual time series of AVHRR-derived land surface temperature. *Adv. Space Res. 14*, (3)27-(3)30.

Gutman, G., Csiszár, I. and *Romanov, P.*, 2000: Using NOAA/AVHRR products to monitor El Niño impacts: Focus on Indonesia in 1997–1998. *Bull. Amer. Meteorol. Soc. 81*, 1189-1205.

Gutman, G., Tarpley, D., Ignatov, A. and *Olson, S.*, 1995: The enhanced NOAA Global Land Dataset from the Advanced Very High Resolution Radiometer. *Bull. Amer. Meteorol. Soc. 76*, 1141-1156.

Gutman G. and *Ignatov, A.*, 1998: The derivation of the green vegetation fraction from NOAA/AVHRR data for use in numerical weather prediction models. *Int. J. Rem. Sens. 19*, 1533-1543.

Gutman, G., 1999a: On the use of long-term global data of land reflectances and vegetation indices derived from the advanced very high resolution radiometer. *J. Geophys. Res. 104*, D6, 6241-6255.

Gutman, G., 1999b: On the monitoring of land surface temperatures with the NOAA/AVHRR: Removing the effect of satellite orbit drift. *Int. J. Remote Sens. 20*, 3407-3413.

Hurtado, E., Artigao, M.M. and *Caselles, V.*, 1994: Estimating maize (Zea mays) evapotranspiration from NOAA-AVHRR thermal data in the Albacete area, Spain. *Int. J Remote Sensing* **15**, 2023-2037.

Ignatov, A. and *Gutman, G.*, 1999: Monthly mean diurnal cycles in surface temperatures over land for global climate studies. *J. Climate 12*, 1900-1910.

Jin, M. and *Dickinson, R.E.*, 1999: Interpolation of surface radiative temperature measured from polar orbiting satellites to diurnal cycle. *J. Gephys. Res. 104*, 2105-2116.

Kidwell, K, 1997: *Global Vegetation Users' Guide*. NOAA/NESDIS National Climatic Data Center, U.S Dep. of Commer., Washington, D.C.

Kogan, F.N., 1997: Global drought watch from space. *Bulletin Amer. Meteorol. Soc. 78*, 621-636.

Nemani, R.R., Running, S.W., Pielke, R.A. and *Chase, T.N.*, 1996: Global vegetation cover changes from coarse resolution satellite data. *J. Geophys. Res. 101*, 7157-7162.

Price, J.C., 1985: On the analysis of thermal infrared imagery: The limited utility of apparent thermal inertia. *Remote Sens. Environ. 18*, 59-73.

Price, J.C., 1993: Estimating leaf area index from satellite data. *IEEE Transactions Geosci. Remote Sens. 31*, 727-734.

Rao, C.R.N. and *Chen, J.*, 1995: Intersatellite calibration linkages for the visible and near-infrared channels of the advanced very high resolution radiometer on the NOAA 7, 9, 11 spacecraft. *Int. J. Remote Sens. 16*, 1931-1942.

Rao, C.R.N. and *Chen, J.*, 1996: Postlaunch calibration of the visible and near-infrared channels of the advanced very high resolution radiometer on the NOAA 14 spacecraft, 1. *Int. J. Remote Sens. 17*, 2743-2747.

Seguin, B. and *Itier, B.*, 1983: Using midday surface temperature to estimate daily evaporation from satellite thermal IR data. *Int. J. Remote Sensing 4*, 371-383.

Sobrino, J.A. and *El Kharraz, M.H.*, 1999: Combining afternoon and morning NOAA satellites for thermal inertia estimation 1. Algorithm and its testing with Hydrologic Atmospherci Pilot Experiment-Sahel data. *J Geophys. Res. 104*, 9445-9453.

Stowe, L., Davis, P. and *McClain, E.P.*, 1999: Scientific basis and initial evaluation of the CLAVR-1 global clear/cloud classification algorithm from the Advanced Very High Resolution Radiometer. *J. Atmos. Oceanic Technol. 16*, 656-681.

Tänczer, T., Rimóczi-Paál, A. and *Csiszár, I.*, 1995: Prediction of daily amplitudes of canopy temperatures using satellite information. *Adv. Space Res.* 16, (10)181-(10)184.

Tarpley, J.D., 1994: Monthly evapotranspiration from satellite and conventional meteorological observations. *J. Climate 7*, 704-713.

IDŐJÁRÁS

Quarterly Journal of the Hungarian Meteorological Service
Vol. 105, No. 1, January–March 2001, pp. 29–38

Visibility and fog forecasting based on decision tree method

Ferenc Wantuch

Hungarian Meteorological Service,
P.O. Box 38, H-1525 Budapest, Hungary; E-mail: wantuch.f@met.hu

(Manuscript received 6 April 2000; in final form 15 December 2000)

Abstract—The paper describes a visibility and fog forecasting model developed and used at the Hungarian Meteorological Service (HMS) for last 3 years. The investigated model is a perfect prognostical model (PP). Characteristics of the model, such as input data, statistical approach, decision trees and threshold numbers are described in this paper. The model was tested for both measured sounding and predicted data. Verification of the model led to very good results, so it was applied to aeronautical forecasting as well as to nowcasting. Information and short review about different types of other visibility models are also given.

Key-words: NWP parameters, perfect prognosis (PP), model output statistics (MOS), FOGSI index, decision tree.

1. Introduction

Visibility forecast is very important for transportation, especially for air traffic where its accuracy is prominent. The WMO/ICAO requirements are very rigorous in aviation meteorology (*ICAO*, 1998). Verifications of aeronautical forecasts show that the reason of poor terminal weather forecasts—in about 70 per cent of all cases—is a weak or not suitable visibility prediction. It have not been available any special numerical methods at the HMS before, which could be an aid for forecasters in the prediction of the visibility, so they could use only traditional tools.

The European forecasters use different methods in the practice. One possibility is the diagnosis of fog from satellite images (*Kerényi et al.*, 1995). Some organisations, e.g., EUMETSAT, Central Institute for Meteorology and Geodynamics Austria (ZAMG), Swedish Meteorological Institute (SMHI) and Météo France use NOAA AVHRR and Meteosat images in order to analyse fog

and low cloud from satellite data. Another possibility is the improvement of 1-D-models applied in UK, Sweden, Portugal, Belgium (*Stessel* and *Ottoy,* 1999) and also in France. Some case studies have been validated with promising results.

The third way is the use of statistical methods and decision support systems for fog and low cloud forecasting. In the frame of it different methods, like decision trees, linear regression, Kalman-filter (*Kilpinen,* 1992) and neural network (*Pasini et al.,* 1999) were considered for probability forecasts. In general, the results of all these methods were promising, so we considered the problem from statistical point of view.

Let us denote by y the estimated parameter, that is the predictand and by $x_1, x_2, ..., x_p$ the detected meteorological elements, which are the predictors. In this case we have to construct a function:

$$y = f(x_1, x_2, ..., x_p) + \varepsilon, \tag{1}$$

where ε is the error of the method. One can use this function in the following estimated form:

$$\tilde{y} = f(\tilde{x}_1, \tilde{x}_2, ..., \tilde{x}_p), \tag{2}$$

where $\tilde{x}_1, \tilde{x}_2, ..., \tilde{x}_p$ are known from NWP. This is the basic concept of the perfect prognosis method. Suppose that Eq. (2) is constructed directly from $\tilde{x}_1, \tilde{x}_2, ..., \tilde{x}_p$, so

$$y = f(\tilde{x}_1, \tilde{x}_2, ...\tilde{x}_{,p}) + \varepsilon. \tag{3}$$

In this way we get a model output statistical method. Based on this idea, an automatic visibility forecast method can be constructed. The input data of the visibility prediction is, in the given case, the ALADIN mesoscale model output. This is a hydrostatic, spectral limited area numerical weather prediction model, which was developed by collaboration among Météo-France and some Central- and East-European hydrometeorological services including HMS. The main dynamical characteristics of the model, like the preparation of initial and lateral boundary conditions, the physics and post-processing were discussed by *Horányi et al.* (1996).

In order to find a connection with visibility, first we made a comprehensive statistical research on direct measurements and derived physical quantities. The best correlation was received by the fog stability index. The index was calculated according to the following formula:

$$FOGSI = 2 \mid T_{sfc} - T_{850} \mid + 2\,(T_{sfc} - T_{d\,sfc}) + 2\,W_{850}, \tag{4}$$

where

T_{sfc} temperature near the surface,
$T_{d\,sfc}$ dew point near the surface,
T_{850} temperature on 850 hPa level,
W_{850} wind speed on 850 hPa level.

FOGSI index takes into account the temperature gradient (that is the measure of the stability), the impact of moisture near the surface and the mixing by wind.

2. Results of statistical research

The FOGSI index is highly correlated with the observed visibility, especially in autumn-winter time when fog and mist frequently occur. Because of the strong relationship, we could use a regression connection based on a two years long dataset as follows:

$$Visibility = -1.33 + 0.45 \times FOGSI \tag{5}$$

Fig. 1 shows connection between the FOGSI index and the observed visibility (measured in kms) in October 1996. Based on this figure we can make the following considerations. There is a critical interval of FOGSI. Above the upper limit of this interval the calculation of visibility by regression is adequate to use. On the other hand, if the FOGSI number is smaller than the lower limit of this domain, one can predict fog in all cases. The variance of the visibility values inside the critical interval is very high, consequently the statistical method is uncertain. It means that in this interval one can not decide about the visibility based on FOGSI, e.g., if FOGSI is equal to 25, it might represent fog, mist or good visibility at the same time. If data are taken into account only from the critical interval, then the statistical connection between FOGSI and visibility becomes very poor (*Fig. 2*). Its physical reason is that several other effects, which play a great role in development of visibility, were neglected in FOGSI definition. Therefore, one has to introduce some new weather predictors and methods. Parameters, which can be computed from TEMP data and NWP model output as well, are reasonable to select. After thorough investigation, the mean relative humidity of lower air layers (925 hPa - surface) and upper layers (850–700 hPa), the near surface wind speed and relative humidity were chosen to be included into the decision process.

Having examined a large number of cases, it was found that in winter period the cold air can be accumulated near the surface, mainly in the valleys and basins. Sometimes the surface temperature is 2–5 degrees colder than the temperature of the 850 hPa level, in extreme cases this difference reaches 10°C. This inversion stratification is called "the cold air pad" (*Tóth,*1984; *Bóna,*

1986), which represents a very stable state of the atmosphere. We came to the conclusion, that it is necessary to treat cold air pad situations separately and for these days other threshold numbers have to be determined. In order to specify different visibility categories inside the critical interval, one had to work out a new procedure. The steps of the process are summarized in *Fig. 3.*

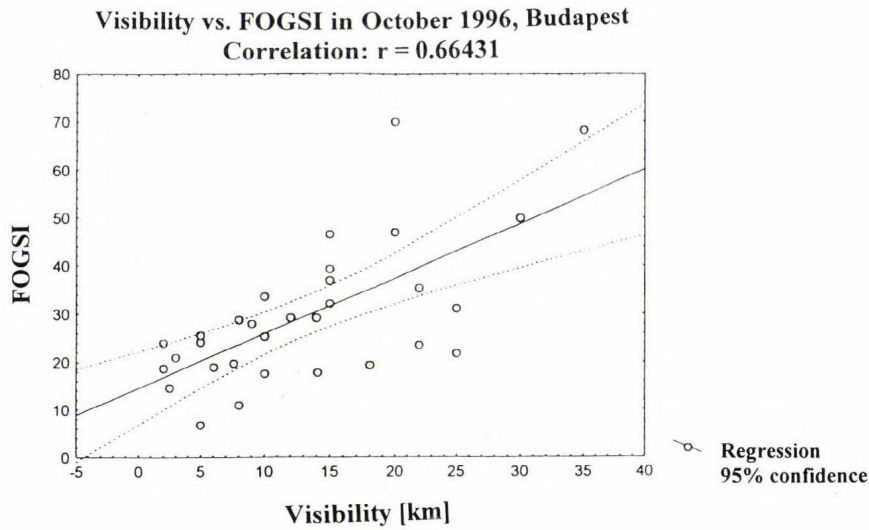

Fig. 1. Correlation between FOGSI and observed visibility.

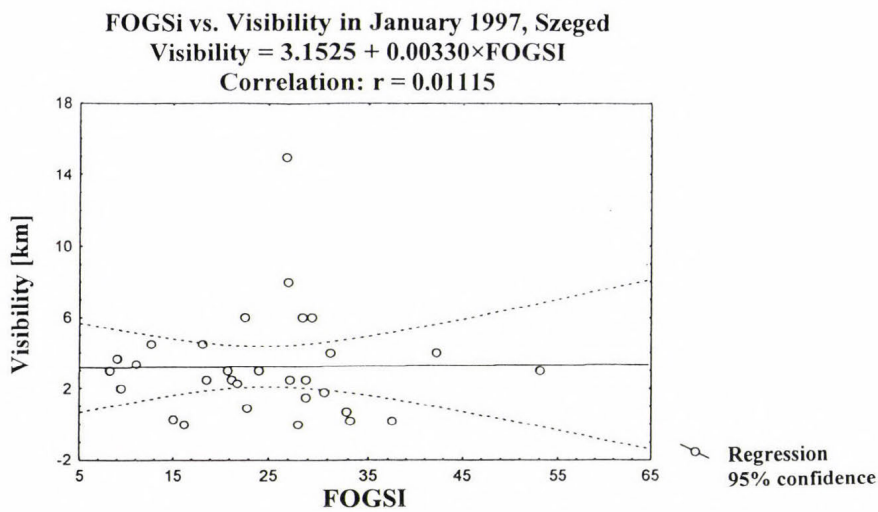

Fig. 2. Correlation between FOGSI and observed visibility (all data derived from critical domain).

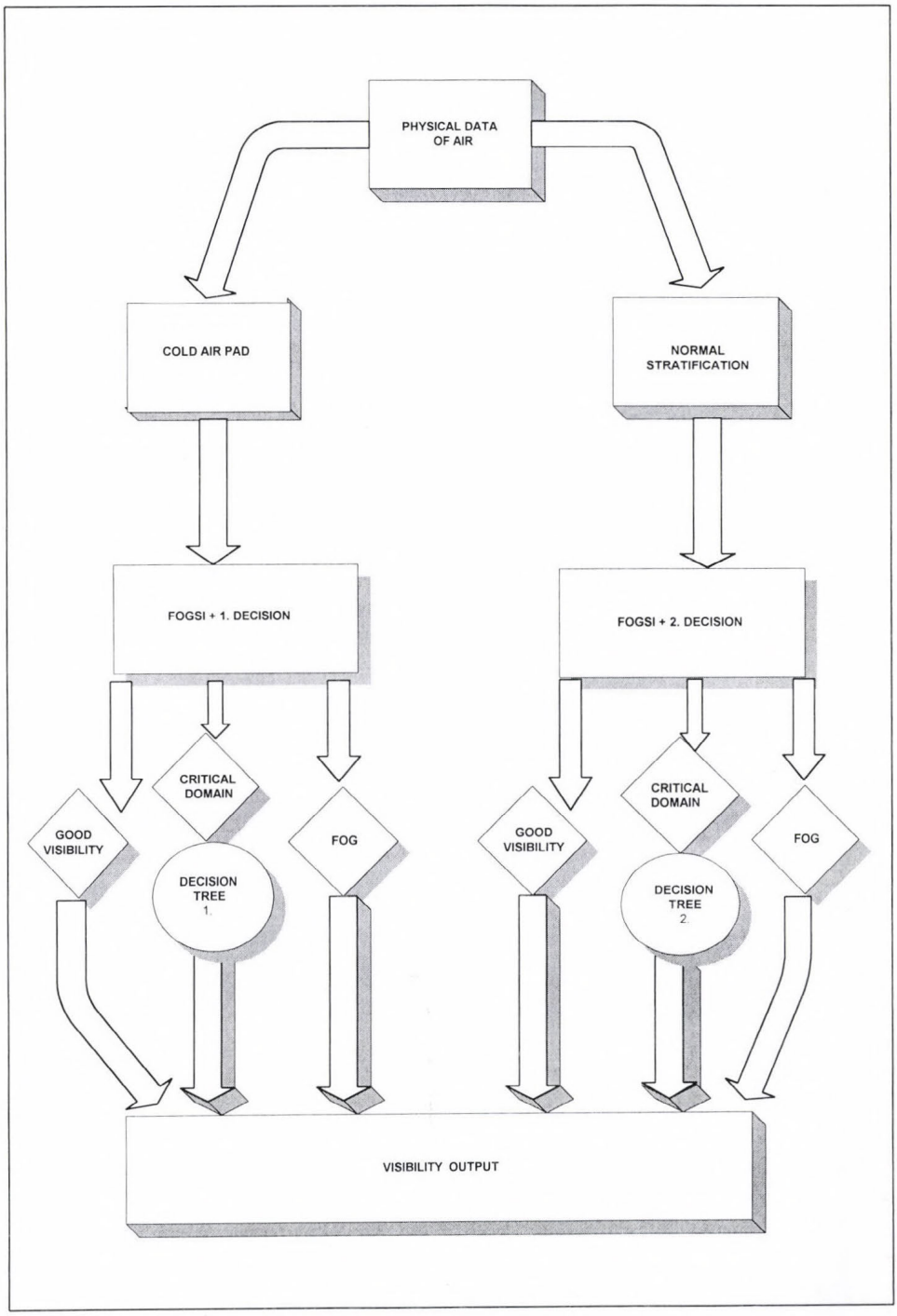

Fig. 3. The first steps of the process.

3. Decision tree

In this chapter the principles and steps of the decision-making procedure will be discussed and demonstrated in *Fig. 4*. Each box represents an important physical condition of the air column. The threshold numbers are based on two years of surface and radiosonde measurements of Budapest-Lőrinc.

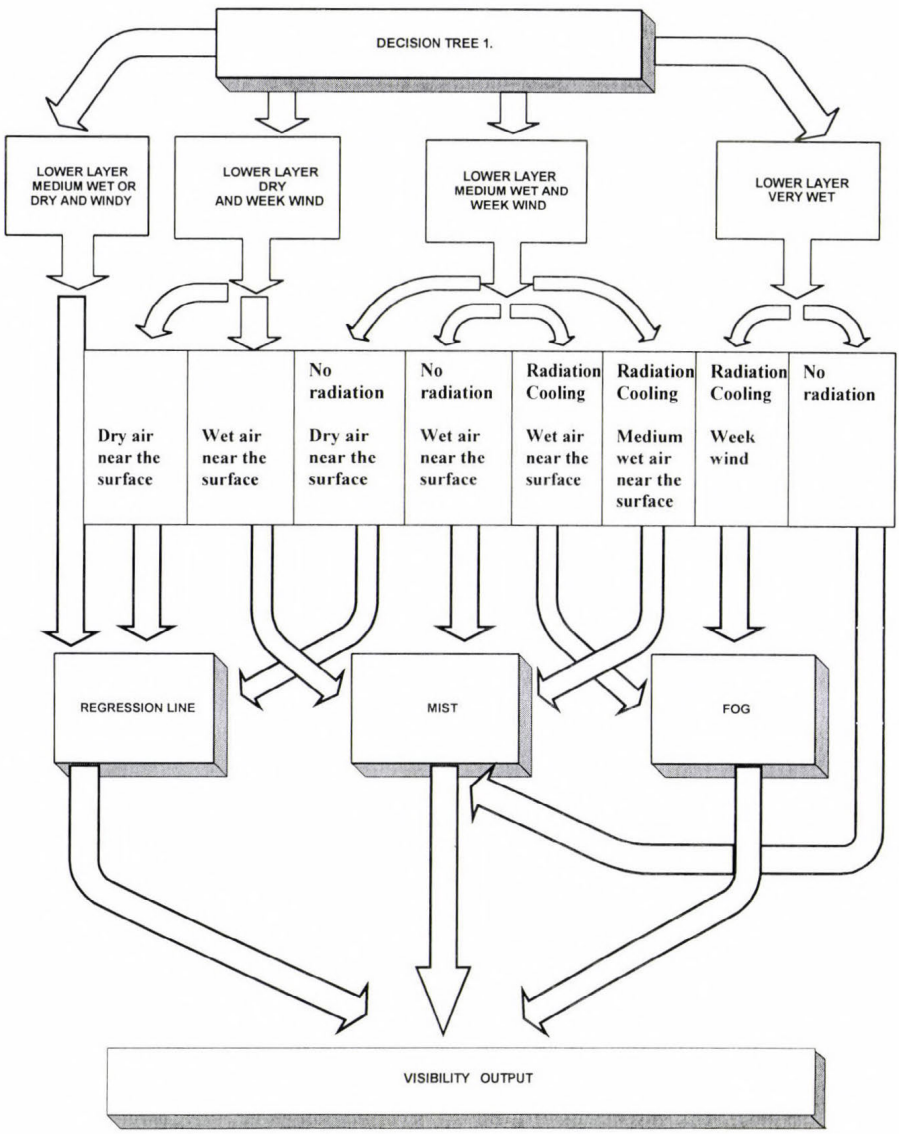

Fig. 4. Decision tree in case of normal stratification.

Suppose that the lowest layer of the air (between surface and 925 hPa) is dry or moderately wet and windy, then the visibility depends on the water content near the surface. In this case the process uses simply the regression line for determining the visibility. If the lowest layer is dry (relative humidity <80%) and the wind is weak, then the visibility depends on the water content of the air near the surface. If this layer is wet, then we choose mist, otherwise a good visibility category is selected. If the lowest layer is medium wet (80%< relative humidity <90%), then four subclasses are constructed. In these subclasses the radiative cooling effects of the atmosphere above a ground level point are represented. This influence is modeled as the difference of mean relative humidity between the upper and the lower layers as follows:

(1) If the air near the surface is dry and we do not include radiative cooling effect near the surface, then visibility can be calculated by the help of the regression line.
(2) If the air near the surface is wet and we have no radiative cooling influence in the air column, then the decision is the misty weather.
(3) If the air near the ground level is wet and we have radiative cooling effect, then fog formation is expected.
(4) If the air near the surface is medium wet and we include radiative cooling, misty weather is predicted.
(5) Finally, supposing that the air near the ground level is very wet (relative humidity >90%), then in case of radiative cooling we expect foggy, otherwise misty category.

For cold air pad situations similar decision tree was constructed. The main differences are in the values of the threshold numbers. If very high relative humidity and weak winds occur together, it will be foggy weather.

4. Test results

The test of diagnostic method presented in this paper led to the following results. *Fig. 5* illustrates the visibility at 00 UTC for each day of January in 1997, where JANAKTL means the measured, JANMODSZ the computed values. With regard to reliable visibility forecast, good estimation of the small values is especially important. As it is shown, under 5 km both lines give similar range of sight, even if the dotted line sometimes a little bit underestimates the real data, so it makes the prediction more safe, e.g., for aviation. For larger visibility values the difference is not so important.

The next two figures illustrate the correlations between measured and computed visibilities with (JANMODSZ in *Fig. 6*) and without (JANSSI *Fig. 7*) the use of decision tree procedure. High correlation (0.83) was reached with the

more developed method, as opposed to the low correlation (0.40) received applying only the simple FOGSI index (Eq. (4)). According to our experiences, the described decision tree procedure improves the results in all cases.

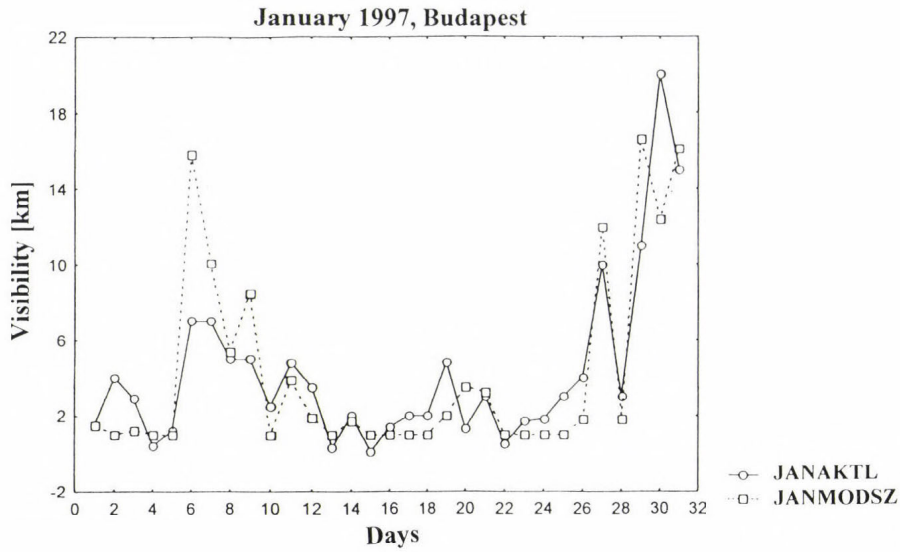

Fig. 5. Observed and diagnosed visibility.

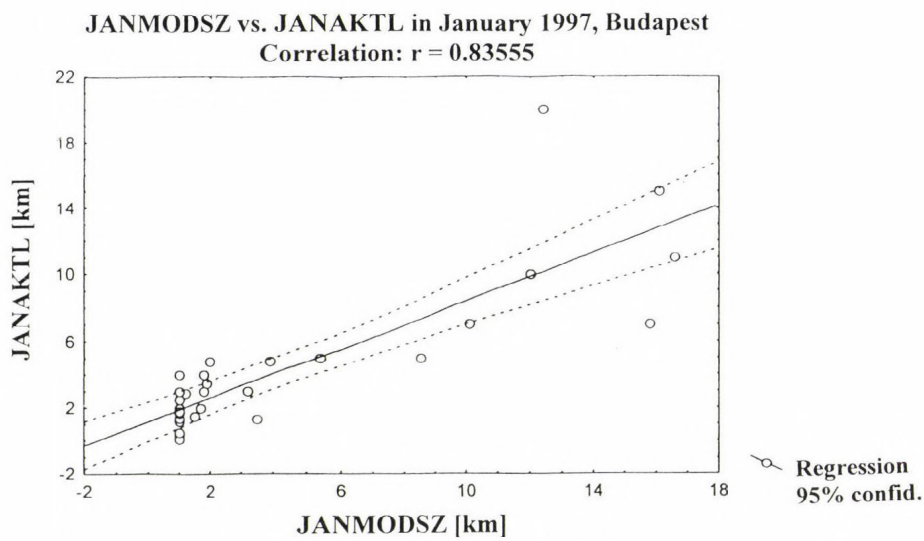

Fig. 6. Correlation between observed and calculated visibility using the decision tree.

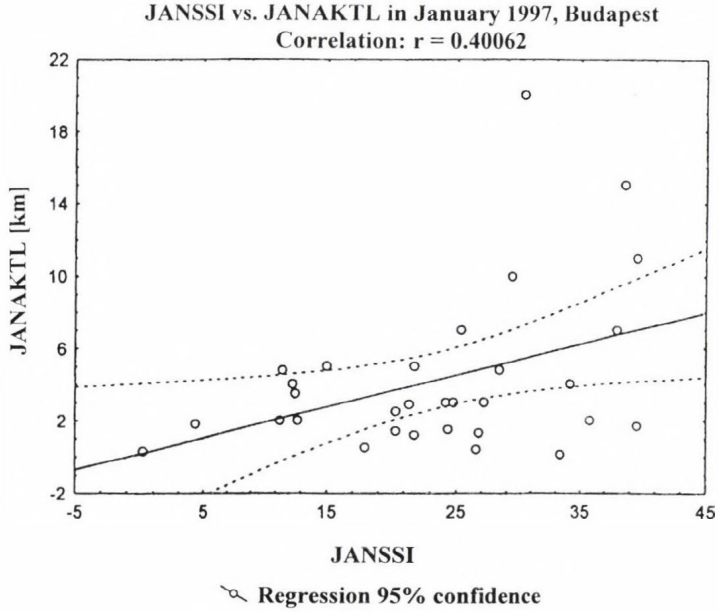

Fig. 7. Correlation between observed and diagnosed visibility.

An even more illustrative picture is presented in *Fig. 8*, where one can follow the hour by hour (continuos line) changes of real visibility compared to the 48-hour forecasts (columns). The run of observed and predicted visibility values is comparable to each other, although at some hours long shift might be detected. Regression coefficients were calculated based on the radiosounding data of Budapest and used for Szeged. It can be concluded, that Eq. (5) is adequate for most of the places of Hungary. A possible explanation is, that it is due to the relatively smooth surface of the country.

5. Conclusion

The described method is mainly used in aeronautical meteorology. After the test period this method was installed at the HMS Weather Forecasting and Aviation Meteorology Department. According to 3 years long experience, efficiency of the method strongly depends on the quality of the ALADIN model output near the ground level.

Another application area is nowcasting, where the application of the above outlined procedure for fog formation and dissipation, as well as the horizontal visibility led to significant improvements.

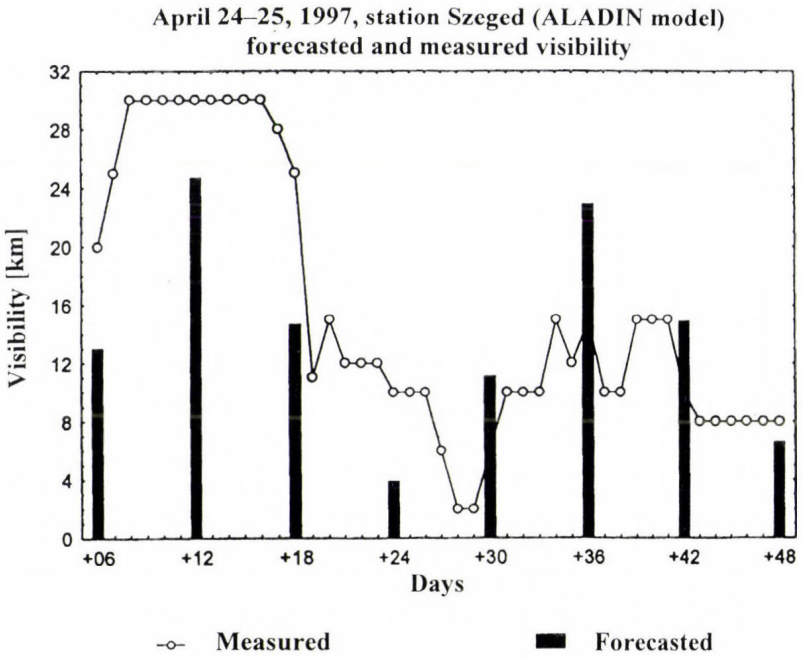

Fig. 8. Predicted and observed visibility in Szeged.

References

Bóna, M., 1986: Aerosynoptical research of cold air pad (in Hungarian). *Meteorológiai Tanulmányok*, No. 54, Országos Meteorológiai Szolgálat, Budapest.

Horányi, A., Ihász, I. and *Radnóti, G.*, 1996: ARPEGE/ALADIN: A numerical weather prediction model for Central-Europe with the participation of the Hungarian Meteorological Service. *Időjárás 100*, 277-301.

ICAO, 1998: *International Standards and Recommended Practices, Meteorological Service for International Air Navigation To the Convention on International Civil Aviation*. Thirteenth edition.

Kerényi, J., G. Szenyán, I., Putsay, M. and *Wantuch, F.*, 1995: Cloud detection on treshold technique for NOAA-AVHRR images for the Carpathian Basin. *Proc. of 1995 Meteorological Satellite Data Users' Conference*. Winchester, United Kingdom, 4-8 Sep 1995, 565-569.

Kilpinen, J., 1992: The application of Kalman filter in statistical interpretation of numerical weather forecasts. *12th Conference on Probability and Statistics in the Atmospheric Sciences*, June 22-26, 1992, Toronto, Ont., Canada, 11-16.

Pasini, A., Pelino, V. and *Potestà, S.*, 1999: A Neural Network model for visibility nowcasting from surface observations: results and sensitivity to physical input variables. Submitted to *Journal of Geophysical Research, D.*

Stessel, J.-P. and *Ottoy, H.*, 1999: Dense fog forecasting with an interactive expert. In *COST-78 Project II. 3, Final Report. Fog and Low Clouds: Statistical Methods and Decision Support Systems for Fog and Low Cloud Forecasting.*

Tóth, P., 1984.: Parameterization in the analysis of cold air pad forming and dissipation (in Hungarian). *Meteorológiai Tanulmányok*, No. 51. Országos Meteorológiai Szolgálat, Budapest.

IDŐJÁRÁS

Quarterly Journal of the Hungarian Meteorological Service
Vol. 105, No. 1, January–March 2001, pp. 39–58

Splitting method and its application in air pollution modeling

Ágnes Havasi[1], **Judit Bartholy**[1] and **István Faragó**[2]

[1]*Department of Meteorology, Eötvös Loránd University*
P.O. Box 32, H-1518 Budapest, Hungary
E-mails:hagi@nimbus.elte.hu; bari@nimbus.elte.hu

[2]*Department of Applied Analysis, Eötvös Loránd University,*
Kecskeméti u. 10, H-1053 Budapest, Hungary

(Manuscript received 1 August 2000; in final form 15 December 2000)

Abstract—The problems concerning the numerical solution of the chemistry-transport equations — the basis of all air pollution models — and the operator splitting procedure are discussed. The main aim of the paper is to clarify the mathematical background of operator splitting. The connection between Lie-algebra and the splitting procedure with its error (the so-called splitting error) is studied. Two important examples of the splitting technique are introduced (DEM splitting, physical splitting).

Key-words: air pollution problem, chemistry-transport equations, operator splitting, Lie-algebra.

1. Introduction

Nowadays air pollution is among the major environmental problems, especially in the developed industrial regions of the world. A considerable part of the total pollutant concentration emitted into the atmosphere is of anthropogenic origin. Recently atmospheric chemistry becomes one of the key disciplines of our understanding of air pollution and climatic processes. In 1995 Crutzen did win the Nobel Prize for chemistry for research results on this issue (*Crutzen* and *Zimmermann*, 1991; *Crutzen*, 1995; *Möller*, 1999). Approximately 20 billion tons of carbon-dioxide are discharged into the air every year solely due to the combustion of fossil fuels. Carbon-dioxide is the major anthropogenic greenhouse gas, therefore its increasing amount will probably lead to the warmth of the global climate in the forthcoming decades. Continuous monitoring of atmospheric CO_2 at Mauna Loa Observatory, Hawaii (*Keeling et al.,* 1989) indicates that the concentration of CO_2 gas has increased by about 26 percent over the pre-industrial level. With sophisticated climate model simulations we do have several climate

scenarios for the next 100 years, but on the base of some new findings by *Broecker* (1987) some are questionable. Hard to estimate the role of the ocean conveyor circulation (*Broecker*, 1991), but many evidences are available on its existence. Radiocarbon measurements of the GEOSECS programme imply that the conveyor circulation of the ocean could impact temporal changes in the $^{14}C/^{12}C$ ratio for atmospheric CO_2. Another important greenhouse gas is the tropospheric ozone, which is harmful not only to plants and animals, but also to human health. This gas is created from nitrogen-oxides and volatile organic compounds; all being dangerous toxic species. Another example is the discharge of toxic heavy metals (e.g., lead), which can get into the cycle of nutrients, so damaging the living organisms.

Reducing the emissions of the air pollutants is an important task, which requires international efforts (*Houghton*, 1995), since the high concentration values are not limited to the areas where the emission sources are located. First of all it is necessary to determine those critical concentration values, which should not be exceeded. The critical level for a given pollutant is the highest concentration value that will not cause damage to biological systems. (It is not reasonable to reduce the concentrations too much below critical levels, because the extra efforts may be very expensive and could cause economical difficulties.) Taking into account the critical levels, we have to work out control strategies on exactly where and how to reduce the emissions.

In the solution of the problem sketched above, the most efficient tools are the so-called chemistry-transport models. The development of such models is necessarily an intensive procedure requiring sensitivity studies of model components as well as validation against observations. The models are based on the mass conservation law, which is expressed in the form of a system of partial differential equations: the so-called (chemistry-)transport equations. To find the analytical solution of these equations is practically impossible, therefore we use some numerical method. However, the numerical treatment of the global problem is rather complicated. (Approximations of differential operators of different types, huge coupled discretized systems, etc.) That is why we apply a decoupling procedure, the so-called splitting technique. The point of this method is as follows. The original system of differential equations describes different processes (e.g., advection diffusion, etc.) that act simultaneously in the atmosphere. We replace this model with one in which appropriately chosen groups of these processes take place successively in time. This allows us to solve a few simpler systems instead of the whole one. However, the application of operator splitting usually implies some error, the so-called splitting error. The mathematical background of this error has not yet been completely clarified. The main aim of the paper is to introduce the technique of operator splitting and make clear both the background and the role of the splitting error.

In this article first we discuss the basic questions concerning the numerical treatment of the chemistry-transport equations. In Chapter 2 we introduce the

two basic approaches that can be applied in the numerical solution of this system: the Eulerian and the Lagrangian approach. In Chapter 3 we consider the basic questions related to the numerical solution of partial differential equations in general. In Chapter 4 we point out that some of the arising difficulties can be avoided by applying the useful technique of operator splitting. In the last three chapters we clarify the mathematical background and the role of operator splitting. First we investigate the splitting procedure on the simple problem of linear, constant coefficient systems. In Chapter 5 we move on to the more general case of linear operators. Here we describe the connection between Lie-algebras and Lie-groups, which serves as the mathematical background of operator splitting. Finally, in Chapter 7 we deal with the non-linear case, which, by the use of the Lie-operator formalism, leads back to the results of the previous chapter. Also, we formulate some conditions under which the splitting error vanishes.

2. The transport equations

Atmospheric transport of air pollutants is, in principle, a well-understood process (*Trenberth,* 1992). Assume that the concentration changes of m different chemical species are to be studied. Let $\mathbf{c}$ denote the vector in $\mathbf{R}^m$ containing the m concentration values. (In general, $\mathbf{c}$ may vary in space and time, so $\mathbf{c} = \mathbf{c}(\mathbf{x},t)$). If $\mathbf{u} = \mathbf{u}(\mathbf{x},t)$ denotes the three-dimension velocity vector, and c is the concentration of any of the m species then the changes of c can be described mathematically by the partial differential equation (PDE)

$$\frac{\partial c}{\partial t} + \nabla(\mathbf{u}c) = \nabla(\mathbf{K}\nabla c) + R(\mathbf{x},\mathbf{c}) + E + \sigma c \tag{1}$$

with the corresponding initial and boundary conditions. The m equations are coupled through the function $R(\mathbf{x},\mathbf{c})$ and so form a system of PDE's.

The different terms in the system (1) have the following physical meaning:

- The second term on the left-hand side describes the transportation due to the velocity field and is called the advection term. Advection transport plays an important role in the evolution of air pollutants and therefore appears in almost all air pollution models.
- The first term on the right-hand side expresses the turbulent diffusion. Here $\mathbf{K} = \mathbf{K}(\mathbf{x},t)$ is the so-called diffusion coefficient matrix.
- Term $R(\mathbf{x},\mathbf{c})$ represents the chemical reactions that take place during the atmospheric transport of the pollutants. The reactions included in air pollution models are usually of first and second order; in the latter case the vector function R is quadratically non-linear. The coefficients of the linear and the quadratic chemical terms express the rate at which the reactions proceed. The rates

of the different reactions can vary by several orders of magnitude, therefore the lifetime of the species can range from microseconds (e.g., hydrogen atoms) to centuries (e.g., nitrous oxide molecules).

- Term E expresses the emission, that is the discharge of the pollutants into the air either by natural (e.g., volcanic eruption of forest fires) or anthropogenic sources (e.g., urban traffic or combustion of fossil fuels).
- Finally, the residual σc term describes the deposition process, that is the removal of the pollutant particles from the air. We distinguish two basic types of deposition: wet and dry deposition. Wet deposition — or in other words precipitation scavenging — means removal of the particles by any kind of falling precipitation. Dry deposition includes gravitational sedimentation (particularly efficient for large particles), impaction on vegetation and absorption or reaction processes on the surface of the earth.

The above system of PDE's will simply be referred to as chemistry-transport (or simply transport) equations in the sequel (*Zlatev*, 1995). If we were able to solve the system (1) analytically, we could forecast the spatial and temporal changes of the continuous concentration fields. However, to find the analytical solution is practically impossible, unless some very unrealistic assumptions are made. The system is so complicated that we cannot even guarantee the existence of the unique solution, except in very special cases. The major difficulties are the following: (1) the reaction term $R(\mathbf{c})$ is usually non-linear; (2) the coefficients $\mathbf{u}$, $\mathbf{K}$ and σ are not constant and not necessarily continuous. Therefore in the sequel we assume the existence of the unique solution, which is a reasonable assumption because the model adequately describes the physics of air pollution transport. In the absence of any tools to obtain the analytical solution, the system must be treated numerically.

There are two main approaches that can be applied in the numerical treatment of the system (1). The first one is the so-called Eulerian approach, which is based on the following conception. A grid is defined on the space domain of interest, and the spatial derivatives in the system are discretized over the grid. As a result of the spatial discretization, we obtain an ordinary differential equation (ODE) at each gridpoint P_i (and for each chemical species) for the unknown time-depending function $c_d^i(t)$ approximating the concentration at the given point. (This procedure is called semi-discretization.) The obtained system of ODE's with the corresponding initial values is then solved numerically.

In the other approach — the so-called Lagrangian approach — the system of PDE's is simplified to a system of ODE's in the following way. Let us suppose that the wind components $u(x,y,t)$ and $v(x,y,t)$ are known, neglect the third velocity component w and consider a pollutant parcel in the spatial point (x_0,y_0) at time t. It is assumed that there is no diffusion, and the parcel as one piece is transported by the wind. This allows us to reduce the dimension of the problem. The trajectory of the parcel can be determined by solving the

$$\frac{dx}{dt} = u(t), \quad x(0) = x_0, \qquad \frac{dy}{dt} = v(t), \quad y(0) = y_0 \tag{2}$$

initial value problem. Our aim is to describe the concentration changes of the parcel along the trajectory. The concentration is influenced by chemical reactions, emission and deposition taking place along the trajectory. So the system

$$\frac{dc}{dt} = R(\mathbf{x},\mathbf{c}) + E(x(t), y(t), t) + \sigma c(x(t), y(t), t) \tag{3}$$

with the known functions $x(t)$, $y(t)$ is to be solved, which is a system of ODE's with the unknown function c depending only on time now. In practice, the system of Eqs. (2) and (3) can be solved numerically for example in the following steps:

- we discretize the time interval [0,T] using some Δt timestep,
- we solve the system (2) applying some numerical method (usually of Runge–Kutta type), and
- along the trajectory that we obtained numerically in the previous step, we solve the system (3).

In the solution of the two systems we should work with matching timesteps. We remark that the numerical method is not usually the same in the two cases. The system (2) is of very simple type, and it can even be solved by an explicit method. However, the system (3) is a so-called stiff system (because of the nonlinear $R(\mathbf{x},\mathbf{c})$ term), which means that stability may impose a restriction to the choice of the timestep. In the case of a stiff system, we should apply a so-called A-stable method, which allows us to choose an arbitrary timestep, that is in the choice of the timestep only accuracy and not stability accounts.

Both kinds of modeling have advantages as well as disadvantages. The main benefit of the Eulerian models is the use of the original equations describing all important physical processes that take place during the air pollution transport. Eulerian models perform better than Lagrangian ones

- if there are many emission sources;
- if all chemical reactions are taken into account during the transport; and
- if the air pollution transport is considered on a long time-scale.

However, running an Eulerian model is usually very expensive because of the high resolution. In addition to this, Eulerian models have problems with a strong single source resulting in sharp concentration gradients. An example of an Eulerian model is MEDIA, which was developed at the French Weather Service in 1990 and has been used operationally since 1998 at the Hungarian Meteorological Service (HMS) as well. The model was first validated on the Chernobyl re-

lease (*Piedelievre et al.,* 1990) and was successfully used among others in the case of the Algeciras nuclear accident (Spain) in May, 1998.

On short-scale and in the case of a single source, the use of a Lagrangian model is usually more advantageous. The system of ODE's obtained along the trajectories is easier to treat numerically than the original system of PDE's. Due to the simple conception, the results of a Lagrangian model are easier to interpret. These models are good for experimental purposes and they are especially useful when the origin of the pollutant is to be determined. To this end so-called backward trajectories are calculated, that is the pathway of the pollutant parcel is computed backward in time. A report on the application of a Lagrangian model can be found in *Eliassen et al.* (1982), where a Norwegian case study is analysed, and it is pointed out that the high Scandinavian ozone levels are not due to Scandinavian sources but probably to emissins of primary pollutants in Eastern Europe. For other applications of Lagrangian models see also *Olson et al.* (1992) and *Simpson* (1992, 1993).

The major disadvantage of Lagrangian models is the low accuracy, especially distant to the source, because of the ignorance of the diffusion and the exponential increase of errors in the trajectory calculations. In some situations the combination of a Lagrangian and an Eulerian model may be the best choice, e.g., when the long-range transport of pollutants discharged by a sharp single source (such as an accidental release from a nuclear power plant) is to be studied. In this case it is advisable to apply a Lagrangian model near the source, but from a certain distance it is better to switch over to an Eulerian one. A critical point of this procedure is the coupling of the two models at the boundary of the Lagrangian and the Eulerian domain (*Brandt et al.*, 1998).

The numerical treatment of the system of PDE's (1) is not a simple problem. In the next chapter we consider the main aspects of selecting a proper numerical method for solving the system (1).

3. Numerical solution of the transport equations

The numerical solution of the system of PDE's (1) is based on defining a mesh sequence on the domain of the system. Discretization of the model equations over the meshes leads to a discrete model sequence. We determine a numerical solution on each mesh. It is also necessary to define a measure (or norm) of the elements on each mesh, which can be, for example, the maximum of the grid-point values or the square sum. Of course, when realising the numerical method, we cannot work with the infinite mesh sequence, but we stop after a finite number of steps. (We use a so-called stopping criterion. For example we stop when the difference between the numerical solutions following one another is sufficiently small. For details see *Marchuk* (1980) and *Thomée* (1990)). In the fol-

lowing we turn our attention to the questions concerning the numerical solution obtained as above.

• **Efficiency.** The discretization of the system leads to a huge computational problem, especially in the case of Eulerian models. Therefore it is crucial to perform efficiently the most time-consuming calculations in the numerical solution.

• **Consistency.** The exact solution of the continuous model does not usually satisfy the discrete model equations. We introduce the notion of the local error to measure how well the exact solution satisfies the numerical model. The local error of one discrete model in the model sequence is the quantity obtained by substituting the exact solution into the discrete model. The method is called consistent if the local error in the discrete model sequence tends to zero, that is in limit the exact solution satisfies the discrete model.

• **Stability.** We expect the numerical method to be stable, which means that for all input data the numerical solution in absolute value remains under a bound. This is important because the input data usually come from measurements and go through some data-processing procedures (e.g., interpolation on the grid) and, therefore, unavoidably contain errors. In the case of certain methods, a relation between the spatial and the temporal stepsize (a so-called stability criterion) has to be fulfilled so that the method is stable. In practice this means a limitation for the choice of the timestep-size at a given spatial stepsize. It is most advantageous if the method is unconditionally stable, i.e., there is no restriction for stability. We remark that the notion of stability is norm-dependent.

• **Convergence.** The approximation is called convergent if the difference between the exact and the numerical solution in the discrete model sequence (the so-called global error) tends to zero. Convergence is closely related to stability according to Lax's equivalence theory, which roughly says that in the case of consistency stability is a necessary and sufficient condition for convergence.
Obviously, the speed of the convergence is also of great importance, since in practice the timestep-size cannot be chosen to be arbitrarily small.

• **Preservation of main qualitative properties.** Some methods satisfy all the above requirements, however, the numerical solution is not acceptable, because it does not preserve some basic qualitative property of the exact solution. Suppose that the numerical solution is convergent, and the exact solution at a given point is a small positive concentration value. It can happen that though the numerical solution tends to this positive value, in the case of the given mesh it gives a negative value at this point. This should be avoided because (1) negative concentration values have no physical meaning, and (2) the physically impossible values can cause difficulties when these are used as input data in another model.

A further important qualitative property is the preservation of the shape of the exact solution (e.g., convexity, monotonicity). From a physical point of view, an especially important qualitative property is mass conservation. The transport equations express a fundamental physical law: the local change of the concentration at a point is equal to the amount that is transported to that point by

different transport processes. However, this physical principle can be broken when the continuous equations are discretized, which leads to unrealistic results. Stability in an arbitrary norm is not usually sufficient for the preservation of the above properties, but roughly speaking, stability in the maximum norm is already enough in most cases.

We remark that though so far we have focused on the qualitative properties of the exact solution of the continuous model, the ultimate aim of modeling is to describe the behaviour of a physical system. In some cases the exact solution of the continuous model does not reflect the real behaviour of the physical system. For example, the analytical solution of the heat equation results in an infinite velocity of heat, which contradicts any experience. However, certain numerical methods do not have this bad property, so the numerical solution may even improve the continuous model. (More details for a special heat equation can be found in *Faragó et al.* (1993)).

The above requirements are natural, and it is highly desirable to satisfy all of them simultaneously when solving numerically the transport equations. However, this is not a simple task. Since the terms on the right-hand side have different properties, the system is too complicated and theoretical results are not applicable. Therefore, it is impossible to satisfy all the requirements simultaneously, if we apply direct approximation to the system. A possible approach to the solution of this problem is operator splitting, which will be introduced in the next chapter.

4. Operator splitting

Operator or time splitting is commonly used in air pollution modeling. The basic idea behind this procedure is dividing the spatial differential operator of the system (1) into a few simpler operators, and solving the corresponding systems — which are connected to each other through the suitable initial conditions — successively in each timestep (*Marchuk,* 1988; *Yanenko,* 1962; *Lanser* and *Verwer*, 1999).

Operator splitting is usually applied according to the different physical processes involved in the model. As an example, we introduce the splitting procedure of the Danish Eulerian Model (DEM). In this long-range air pollution model, the splitted sub-systems describe the horizontal advection (Eq. (4)), the horizontal diffusion (Eq. (5)), the chemical reactions with the emission (Eq. (6)), the deposition (Eq. (7)) and the vertical exchange (Eq. (8)).

$$\frac{\partial c^{(1)}}{\partial t} = -\frac{\partial (uc^{(1)})}{\partial x} - \frac{\partial (vc^{(1)})}{\partial y} \tag{4}$$

$$\frac{\partial c^{(2)}}{\partial t} = \frac{\partial}{\partial x}\left(k_1 \frac{\partial c^{(2)}}{\partial x}\right) + \frac{\partial}{\partial y}\left(k_2 \frac{\partial c^{(2)}}{\partial y}\right) \tag{5}$$

$$\frac{\partial c^{(3)}}{\partial t} = E + R(\mathbf{c}^{(3)}) \tag{6}$$

$$\frac{\partial c^{(4)}}{\partial t} = \sigma c^{(4)} \tag{7}$$

$$\frac{\partial c^{(5)}}{\partial t} = -\frac{\partial (w c^{(5)})}{\partial z} + \frac{\partial}{\partial z}\left(k_3 \frac{\partial c^{(5)}}{\partial z}\right). \tag{8}$$

In the above splitting procedure, the original system of PDE's has been split into five simpler systems, which are to be solved in each timestep one after the other in the following way. Assume that some approximation to the concentration vector **c** at time t has been found. The first system is solved by using this vector as a starting vector. The obtained solution will serve as the initial vector in the treatment of the second system and so on. The solution of the fifth system is accepted as an approximation to the concentration vector at the end of the timestep.

Operator splitting has several advantages:

- The splitted sub-systems are easier to treat numerically than the original system.
- We can exploit the special properties of the different sub-systems and apply the most suitable method for each.
- If each method is stable and preserves the main qualitative properties then so does the global model.

It is obvious that this kind of de-coupling procedure may cause inaccuracy in the solution. This is called splitting error, which will be described in more details in the next chapters.

5. Investigation of splitting method on a simple problem

First let us consider the simple linear, constant coefficient system

$$\frac{d\mathbf{w}}{dt} = \mathbf{A}\mathbf{w}(t) + \mathbf{B}\mathbf{w}(t) \tag{9}$$

with the initial condition

$$\mathbf{w}(0) = \mathbf{w}_0,$$

where $\mathbf{w}$: $\mathbf{R} \rightarrow \mathbf{R}^n$ is the unknown vector function, and $\mathbf{A}$ and $\mathbf{B}$ are matrices of type $\mathbf{R}^{n \times n}$. The exact solution of the above initial value problem at a time τ is

$$\mathbf{w}(\tau) = e^{(\mathbf{A}+\mathbf{B})\tau}\mathbf{w}_0. \tag{10}$$

Now let us split the problem into the following two simpler problems:

$$\left.\begin{aligned} \frac{d\mathbf{w}^{(1)}}{dt} &= \mathbf{A}\mathbf{w}^{(1)}(t) \\ \mathbf{w}^{(1)}(0) &= \mathbf{w}_0 \end{aligned}\right\} \tag{11}$$

and

$$\left.\begin{aligned} \frac{d\mathbf{w}^{(2)}}{dt} &= \mathbf{B}\mathbf{w}^{(2)}(t) \\ \mathbf{w}^{(2)}(0) &= \mathbf{w}^{(1)}(\tau) \end{aligned}\right\}. \tag{12}$$

The solution of the first system at time τ is

$$\mathbf{w}^{(1)}(\tau) = e^{\mathbf{A}\tau}\mathbf{w}_0\,, \tag{13}$$

which is applied as the initial value for the second system. So the exact solution of the splitted problem at time τ is

$$\mathbf{w}_{Sp}(\tau) = \mathbf{w}^{(2)}(\tau) = e^{\mathbf{B}\tau}e^{\mathbf{A}\tau}\mathbf{w}_0\,. \tag{14}$$

The splitting error is defined as the difference between (10) and (14), that is

$$Err_{Sp} := \mathbf{w}(\tau) - \mathbf{w}_{Sp}(\tau) = e^{(\mathbf{A}+\mathbf{B})\tau}\mathbf{w}_0 - e^{\mathbf{B}\tau}e^{\mathbf{A}\tau}\mathbf{w}_0\,. \tag{15}$$

Clearly, for any initial vector, the splitting error is zero if and only if the equality

$$e^{(\mathbf{A}+\mathbf{B})\tau} = e^{\mathbf{B}\tau}e^{\mathbf{A}\tau} \tag{16}$$

holds. Let us compare the two sides. According to the definition of the matrix exponential

$$e^{(\mathbf{A}+\mathbf{B})\tau} = \mathbf{I} + (\mathbf{A}+\mathbf{B})\tau + \frac{1}{2!}(\mathbf{A}+\mathbf{B})^2\tau^2 + o(\tau^3) =$$

$$= \mathbf{I} + (\mathbf{A}+\mathbf{B})\tau + \frac{1}{2!}(\mathbf{A}^2+\mathbf{B}^2)\tau^2 + \frac{1}{2!}(\mathbf{AB})\tau^2 + \frac{1}{2!}(\mathbf{BA})\tau^2 + o(\tau^3) \tag{17}$$

and

$$e^{\mathbf{B}\tau}e^{\mathbf{A}\tau} = (\mathbf{I} + \mathbf{B}\tau + \frac{1}{2!}\mathbf{B}^2\tau^2 + o(\tau^3))(\mathbf{I} + \mathbf{A}\tau + \frac{1}{2!}\mathbf{A}^2\tau^2 + o(\tau^3)) =$$

$$= \mathbf{I} + \mathbf{A}\tau + \frac{1}{2!}\mathbf{A}^2\tau^2 + \mathbf{B}\tau + \mathbf{BA}\tau^2 + \frac{1}{2!}\mathbf{B}^2\tau^2 + o(\tau^3) =$$

$$= \mathbf{I} + (\mathbf{A} + \mathbf{B})\tau + \frac{1}{2!}(\mathbf{A}^2 + \mathbf{B}^2)\tau^2 + \mathbf{BA}\tau^2 + o(\tau^3). \tag{18}$$

It is seen that the terms of order $o(\tau^2)$ in the expression of the error vanish if

$$\frac{1}{2}\mathbf{AB} + \frac{1}{2}\mathbf{BA} = \mathbf{BA},$$

that is if

$$\mathbf{AB} = \mathbf{BA},$$

or in other words, the matrices **A** and **B** commute. It is easy to see that in case the matrices **A** and **B** do not commute, then the splitting error is of $o(\tau^2)$. Furthermore, provided that the matrices commute, the difference resulting from the higher order terms in Eqs. (17) and (18) also turns into zero, that is there is no splitting error. The proof of this assertion will be given for the more general case of linear operators in the following chapter.

6. Splitting for linear operators

In the remaining two chapters we will consider operators of type S $\rightarrow$ S, where S is a normed space of functions. In this space we can define the composition in the usual sense, that is for any $\mathbf{C}_1$, $\mathbf{C}_2$: S$\rightarrow$S $(\mathbf{C}_1 \circ \mathbf{C}_2)(x)$ means $\mathbf{C}_1(\mathbf{C}_2(x))$. First we have to introduce the notion of the operator exponential, since it will play an important role in our investigations. Let **C** be an operator mapping from S to S. Suppose that the series

$$\mathbf{I}(x) + \frac{1}{1!}\mathbf{C}(x) + \frac{1}{2!}(\mathbf{C} \circ \mathbf{C})(x) + \frac{1}{3!}(\mathbf{C} \circ \mathbf{C} \circ \mathbf{C})(x) + \cdots \tag{19}$$

is convergent to an element $x^* \in$ S for all $x \in$ H $\subset$ D(**C**). (Here the letter I stands for the identity operator of type S$\rightarrow$S.)

Definition: The operator $e^{\mathbf{C}}$: $x \rightarrow x^*$, D($e^{\mathbf{C}}$):= H is called the exponential of the operator **C**.

In this chapter we restrict our attention to linear problems, that is we consider the system

$$\frac{d\mathbf{w}}{dt} = \mathbf{L}_1\mathbf{w}(t) + \mathbf{L}_2\mathbf{w}(t) \tag{20}$$

with the initial condition

$$\mathbf{w}(0) = \mathbf{w}_0.$$

Here $\mathbf{w} \in S$ is the unknown function, and $\mathbf{L}_1$, $\mathbf{L}_2$ on the right-hand side denote two linear operators of type S→S. The splitted subproblems have the form

$$\left.\begin{aligned} \frac{d\mathbf{w}^{(1)}}{dt} &= \mathbf{L}_1\mathbf{w}^{(1)}(t) \\ \mathbf{w}^{(1)}(0) &= \mathbf{w}_0 \end{aligned}\right\} \tag{21}$$

and

$$\left.\begin{aligned} \frac{d\mathbf{w}^{(2)}}{dt} &= \mathbf{L}_2\mathbf{w}^{(2)}(t) \\ \mathbf{w}^{(2)}(0) &= \mathbf{w}^{(1)}(\tau) \end{aligned}\right\}. \tag{22}$$

As we mentioned before, we assume that both the original problem and the splitted subproblems have a unique solution. It is known (see for example *Engel* and *Nagel* (2000)) that in this case the solution can be given again with the help of exponentials. Namely, the solution of the first splitted subsystem at time τ is

$$\mathbf{w}^{(1)}(\tau) = e^{\mathbf{L}_1\tau}\mathbf{w}_0, \tag{23}$$

and the exact solution of the whole splitted problem at time τ has the form

$$\mathbf{w}_{Sp}(\tau) = \mathbf{w}^{(2)}(\tau) = e^{\mathbf{L}_2\tau}\, e^{\mathbf{L}_1\tau}\mathbf{w}_0. \tag{24}$$

It is seen that the error of the splitting procedure is related to the difference between the expressions $e^{\mathbf{L}_2\tau}\, e^{\mathbf{L}_1\tau}$ and $e^{(\mathbf{L}_1+\mathbf{L}_2)\tau}$, similarly to the case of the matrices. The splitting error vanishes for all initial functions $\mathbf{w}_0$ if and only if $e^{\mathbf{L}_2\tau}\, e^{\mathbf{L}_1\tau} = e^{(\mathbf{L}_1+\mathbf{L}_2)\tau}$. This equality expresses that the product of $e^{\mathbf{L}_2\tau}$ and $e^{\mathbf{L}_1\tau}$ can be obtained by applying the exponential function to the sum $\mathbf{L}_1\tau + \mathbf{L}_2\tau$. The following questions arise naturally:

(1) What is the condition of the equality?

(2) If the equality does not hold, then, instead of the exponential function, what kind of function (if such exists) connects the product and the sum?

To formulate this connection, we will need the notions of Lie-algebra and Lie-group. Let $(V, +, \cdot)$ be a vector space (in the usual sense) and $[\cdot, \cdot]: V \times V \to V$ an additional operation called commutation with the following properties:

(1) $[\lambda_1 X_1 + \lambda_2 X_2, Y] = [\lambda_1 X_1, Y] + [\lambda_2 X_2, Y]$,

(2) $[X, Y] = -[Y, X]$,

(3) $[X,[Y,Z]] + [Y,[Z,X]] + [Z,[X,Y]] = 0$

for all X, X_1, X_2, Y, Y_1, Y_2 and $Z \in V$. The first property is called bilinearity, the second one is the scew-symmetry and the third one is the so-called Jacobi-identity. $[X, Y]$ is called the commutator of the elements X and Y.

It is easy to check that provided a natural product $(X, Y) \to Y$ exists between the elements of the vector space V, then with the operation

$$[X, Y] := XY - YX, \quad X, Y \in V$$

the vector space V forms a Lie-algebra. Particularly, if V is identified with a function space, then we can define this natural product of X and Y in V as the function composition $X \circ Y$. Therefore, the operation

$$[X, Y] := X \circ Y - Y \circ X$$

determines a Lie-algebra.

In the case when a natural product exists on the vector space V, we can define the exponentials of the elements of V. Let L denote the exponentials of those elements of V, for which their exponential exists. Let us provide this set of exponentials with an appropriate product between the elements to obtain a group L. If $V \equiv \mathrm{Hom}(S)$ (linear operators of type $S \to S$), then the exponentials of the elements are operators of type $S \to S$, and the composition of these exponential operators is a group product. It is important that in our case the vector space Hom(S) with the induced operator norm is topological (because it is a normed space), therefore the above group of exponentials forms a so-called Lie-group. The connection between a Lie-algebra and its Lie-group is expressed by the following theorem (see *Varadarajan*, 1974).

Theorem. (Baker–Campbell–Hausdorff-formula) Let $(V, [\cdot, \cdot])$ be a Lie-algebra, and L its Lie-group. Then for all X and Y in V and for any scalar t the product of e^{Xt} and $e^{Yt} \in L$ can be given in the form

$$e^{Xt} e^{Yt} = e^{\sum_{n=0}^{\infty} t^n c_n(X,Y)}, \tag{25}$$

where the functions $c_n(X,Y)$: $V \times V \to V$, $n = 1, 2, \ldots$ are obtained recursively as follows:

$$c_0(X,Y) = 0,$$

$$c_1(X,Y) = X + Y,$$

$$(n+1)\, c_{n+1}(X,Y) = \frac{1}{2}[X - Y, c_n(X,Y)]$$
$$+ \sum_{p \geq 1,\, 2p \leq n} K_{2p} \sum_{\substack{k_1, \ldots, k_{2p} > 0 \\ k_1 + \cdots + k_{2p} = n}} [c_{k_1}(X,Y), [\ldots [c_{k_{2p}}(X,Y), X + Y] \ldots]],$$

where $k_1, \ldots, k_{2p}$ are natural numbers, and $K_2, \ldots, K_{2p}$ are given constants. We remark that the coefficients $c_0(X,Y)$ and $c_1(X,Y)$ can be easily obtained by direct comparison of the series

$$e^{Xt} e^{Yt} = \left(I + Xt + \frac{1}{2!} X^2 t^2 + \ldots\right)\left(I + Yt + \frac{1}{2!} Y^2 t^2 + \ldots\right) = I + (X+Y)t + \ldots$$

and

$$e^{\sum_{n=0}^{\infty} t^n c_n(X,Y)} = I + \left(c_0 + c_1 t + \frac{1}{2!} c_2 t^2 + \ldots\right) + \frac{1}{2!}\left(c_0 + c_1 t + \ldots\right) + \ldots$$

We seek the condition of the equality

$$e^{Xt} e^{Yt} = e^{(X+Y)t}. \tag{26}$$

Comparing the right-hand sides of Eq. (25) and Eq. (26) we see that Eq. (26) holds if and only if $c_i(X,Y) = 0$ for all $i \geq 2$.

Substituting $n = 1$ into the recursive formula we obtain that

$$c_2(X,Y) = \frac{1}{2}[X,Y],$$

which means that

$$[X,Y] = 0 \tag{27}$$

is a necessary condition of the equality (26). Substituting greater values of n we see that if Eq. (27) holds then the coefficients $c_3(X,Y)$, $c_4(X,Y)$, etc., of the higher order terms also turn into zero. So, the equality (26) holds if and only if $[X,Y] = 0$.

This result is directly applicable to the splitting problem Eqs. (20) to (22), as follows. Let $V \equiv \mathrm{Hom}(S)$, and let us define the commutator of $\mathbf{L}_1$ and $\mathbf{L}_2$ in S as

$$[\mathbf{L}_1,\mathbf{L}_2] := \mathbf{L}_1 \circ \mathbf{L}_2 - \mathbf{L}_2 \circ \mathbf{L}_1.$$

In such a way we have obtained a Lie-algebra over the topological (normed) vector space Hom(S). As we pointed out earlier, the splitting error vanishes if and only if

$$e^{\mathbf{L}_2\tau}\, e^{\mathbf{L}_1\tau} = e^{(\mathbf{L}_1+\mathbf{L}_2)\tau}. \tag{28}$$

The expression on the right-hand side is the composition of the exponentials of $\mathbf{L}_2\tau \in \mathrm{Hom}(S)$ and $\mathbf{L}_1\tau \in \mathrm{Hom}(S)$. The set of the exponentials of the elements in Hom(S) provided with the composition operation forms a Lie-group. Therefore, according to our previous considerations, the equality (28) holds if and only if

$$[\mathbf{L}_1, \mathbf{L}_2] = 0,$$

which yields that the splitting error vanishes if and only if

$$\mathbf{L}_1 \circ \mathbf{L}_2 = \mathbf{L}_2 \circ \mathbf{L}_1.$$

7. Splitting for non-linear operators

In the general non-linear case the splitting error is related to the notion of L-commutativity. Let **F** and **G**: S→S be usually non-linear differentiable mappings. We define the operator $\mathbf{E}_{F,G}$: S→S as follows:

$$\mathbf{E}_{F,G}(s) := (\mathbf{G}'(s) \circ \mathbf{F})(s) - (\mathbf{F}'(s) \circ \mathbf{G})(s), \tag{29}$$

where ' refers to the derivative. (The operators **F**'(s) and **G**'(s) are in Lin(S), where Lin(S) denotes the space of continuous linear operators of type S→S.)

Definition: The operator $\mathbf{E}_{F,G}$ is called the commutator of the mappings **F** and **G**.

Definition: We say that the operators **F** and **G** L-commute if their commutator is zero, that is if $\mathbf{E}_{F,G} = 0$.

In the following we will show the connection between the L-commutativity and the splitting error with the help of the so-called Lie operator formalism.

Let us consider the general non-linear problem

$$\frac{\partial \mathbf{c}}{\partial t}(\mathbf{x},t) = \mathbf{F}(\mathbf{c}(\mathbf{x},t)), \tag{30}$$

where $\mathbf{c}(\mathbf{x},t)$ is vector-valued in $\mathbf{R}^m$, and $\mathbf{F}$ represents a usually non-linear operator. As before, we assume that the system has a unique solution $\mathbf{c}(\mathbf{x},t)$ and it is an analytical function. Then the Taylor-series expansion of the solution according to the variable t reads

$$\mathbf{c}(\mathbf{x},t+\tau) = \mathbf{c}(\mathbf{x},t) + \tau\frac{\partial \mathbf{c}}{\partial \mathbf{t}}(\mathbf{x},t) + \tau^2\frac{1}{2!}\frac{\partial^2 \mathbf{c}}{\partial t^2}(\mathbf{x},t) + \ldots + \tau^k\frac{1}{k!}\frac{\partial^k \mathbf{c}}{\partial t^k}(\mathbf{x},t) + \ldots \tag{31}$$

Substituting Eq. (30) into Eq. (31) we get the relation

$$\mathbf{c}(\mathbf{x},t+\tau) = \mathbf{c}(\mathbf{x},t) + \tau\mathbf{F}(\mathbf{c}(\mathbf{x},t)) + \tau^2\frac{1}{2!}\frac{\partial}{\partial t}\mathbf{F}(\mathbf{c}(\mathbf{x},t)) + \ldots + \tau^k\frac{1}{k!}\frac{\partial^{k-1}}{\partial \mathrm{t}^{k-1}}\mathbf{F}(\mathbf{c}(\mathbf{x},t)) + \ldots \tag{32}$$

Now with the given operator $\mathbf{F}$ we associate a new operator, which we will denote by $\hat{\mathrm{F}}$. This is the so-called Lie operator which acts on the space of the differentiable operators of type S→S and maps each operator $\mathbf{G}$ into the new operator $\hat{\mathrm{F}}(\mathbf{G})$, such that for any element $\mathrm{c} \in \mathrm{S}$

$$(\hat{\mathrm{F}}(\mathbf{G}))(\mathbf{c}) = (\mathbf{G}'(\mathbf{c}) \circ \mathbf{F})(\mathbf{c}). \tag{33}$$

It is easy to see that the Lie operator is linear. Applying the operator $\hat{\mathrm{F}}(\mathbf{G})$ to the element $\mathbf{c}(\mathbf{x},t)$ and using Eq. (30) and the well-known chain rule of differentiating, we obtain that

$$\begin{aligned}(\hat{\mathrm{F}}(\mathbf{G}))(\mathbf{c}(\mathbf{x},t)) &= (\mathbf{G}'(\mathbf{c}(\mathbf{x},t)) \circ \mathbf{F})(\mathbf{c}(\mathbf{x},t)) = (\mathbf{G}'(\mathbf{c}(\mathbf{x},t)))(\mathbf{F}(\mathbf{c}(\mathbf{x},t))) = \\ &= (\mathbf{G}'(\mathbf{c}(\mathbf{x},t)))(\frac{\partial \mathbf{c}}{\partial t}(\mathbf{x},t)) = \frac{\partial}{\partial t}\mathbf{G}(\mathbf{c}(\mathbf{x},t)).\end{aligned} \tag{34}$$

From induction follows that the k^{th} power of the Lie-operator $\hat{\mathrm{F}}$ applied to some operator $\mathbf{G}$ can be expressed as the k^{th} derivative of $\mathbf{G}$, that is the relation

$$(\hat{\mathrm{F}}^{\mathrm{k}}(\mathbf{G}))(\mathbf{c}(\mathbf{x},t)) = \frac{\partial^k}{\partial t^k}\mathbf{G}(\mathbf{c}(\mathbf{x},t)) \tag{35}$$

is valid for all $\mathrm{k} = 1, 2\ldots$.

Taking into account Eq. (32) and Eq. (35), for the function $\mathbf{c}(\mathbf{x},t)$ the relation

$$\mathbf{c}(\mathbf{x},t+\tau) = \mathbf{I}(\mathbf{c}(\mathbf{x},t)) + \frac{1}{1!}(\tau\hat{\mathrm{F}}(\mathbf{I}))\,(\mathbf{c}(\mathbf{x},t)) + \ldots + \frac{1}{k!}(\tau^k\hat{\mathrm{F}}^k(\mathbf{I}))\,(\mathbf{c}(\mathbf{x},t)) + \ldots =$$

$$= (\mathbf{I} + \frac{1}{1!}(\tau\hat{\mathrm{F}})\,(\mathbf{I}) + \ldots + \frac{1}{k!}(\tau^k\hat{\mathrm{F}}^k)\,(\mathbf{I}) + \ldots)\,(\mathbf{c}(\mathbf{x},t)) \equiv (e^{\tau\hat{\mathrm{F}}}(\mathbf{I}))\,(\mathbf{c}(\mathbf{x},t)) \qquad (36)$$

is valid, where the defining equality is right, because the series on the right-hand side is convergent.

Let us split the operator $\mathbf{F}$ into the sum $\mathbf{F_1} + \mathbf{F_2}$. From the above consideration follows that the splitting error is

$$\mathrm{Err}_{\mathrm{Sp}} = (e^{\tau(\hat{\mathrm{F}}_1+\hat{\mathrm{F}}_2)}(\mathbf{I}) - (e^{\tau\hat{\mathrm{F}}_2}\,e^{\tau\hat{\mathrm{F}}_1})\,(\mathbf{I}))\,(\mathbf{c}(\mathbf{x},t))\,. \qquad (37)$$

This error vanishes for all $\mathbf{c}(\mathbf{x},t)$ if and only if

$$e^{\tau(\hat{\mathrm{F}}_1+\hat{\mathrm{F}}_2)}(\mathbf{I}) = (e^{\tau\hat{\mathrm{F}}_2}\,e^{\tau\hat{\mathrm{F}}_1})\,(\mathbf{I})\,. \qquad (38)$$

At this point the previous results are again applicable. If we define the usual addition operation between the Lie-operators, that is

$$(\hat{\mathrm{F}}_1+\hat{\mathrm{F}}_2)\,(\mathbf{G}) := \hat{\mathrm{F}}_1(\mathbf{G}) + \hat{\mathrm{F}}_2(\mathbf{G})$$

and

$$(\lambda\hat{\mathrm{F}})\,(\mathbf{G}) := \lambda\hat{\mathrm{F}}(\mathbf{G}),$$

then the set of Lie-operators form a vector space. Moreover, defining the commutation operation by

$$[\hat{\mathrm{F}}_1,\hat{\mathrm{F}}_2] := \hat{\mathrm{F}}_1 \circ \hat{\mathrm{F}}_2 - \hat{\mathrm{F}}_2 \circ \hat{\mathrm{F}}_1,$$

we obtain a Lie-algebra. As $e^{\tau\hat{\mathrm{F}}_2}\,e^{\tau\hat{\mathrm{F}}_1}$ is given by the Baker–Campbell–Hausdorff-formula, therefore, for an operator $\mathbf{G}$ the relation

$$e^{\tau(\hat{\mathrm{F}}_1+\hat{\mathrm{F}}_2)}(\mathbf{G}) = (e^{\tau\hat{\mathrm{F}}_2}\,e^{\tau\hat{\mathrm{F}}_1})\,(\mathbf{G})$$

holds if and only if the equality

$$(\hat{\mathrm{F}}_1 \circ \hat{\mathrm{F}}_2)\,(\mathbf{G}) = (\hat{\mathrm{F}}_2 \circ \hat{\mathrm{F}}_1)\,(\mathbf{G})$$

is satisfied. We expect this equality to be valid only for the identity operator $\mathbf{I}$, that is we only need the equality

$$((\hat{F}_1 \circ \hat{F}_2)(\mathbf{I}))(\mathbf{c}) = ((\hat{F}_2 \circ \hat{F}_1)(\mathbf{I}))(\mathbf{c}) \tag{39}$$

to be satisfied for all $\mathbf{c} \in S$. Applying the definition of the Lie operator we can see that Eq. (39) is equivalent to the relation

$$(\mathbf{F}_1'(\mathbf{c}) \circ \mathbf{F}_2)(\mathbf{c}) = (\mathbf{F}_2'(\mathbf{c}) \circ \mathbf{F}_1)(\mathbf{c}) \tag{40}$$

for all $\mathbf{c} \in S$, which means that the operators $\mathbf{F}_1$ and $\mathbf{F}_2$ L-commute. If $\mathbf{F}_1$ and $\mathbf{F}_2$ do not commute, then the splitting error is of $o(\tau^2)$.

The condition (40) can be used to analyse the splitting error of a given splitting procedure. At the beginning of the chapter we introduced DEM splitting. An alternative procedure can be the splitting of the spatial differential operator on the right-hand side of the system (1) purely according to the physical processes, which means that we have the splitted operators

- $\mathbf{F}_1(\mathbf{c}) = -\nabla(\mathbf{uc})$ for the advection,
- $\mathbf{F}_2(\mathbf{c}) = \nabla(\mathbf{K}\nabla\mathbf{c})$ for the diffusion,
- $\mathbf{F}_3(\mathbf{c}) = \boldsymbol{\sigma}\mathbf{c}$ for the deposition,
- $\mathbf{F}_4(\mathbf{c}) = \mathbf{E}$ for the emission, and
- $\mathbf{F}_5(\mathbf{c}) = \mathbf{R}(\mathbf{c})$ for the chemistry.

Here for example the commutator of the advection and diffusion operators reads

$$\mathbf{E}_{1,2}(\mathbf{c}) = (\mathbf{F}_2'(\mathbf{c}) \circ \mathbf{F}_1)(\mathbf{c}) - (\mathbf{F}_1'(\mathbf{c}) \circ \mathbf{F}_2)(\mathbf{c}) = \nabla[\mathbf{K}\nabla(-\nabla(\mathbf{uc}))] + \nabla[\mathbf{u}(\nabla(\mathbf{K}\nabla\mathbf{c}))].$$

The L-commutativity of all pairs of operators in the physical splitting is analysed in details in *Dimov et al.* (1999). For example it is shown that provided the diffusion coefficient matrix $\mathbf{K}$ and the velocity field $\mathbf{u}$ are independent of $\mathbf{x}$, then the above commutator $\mathbf{E}_{1,2}$ equals zero, that is no splitting error occurs between advection and diffusion. A similar analysis leads to the following results. In the case

$$\nabla\mathbf{K} = 0, \quad \nabla\mathbf{u} = 0, \quad \nabla\sigma = 0, \quad \nabla\mathrm{E} = 0$$

any pair of the operators $\mathbf{F}_1$, $\mathbf{F}_2$, $\mathbf{F}_3$ and $\mathbf{F}_4$ L-commute, except for $\mathbf{F}_3$ and $\mathbf{F}_4$. Moreover, if the operator $\mathbf{F}_5$ is independent of $\mathbf{x}$, then it L-commutes with $\mathbf{F}_1$, and under some additional conditions with $\mathbf{F}_2$ and $\mathbf{F}_3$ as well. However, the operator $\mathbf{F}_4$ does not L-commute with the operators $\mathbf{F}_3$ and $\mathbf{F}_5$. (For details see *Dimov et al.* (1999).)

In practice the conditions for the non-existence of the splitting error are not usually satisfied. However, in certain meteorological situations they may be ap-

proximately satisfied. For example if the diffusion coefficient matrix **K** decreases to very small values (which is typical of night-time periods because of the increased stability of the atmosphere), the commutators between diffusion and advection and diffusion and chemistry strongly decrease, which presumably leads to a significant decrease of the splitting error.

In addition to the two different splitting procedures introduced in this chapter, other splittings can also be applied. We can divide the spatial differential operator into even more parts and obtain more systems that are even simpler. It is also possible to combine the splitting methods and apply different splittings over different time intervals. However, it is better to minimize the number of the splitted operators, because the splitting error is, as a rule, difficult to estimate.

8. Summary

Nowadays air pollution is one of the most urgent environmental problems, which necessitates the reliable modeling of the atmospheric transport of pollutants. Air pollution models are based on the (chemistry-)transport equations, a system of partial differential equations describing the concentration changes of the pollutants in the atmosphere due to several transport processes. This system can only be solved numerically.

In the paper first we introduce the transport equations, and then summarize the problems concerning the numerical solution of a system of partial differential equations in general. A reliable numerical method is expected to satisfy several requirements simultaneously also in the case of the transport equations. However, this system is so complicated that we cannot guarantee these important properties. In the paper we discuss a procedure which allows us to solve a few simpler systems instead of the whole one. This procedure is called operator splitting and is widely used in air pollution modeling, however, so far little investigation has been carried out into it. In the article we clarify the mathematical background and the role of operator splitting with the use of the Lie-algebra theory and give some examples of splitting procedures (DEM splitting, physical splitting).

When applying splitting in a mathematical model, it is important to know the error resulting from the splitting procedure itself, the so-called splitting error, which we also discuss in more details. We give some cases when this error vanishes, but in practical applicatons this rarely happens. Obviously, this error (together with the effect of other numerical errors) should be minimal. Therefore, it is important to analyse the splitting error of the applied schemes and possibly find others in which the error is even more reduced.

Acknowledgement—The authors are indebted to the referees for the valuable suggestions.

References

Brandt, J., Bastrup-Birk, A., Christensen, J. H., Mikkelsen, T., Thykier-Nielsen, S. and *Zlatev, Z.*, 1998: Testing the importance of accurate meteorological input fields and parameterizations in atmospheric transport modelling using DREAM - Validation against ETEX-1. *Atmospheric Environment 32*, 4167-4186.

Broecker, W.S., 1987: Unpleasant surprises in the greenhouse? *Nature 328*, 123-126.

Broecker, W. S., 1991: The great ocean conveyor. *Oceanography 4*, 79-89.

Crutzen, P.J. and *Zimmermann, P.H.*, 1991: The changing photochemistry of the troposphere. *Tellus 43A/B*:136.

Crutzen, P.J., 1995: Overview of tropospheric chemistry: Developments during the past quarter century and a look ahead. Faraday discussions 100:1.

Dimov, I., Faragó, I. and *Zlatev, Z.*, 1999: Commutativity of the operators in splitting methods for air pollution models. *Technical report 04/99.* Bulgarian Academy of Sciences.

Eliassen, A., Hov, O., Isaksen, J. S., Saltbones, J. and *Stordal, F.*, 1982: A Lagrangian long-range model with atmospheric boundary layer chemistry. *Journal of Applied Meteorology 21*, 1615-1661.

Engel, K.-J. and *Nagel, R.*, 2000: *One-Parameter Semigroups for Linear Evolution Equations.* Springer, New York.

Faragó, I., Hariton, H. A., Komáromi, N. and *Pfeil, T.*, 1993: The heat equation and the qualitative properties of its numerical solution I-II. Alkalmazott Matematikai Lapok 17, 101-141.

Houghton, J. T., Meira Filho, L. G., Callander, B. A., Harris, N., Kattenberg, A. and *Maskell, K.*, 1995: Climate Change 1995. The science of climate change. Published for the Intergovernmental Panel on Climate Change, Cambridge University Press, p. 572.

Keeling, C. D., Bacastow, R. B., Carter, I. F., Piper, S. C., Whorf, T. P., Heimann, M., Mook, W. G. and *Roeloffzen, H.*, 1989: A three-dimensional model of atmospheric CO_2 transport based on observed winds. 1. Analysis of observational data. *Geophis. Mono.*, Am. Geophys. Union, Washington, DC, 165-231.

Lanser, D. and *Verwer, J. G.*, 1999: Analysis of operator splitting for advection-diffusion-reaction problems in air pollution modelling. *J. Compute. Appl. Math. 111*, 201-216.

Marchuk, G. I., 1980: *Methods of Computational Mathematics* (in Russian). Nauka, Moscow.

Marchuk, G. I., 1988: *Methods of Splitting* (in Russian). Nauka, Moscow

Möller, D., 1999: Atmospheric environmental research. Critical decisions between technological progress and preservation of nature. Springer p. 185.

Olson, M. P., Bottenheim, J. W. and *Oikawa, K. K.*, 1992: Nitrogen source receptor matrices and model results for eastern Canada. *Atmospheric Environment 26A*, 2323-2340.

Piedelievre, J. P., Musson-Genon, L. and *Bompay, F.*, 1990: MEDIA - An Eulerian model of atmospheric dispersion, first validation on the Chernobyl release. *Journal of Applied Meteorology 29*, 1205-1220.

Simpson, D., 1992: Long-period modelling of photochemical oxidants in Europe. Model calculations for July 1985. *Atmospheric Environment 26A*, 1609-1634.

Simpson, D., 1993: Photochemical model calculations over Europe for two extended summer periods, 1985 and 1989. Model results and comparisons with observations. *Atmospheric Environment 27A*, 921-943.

Thomée, V., 1990: *Finite Difference Methods for Linear Parabolic Equations.* Elsevier, North-Holland.

Trenberth, K. E., 1992: *Climate System Modeling.* Cambridge University Press, 491-517.

Varadarajan, V. S., 1974: *Lie Groups, Lie Algebras and Their Representations.* Prentice-Hall, Inc., Englewood Cliffs, New Jersey.

Yanenko, N. N., 1962: On convergence of the splitting method for heat equation with variable coefficients (in Russian). *Journal of Comp. Math. and Math. Phys. 2.*

Zlatev, Z., 1995: *Computer Treatment of Large Air Pollution Models.* Kluwer Academic Publishers.

BOOK REVIEW

Warneck, P., 1999: **Chemistry of the Natural Atmosphere**. Academic Press, San Diego, San Francisco, New York, Boston, London, Sidney and Tokyo. 923 pages, a large quantity of tables, figures and supplementary tables with important data, a huge amount of references on 127 pages and a detailed index.

One of the milestones in the short history of atmospheric chemistry research was the publication of the book of *Christian E. Junge* in 1963 (*Air Chemistry and Radioactivity*) by the Academic Press in its famous International Geophysics Series. The present book is dedicated to the memory of the late professor Junge (1912–1996), "a pioneer in the exploration of atmospheric trace substances" and is written by a former Junge's associate. We have to note that the volume is worthy of the name of the late master. It can also be considered as a milestone in such a way that it summarizes in an excellent manner practically everything which has happened in this field during the last hundred fifty years, but mainly during the last part of the 20th century. In other words this book closes the first important time period of this field of atmospheric science. If the Junge's book announced the birth of a new branch of science, Warneck's book is a signal of its maturity.

Let us imagine that when the writer of the present review was a student, more than forty years ago, he learned at the University of Budapest that the atmosphere, beside oxygen, nitrogen and noble gases, contains as minor constituents only water vapor, carbon dioxide and "dusts" and that ozone is simply a substance which indicates the motion of atmospheric pressure systems, that is the mixing efficiency between the stratosphere and troposphere. Since that time we have understood that in the air we can find a lot of trace substances which are in a continuous chemical interactions with one another and water, that atmospheric oxygen level has a history and that the composition of the atmosphere is a consequence of a huge material flow in nature called biogeochemical cycles. Research in atmospheric chemistry has become more and more active due to the recognition that human activities influences the atmospheric composition including the acidity of atmospheric deposition ("acid rain") as well as ozone formation and removal in the stratosphere ("ozone hole") and troposphere ("smog"). For their results in this latter field three research workers (*P. Crutzen, M. Molina* and *F. S. Rowland*) were rewarded by Nobel price in 1995. This was the first Nobel price given for research in atmospheric science. During the last decades, owing to intensive studies in atmospheric physics and chemistry, we recognized that the burning of fossil fuels by man contributes significantly to the atmospheric greenhouse and man-made aerosol particles can modify not only

the cloud and precipitation formation, but also the solar radiation transfer, consequently the climate.

The reader can learn from Warneck's book the history and present state of our knowledge concerning the problems mentioned. At the same time the volume is prepared with a scientific deepness necessary for helping all young people who want to make research in this important field: its reading is an excellent and unavoidable starting point for any further activity in this field. On the other hand, it gives a good reference book for senior researchers specialized in a narrow sector of air chemistry. The content is divided in twelve chapters from basic concepts of the composition, structure and dynamics of the air to the evolution of the Earth's atmosphere. A chapter on photochemical processes and elementary reactions gives a good introduction of the subject for potential non-chemist readers. Further, we can find specialized chapters on the chemistry and cycle of ozone, organic species, as well as of nitrogen and sulfur compounds. One chapter is devoted to the discussion of the physics and chemistry of the atmospheric aerosol, an other one deals with the role of clouds and precipitation in the control of atmospheric pathways of other trace components. Last but not least, a chapter provides a good survey of the geochemistry of carbon dioxide. It should also be emphasized that the supplementary tables contain kinetic data of all possible chemical reactions in the atmosphere necessary for model calculations.

In the last years several books have been published on atmospheric chemistry. Without estimating the values of these books we note that the content and the deepness of the chapters reflect generally the interest of the author(s) which is rather understandable. If a book is good, for example, in atmospheric photochemistry, it is not too detailed concerning the atmospheric aerosol particles and clouds, and *vice versa*. The reviewer believes that even in this respect the present volume is unique: the author presents all the problems at the same high scientific level. Shortly, it is the best book on atmospheric chemistry published until now. Thus, it goes without saying that its reading is recommended to all present and future scientists interested in this young, but very attractive and promising field of atmospheric science.

E. Mészáros

ATMOSPHERIC ENVIRONMENT

an international journal

To promote the distribution of Atmospheric Environment *Időjárás* publishes regularly the contents of this important journal. For further information the interested reader is asked to contact *Prof. P. Brimblecombe*, School for Environmental Sciences, University of East Anglia, Norwich NR4 7TJ, U.K.; E-mail: atmos_env@uea.ac.uk

Volume 35 Number 1 2001

Short Communications

Volume 35 Number 2 2001

NOTES TO CONTRIBUTORS

The purpose of *Időjárás* is to publish papers in the field of theoretical and applied meteorology. These may be reports on new results of scientific investigations, critical review articles summarizing current problems in certain subject, or shorter contributions dealing with a specific question. Authors may be of any nationality but papers are published only in English.

Papers will be subjected to constructive criticism by unidentified referees.

* * *

The manuscript should meet the following formal requirements:

Title should contain the title of the paper, the names(s) of the author(s) with indication of the name and address of employment.

The title should be followed by an *abstract* containing the aim, method and conclusions of the scientific investigation. After the abstract, the *key-words* of the content of the paper must be given.

Three copies of the manuscript, typed with double space, should be sent to the Editor-in-Chief: *P.O. Box 39, H-1675 Budapest,* Hungary.

References: The text citation should contain the name(s) of the author(s) in Italic letter or underlined and the year of publication. In case of one author: *Miller* (1989), or if the name of the author cannot be fitted into the text: *(Miller,* 1989); in the case of two authors: *Gamov* and *Cleveland* (1973); if there are more than two authors: *Smith et al.* (1990). When referring to several papers published in the same year by the same author, the year of publication should be followed by letters a,b etc. At the end of the paper the list of references should be arranged alphabetically. For an article: the name(s) of author(s) in Italics or underlined, year, title of article, name of journal, volume number (the latter two in Italics or underlined) and pages. E.g. *Nathan, K. K.,* 1986: A note on the relationship between photosynthetically active radiation and cloud amount. *Időjárás 90,* 10-13. For a book: the name(s) of author(s), year, title of the book (all in Italics or underlined with except of the year), publisher and place of publication. E.g. *Junge, C. E.,* 1963: *Air Chemistry and Radioactivity.* Academic Press, New York and London.

Figures should be prepared entirely in black India ink upon transparent paper or copied by a good quality copier. A series of figures should be attached to each copy of the manuscript. The legends of figures should be given on a separate sheet. Photographs of good quality may be provided in black and white.

Tables should be marked by Arabic numbers and provided on separate sheets together with relevant captions. In one table the column number is maximum 13 if possible. One column should not contain more than five characters.

Mathematical formulas and *symbols:* non-Latin letters and hand-written marks should be explained by making marginal notes in pencil.

The final text should be submitted both in manuscript form and on *diskette.* Use standard 3.5" or 5.25" DOS formatted diskettes for this purpose. The following word processors are supported: WordPerfect 5.1, WordPerfect for Windows 5.1, Microsoft Word 5.5, Microsoft Word 6.0. In all other cases the preferred text format is ASCII.

* * *

Authors receive 30 *reprints* free of charge. Additional reprints may be ordered at the authors' expense when sending back the proofs to the Editorial Office.

Published by the Hungarian Meteorological Service

Budapest, Hungary

INDEX: 26 361

HU ISSN 0324-6329

IDŐJÁRÁS

QUARTERLY JOURNAL
OF THE HUNGARIAN METEOROLOGICAL SERVICE

CONTENTS

****

http://omsz.met.hu/firat/ido-e.html

VOL. 105 * NO. 2 * APRIL–JUNE 2001

IDŐJÁRÁS

Quarterly Journal of the Hungarian Meteorological Service

Editorial Office: P.O. Box 39, H-1675 Budapest, Hungary or
Gilice tér 39, H-1181 Budapest, Hungary
E-mail: prager.t@met.hu or *antal.e@met.hu*
Fax: (36-1) 346-4809

Subscription by

mail: IDŐJÁRÁS, P.O. Box 39, H-1675 Budapest, Hungary
E-mail: prager.t@met.hu or *antal.e@met.hu*; *Fax: (36-1) 346-4809*

IDŐJÁRÁS

Quarterly Journal of the Hungarian Meteorological Service
Vol. 105, No. 2, April–June 2001, pp. 63–80

A brief history of aerosol research in Hungary

E. Mészáros[1] and **A. Molnár**[2]

[1]*Department of Earth and Environmental Sciences, University of Veszprém*
[2]*Air Chemistry Group of the Hungarian Academy of Sciences*
P.O. Box 158, H–8201 Veszprém, Hungary
E-mail: meszaros@anal.venus.vein.hu

(Manuscript received 8 February 2001)

Abstract—The aim of this paper is to summarize the history of Hungarian research carried out during the last forty years to study the atmospheric aerosol. This period can be divided in three parts. In the first part (between 1960 and 1980) the water soluble inorganic ions were investigated to understand the role of aerosol particles in the cloud formation The studies showed that water soluble particles are composed mainly of ammonium sulfate and about the half of the mass of this compound can be identified in the size range of particles with a diameter below 0.2 μm. The sampling program done over the remote ocean indicated that sulfate particles give the major part of the number of aerosol particles even under oceanic conditions, far from the continents. Sulfur budget calculations made it evident that sulfate particles in the continental air are of anthropogenic origin. This meant that human activities control in a great measure the formation of cloud condensation nuclei. Research in the second part (between 1981 and 1995) was devoted to the study of elemental composition of aerosol particles including some toxic metals like lead, zinc and vanadium. Since about 1995, in the third part, one of our main aims has been the investigation of organic species in the atmospheric aerosol. These studies demonstrated that an important fraction of organic matter consists of macromolecules like humic substances in the soils. A non negligible part of these macromolecules are soluble in water. The second goal after 1995 has been to study the effects of the optical properties of aerosol particles on the solar radiation transfer for understanding the role of aerosol particles in visibility control and climatic variation.

Key-words: atmospheric aerosol composition, cloud condensation nuclei, light extinction, Hungary.

1. Introduction: the beginnings

The existence of aerosol particles in the air was first demonstrated by *Coulier* (1875) and *Aitken* (1880) in the second half of the nineteenth century. Their expansion chamber experiences showed that water droplets formed on "dust" particles served as condensation nuclei. They also demonstrated that dust parti-

cles could be eliminated from the air by several subsequent expansions. Thus, Aitken noted that "if there were no dust in the air there would be no fogs, no clouds, no mist and probably no rain". On the other hand at the beginning of the twentieth century *Mie* (1908) further developed the earlier proposition of Lord Raleigh according to which the particles in the air are optically active, mainly those having a size comparable with the wavelength of the solar radiation. The concept that the Earth's atmosphere constitutes a huge colloidal system was introduced by *Schmauss* and *Wigand* in 1929. *Junge* (1952) was the first to demonstrate that particles in different size domains investigated by different aims and methods have a continuous size distribution.

Until the fifties the chemical composition of atmospheric particles remained practically unknown, in spite of the fact that, beside dust of continental origin, the presence of sea salt particles were already indirectly indicated by fog and frost analyses as well as by their effect on visibility. Another broad class of particles, which can be observed even in naked eye was named "combustion particles", or simply "smoke". In the fifties some important new results were obtained. Thus, the classical measurements of *Junge* (1963) made it clear that a major part of water soluble particles with a radius between 0.1 and 1.0 μm consisted of sulfuric acid and ammonium sulfate formed in the air by chemical reactions followed by condensation. On the other hand, his results also indicated that near the seas in the radius range above 1.0 μm water soluble particles were composed of sea salt (mostly sodium and chloride ions) in agreement with the results of pioneering aircraft flights of *Woodcock* (1953) carried out under oceanic conditions.

At that time, owing to research in cloud physics, it was already evident that only a fraction of aerosol particles serves as condensation nuclei in natural clouds. This idea was based on the fact that the number of cloud droplets was found to be smaller than the concentration of particles measured by expansion chambers (*Mason*, 1957). On the basis of his observation Junge proposed that this active fraction is in the radius range of 0.1–1.0 μm where ammonium sulfate particles are predominant. This proposition was in disagreement with the general earlier belief that sea salt particles serve as active condensation nuclei, called later cloud condensation nuclei (CCN) by *Twomey* (1959).

This was briefly the situation in 1960 when Hungarian aerosol research started. Our first goal was to check whether sea salt particles have an important effects on cloud and precipitation formation over Central Europe and, generally speaking, what kind of water soluble particles do exist in the air above our country. The second direction was to determine the concentration and deposition of different metals. Finally, the role of aerosol particles in the control of radiation transfer was also investigated. The aim of this paper is to summarize the main results of Hungarian investigation made in this field between 1960 and 2000.

2. *The water soluble inorganic fraction*

The first research goal was to clarify the role of chloride particles in cloud formation over Hungary. On the surface, the sampling was carried out by an impactor, while aloft small slides, exposed from a light aircraft, were used to capture the particles. In both cases the particles were collected on a gelatin surface sensitized by silver nitrate. The surface measurements in suburban Budapest (see *Fig. 1*) and aircraft flights indicated that the concentration of chloride particles is higher in air masses of maritime origin as expected. The concentrations increased generally with height (*Mészáros*, 1963) in agreement with earlier observations of *Byers et al.* (1957) made over North America. It was also found that the number of chloride particles is too low to be important in cloud formation. There was an indication that even the number of all particles with a diameter above 0.2 μm was not sufficient. This was later proved by capturing particles by membrane filters below freshly formed small cumulus clouds with parallel droplet samplings above the cloud base (*A. Mészáros*, 1969). The results of this program are summarized in *Table 1*.

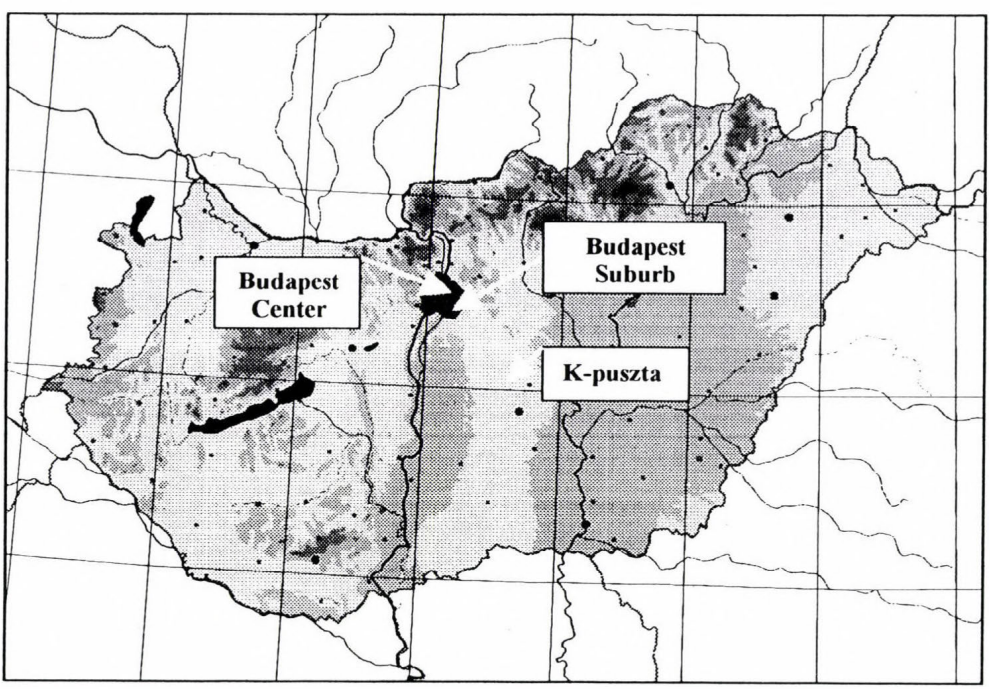

Fig. 1. Aerosol sampling sites referred in the text.

Table 1. Comparison of below-cloud aerosol particle concentration (N, with d > 0.2 μm) and cloud droplet number (n) above the base of freshly formed cumuli in different days (N°).

N° →	1	2	3	4	5
N (cm^{-3})	330	350	300	220	500
n (cm^{-3})	2300	1080	1660	1100	2300
N/n (%)	14	32	18	20	22

Data tabulated clearly show that the concentration of particles in the size range above 0.2 μm is much lower than that of droplet concentration. It is interesting to note that similar results were obtained by *Hidy et al.* (1970) over Northeastern Colorado. Thus, one concluded that particles smaller than the above size give a major part of CCN. According to thermodynamic calculations small particles can serve as CCN only if they are soluble in water. However, at that time the chemical composition of small particles was an open question. For this reason we sampled the particles by a cascade impactor of four stages backed up by suitable filters. The samples were analyzed with nephelometric and colorimetric chemical methods. This program indicated (*Mészáros*, 1968) that the fraction of water soluble substances increases with decreasing diameter and soluble aerosol material in the size range below 0.2 μm is composed mostly of sulfate and ammonium ions, while the quantity of nitrate and chloride ions is lower and in many cases it can practically be neglected[1]. It was also found that the half of the mass of ammonium and sulfate ions is in this size range (see *Table 2*). This involved that on number basis the great majority of ammonium sulfate particles has a very small size.

Table 2. Size distribution of various ions in percentage of their total mass (*Mészáros*, 1968). Note that *d* is the particle diameter.

Size range	Ammonium	Sulfate	Chloride
d > 2 μm	8	12	33
2 > d > 0.2 μm	45	45	49
d < 0.2 μm	47	43	18

[1] The origin of chloride ions in the size range of d < 0.2 μm is not clear. It is assumed, however, that they are of anthropogenic origin.

Thus, it was concluded that CCN consist of ammonium sulfate particles with diameter below 0.2 μm. The same conclusion was drown by *Twomey* (1968) by measuring the size and volatility of CCN. Research in Hungary also demonstrated that sulfate particles in summer daylight form by photochemical reactions (*Mészáros,* 1973), while in winter some other processes also play a part. Although there are other possibilities (formation in liquid water), we found later that in night mainly during the winter half-year sulfate ions come into being on the surface of elemental carbon particles (*Mészáros* and *Mészáros*, 1988).

The conclusion that CCN are composed of ammonium sulfate was widely accepted in the literature. The work of many other scientists pointed into this direction. Thus, on the basis of research done in the U.S.A. in this field (e.g., *Dinger et al.*, 1970; *Hudson*, 1991) one proposed without doubt that CCN are composed of sulfates. At the beginning of seventies the first aerosol measurements were made in the air over remote oceans. Hungarian samplings were carried out on board a Soviet research vessel by means of membrane filters. The samples obtained were evaluated on the basis of particle morphology by an electron microscope. The results showed (*A. Mészáros* and *Vissy*, 1973) that particles identified are composed mainly of ammonium sulfate in the size range of fine particles (d<1 μm), while coarse aerosol (with particle diameter above 1 μm) consisted of sea salt particles (*Fig. 2*). This means that in the control of the composition of fine background aerosol sulfate particles play an essential role.

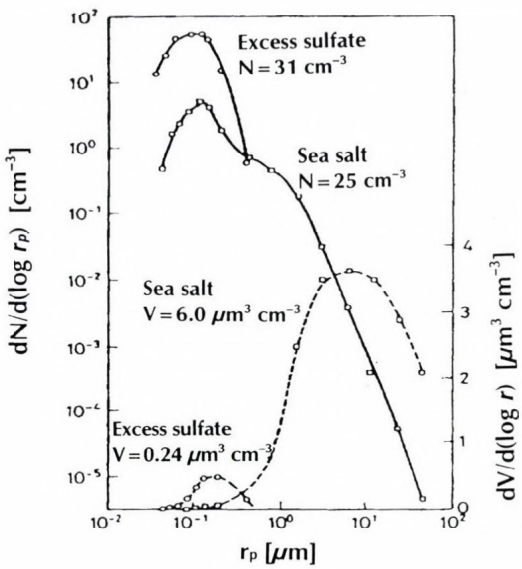

Fig. 2. Number (N) and volume (V) size distributions of sea salt and excess sulfate in the air over the oceans (r_p denotes the radius of aerosol particles).

Atmospheric sulfur budget calculations indicated that sulfate particles in oceanic air form by the gas-to-particle conversion of dimethyl sulfide emitted by the oceanic biota. On the other hand the precursor gas of continental sulfate particles is predominantly sulfur dioxide emitted because of the combustion of fossil fuels by man (see e.g., *Langner* and *Rodhe*, 1991). In other words CCN over the continents are of anthropogenic origin. This conclusion involves indirectly the following interesting question (*Mészáros*, 1992): what particles did serve as CCN before the industrial revolution, and what was the structure of continental clouds some hundred years ago? Since there were clouds and precipitation even at that time, we may ask: on what kind of particles formed cloud droplets before human influences over the continents? Are there water soluble fine particles other than sulfate which serve as CCN even now? These questions obviously involve that further research is needed in this field. Since the water soluble fraction of inorganic substances in the aerosol is well known, we concluded that we have to look for organic water soluble species. However, before discussing this problem let us summarize the results of Hungarian research aimed to study the elemental composition and mass balance of atmospheric aerosol particles which preceded in time the measurements of organic compounds.

3. Elemental composition: metals in the atmosphere

Beside condensation, the study of the atmospheric aerosol is important for the chemistry of other media of our environment. This is caused by the fact that, by means of dry and wet deposition, different elements in the aerosol are deposited onto the hydrosphere, pedosphere and biosphere. For this reason the investigation of these deposition processes is also of interest for solving many environmental problems, including anthropogenic effects on biogeochemical cycles of aerosol components. Thus, beside sulfur, nitrogen and chlorine in water soluble form, in the eighties the main aim of our research was to study the atmospheric concentration and deposition of different metals and metalloids in the air. For this purpose aerosol particles were captured under different conditions on Nuclepore filters and the elemental composition was determined by nuclear methods (PIXE: *P*article *I*nduced *X*-ray *E*mission). At the same time precipitation water, collected at several sites in Hungary, was analyzed by the ICP emission analysis (*I*nductively *C*oupled *P*lasma). In some cases aerosol samplings with a Berner-type cascade impactor (analyses by atomic absorption spectrometry) was also made to gain further insight into the size distribution of the elements.

The concentration of some selected elements under different environmental conditions (see Fig. 1) are summarized in *Table 3*. In parenthesis the enrichments factors relative to aluminum are also given.

Table 3. Concentration and enrichment factor (in parenthesis) of some selected elements under different conditions in Hungary. Concentrations are expressed in ng m^{-3} (*Molnár et al.*, 1993).

Sampling site →	City center	Suburb	Background
Al	274 (1)	290 (1)	131 (1)
Mn	13.4 (5.9)	13.4 (5.6)	3.4 (3.1)
Pb	203 (2710)	82.3 (2950)	10.4 (824)
V	6.1 (28.5)	4.4 (19.4)	2.0 (19.3)
Cu	21.5 (158)	11.5 (79.9)	4.4 (68.0)

One can see from data tabulated that the concentrations decreases from city center to background as expected. The ratio of city (Budapest) concentration to the value measured at K-puszta site (background) is high in particular for lead and in a lesser way for copper. This is mainly due to traffic density and coal combustion, respectively. The man-made origin is also proved by the high values of the enrichment factor. Vanadium is a notorious pollutant of oil combustion. Its concentration decreases from city to background but its enrichment is smaller than for copper. It is interesting that even aluminum and manganese, considered of crustal origin, show a similar trend than elements of mostly anthropogenic origin. In spite of this result we used aluminum to calculate the enrichment factors for obtaining values generally published in literature.

To gain further insight into the properties of different elements, their size distribution was also studied on the basis of samplings carried out in Veszprém (*Mészáros et al.*, 1997), which is a relatively clean university town in western Hungary (see Fig. 1). This is proved by the fact that concentrations measured in this town are only slightly different from those obtained at K-puszta station. The size distribution of four elements according to sampling in eight size ranges is represented in *Fig. 3* (note that the size spectrum for copper is not given, which is very similar to that of vanadium). It follows from these spectra that different elements can have different size distributions which is obviously caused by formation and dynamic processes. Thus, manganese of soil origin has a maximum in the size range of particles having a diameter above 1 μm (coarse particles). The main maximum of aluminum also can be found in this size interval. However, a smaller peak also exists in the smaller size range indicating some other, but less important sources. Lead has an unimodal distribution which is probably caused either by the condensation of lead containing species on particles with diameter above 0.25 μm during their emission, or by the particle coagulation. Contrary to this, a non-negligible fraction of vanadium (and copper) consists of particles smaller than 0.125 μm indicating fresh aerosol.

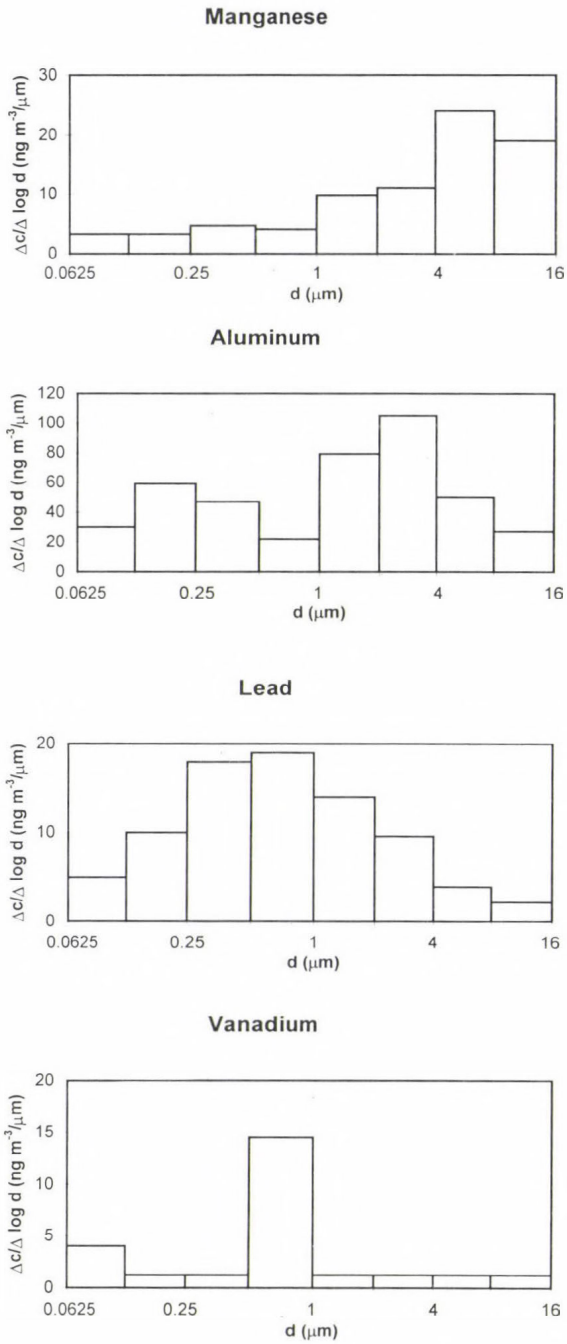

Fig. 3. Size distribution of the mass (c) of manganese, aluminum, lead and vanadium containing particles in Veszprém air. (Note that *d* is the particle diameter.)

These results make it obvious that the size distributions must be taken into account when we calculate the dry deposition and health effects of different metals (*Molnár et al.*, 1995). However, the comparison of the values calculated with the wet depositions shows that wet deposition plays a more important role in the self-cleaning of the atmosphere as does dry deposition.

Hungarian elemental aerosol data was also elaborated according to the direction of air trajectories. This work showed (*Koltay*, 1994), among other things, that in the cases of north-west trajectories the non-crustal Mn/V ratios were close to the value found in western Europe (about 2). However, for the air arriving from the north-eastern sector, the corresponding value is as large as 8.3 indicating the effect of coal burning and industrial activity. This study clearly indicates the importance of elemental ratios in the study of the origin of air pollution.

4. Mass balance calculated in 1990

In 1990 we believed that we have sufficient amount of data to try to calculate the mass balance of atmospheric aerosol particles. This means that the mass of different compounds calculated on the basis of inorganic ion and PIXE measurements is summed up and the results are compared with the total mass measured directly by weighing aerosol filters before and after the sampling. The input data for this calculation based on PIXE and wet chemistry analyses are given in *Table 4* (*Mészáros,* 1991). The table contains the fourteen most frequent elements found in the Hungarian aerosol. It can be seen that the first six elements as well as magnesium in the last row have an enrichment near one (within a factor of about two). Consequently they are considered as mineral dust components. The rest of elements are characterized by an enrichment factor much higher than 1. It is high in particular for sulfur and nitrogen: these elements are obviously of non-crustal origin. It is to be noted that the relatively high sodium concentration/enrichment is due to the fact that in the Hungarian Great Plain the soils contain much more sodium carbonate than the "average" soils used in the calculation.

Data in Table 4 shows that the concentration of sulfur as well as ammonium- and nitrate nitrogen is very important. Except some nitrate, these species can be found in the fine particles (see later), together with elemental carbon. On the other hand the level of sodium, silicon, aluminum and calcium is also significant, especially in the summer half-year (see *Borbély-Kiss et al.*, 1991). These elements constitute the soil derived aerosol particles.

On the basis of these data the main compound in the aerosol was estimated as listed in *Table 5*. For constructing the table the main composition of

Hungarian soils was also taken into consideration. According to this first approximation sodium carbonate is an important component in the coarse size range. This is partly caused by the water content of its crystals. On the other hand in the fine size range the composition is controlled by ammonium sulfate. This involves that oxygen is a major element in the aerosol over Hungary.

Table 4. Elemental composition of atmospheric aerosol particles under background conditions in Hungary measured by PIXE and wet chemistry (denoted by an asterisk) methods. *Ef* is the enrichment factor relative to titanium (it is equal to one if the element is of soil origin)

Element	Concentration (ng m^{-3})	Ef
Si	945	0.4
Al	340	0.6
Ca	495	2.6
Fe	324	1.1
K	265	2.1
Mn	12.8	2.7
S	1778	1507
Cl	22.1	31
Pb	24.8	457
Zn	29.9	106
NH_4-N*	1268	
NO_3-N*	352	6568
Na*	2880	18.9
Mg*	250	2.2

We have to emphasize, however, that Table 5 is based on elements and ions tabulated in Table 4. This means that aerosol particles may contain other substances which were not identified. This possibility is supported by the fact that that the total mass concentration of aerosol particles, measured by direct weighing in 1988, is 54 μg m^{-3} on an average. By comparing this latter value with the total concentration in Table 5, we can conclude that the compounds tabulated constitute only 64 % of the total mass. In other words this means that there is an important unidentified fraction. It was obvious to suppose again (see Section 2 of this paper) that this fraction consists of organic materials. For this reason in the second half of nineties our main aim has been to look for organic matter in the aerosol.

Table 5. Mass of different species in atmospheric aerosol particles over Hungary. Note: elemental carbon was measured by means of an optical method (*Heintzenberg* and *Mészáros*, 1985).

Size	Compound	Concentration (ng m^{-3})
Coarse	$KAlSi_3O_8$	1889
	$NaAlSi_3O_8$	1166
	$Al(OH)_3$	225
	$Na_2CO_3.10H_2O$	17271
	$FeCO_3$	705
	$CaCO_3$	1238
	$MgSO_4.7H_2O$*	2563
	Subtotal	**25057**
Fine	NH_4NO_3	2012
	$(NH_4)_2SO_4$	4381
	H_2SO_4	2130
	Elemental carbon	810
	Subtotal	**9333**
Coarse + Fine	**Total**	**34390**

*Mg was considered as $MgSO_4$ since water soluble magnesium was identified

5. Organic compounds

The philosophy of our research aiming to study the organic substances is as follows. It is well known that in the U.S.A. several series of measurements have been carried out to identify organic species. In these programs organic solvents were used to dissolve organic compounds from aerosol samples. The results of these studies show that only a small fraction of organic compounds can be identified individually in this way (see e.g., *Rogge et al.*, 1993). For this reason our aim has been to characterize the group of organic compounds with special emphasis on water soluble fraction. In the atmosphere the main solvent is water, and one of the main questions is whether particles are water soluble or not. Thus, the goal of our program has been to look for water soluble organic substances. We hoped that in this way we can explain in a more deeper manner the nature of CCN as outlined in Section 2 of this paper.

Briefly, the atmospheric particles were captured in this case by high volume samplers and an impactor of two stages backed-up by suitable filters. The samples were analyzed by different up-to date chemical methods like capillary electrophoresis, gas chromatography-mass spectrometry, high performance liquid chromatography etc. Total, elemental and organic carbon was measured

by the evolved gas analysis. In the last years for particle sampling and characterization an *e*lectric *l*ow *p*ressure *i*mpactor (ELPI) was applied (*Laitinen et al.*, 1996). In this device particles are electrically charged before entering the impactor. According to their inertia the charged particles impact onto metal foils to create electric signals which are in real-time counted, while samples can be subsequently analyzed. All the samplings were carried out under background conditions at K-puszta site.

The first result of this program is that total carbon concentration in the fine particle size range is comparable or higher than sulfate ion concentration. The majority of total carbon consists of organic carbon, while the mass of elemental carbon is relatively low. The organic carbon concentration can be as high as 10 $\mu g\ m^{-3}$ which is sufficient to explain the missing mass in the fine size range (see Table 5), mainly if we recalculate the mass of carbon as an element into the mass of carbon compounds by using the conversion factor of 1.8 we found (*Kiss et al.*, 2000).

The second interesting finding is that at least the half of the mass of organic carbon is soluble in water (*Zappoli et al.*, 1999; *Kiss et al.*, 2000). Further, there is some indication that this water soluble fraction is composed of macromolecular species which behave very similarly as humic acids in the soils[2]. This idea was based on the laboratory comparison of UV spectra, electropherograms and thermal behavior of humic acid standards to those of aerosol samples. The pyrolysis of aerosol samples also indicates that macromolecules in the fine size range are composed of polysaccharides, lignins, proteins and lipids very similarly to major soil compounds (*Gelencsér et al.*, 2000). This possibility was first demonstrated by *Mukai* and *Ambe* (1986), but these Japanese workers found humic substances in a much lower concentration. Moreover, macromolecular substances in aerosol samples were identified in street dust by *Havers et al.* (1998) in Germany. Finally, *Likens et al.* (1983) showed that in precipitation water a major part of dissolved carbon is in macromolecular form. This finding is interesting in particular if we consider that practically no humic substances are found in the coarse particle size range which excludes the possibility that these substances in the air originate from the mechanical disintegration of soils. Since such molecules cannot be formed in the air by chemical reactions, *Gelencsér* (2001) supposes that macromolecules are released from the soils in gaseous form and condensed in the air by homogeneous or heterogeneous nucleation.

Unfortunately the size distribution of water soluble organics (or humic acid-like substances) is not yet known. However, our measurements made by

[2] The concentration of different carboxylic acids in aerosol phase was found to be rather low in Hungary, although in clean air in the Swiss Alps their role is more important (*Sárvári et al.*, 1999).

ELPI show that organic carbon and sulfate ions have very different size distributions (*Fig. 4*). While sulfate ions are accumulated in the size range of 0.25–1.0 μm, an important part of the *mass* of organic carbon particles have diameters below 0.06 μm. This means that on *number* basis the majority of aerosol particles consists of organics in agreement with the finding of *Novakov* and *Penner* (1993). If these small organic carbon particles are soluble in water, one can assume that they can serve as CCN. By accepting this hypothesis we can conclude that an important part of CCN under continental conditions (at least in Europe) is independent of, or only indirectly related (through agriculture) to human activities. It goes without saying that this conclusion should be verified by further research. Anyway, fog studies in Po Valley, Italy, demonstrate (*Facchini et al.*, 1999) that polar water soluble organic species (giving the majority of total organic mass) can be found mostly in droplet phase, while insoluble carbon is detected preferentially in interstitial particles.

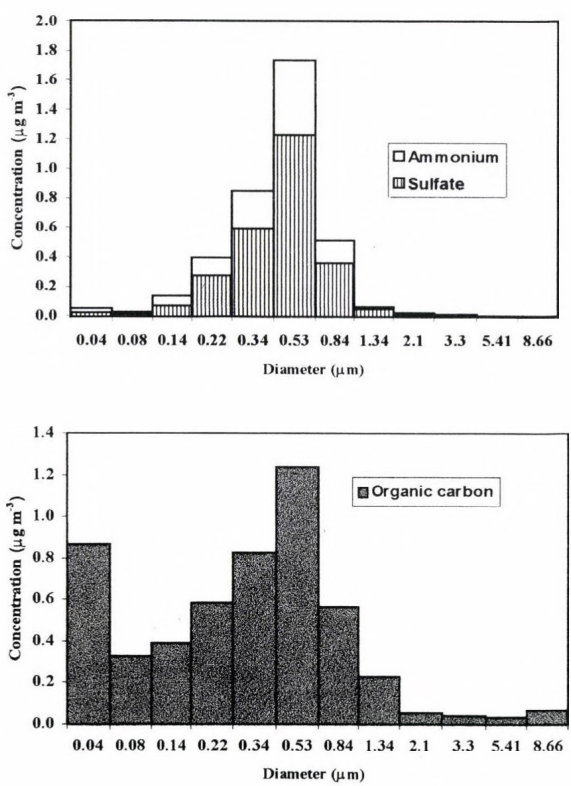

Fig. 4. Size distribution of ammonium sulfate and organic carbon particles.

An other interesting fact emerging from the figure is that ammonium sulfate particles detected in 1995–1996 have larger sizes than they had thirty years ago (see Table 2; *Mészáros*, 1968) when sulfate concentrations were higher than today. If we do not consider differences in sampling methods, one can speculate that temporal variations in sulfate concentrations and size distributions are the result of the decrease of sulfur dioxide emissions in Hungary and generally speaking in Europe (*Mylona*, 1996). Higher emission rates resulted not only in higher sulfate concentrations, but also in smaller particles due to the continuous aerosol formation by gas-to-particle conversion. This involves that the relative importance of sulfate ions in condensation processes *versus* the effects of organic carbon was higher some decades ago than presently.

6. Optical properties and chemical composition

Aerosol particles in the air scatter and absorb solar radiation. This aerosol extinction is important not only in the regulation of visibility, but also in the control of solar radiation transfer. Since solar radiation transfer determines the radiation budget, changes in aerosol characteristics contribute to climatic variations (*Charlson et al.*, 1991). For this reason, parallel with chemical measurements, optical properties of fine aerosol are also monitored at K-puszta station. The scattering and absorption coefficients are observed by an integrating nephelometer (working at 535 nm) and a particle soot absorption photometer (550 nm), respectively. The aim of the program is to look for correlation between these optical parameters averaged for 12 or 24 hours and the chemical composition. It should be noted that the values of the scattering coefficient varies typically between 50 and 100 Mm^{-1}, while the range of the absorption coefficient is generally 5–10 Mm^{-1}. This means that the extinction of solar radiation by aerosol particles is controlled by light scattering.

The first evaluation of data showed that in winter the scattering coefficient correlates significantly with sulfate concentration and the absorption coefficient is determined by elemental carbon. In summer the situation is more complicated: the correlation between the sulfate concentration and scattering is weaker (*Mészáros et al.*, 1998). A more detailed analysis of data revealed that the summer situation can be interpreted if the concentration of organic compounds is also considered (*Molnár et al.*, 1999). That is, in summer daylight the correlation between sulfate and scattering coefficient is significant only when the weather is characterized by the passage of cold fronts with relatively low temperature, more or less cloudy sky and temporary precipitation. In these cases the correlation coefficient between sulfate and scattering is 0.96, while the corresponding figure for ammonium is 0.95. On the other hand, during hot

and stable weather with sunshine, weak wind speeds and high ozone concentrations, both scattering and absorption coefficients correlate well with organic species. *Table 6* gives the correlation coefficients for this type of weather period. We note that, considering the number of cases, the relationship is significant at a probability level of 0.1% if the correlation coefficient is equal to or larger than 0.80.

It would be very interesting to know what the difference is between the organic species occurred during these two weather types. One possibility is that in these two weather periods the size distribution of organic particles is different. One can speculate for example that in the case of the first weather period the aerosol contains organic particles with an average size below the optically active size range. An other explanation can be the different chemical composition in the bulk organic fraction. Anyway, the interpretation of the data needs further, more detailed investigation.

Table 6. Correlation coefficients between the concentration of carbonaceous particles and optical properties. WS denotes the water soluble fraction.
Note that oxalate constitutes the most important carboxylic acid in aerosol phase.

Species →	**Oxalate**	**Total carbon**	**WS carbon**
Scattering	0.85	0.80	0.80
Absorption	0.84	0.96	0.88

On the basis of this study one can conclude that in certain situations the organic species play an important role in the control of the optical properties of the aerosol. Under other conditions their role is secondary in comparison with that of sulfate particles. Thus, the chemical properties controlling the optical parameters can change significantly from day to day. This conclusion rises the question how we can apply aerosol composition averaged for large time and spatial scales for understanding the behavior of the aerosol optics and radiation transfer in the air in a deeper way.

7. Conclusions

On the basis of the above discussion one can conclude that Hungarian aerosol research has contributed to the formulation of the following conclusions:

- Under continental conditions sea salt particles do not play a role in the control of the formation of clouds and precipitation.

- Both in the air over the oceans and continents ammonium sulfate is the most essential water soluble inorganic compound in the atmospheric aerosol. Considering their size and number these particles constitute an important part of cloud condensation nuclei.
- Taking into account that under continental conditions sulfate particles are presently of anthropogenic origin, in the past, before the industrial revolution, other aerosol type took part in the cloud formation. This fraction is consisted with a high probability of organic substances of biogenic origin.
- The deposition of different toxic elements, mainly in the wet deposition, supplies an non-negligible material flux into continental ecosystems.
- The mass balance of aerosol particles is improved considerably if organic substances are also considered. These macromolecular substances are partly water soluble and contribute to the control of cloud formation and solar radiation transfer in the atmosphere.
- In spite of the great progress in atmospheric aerosol research, world-wide and in Hungary further research is needed, mainly in the field of organic particles, to elucidate in a deeper way the role of aerosol particles in the control of environmental processes including weather and climate.

References

Aitken, J., 1880: On dust, fogs, and clouds. *Trans. Roy. Soc. Edinburgh 30*, 337368.

Borbély-Kiss, I., Bozó, L., Koltay, E., Mészáros, E., Molnár, A. and *Szabó, Gy.*, 1991: Elemental composition of aerosol particles under background conditions in Hungary. *Atmospheric Environment 25A*, 661-668.

Byers, H.R., Sievers, J.R. and *Tufts, B.J.*, 1957: Distribution in the atmosphere of certain particles capable of serving as condensation nuclei. In *Artificial Stimulation of Rain* (eds.: *H. Weickmann* and *W. Smith*). Pergamon Press, London and New York, 47-72.

Charlson, R.J., Langner, J., Rodhe, H., Leovy, C.B. and *Warren, S.*, 1991: Perturbation of northern hemisphere radiative balance by backscattering from anthropogenic sulfate aerosols. *Tellus 43AB*, 152-163.

Coulier, M., 1875: Note sur une nouvelle propriété de l'air. *J. Pharm. Chim. 22*, 165.

Dinger, J.E., Howell, H.B. and *Woyciechowski, T.A.*, 1970: On the source and composition of cloud nuclei in a subsident air mass over the North Atlantic. *J. Atmospheric Sci. 27*, 741-747.

Facchini, M. C., Fuzzi, S., Zappoli, S., Andracchio, A., Gelencsér, A., Kiss, G., Krivácsy, Z., Mészáros, E., Hansson, H. C., Alsberg, T. and *Zebühr, Y.*, 1999: Partitioning of the organic aerosol component between fog droplets and interstitial air. *J. Geophys. Res. 104*, 26,821-26,832.

Gelencsér, A., Hoffer, A., Krivácsy, Z., Kiss, G., Molnár, A. and *Mészáros, E.*, 2001: On the possible origin of humic matter in fine continental aerosol. Submitted to *J. Geophys. Res.*

Gelencsér, A., Mészáros, T., Blazsó, M., Kiss, Gy., Krivácsy, Z., Molnár, A. and *Mészáros, E.*, 2000: Structural characterisation of organic matter in fine tropospheric aerosol by pyrolysis — gas chromatography — mass spectrometry. *J. Atmospheric Chem. 37*, 173-183.

Havers, N., Burba, P., Lambert, J. and *Klockow, D.*, 1998: Spectroscopic characterization of humic-like substances in airborne particulate matter. *J. Atmospheric Chem. 29*, 45-54.

Heintzenberg, J. and *Mészáros, A.*, 1985: Elemental carbon, sulfur and metals in aerosol samples at a Hungarian regional air pollution station. *Időjárás 89*, 313-319.

Hidy, G.M., Bleck, R., Blifford, I.H., Brown, P.M., Langer, G., Lodge, J.P., Rosinsky, J. and *Sedlovsky, J.P.*, 1970: *Observations of Aerosol over North Eastern Colorado*. NCAR Technical Notes 49, Boulder.

Hudson, J.G., 1991: Observations of anthropogenic cloud condensation nuclei. *Atmospheric Environment 25A*, 2449-2455.

Junge, C., 1952: Gesetzmässigkeiten in der Grössenverteilung atmosphärischer Aerosole über dem Kontinent. *Berichte der Deutcher Wetterdienst. US Zone, Nr. 35*, 261-277.

Junge, C.E., 1963: *Air Chemistry and Radioactivity*. Academic Press, New York.

Kiss, G., Gelencsér, A., Hoffer, A., Krivácsy, Z., Mészáros, E., Molnár, A. and *Varga, B.*, 2000: Chemical characterization of water soluble organic compounds in tropospheric fine aerosol. Presented at 15th ICNAA, Rolla, 2000.

Koltay, E., 1994: The application of PIXE and PIGE techniques in the analytics of atmospheric aerosol. *Nuclear Instrument and Methods in Physical Res. B85*, 75-83.

Laitinen, A., Hautanen, J., Keslkinen, J., Moision, M., Marjamäki, M. and *Elsilä, A.*, 1996: Real time measurement of the size distribution of urban air aerosols with electric low pressure impactor. *J. Aerosol Sci. 27*, (Supplement 1) S299-S300.

Langner, J. and *Rodhe, H.*, 1991: A global three-dimensional model of the tropospheric sulfur cycle. *J. Atmospheric Chem. 13*, 225-264.

Likens, G.E., Edgerton, E.S. and *Galloway, J.N.*, 1983: The composition and decomposition of *organic* carbon in precipitation. *Tellus 35B*, 16-24.

Mason, B.J., 1957: *The Physics of Clouds*. Clarendon Press, Oxford.

Mészáros, A., 1969: Vertical profile of large and giant particles in the lower troposphere. *Proc. 7th Inernat. Conference on Condensation and Ice Nuclei*. 364-368. Academia, Prague.

Mészáros, A. and *Mészáros, E.*, 1988: Sulfate formation on elemental carbon particles. *Aerosol Sci. Technol. 10*, 337-342.

Mészáros, A. and *Vissy, K.*, 1974: Concentration, size distribution and chemical nature of atmospheric aerosol particles in remote oceanic areas. *J. Aerosol Sci. 5*, 101-110.

Mészáros, E., 1963: Répartition verticale de la concentration des particules de chlorures dans les basses couches de l'atmospheres. *J. de Rech. Atmosph. 1 (2e année)*, 1-10.

Mészáros, E., 1968: On the size distribution of water soluble particles in the atmosphere. *Tellus 20*, 443-448.

Mészáros, E., 1973: Evidence of the role of indirect photochemical processes in the formation of atmospheric sulphate particulate. *J. Aerosol Sci. 4*, 429-434.

Mészáros, E., 1991: Study of the chemical composition of atmospheric aerosol particles in Hungary: a review. *Atmospheric Research 26*, 275-283.

Mészáros, E., 1992: Structure of continental clouds before the industrial era: a mystery to be solved. *Atmospheric Environment 26A*, 2469-2470.

Mészáros, E., Barcza, T., Gelencsér, A., Hlavay, J., Kiss, Gy., Krivácsy, Z., Molnár, A. and *Polyák, K.*, 1997: Size distributions of inorganic and organic species in the atmospheric aerosol in Hungary. *J. Aerosol Sci. 28*, 1163-1175.

Mészáros, E., Molnár, A. and *Ogren, J.*, 1998: Scattering and absorption coefficients *vs.* chemical composition of fine atmospheric aerosol particles under regional conditions in Hungary. *J. Aerosol Sci. 29*, 1171-1178.

Mie, G., 1908: Reports on the optics of turbid media, especially metallic colloidal suspensions (in German). *Annalen der Physic 25*, 377-445.

Molnár, A., Mészáros, E. and *Ogren, J.A.*, 1999: On the possible role of carbonaceous particles in the control of optical properties of fine atmospheric aerosol. *J. Aerosol Sci. 30 (Supplement 1)*, S859-S860.

Molnár, A., Mészáros, E., Bozó, L., Borbély-Kiss, I., Koltay, E and *Szabó, Gy.*, 1993: Elemental composition of atmospheric aerosol particles under different conditions in Hungary. *Atmospheric Environment 27A*, 2457-2461.

Molnár, A., Mészáros, E., Polyák, K., Borbély-Kiss, I., Koltay, E., Szabó, Gy. and *Horváth, Zs.*, 1995: Atmospheric budget of different element in aerosol particles over Hungary. *Atmospheric Environment 29*, 1821-1828.

Mukai, H. and *Ambe, Y.*, 1986: Characterization of a humic acid like brown substance in airborne particulate matters and tentative identification of its origin. *Atmospheric Environment 20*, 813-819.

Mylona, S., 1996: Sulphur dioxide emissions in Europe 1880-1991 and their effects on sulphure concentrations and depositions. *Tellus 48B*, 662-689.

Novakov, T. and *Penner, J.E.*, 1993: Large contribution of organic aerosol to cloud-condensation nuclei concentration. *Nature 365*, 823-826.

Rogge, W.F., Mazurek, M.A., Hildemann, L.M. and *Cass, G.R.*, 1993: Quantification of urban organic aerosols at a molecular level: identification, abundance and seasonal variation. *Atmospheric Environment 27A*, 1309-1330.

Sárvári, Zs., Krivácsy, Z., Baltensperger, U., Nyeki, S., Weingartner, E., Wessel, S.. and *Jennings, S.G.*, 1999: Low-molecular weight carboxylic acids in atmospheric aerosol at different European sites. *J. Aerosol Sci. 30 (Supplement 1)*, S261-S262

Schmauss, A. and *Wigand, A.*, 1929: *Die Atmosphäre als Kolloid*. Vieweg und Sohn, Braunschweig.

Twomey, S., 1959: The nuclei of natural cloud formation. Part I: The chemical diffusion method and its application to atmospheric nuclei. *Geofisica Pura e Applicata 43*, 227-242.

Twomey, S., 1968: On the composition of cloud nuclei in north-eastern United States. *J. Rech. Atmos. 4*, 281-285.

Woodcock, A.H., 1953: Salt nuclei in marine air as a function of altitude and wind force. *J. Meteorology 10*, 362-371.

Zappoli, S., Andracchio, A., Fuzzi, S., Facchini, M.C., Gelencsér, A., Kiss, G., Krivácsy, Z., Molnár, A., Mészáros, E., Hansson, H.-C., Rossman, K. and *Zebühr, Y.*, 1999: Inorganic, organic and macromolecular components of fine aerosol in different areas of Europe in relation to their water solubility. *Atmospheric Environment 33*, 2733-2743.

IDŐJÁRÁS

Quarterly Journal of the Hungarian Meteorological Service
Vol. 105, No. 2, April–June 2001, pp. 81–91

Estimation of hourly temperature for the application of agrometeorological models

A. Cappugi[1], G. Maracchi[2] and S. Orlandini[1*]

[1]*Department of Agronomy and Land Management (DISAT), University of Florence*
Piazzale delle Cascine 18, 50144 Florence, Italy
E-mail: orlandini@iata.fi.cnr.it

[2]*Institute of Agrometeorology and Environmental Analysis Applied to Agriculture (CNR-IATA), National Research Council*
Piazzale delle Cascine 18, 50144 Florence, Italy

(Manuscript received 15 December 2000; in final form 25 May 2001)

Abstract—The importance of agrometeorological models and their application to improve cultivation techniques are growing day after day. This is mainly due to the need of an integrated agriculture, in which expensive and polluting input has to be substituted by more sustainable agronomic practices. Unfortunately, weather data used as input for these models are not always available, so methods to estimate the missing data have high importance. Starting from these considerations, some models to calculate hourly temperature from maximum and minimum daily values were used to simulate thermal pattern during seven different years (from 1994 to 2000). The obtained results were first compared with the measured values of hourly temperature to control the accuracy of the models. Then, calculated temperatures were used as input of an agrometeorological model simulating the development of *Plasmopara viticola* on grapevine (*Vitis vinifera*). Simulations, using measured and predicted temperatures, were compared to evaluate the possibility of applying temperature models to generate input data of biological systems. The Parton model showed the higher accuracy, while the Ephrath, Wcalc and Goudriaan models presented a decreasing precision in the simulation of thermal pattern. However, all the methods allowed a good substitution of measured temperatures for the application of agrometeorological models.

Key-words: generation of weather data, epidemiological models, sine-exponential models, deviance indexes.

* Corresponding author

1. Introduction

Temperature and other weather variables obviously have a very important effect on many physiological processes taking place in plants. Often temperature is one of the critical variables that drive biological systems, affecting crop growth and development, disease and insect attacks. Consequently thermal pattern has fundamental importance in model simulation, representing the main driving variable (*Benincasa et al.,* 1991). Usually, the available temperature data consist of daily average or daily maximum and minimum values. This is particularly true for historical climatic series, marginal areas and developing countries, where economical limitations obstacle the diffusion of automatic weather stations. However extreme values offer a good representation of the average meteorological conditions and probably they are sufficient in some situations, such as bioclimatic characterisation (*Orlandini et al.,* 2000). In biological models, however, the use of daily average or maximum and minimum values can cause deviations. In fact many biological processes, such as photosynthesis, respiration, transpiration and disease infection respond continually to weather variables (*Bjorkman*, 1979), so that daily totals or means of the required weather data are not sufficient (*Eprath et al.,* 1996). For many models and applications it is then crucial to obtain an approximation of hourly temperature, starting from daily maximum and minimum values. These considerations have stimulated the development of algorithms that allow to calculate hourly temperature from daily extreme data generating the driving variables to be used as input of many agrometeorological models (*Friend,* 1996).

The two most frequently used techniques for simulating the shape of daily curves of air temperature are the empirical and the energy budget model (*Parton* and *Logan,* 1981). The application of the latter is generally difficult because energy budget models require extensive computer time and data input (i.e., solar radiation, wind-speed, dew point). Empirical models draw the shape of the diurnal temperature curve in a variety of ways, varying from simple curve-fitting models based upon sine-exponential curves (*Parton* and *Logan,* 1981; *Wilkerson et al.,* 1983; *Eprath et al.,* 1996) to more sophisticated techniques utilising Fourier analysis (*Carson* and *Moses*, 1963). It is not easy to represent the shape of daily temperature by few terms of a Fourier series, since many of the observed diurnal temperature curves are a combination of periodic sine and exponential decay curves (*Reicosky et al.,* 1989). Whereas sine-exponential models require only daily maximum and minimum temperatures, julian day and latitude to calculate hourly temperature.

The purpose of this work was to investigate the accuracy of several methods for calculating hourly air temperature from daily maximum and minimum values, collected in Chianti area (Tuscany, central Italy). Methods were se-

lected from the literature on the basis of their simplicity, in terms of the number of input data and procedures of computing, so to allow a wide range of possible applications. The accuracy of models was studied first comparing model predictions with real hourly values of temperature collected in seven subsequent years (from 1994 to 2000) and then using predicted values as input of the agrometeorological model PLASMO (*Orlandini* and *Rosa,* 1997), simulating the development of *Plasmopara viticola* on grapevine (*Vitis vinifera*).

2. Material and methods

2.1 Data collection

Weather data were measured at the Mondeggi farm station (latitude 43°42'N, longitude 11°20'E), with 1 hour interval, for the period going from April to August, during seven years (from 1994 to 2000). In particular, temperature data were collected using a thermistor (Vaisala HMP 35A, Helsinki, Finland) with an accuracy of ±0.2°C at +25°C. Thermistor was placed, at the height of 2 m, in a shaded and ventilated chamber to prevent direct solar radiation from influencing the readings. All data were logged directly in digital format, using a data-logger (Delta-T, Cambridge, England) placed in the station. Maximum and minimum daily values were used to apply for the temperature models, while hourly values were used to analyse model performance. Complete data sets of measured weather parameters were applied to run PLASMO model. It is based on temperature, relative humidity, rainfall and leaf wetness hourly values, to simulate the attack degree in percentage terms (ratio between infected and total leaf area) of grapevine downy mildew.

Temperature data collected during 1994 were used to calibrate the models by reducing the values of the average deviation of simulated from measured temperatures.

2.2 Temperature models

Four different methods were selected to calculate hourly temperature according to their limited input request and simplicity of computing. The chosen models were: Parton, described by *Parton* and *Logan* (1981); Wcalc, described by *Wilkerson et al.* (1983); Ephrath, described by *Eprath et al.* (1996); Goudriaan, described by *Goudriaan* and *van Laar* (1994). For the detailed mathematical description of the model equations it is possible to refer to the original papers. A general overview of model structure is only presented (*Table 1*).

Table 1. Main characteristics of temperature models.
Legend: Smh = time of maximum solar height; p and c = tuning parameters

Model	Function for daytime temperature	Function for night-time temperature	Time of maximum temperature (Local Time)	Time of minimum temperature (Local Time)	Number of parameters
Ephrat	Sinusoidal	Exponential	Smh + p	Sunrise	3
Parton	Sinusoidal	Exponential	Smh + p	Sunrise + c	1
Goudriaan	Sinusoidal	Exponential	13:30	Sunrise	3
Wcalc	Sinusoidal	Linear	14:00	Sunrise+2 hours	0

All models have some common assumptions: maximum temperature happens during daytime, before sunset; minimum temperature happens about at sunrise; the time of minimum and maximum temperature are fixed; daily minimum and maximum air temperature are the main input; Julian Day and latitude are used to calculate sunrise and sunset times from standard meteorological equations.

All methods selected are empirical and they describe the shape of the daytime temperature curve by a sinusoidal equation (*Fig. 1)*. Three models use an exponential decay curve for calculating night-time hourly temperature, while Wcalc uses a linear equation. Ephrat and Parton models fix the time of maximum temperature adding to the time of maximum solar height (12:00) as a parameter. That parameter represents the delay in the maximum air temperature with respect to the time of maximum solar height, caused by heat storage in the atmosphere and in the surface layers of the soil (*Ephrath et al.*, 1996). The other models fix the time of maximum temperature at 13:30 (Goudriaan) and at 14:00 (Wcalc). The time of minimum temperature is fixed at sunrise in Ephrath and Goudriaan models, at sunrise plus a parameter in Parton and at sunrise plus 2 hours in Wcalc. Several tuning parameters are included in the models allowing a better fitting of simulations to different situations.

All models were implemented in computer programs using Fortran 32 language.

2.3 Analysis of model performance

To test the performance of the models two different analyses were carried out. First, in order to evaluate the accuracy of models describing the hourly trend of thermal pattern, temperatures measured at hourly intervals were compared to the calculated values.

Second, the possibility of using calculated data as input of agrometeorological models was assessed, by using predicted hourly temperatures as input data for a model simulating the development of grapevine downy mildew. The results of simulations were then compared with those obtained by using measured hourly temperature as input. The "goodness of fit" of each model was then evaluated by applying several statistical indices (*Mayer* and *Butler,* 1993).

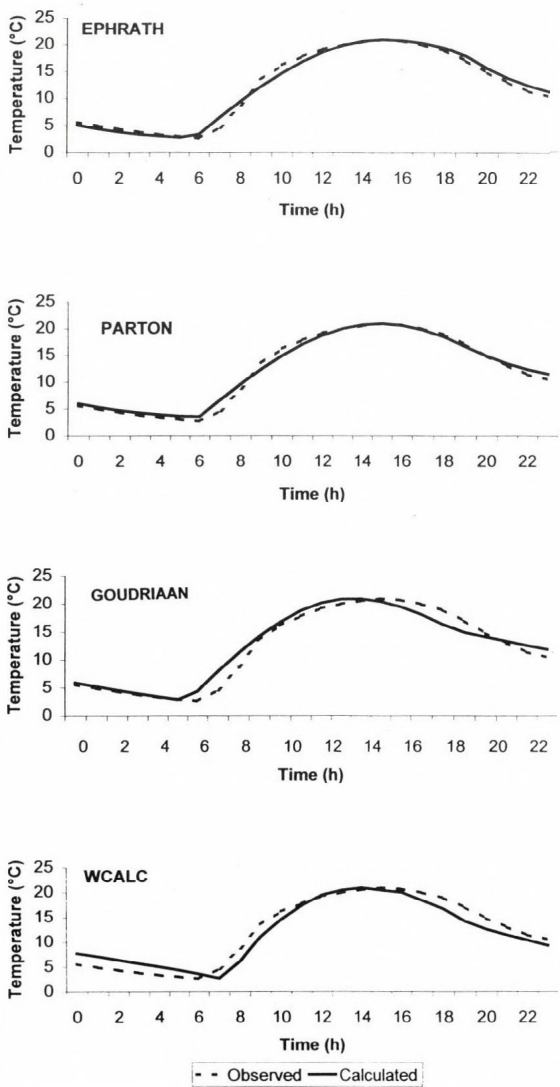

Fig. 1. Comparison of observed and calculated hourly courses of temperature for a typical day.

Mean bias error (MBE) and mean bias percent error (MB%E) allow to evaluate the average deviation calculated from measured values. A negative result of MBE and MB%E indicates that, generally, the model overestimates temperature with respect to the observed one.

Mean absolute error (MAE) and mean absolute percent error (MA%E) were used to evaluate the variation of simulated data around the observed patterns. Low values of MAE and MA%E indicate a low deviation of simulated values with respect to the measured values and so a higher accuracy of model.

$$MBE = \frac{\left(\sum_{i=1}^{n}(T_m - T_c)\right)}{n}, \tag{1}$$

$$MB\%E = 100\ \frac{\left(\sum_{i=1}^{n}\left(\frac{T_m - T_c}{T_m}\right)\right)}{n}, \tag{2}$$

$$MAE = \frac{\left(\sum_{i=1}^{n}|T_m - T_c|\right)}{n} \quad \text{and} \tag{3}$$

$$MA\%E = 100\ \frac{\left(\sum_{i=1}^{n}\left(\frac{|T_m - T_c|}{|T_m|}\right)\right)}{n}, \tag{4}$$

where n is the number of observations, $T_{m,i}$ is the i*th* measured value and $T_{c,i}$ is the i*th* calculated value.

3. Results and discussion

The values of MAE and MA%E indicated that Parton and Ephrath models had a lower deviation of simulated temperatures with respect to the measured values. In particular, Parton model showed the lowest MAE, while Ephrath the lowest MA%E (*Table 2*). The bigger accuracy of Parton and Ephrath models with respect to the others models was probably due to the higher number of tuning parameters allowing a better calibration of models to the observed temperature pattern.

In particular, analysing the influence of each parameter, it was possible to point out the importance of parameter for fixing the time of maximum tem-

perature with regard to the time of maximum solar height. As matter of fact, Goudriaan model had only a parameter for determining night-time temperature and it showed almost the same error as for Wcalc model which did not have any parameters. On the other hand, the other two models included parameters both for the night-time and the time of maximum temperature position obtaining the best estimation.

Table 2. Statistical measures of model performance.
Legend: MAE = mean absolute error; MA%E = mean absolute percent error; MBE = mean bias error; MB%E = mean bias percent error

Model	MAE (°C)	MA%E	MBE (°C)	MB%E
Ephrath	1.11	8.33	-0.38	-1.58
Parton	1.10	8.79	-0.45	-2.50
Goudriaan	1.64	11.49	-0.20	-1.37
Wcalc	1.60	11.55	0.51	1.72

These considerations were confirmed by the decade analysis of error trend (*Fig. 2*). Parton and Ephrat presented the same level of error, that was quite stable enough during the whole vegetative season. Wcalc and Goudriaan model errors were observed at a higher level, particularly during the warmer months of the year, when the hourly trend is strongly affected by the delay of maximum temperature. Considering the decade trend of MA%E (*Fig. 3*) it was possible to point out, that during the spring the relative errors of all the models were higher, probably because of the lower levels of air temperature and the high weather variability. This variability maybe caused an alteration of normal sinusoidal daytime trend of temperature increasing the error of model result.

The values of MBE and MB%E indicated that, on average, Wcalc model underestimated the observed temperature, while the other models overestimated the real thermal pattern (Table 2). Moreover, Parton model showed a higher value of bias percent error with respect to Ephrath. As it is possible to emphasize from *Fig. 4,* this difference was mainly due to the higher underestimation of night-time temperatures of Ephrath model, that compensated for daytime overestimation reducing the daily amount of MB%E.

The purpose of this work was also to investigate the possibility of using calculated temperatures, instead of measured values, as input in simulation models. For this aim PLASMO simulations, performed with calculated and measured temperature values, were compared.

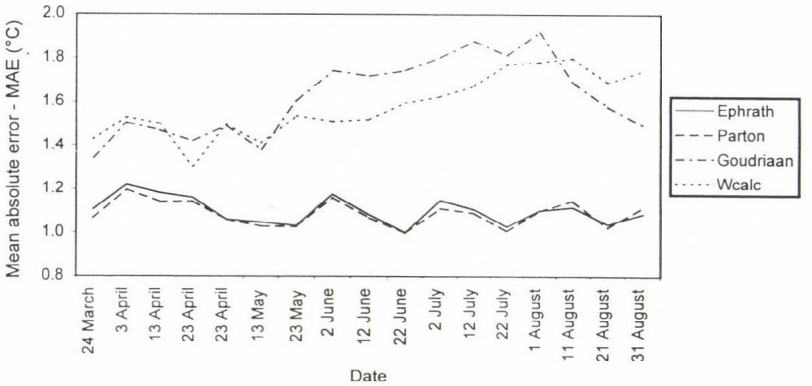

Fig. 2. Analysis of decade value of MAE.

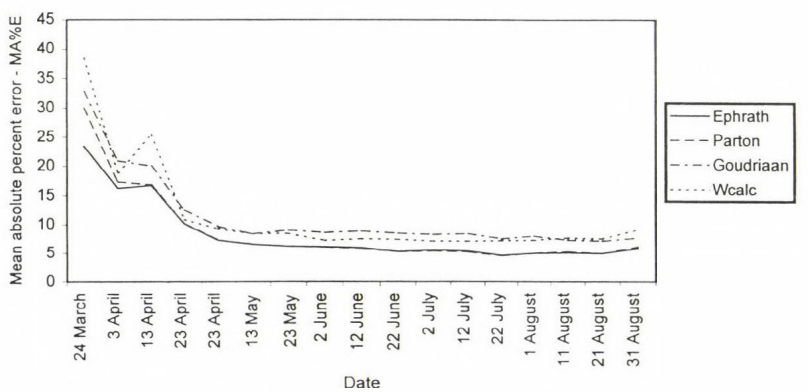

Fig. 3. Analysis of decade value of MA%E.

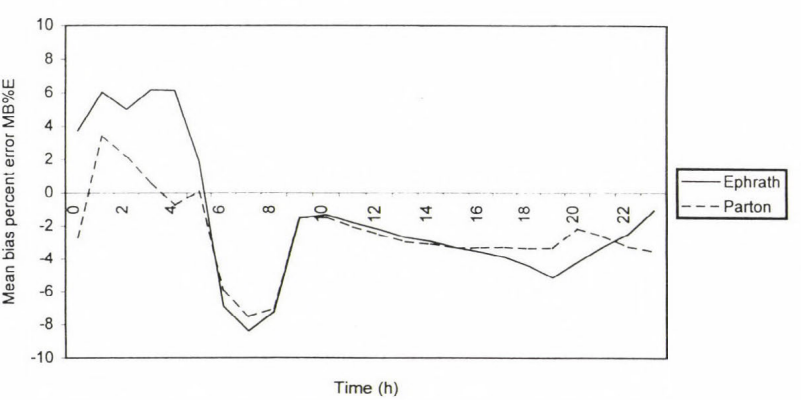

Fig. 4. Analysis of hourly curve of MB%E for Ephrath and Parton models.

The analysis of the PLASMO simulations was first carried out calculating the values of statistical indices of deviance (MAE, MA%E, MBE, MB%E) and then comparing the attack degree simulated by the model at three different periods of the year, using predicted and measured hourly temperature series of input data. The number of infections reported during the season was not analysed, because it is not a function of temperature but affected by relative humidity, leaf wetness and rainfall.

For all the models low average errors were observed, but Ephrath showed the best mean value for the whole analysed period (*Table 3*). This consideration was in agreement with the accuracy of model with respect to the measured temperature (Table 2).

Table 3. Average deviance of PLASMO simulation performed with calculated temperature with respect to simulation performed with measured values of air temperature.
Legend: MAE = mean absolute error; MA%E = mean absolute percent error; MBE = mean bias error; MB%E = mean bias percent error

Model	MAE (°C)	MA%E	MBE (°C)	MB%E
Ephrath	0.24	13.28	-0.04	-3.45
Parton	0.32	13.43	-0.27	-9.72
Goudriaan	0.42	19.12	0.08	-3.19
Wcalc	0.42	16.30	-0.13	-7.05

During four of the six considered years the attack degree of *Plasmopara viticola* was very low (*Table 4*) and this had probably influenced the percentage errors, increasing their values. The level of MBE and MB%E indicated that Goudriaan model had a little trend to underestimate attack degree, while the other models overestimated the intensity of pathogen infection during the season (Table 3).

Table 4 presents the attack degree simulated by all the models at three different days of the six considered years using temperature measured or calculated. The differences between the attack degrees were very low for all models. Moreover, the differences showed an increasing trend from the beginning to the end of the season. Ephrath showed the lowest differences confirming its accuracy in simulating the hourly temperature.

Table 4. Attack degree values (%) simulated by PLASMO model using calculated and measured temperatures at three different days of the year

	1995			1996		
	June 30	July 31	August 31	June 30	July 31	August 31
Measured	0.49	3.80	29.72	0.47	0.49	1.20
Ephrath	0.49	3.44	30.47	0.47	0.60	1.67
Parton	0.50	3.97	31.72	0.48	0.55	1.67
Goudriaan	0.49	3.03	28.41	0.47	0.59	1.62
Wcalc	0.48	4.08	32.72	0.46	0.47	1.33

	1997			1998		
	June 30	July 31	August 31	June 30	July 31	August 31
Measured	0.58	1.05	5.71	0.97	3.94	6.01
Ephrath	0.57	0.93	5.07	1.38	1.57	6.81
Parton	0.57	1.04	5.81	1.41	3.39	6.01
Goudriaan	0.57	0.86	4.66	1.45	3.70	6.74
Wcalc	0.57	0.90	5.11	1.19	2.43	4.39

	1999			2000		
	June 30	July 31	August 31	June 30	July 31	August 31
Measured	0.27	1.94	1.88	1.95	5.09	20.70
Ephrath	0.29	2.38	2.31	1.91	5.04	20.21
Parton	0.30	2.55	2.48	2.07	5.89	22.75
Goudriaan	0.30	2.73	2.65	1.75	4.27	17.38
Wcalc	0.31	2.94	2.86	1.85	4.95	20.69

4. Conclusions

This study referred to select and calibrate some models to estimate hourly air temperature using daily data for Chianti zone. The models showed a different accuracy in simulation of diurnal thermal pattern with respect to the observed data. A particular attention must be devoted to calibration of models, also considering that the same parameters should be modified during the season to take into account for the variation of solar radiation regime, as affecting the pattern of hourly temperature. With this aim, also the area of model formulation and calibration represents a fundamental element for the successful application of the model in different areas and periods of the year.

The use of calculated temperature as input data in a model for grapevine downy mildew allowed a good simulation of pathogen infection, with low deviance from the results obtained by using measured temperature values. However this assumption can not be considered true for every agrometeorological model, also depending by model sensibility to the specific weather parameter (*Cappugi,* 2000).

The always growing importance of agrometeorological models and decision support systems in modern agriculture demands the study of methods for the estimation of other weather and agrometeorological variables, such as relative humidity and leaf wetness. This will increase the possibility of application of these important instruments, also in areas, where economical or technical problems may reduce the diffusion of weather stations.

References

Benincasa, F., Maracchi, G. and *Rossi, P.*, 1991: *Agrometeorologia.* Patron Editore, Bologna.

Bjorkman, O., 1979: The response of photosynthesis to temperature. In *Plant and Their Atmospheric Environment* (eds.: *J. Grace, E.D. Fored* and *P.G. Jarvis*). Blackwell Scientific Publisher, Boston.

Carson, J.E. and *Moses, H.*, 1963: Analysis of soil and air temperature by Fourier techniques. *Journal Geophysical Research 68, 2217-2232.*

Cappugi, A., 2000: Stima dei dati agrometeorologici per l'utilizzo dei sistemi di supporto alle decisioni degli agricoltori. Degree dissertation in Agricultural Science, University of Florence.

Ephrath, J.E., Goudriaan, J. and *Marani, A.*, 1996: Modelling diurnal patterns of air temperature, radiation, wind speed and relative humidity by equations from daily characteristic. *Agricultural Systems 51*, 377-393.

Friend, A.D., 1996: Parameterisation of global daily weather generator for terrestrial ecosystem and biogeochemical modelling. *Ecological Modelling 4*, 334-350.

Goudriaan, J. and *van Laar, H.H.*, 1994: *Modelling Potential Crop Growth Processes.* Kluwer Academic Publisher, The Netherlands.

Mayer, D.G. and *Butler, D.G.*, 1993: Statistical validation. *Ecological Modelling 68,* 21-32.

Orlandini, S. and *Rosa, M.*, 1997: A model for the simulation of grapevine downy mildew. *Proc. 1th Workshop on Successful Applications of Information and Communication Technologies in Plant Protection*, 28-29 November, Rome.

Orlandini, S., Mancini, M. and *Moriondo, M.*, 2000: Bioclimatic charachterisaion of hilly area. *Proc. of Third European Conference on Applied Climatology*, 16-20 October, Pisa.

Parton, W.J. and *Logan, J.A.*, 1981: A model for diurnal variation in soil and air temperature. *Agricultural and Forest Meteorology 23*, 205-216.

Reicosky, D.C., Winkelman, L.J., Baker, J.M. and *Baker, D.G.*, 1989: Accuracy of hourly air temperatures calculated from daily maxima and minima. *Agricultural and Forest Meteorology 46*, 193-209.

Wilkerson, C.G., Jones, J.W., Ingram, K.T. and *Mishoe, J.W.*, 1983: Modelling soybean growth for crop management. *Transactions of the American Society of Agricultural Engineers (ASAE) 26*, 63-67.

IDŐJÁRÁS

Quarterly Journal of the Hungarian Meteorological Service
Vol. 105, No. 2, April–June 2001, pp. 93–107

Analysis of drought severity using PDSI and SPI indices

Péter Domonkos, Sándor Szalai and **Judit Zoboki**

Hungarian Meteorological Service
P.O. Box 38, H-1525 Budapest, Hungary; E-mail: domonkos.p@met.hu

(Manuscript received 14 March 2001; in final form 1 June 2001)

Abstract–The Great Hungarian Plain, which is the most important agricultural area of the country, is often stricken by drought. Dry years were particularly frequent in the last fifth of the 20th century. Tendencies of seasonal and annual precipitation totals during the 20th century were analysed using data series of monthly precipitation amounts from 14 Hungarian observing stations. Efficiencies of PDSI and SPI were investigated focusing the examples of unusual large changes in water supply anomalies between November 1999 and October 2000.

Our results show that precipitation has clearly decreased during the 20th century, particularly in early spring and early autumn. The decrease of annual totals is significant at the 0.95 level in all parts of Hungary. Frequency of severe drought events has markedly increased, although very wet periods also occurred in the recent years. PDSI and SPI are widely applied tools to characterise natural water supply. The various indices have different advantages and disadvantages. For example, while SPI for 6 months seems to be the best indicator of natural water supply for an average plant, SPI for 3 months is the better tool for sensitive, shallow-rooted plants.

Key-words: precipitation trend, water supply anomalies, drought, drought indices, Hungary.

1. Introduction

Drought is a recurrent phenomenon in Hungary causing frequent and substantial damages in the agricultural production. As high as 36% of the overall agricultural loss originates from drought, followed by hail, floods and frosts in the order of mean rates (*Dunay* and *Czakó*, 1987). Albeit drought has never been rare in the past, the period from 1983 to 1995 was exceptionally dry. In this 13 years the drought was chronic with relatively short interruptions of wetter subperiods, and 8 of the 13 years were extremely dry. This long series of dry

years is unique in the 20th century in the Carpathian Basin, and only the period from 1943–1952 (*Gunst*, 1993) was accompanied by similarly frequent disastrous drought events. In the late 90's some very wet years followed, but the growing season of 2000 was extraordinarily dry again.

Hungary is situated in Central Europe, close to the 47°N geographical latitude, in the Carpathian Basin. The climate of Hungary is strongly influenced by the circulation patterns carrying maritime, continental or Mediterranean air masses, and the basic features originated from the macrosynoptic effects are modified by the topography of the basin and some other local factors. In most part of the country the climate is continental with semiarid features, since it can be characterized by 450–600 mm annual precipitation and 800–1000 mm $year^{-1}$ potential evapotranspiration (PE). One fifth of the country in the Southwest and the mountainous regions in the North part are slightly wetter, with 600–800 mm typical yearly sum for both precipitation and PE. The wettest month of the year is June (60–90 mm), and the lowest monthly values are measured between January and March (25–40 mm) on average. However, the Great Hungarian Plain, which is the most important agricultural area of the country, particularly often suffers from insufficient water supply during the summer months. Frequent occurrence of water shortage in summer can be explained by the higher PE and in connection with it the increased water demand of plants under sunny and warm weather conditions, as well as the very large variability of precipitation amounts. While, on the one hand, cloudbursts with 50–100 mm precipitation may cause local floods, and monthly precipitation sum can sometimes exceed 200 mm, on the other hand, months without any precipitation and 3 month periods with below 100 mm total may occur at any time of the year. The importance of sufficient plant water supply is the highest in the growing season (April–September), and unfortunately, the highest variation of precipitation amount is detected in the same part of the year.

Numerous appropriate methods are known for characterizing different levels of water supply, especially drought events. The Palmer Drought Severity Index (PDSI) developed by *Palmer* (1965) is one of the most popular drought indices nowadays (*Briffa et al.*, 1994; *Scian* and *Donnari*, 1997; *Cook et al.*, 1999, etc.). However, some limitations of the PDSI have been recognized (e.g., *Alley*, 1984; *Kogan*, 1995; *Guttman*, 1998), and now the Standardized Precipitation Index (SPI) developed at the Colorado State University in the 90's is the mostly recommended drought index by many researchers (*McKee et al.*, 1995; *Edwards* and *McKee*, 1997; *Guttman*, 1998; *Hayes et al.*, 1999). Attempts of introducing some other drought indices are also promising (*Byun* and *Wilhite*, 1999), but these are beyond the scope of this study. Persistent lack of precipitation in 2000 in Hungary, following an unusual wet period,

provides a good opportunity to investigate the efficiencies of PDSI and SPI, and describe the characteristics of a considerably rapid development of a severe summer drought as well.

Systematic changes of monthly, seasonal and annual precipitation totals, as well as efficiencies of PDSI and SPI are discussed in the following sections.

2. Data and methods

2.1 Data

Daily precipitation and monthly temperature data from 6 meteorological observing stations covering the period January 1901–October 2000, monthly precipitation and temperature data from further 8 meteorological observing stations (January 1901–December 1998) as well as county-averages of monthly precipitation for each Hungarian county (November 1999–October 2000) are used in our work. *Table 1* shows the list of the observing stations, their geographical coordinates and some further information related to the used data series. Spatial averages were used in the evaluation of precipitation tendencies, therefore, observing stations are sorted into 3 regions: four stations are sorted into the northern region (N) and five-five stations to the western (W) and southeastern regions (SE).

Table 1. List of the observing stations where the used data series are originated from

Observing stations	Geographical coordinates		Elevation (m)	Daily precipitation data	Region
Sopron	16°36'E	47°41'N	240		W
Szombathely	16°36'E	47°15'N	218	+	W
Keszthely	17°14'E	46°44'N	115		W
Mosonmagyaróvár	17°16'E	47°23'N	122	+	W
Pécs	18°14'E	46°00'N	140	+	W
Budapest	19°02'E	47°31'N	120	+	N
Miskolc	20°46'E	48°07'N	133		N
Debrecen	21°37'E	47°33'N	120	+	N
Nyíregyháza	21°41'E	47°59'N	105		N
Baja	19°11'E	46°11'N	113		SE
Kecskemét	19°46'E	46°54'N	114		SE
Szeged	20°09'E	46°15'N	80	+	SE
Szarvas	20°33'E	46°52'N	83		SE
Túrkeve	20°45'E	47°06'N	87		SE

2.2 Trend analysis

Systematic changes in monthly, seasonal and annual precipitation amounts of the 20th century are analyzed using linear regression technique (based on calculation of least square deviations), supplying with the construction of confidence interval of trend values, as well as applying Mann-Kendall test. These methods are widely used in the analysis of precipitation trends. The regression line fitting method was applied e.g., by *Curtis et al.* (1998), *Akinremi et al.* (1999), *Stafford et al.* (2000); the Mann-Kendall test was applied by *Schönwiese et al.* (1994), *Lettenmaier et al.* (1994), *Rodrigo et al.* (2000), etc.; and both the regression line fitting and the Mann-Kendall test were used by *Brunetti et al.* (2000). Application of other methods also occurs: *Zhang et al.* (2000) use an improved version of the regression line fitting, where, applying a red noise model, the serial autocorrelation in the precipitation series is taken into account; *De Luís et al.* (2000) chose the Spearman's test, which is also a highly recommended method (*Sneyers*, 1992). We have experienced that the results of significance investigations coming from traditional regression analysis are very close to the results of Mann-Kendall test, so application of further methods would likely not lead to essentially different results than those come from the mentioned two techniques. In this paper only trends showing statistical significance at the 0.95 level applying either best linear fitting or Mann-Kendall test are selected as significant.

2.3 Drought indices

PDSI for the investigated period was calculated relying on *Palmer* (1965). The values of this drought index tend to show the departure of water supply from the climatic normal for a date (usually at the end of a specified month). Calculation of the PDSI requires meteorological and soil information, namely values of precipitation amounts, PE and field capacity, as well as the climatic normal values of precipitation and PE. Taking into account that PE depends mostly on temperature in Hungary, and temperature data are available in much higher number and accuracy than measured PE data, the Thornthwaite method was applied to approach PE. At the calculation of climatic normals the 1901–1980 period was specified to be the reference period. Derivation method of the PDSI is recursive, thus monthly PDSI values are sensitive not only to the same month's meteorological conditions, but also to precipitation amounts and temperature values of the previous 6–9 months. While a positive PDSI shows surplus, negative values show shortage of the contemporary water supply. A PDSI value between –2 and –3 means moderate drought, a PDSI of be-

tween –3 and –4 means severe drought, and a PDSI of less than –4 indicates extreme drought.

Calculation of SPI is simpler, and it does not need data beyond monthly precipitation amounts. The source data series is required to be at least 30 year long. At first a gamma distribution is fitted to the source data, then the gamma distribution is converted into standard normal distribution. In this way a particular monthly precipitation amount is coupled with the value of the standard normal distribution having the same probability function value as the precipitation amount has in the source data set. The respective value of the standard normal distribution is the SPI. This method is also applied for precipitation totals of longer than 1 month periods, so one may use 1-month SPI, 2-month SPI, 3-month SPI, and so on. The usual length of the period applied is between 1 and 12 months. Hereafter a number after "SPI" marks the length of the time window, for instance SPI-6 denotes the standard precipitation index for six months.

Owing to the derivation method, the same SPI for different locations or different seasons means the same deviation relative to the climatic normal of the precipitation amounts. So, an SPI value less than –1 occurs 16 times in one hundred years, an SPI of less than –1.5 occurs 6.7 times and an SPI of less than –2 occurs 2.3 times in 100 years, on average. Therefore periods having SPI between –1 and –1.5 are moderately dry, periods having SPI between –1.5 and –2 are severely dry, and SPI values below –2 indicate extremely dry condition.

3. Tendencies of monthly, seasonal and annual precipitation amounts in the 20th century

Fig. 1 shows the long term changes of annual precipitation totals during the period 1901–1998 in Hungary. It seems that fluctuations are rather similar in the different regions, and the W region is the wettest throughout the century. While the earliest part of the investigated period was the wettest in W, in the other two regions the most precipitation fell around 1940. The sign of the mean (linear) change is negative in the whole country: –7.7 mm decade^{-1} in SE, –9.2 mm decade^{-1} in N, and –11.0 mm decade^{-1} in W. All these rates are statistically significant at the 0.95 level.

Rates of systematic changes were not uniform in various periods of the year. *Fig. 2* illustrates the mean rates for the individual months. Although the absolute values are very different, all the monthly trends have negative sign with the only exception of June. While there is hardly any systematic change from May to August, 3–4% per decade decrease has been taken place in the precipitation amounts of early spring and early autumn subperiods.

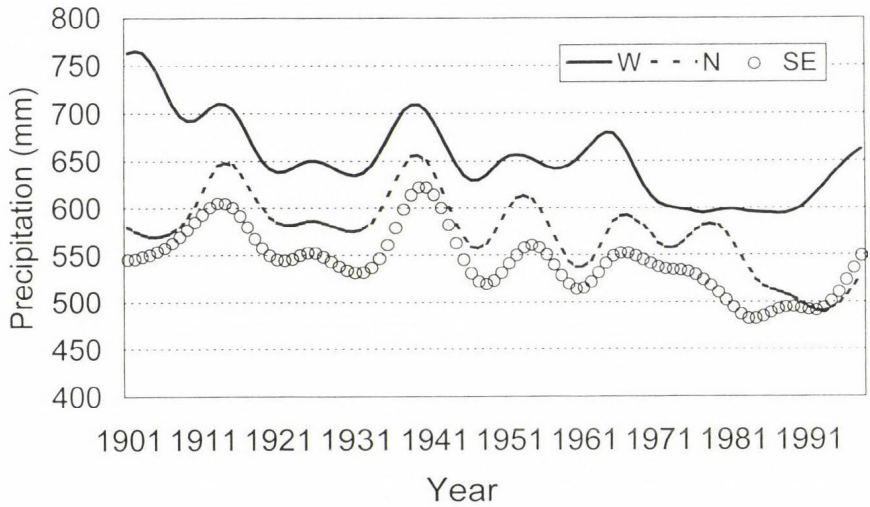

Fig. 1. Annual precipitation totals in the 20th century, over different regions of Hungary. Values are smoothed with a 15-point Gaussian filter.

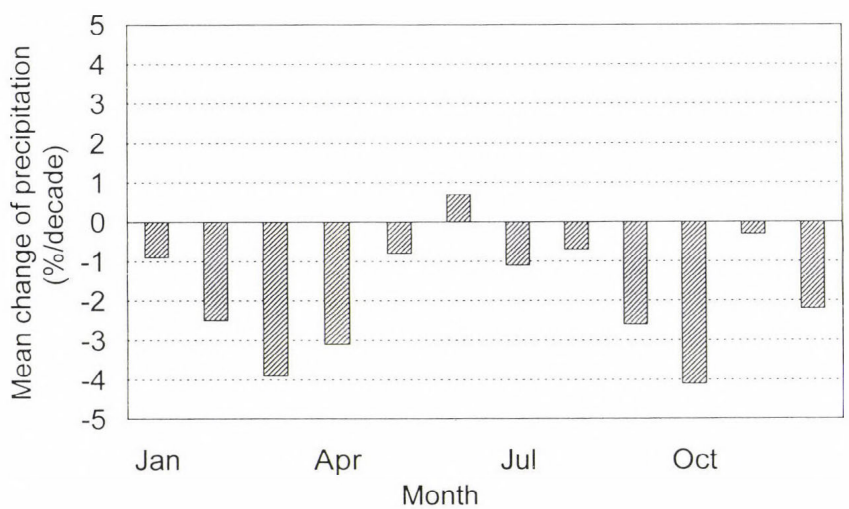

Fig. 2. Mean changes of monthly precipitation amounts in % per decade unit, countrywide averages. (100% = mean value for the 1901–98 period.)

Table 2 presents mean annual changes of precipitation amounts for 1-month and 3-month subperiods. Statistically significant trend values are marked with bold characters. Since the shorter the period, the higher the vari-

ance relative to the average systematic change, trends for individual months are not significant—except for countrywide average precipitation amounts in March (despite of the slightly higher decreasing rate in April and October, the signal-noise ratio is not so clear in any other case). Trends for precipitation totals of 3-month periods are generally not significant either, however, the majority of the trends in Table 2 belonging to early or mid-spring is significant.

Table 2. Mean change of monthly, 3-month and annual precipitation amounts (mm decade^{-1}). Significant trends at the 0.95 level are marked with bold characters

Month	W	N	SE	Mean	3-month	W	N	SE	Mean
January	-0.8	-0.2	0.1	-0.3	DJF	**-3.4**	-2.1	-0.6	-2.0
February	-1.0	-0.6	-0.7	-0.8	JFM	**-3.1**	-2.3	-1.9	**-2.4**
March	-1.3	-1.4	-1.4	**-1.4**	FMA	**-4.1**	-2.7	**-3.8**	**-3.6**
April	-1.8	-0.6	-1.7	-1.5	MAM	**-3.9**	-2.3	**-3.6**	**-3.3**
May	-0.8	-0.2	-0.4	-0.5	AMJ	-1.5	-1.0	-1.8	-1.5
June	1.2	-0.1	0.3	0.5	MJJ	-1.1	-0.9	-0.1	-0.7
July	-1.5	-0.5	0.0	-0.7	JJA	-1.2	-1.1	0.4	-0.6
August	-0.9	-0.4	0.1	-0.4	JAS	-3.8	-2.1	-1.1	-2.4
September	-1.5	-1.1	-1.2	-1.3	ASO	-3.7	-3.6	-3.4	**-3.6**
October	-1.4	-2.1	-2.3	-1.9	SON	-2.6	-3.7	-3.9	-3.3
November	0.3	-0.5	-0.3	-0.2	OND	-2.6	**-3.8**	-2.8	-3.0
December	-1.5	-1.3	-0.2	-1.0	NDJ	-1.9	-2.0	-0.2	-1.3
Annual	**-11.0**	**-9.2**	**-7.7**	**-9.3**					

Fig. 3 shows the long term fluctuations of seasonal precipitation amounts. In accordance with Table 2, slight decreasing trends are visible here. Fig. 3 confirms that the highest amount of precipitation generally falls in summer in Hungary. Nevertheless, it also seems that long term fluctuations and regional differences are the highest in summer too. In the other seasons regional differences are relatively small both in the shapes of the fluctuations and in the absolute values of mean precipitation amounts.

Owing to the decreasing trends in precipitation amounts, frequency of drought events increased during the 20th century. Calculating mean frequencies of PDSI <-3 occurrences from five data series (Mosonmagyaróvár, Budapest, Debrecen, Pécs and Szeged), the results are 8% for the 1901–40 subperiod, 16% for 1941–80 and 24% for 1981–1998. *Szinell et al.* (1998) presented a detailed investigation of drought tendencies in Hungary for the period 1881–1995. According to that, frequency of drought has increased in all sea-

sons. The alterations are mostly significan for moderate drought events, as well as for severe drought events in the eastern–northeastern parts of the country.

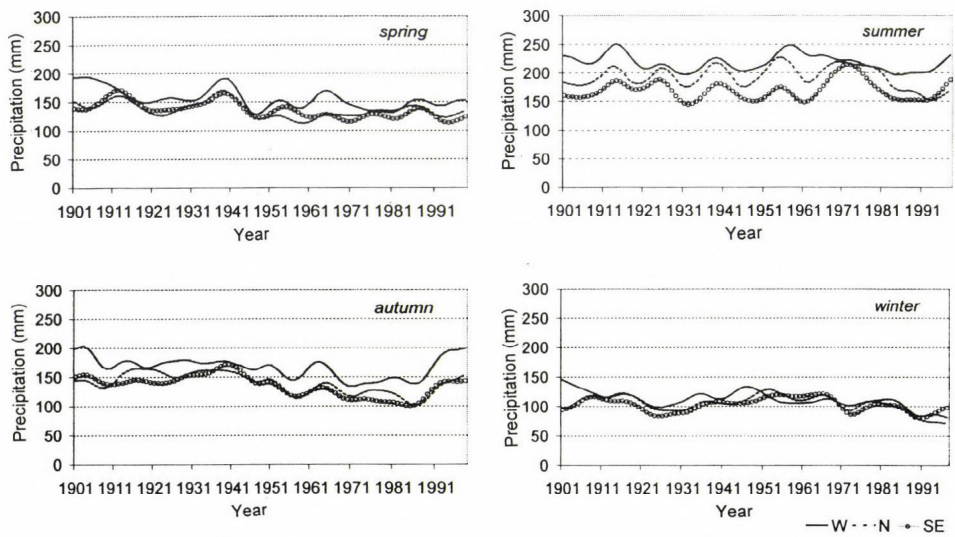

Fig. 3. The same as Fig. 1, but for seasonal precipitation amounts.

Since there are some evidences of a slight global warming in the 20th century (0.5–0.7°C, see *WMO*, 1999) it may be interesting to compare our results with the precipitation change scenario for Hungary referring to a slight global warming. Relying on some statistical connections between local temperature and meteorological variables for the hemispheric scale, some 10% decrease in annual precipitation amount is expected, however, decrease is predicted only for the summer half of the year (*Mika*, 1988; *Molnár* and *Mika*, 1997).

4. Efficiencies of PDSI and SPI in evaluation of drought in 2000

One of the curiosities of drought in 2000 in Hungary was that this event was preceded by an extraordinarily wet period, and there was hardly any transition stage between the two kind of extreme conditions in 1999 and 2000. The time period between September 1998 and December 1999 was unusually wet in the whole territory of Hungary. The precipitation surplus was the highest in the

eastern half of the country, resulting the second wettest year of the 20th century in the Great Hungarian Plain. The area covered by inland waters reached 250 thousand ha in December 1999 and the following 1–2 months. Later on, wetness in the first third of 2000 was changeable. While in January and February the sum of precipitation was half of the climatological average, March and the first week of April was humid again.

The wet early spring was followed by a three months long dryness from April 11 until July 10, the lack of precipitation was rather uniform in the whole country. We note that according to averages of long time series, this 3-month part of the year should be one of the wettest in Hungary, and similar long lasting dry periods very rarely occur in this season. In the beginning the dry weather was favorable for the rapid withdrawal of inland waters. Although at the beginning of May the inland water coverage was still 40 thousand ha, at the same time a considerable large area has already been stricken by the gradually worsening water shortage. By the end of May the inland waters disappeared everywhere, and the moisture-shortage in the upper soil layer reached a severe degree in extensive parts of the country. Since the precipitation falling this time is very important for the plants grown here, the water shortage caused damages in agricultural production. The dry weather still continued in June and in the first third of July. The weather was almost steadily sunny, and daytime temperatures were well above the climatological average. These factors made the PE higher than average worsening the water shortage. As a result of this long lasting unusual weather, a disastrous drought developed in most part of Hungary.

The monthly precipitation amounts compared to the long term averages are shown in *Fig. 4*. In May the precipitation sum was less than half of the usual amount, and in June, which is the wettest month of the year in Hungary on average, the fall was even only the 28% of the climatic normal. The precipitation amounts fell between April 11 and July 10 in Szeged and Mosonmagyaróvár were the lowest ever occurred in the same period of the year in the 20th century. In Miskolc this period of 2000 was the second driest, in Budapest and Szombathely the third driest in the century.

A few weeks of humid weather followed in July, but August was again very dry, the precipitation amount in this month was only 30% of the long term average. The precipitation fell in July could moisten only the upper 20–40 cm layer of the soil, and in August it dried up quickly worsened by the extremely hot weather in the second half of August when the temperature often rose up to 35–40°C. We compared the precipitation amounts fell between May and August with those were measured in the same periods of other years of the 20th century. In Szeged and Budapest the summer of 2000 was the driest in this century, in Szeged 64 mm, in Budapest 79 mm precipitation fell during the

four months. These amounts equal to the sum in one average summer month in Hungary. (In Szeged the new record is only 70% of the earlier measured record.) According to the precipitation fell from May to August, in Mosonmagyaróvár the second, in Miskolc the eighth, in Szombathely the twelfth, in Debrecen the nineteenth, in Pécs the twentieth driest year was the last year of the century. In September and October the dryness continued, but it was spatially not so uniform as before, and in accordance with the seasonal cycle of plants, it caused less harm in the agricultural production than during the previous months.

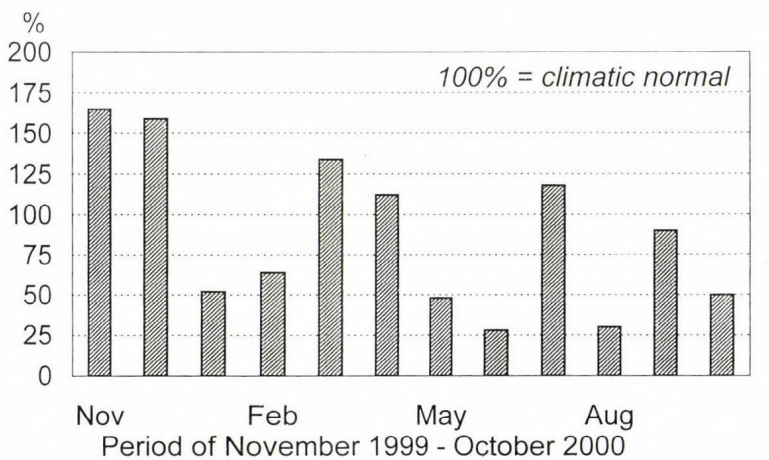

Fig. 4. Monthly precipitation amounts from November 1999 to October 2000, in percentage of climatological normal (1961–1990). Countrywide averages.

Considering that the starting and ending dates of dry periods may occur in any day of a month, drought indices based on merely monthly values of meteorological elements may be insufficient in some cases. For example, the first and very severe dry period leading to the drought focused in this paper lasted from April 7 to July 10, so it was longer than 3 months. As monthly precipitation amounts for April and July were above the normal, the same dryness seems to be substantially shorter relying on the monthly data, and the widely used index values are obviously affected by this shortcoming of the method. Notwithstanding, application of indices derived from monthly precipitation values is appropriate in many cases, especially for characterizing the natural condition in processes which are strongly depend on the long term departures of precipitation amounts.

Considering the different applications, different drought indices may provide the best estimation of a given drought. PDSI and SPI indices for the relevant period were calculated and compared to obtain a more detailed description about the unusually rapid development of drought in 2000. Values of PDSI from November 1999 to October 2000 can be seen in *Fig. 5* for various places of Hungary. In the end of 1999 the values were near normal in the northwestern counties, but extremely high in the Southeast. After December the curves for the southern places show some surprisingly sharp decrease of excess water. This region was very wet in November and December, but in January and February hardly any precipitation fell. In spring and summer the decrease of PDSI values continued throughout the country, but with a much smaller rate than in the beginning of the year in the Southeast. Around the end of the summer the values mostly fell below –3, and the lowest value in Szeged dropped below –5 in October. According to this, the drought was weak or moderate from May to July, but it became severe from the late summer in most part of Hungary.

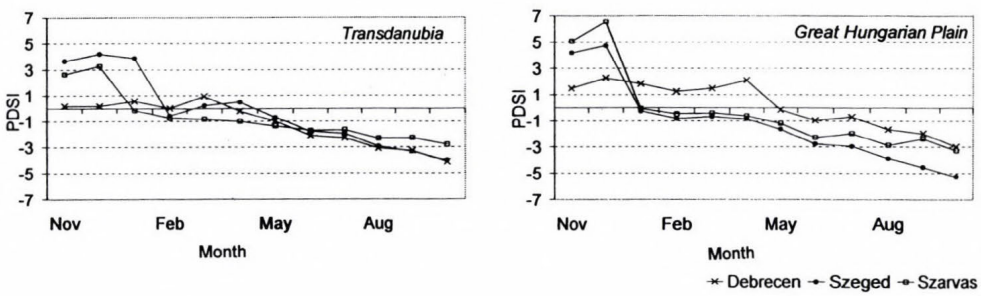

Fig. 5. Values of PDSI from November 1999 to October 2000.

SPI values were calculated for 3, 6 and 9 month periods, for the same locations as the PDSI. These SPI values are presented in *Fig. 6* for the same time period as in Fig. 5. In spring and in summer the prevailing tendency of SPIs is decreasing, similarly to the tendencies of PDSIs. Unusually large decline of SPI values occurred in the Southeast (Szarvas and Szeged) and in Budapest (central-North).

Calculating drought indices, it is obvious that the delay is shorter and the fluctuations are larger for the applications of relatively short time-windows. Among the illustrated indices, the SPI-3 is the most sensitive to the short term changes, and, consequently, it is the only index which indicates moderate wa-

ter shortage even already early in the spring in some places. A few months later, in the beginning of the summer both SPI-3 and SPI-6 indicate drought of moderate to extreme levels in most part of the country. On the contrary, decrease of SPI-9 is rather slow, and indicates moderate drought late in the summer at first.

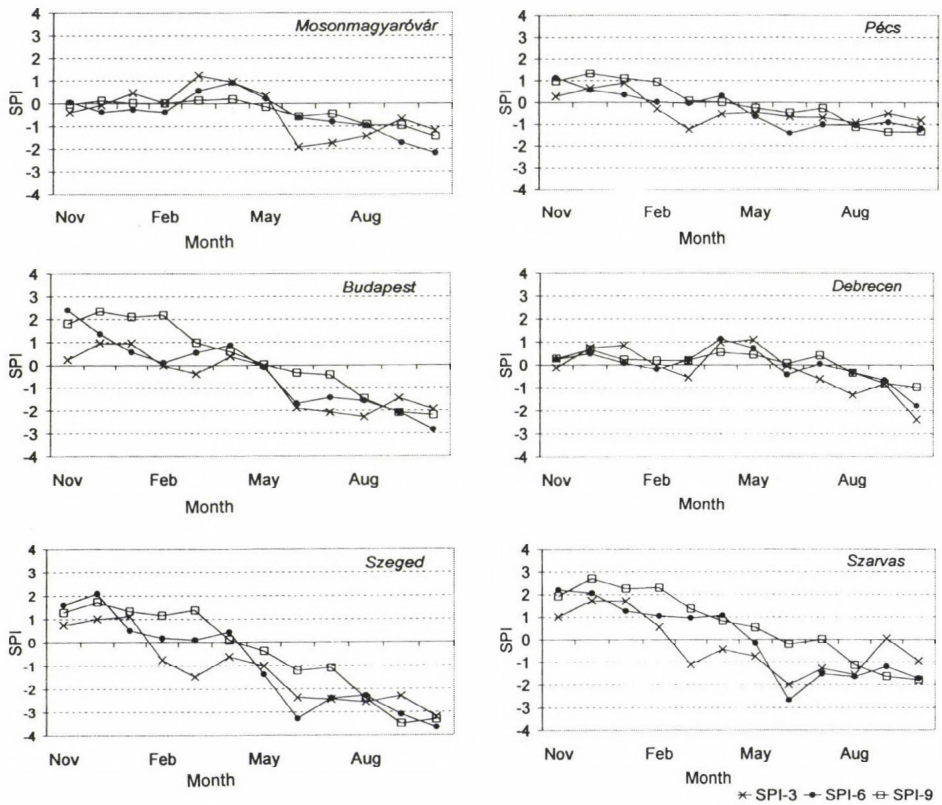

Fig. 6. Values of SPI-3, SPI-6 and SPI-9 from November 1999 to October 2000.

Relying on the presented results, one may conclude that SPI-3 is an appropriate tool for analyzing water supply of sensitive, shallow-rooted plants, since changes of SPI-3 tend to show the changes of moisture content in the upper soil layers in a rather reliable way. SPI-6 can be recommended also for application in the agricultural water management, but for plant species with moderate drought tolerance, since when values of SPI-6 are significantly low, soil must be heavily dried up due to the persistent shortage of precipitation.

SPI-9 and PDSI are not the best tools for indicating a rapid development of agricultural drought, since their persistence is higher than that of originates from the usual storage capacity of available moisture content in the root zone. However, SPI-9 seems to be the most suitable tool for indicating some hydrological conditions: where the water surplus caused extended inland waters in late 1999, values of SPI-9 remained high in the first quarter of the year 2000, and they were still not low late in the spring. The speed of the change in SPI-9 is comparable with the observed withdrawal of the inland waters. SPI-9 may also be appropriate for characterizing the water supply for deep-rooted plants and forests. We cannot state similar good characteristics about PDSI, since we do not know any natural process which would correspond both to the rapid fall after December and to the much slower changes afterwards. This shortcoming of PDSI is a close consequence of its distribution characteristics (*Guttman*, 1998) and known from earlier works (e.g., *Szalai* and *Szinell*, 2000). Limitations in use of PDSI are summarized by *Wilhite et al.* (2000), and similar results related to the effectiveness of PDSI and SPI were found by *Bussay et al.* (2001). SPI is also highly recommended in the two papers last mentioned. Nevertheless we note that use of PDSI also has some advantages: it is a well-known index, and its properties are analyzed in details. Its values are computed and archived over many regions of the world, and as it has only one type, values from any place of the world are comparable well. While application of PDSI seems to be fairly good to obtain a quick survey about changes of water supply, comparative application of SPIs using various time-windows is suggested for a thorough analysis.

5. Conclusions

Systematic changes in precipitation amounts during the 20th century, as well as efficiencies of PDSI and SPI in describing water supply anomalies were investigated using precipitation and temperature data series of observing stations in Hungary. Our main findings are summarized below:

- Annual precipitation amount significantly decreased during the 20th century in all parts of Hungary.
- Precipitation has decreased in all seasons. While the highest decrease rate detected in early and mid-spring, there was hardly any systematic change in early and mid-summer.
- Owing to the decreasing trend of precipitation, frequency of drought events has become higher.

- PDSI and SPI indices follow fairly well the anomalies of plant water supply.
- SPI-6 (SPI-3) is an appropriate tool to characterize water supply condition for plants having average (enhanced) sensitivity to water shortage.
- SPI-9 seems to be an effective tool to follow the slow hydrological processes due to precipitation anomalies.
- Main characteristics of PDSI are similar to those of SPI-6 concerning the time-characteristic of the processes described by them. However, some disadvantages of PDSI were revealed in this study.
- Summarizing our experiences, some kind of parallel use of SPIs applying different time-windows (e.g., SPI-3, SPI-6 and SPI-9 together) may be suggested for overall investigation of natural water supply.

Acknowledgement–This research was funded by the Hungarian Scientific Foundation (OTKA T029374).

References

Akinremi, O.O., McGiun, S.M. and *Cutforth, H.W.*, 1999: Precipitation trends on the Canadian Prairies. *J. Climate 12*, 2996-3003.

Alley, W.M., 1984: The Palmer Drought Severity Index: Limitations and assumptions. *J. Clim. Appl. Meteorol. 23*, 1100-1109.

Briffa, K.R., Jones, P.D. and *Hulme, M.*, 1994: Summer moisture variability across Europe, 1892–1991: An analysis based on the Palmer Drought Severity Index. *Int. J. Climatol. 14*, 475-506.

Brunetti, M., Maugeri, M. and *Nanni, T.*, 2000: Variations of temperature and precipitation in Italy from 1866 to 1995. *Theor. Appl. Clim. 65*, 165-174.

Bussay, A., Hayes, M., Szinell, Cs. and *Svoboda, M.*, 2001: Monitoring drought in Hungary with the Standardized Precipitation Index. *Water Intern.* (in press).

Byun, H.R. and *Wilhite, D.A.*, 1999: Objective quantification of drought severity and duration. *J. Climate 12*, 2747-2756.

Cook, E.R., Meko, D.M., Stahle, D.W. and *Cleaveland, M.K.*, 1999: Drought reconstructions for the continental United States. *J. Climate 12*, 1145-1162.

Curtis, J., Wendler, G., Stone, R. and *Dutton, E.*, 1998: Precipitation decrease in the western Arctic, with special emphasis on Barrow and Barter Island, Alaska. *Int. J. Climatol. 18*, 1687-1707.

De Lúis, M., Raventós, J., González-Hidalgo, J.C., Sánchez, J.R. and *Cortina, J.*, 2000: Spatial analysis of rainfall trends in the region of Valencia (East Spain). *Int. J. Climatol. 20*, 1451-1469.

Dunay, S. and *Czakó, F.*, 1987: Use of meteorological information in agricultural production (in Hungarian). In *Beszámolók az 1984-ben végzett tud. kutatásokról.* Országos Meteorológiai Szolgálat, Budapest, 193-209.

Edwards, D.C. and *McKee, T.B.*, 1997: Characteristics of 20th century drought in the United States at multiple time scales. *Climatology Rep. 97-2*, Dept. of Atmospheric Sci., Colorado State Univ., Fort Collins, CO, 155 pp.

Gunst, P., 1993: The droughts and the Hungarian State (in Hungarian). In *Aszály 1983* (eds.: *Cs. Baráth, B. Győrffy* and *Zs. Harnos*). Kertészeti és Élelmiszeripari Egyetem, Budapest, 131-159.

Guttman, N.B., 1998: Comparing the Palmer Drought Index and the Standardized Precipitation Index. *J. Amer. Water Resour. Assoc. 34*, 113-121.

Hayes, M.J., Svoboda, M.D., Wilhite, D.A. and *Vanyarkho, O.V.*, 1999: Monitoring the 1996 drought using the standardized precipitation index. *Bull. Amer. Meteor. Soc. 80*, 429-438.

Kogan, F.N., 1995: Droughts of the late 1980s in the United States as derived from NOAA polar-orbiting satellite data. *Bull. Amer. Meteor. Soc. 76*, 655-668.

Lettenmaier, D.P., Wood, E.F. and *Wallis, J.R.*, 1994: Hydro-climatological trends in the continental United States, 1948-88. *J. Climate 7*, 586-607.

McKee, T.B., Doesken, N.J. and *Kleist, J.*, 1995: Drought monitoring with multiple time scales. Preprints, *Ninth Conf. on Applied Climatol.*, Dallas, TX, Amer. Meteor. Soc. 233-236.

Mika, J., 1988: Special regional features of global warming in the Carpathian Basin (in Hungarian). *Időjárás 92*, 178-189.

Molnár, K. and *Mika, J.*,1997: Climate as a changing component of landscape: Recent evidences and projections for Hungary. *Zeitschrift für Geomorphologie 110*, 185-195.

Palmer, W.C., 1965: *Meteorological Drought*. US Weather Bureau Research Paper No. 45, Washington DC, 58 pp.

Rodrigo, F.S., Esteban-Parra, M.J., Pozo-Vázquez, D. and *Castro-Díez, Y.*, 2000: Rainfall variability in southern Spain on decadal to centennial time scales. *Int. J. Climatol. 20*, 721-732.

Schönwiese, C.-D., Rapp, J., Fuchs, T. and *Denhard, M.*, 1994: Observed climate trends in Europe 1891-1990. *Z. Meteorol. 3*, 22-28.

Scian, B. and *Donnari, M.*, 1997: Retrospective analysis of the Palmer Drought Severity Index in the semi-arid pampas region, Argentina. *Int. J. Climatol. 17*, 313-322.

Sneyers, R., 1992: Use and misuse of statistical methods for detection of climatic change. In *Climate Change Detection Project, Report on the Planning Meeting on Statistical Procedures for Climate Change Detection*. WCDMP (20), J76-J81.

Stafford, J.M., Wendler, G. and *Curtis, J.*, 2000: Temperature and precipitation of Alaska: 50 year trend analysis. *Theor. Appl., Clim. 67*, 33-44.

Szalai, S. and *Szinell, Cs.*, 2000: Comparison of two drought indices for drought monitoring in Hungary – a case study. In *Drought and Drought Mitigation in Europe* (eds.: *J.V. Vogt* and *F. Somma*). Kluwer, Dordrecht, 161-166.

Szinell, Cs., Bussay, A. and *Szentimrey, T.*, 1998: Drought tendencies in Hungary. *Int. J. Climatol. 18*, 1479-1491.

Wilhite, D.A., Hayes, M.J. and *Svoboda, M.D.*, 2000: Drought monitoring and assessment: Status and trends in the United States. In *Drought and Drought Mitigation in Europe* (eds.: *J.V. Vogt* and *F. Somma*). Kluwer, Dordrecht, 149-160.

WMO, 1999: *WMO Statement on the Status of the Global Climate in 1998*. WMO-No. 896.

Zhang, X., Vincent, L.A., Hogg, W.D. and *Niitsoo, A.*, 2000: Temperature and precipitation trends in Canada, during the 20th century. *Atmosphere – Ocean 38*, 395-429.

IDŐJÁRÁS

Quarterly Journal of the Hungarian Meteorological Service
Vol. 105, No. 2, April–June 2001, pp. 109–126

Selected characteristics of wind climate and the potential use of wind energy in Hungary. Part I

Judit Bartholy and **Kornélia Radics**

Department of Meteorology, Eötvös Loránd University
P.O. Box 32, H–1518 Budapest, Hungary
E-mails: bari@ludens.elte.hu; nelly@nimbus.elte.hu

(Manuscript received 29 December 2000; in final form 12 March 2001)

Abstract—Several authors investigated Hungarian wind characteristics in the last few decades. For instance, *Tar* (1980, 1983) analyzed the entire country. The European Wind Atlas was published in 1989 in Ris , Denmark for the Commission of the European Communities. Shortly after the need of a similar publication for the non-EU member countries emerged and only eight years later just partly satisfied with the Wind Atlas for the Central European Countries (*ZAMG*, 1997). Responding partly for these initiatives, and partly perceiving the increased prosperity of renewable energy resources in this region, in the middle of the 90's a research program started to study and map the wind climate of Hungary to aid on wind energy usage. Within this project, supplementary wind characteristics have been calculated for 13 Hungarian climate stations. Wind measuring field experiments have been performed and analyzed to determine the possible wind energy resources of Hungary. Temporarily operating climate stations have been installed for automated data collection and quality control. Vertical extrapolation of wind potential and calculation of the Weibull parameters have been completed in order to compare available and extractable wind potential. Mean power outputs and errors of using different averaging periods have been estimated. Using the European Digital Terrain Model, the WAsP model have been adapted. Errors of the model have been analyzed by comparing complex (valley of Lake Akkajaure, Sweden) and simple (Hegyhátsál area, Hungary) terrains.

Key-words: renewable energy resources, wind energy, wind climate, statistical time series analysis, wind field modeling.

1. Introduction

Wind energy has been used for a very long time. During the last two millenniums, historical evidence provides information even from Persia, China, and Japan (*Gipe*, 1995). For hundreds of years, wind energy has been used to power

different types of machinery. Later, windmill has been invented to produce an alternate resource. Windmills were utilized first in Denmark (*Hills*, 1994); Paul La Cour built the world's first wind turbine generating electricity in 1891. He was concerned with the storage of energy, and used the electricity from his wind turbines for electrolysis in order to produce hydrogen for the gas light in his school.

At the end of the 19th and beginning of the 20th century, more and more windmills were used to pump water in rural areas and ranches. In Hungary more than 800 windmills worked at that time (*Filep*, 1981). Many of these fell out of use in the 1930s and 1940s, when electricity began to be supplied to these areas. In the 1970s and 1980s, a renewed interest arose in wind technology with rising energy prices and international policy on reduction of emission, but these efforts have once again begun to fall along the wayside despite the potential capacity for development in this area.

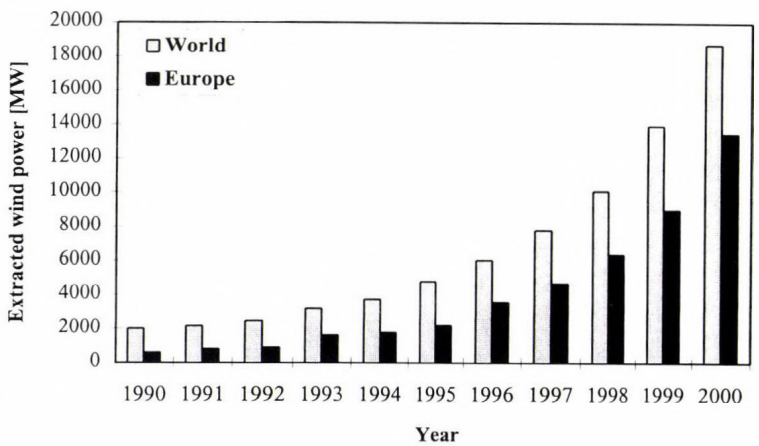

Fig. 1. Extracted wind power in the last decade in Europe and on the whole world (*Heier* and *Kleinkauf*, 2000).

In the last decade, wind energy usage shows definite increasing tendencies in Europe and on the whole world as well (*Fig. 1*). In the 1990–2000 period, the extracted wind power (in MW units) increased approximately twenty times in Europe and eight times in the world (*Heier* and *Kleinkauf*, 2000). Although Hungary is not among the countries having considerable wind power resources, because of the shortage in traditional fuel resources, the rising energy prices, and the unbalanced export-import ratio of energy supply it becomes

necessary to consider and review the usage of our potential renewable energy resources. This was the main purpose of our research project started in 1995. In the first part of this paper we present some of our results on wind climatology and the application of wind energy. First, the main wind characteristics of 13 Hungarian climate stations are discussed. Then, results of two measuring field experiments are presented, comparing available and extractable wind power values. On the basis of the measured time series, errors coming from the different averaging periods are estimated. Finally, two case studies are presented. Namely, wind field simulations have been performed (using the Wind Atlas Analysis and Application Program — WAsP) for two different terrain types to validate the model and verify its adaptability.

2. Wind characteristics of selected stations in Hungary

In order to determine the potentials of wind energy usage in different regions of the country, several wind characteristics have been calculated based on a five year long (1968–1972) hourly time series for 13 meteorological stations in Hungary (*Kovács*, 1996). Wind direction data set is available for 16 sectors, and the accuracy of wind speed data is 0.1 m s^{-1}. Geographical locations and heights of the stations above the sea level are shown in *Fig. 2*. Also, the heights of instruments are indicated. Empirical and statistical data quality controls have been carried out on the raw time series. Because of the different heights of the measuring instruments, further correction was necessary. Wind data have been converted to the standard measuring height (10 m) in order to compare them. Since the necessary parameters for using wind profile equations were not available, only a semi-empirical formula (*Mezősi* and *Simon*, 1981) could be used:

$$v_h = v_{10}\left(0.223 + 0.656 \lg\left(h + 4.75\right)\right), \tag{1}$$

where h indicates height, v_h and v_{10} indicate original and corrected wind speed values, respectively.

Using the transformed wind speed time series, comparative potential wind power study could be carried out for the country. Usually potential wind power is calculated in two different ways. If only wind speed values are known, the available wind power can be defined (*Justus*, 1985) as

$$P = \frac{1}{2}\rho v^3 C, \tag{2}$$

where C is the area of the wind turbine, ρ is the density of air, and v is the

wind speed. To obtain extractable wind power (P^*), the left side of this Eq. (2) should be multiplied with the efficiency (E) of the wind turbine (*Justus*, 1986):

$$P^* = \frac{1}{2} E\rho v^3 C \,. \tag{3}$$

On the other hand, if Weibull parameters are available, potential wind power can be calculated using the gamma function (Γ) (*Troen* and *Petersen*, 1989):

$$P = \frac{1}{2}\rho A^3 \Gamma\left(1+\frac{3}{k}\right), \tag{4}$$

where A and k are the Weibull parameters.

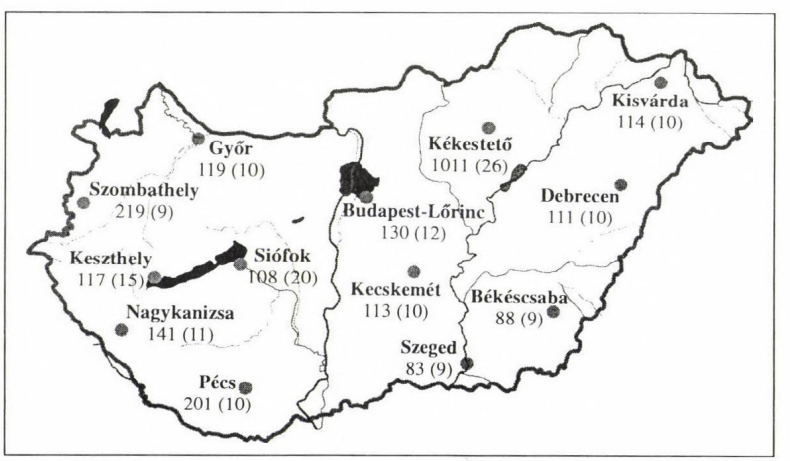

Fig. 2. Geographical locations of meteorological stations.
Height (m) of the station above the sea level and height (m) of the measuring instrument above the surface (in parentheses) are indicated.

In order to provide a better description of regional wind climates, several wind characteristics have been obtained and assembled to climate charts. For this purpose, first we determined seasonality of the wind speed frequencies, annual distribution of wind duration and wind power, monthly wind speed anomalies and their cubic anomalies, relative frequencies of wind speeds in the least windy and the windiest months. For all the 13 stations involved in this research, climatological and energetical diagrams have been assembled considering the structure of the European Wind Atlas (*Troen* and *Petersen*, 1989).

Fig. 3 presents one of the wind climate and energetic diagrams for the meteorological station of Budapest-Lőrinc. On all of these station charts, statistical parameters (at the top) and five diagrams with eleven different climate curves are given as it is detailed below.

(1) Average seasonal variation of wind speed:

a: average seasonal variation of measured wind speed (m s^{-1}) and
b: average seasonal variation of the cube of measured wind speed ($m^3 s^{-3}$).

(2) Wind rose:

c: relative frequencies of wind directions (%),
d: contribution of each sector to total mean speed (%) and
e: contribution of each sector to the cube of total mean speed (%).

(3) Duration and power of wind:

f: duration of wind (hours) and
g: average annual potential power of wind (kWh m^{-2}).

(4) Relative frequencies of wind speeds:

h: relative frequencies for the least windy month,
i: relative frequencies for the windiest month.

(5) Monthly anomalies:

j: monthly average wind speed anomalies (m s^{-1}) and
k: anomalies of the cubes of monthly average wind speeds ($m^3 s^{-3}$).

It is possible to estimate wind potentials of a given region, if potential wind power has been calculated using the Weibull parameters. Based on these results and suggestions of a comparative study on three empirical methods (*Poje* and *Civindi*, 1988), the *Justus* and *Amir Mikhail* (1976) empirical approach has been chosen. This methodology has been applied to extrapolate the Weibull parameters and potential wind power. On the basis of this method, Weibull parameters A and k at level z can be calculated as follows.

$$A(z) = A_a \left(\frac{z}{z_a} \right)^n , \tag{5}$$

$$k(z) = k_a \frac{1 - 0.088 \ln \frac{z_a}{10}}{1 - 0.088 \ln \frac{z}{10}} , \tag{6}$$

where A_a and k_a are parameters at the measuring level z_a and n can be determined as

$$n = \frac{0.37 - 0.088 \ln A_a}{1 - 0.088 \ln \frac{z_a}{10}}. \tag{7}$$

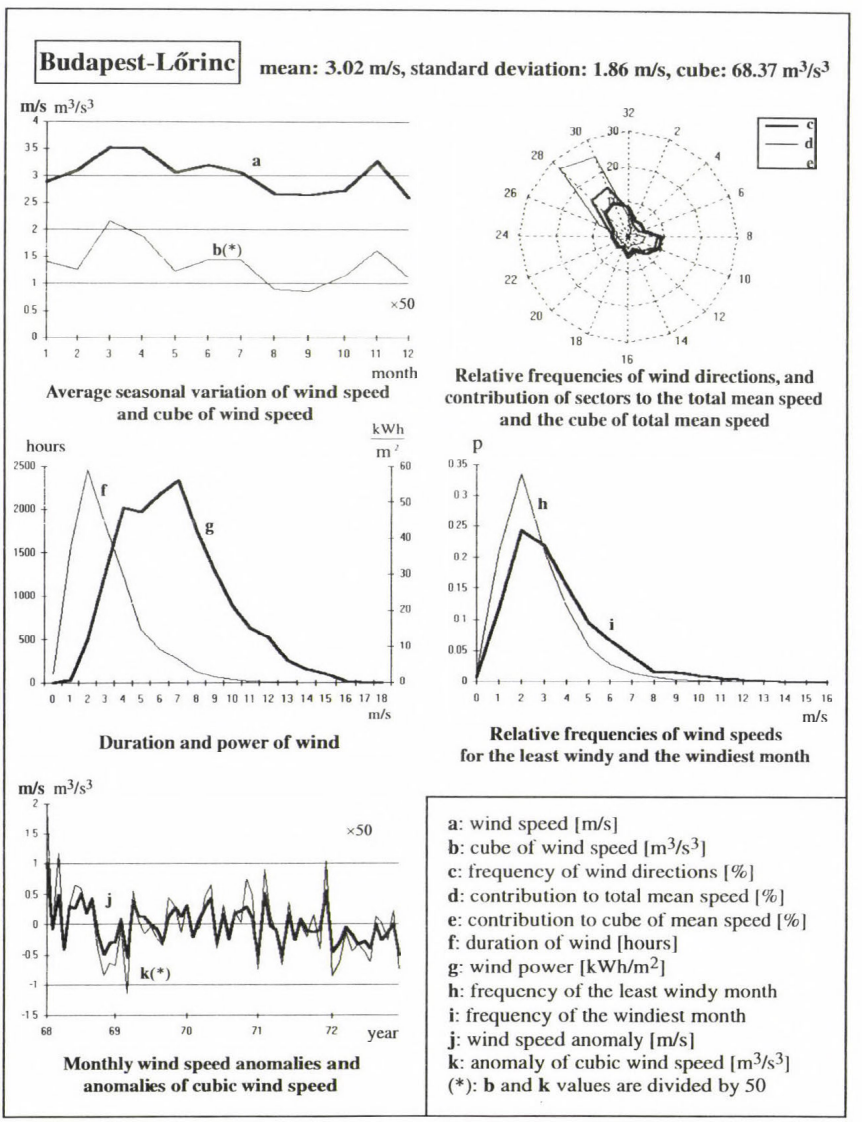

Fig. 3. Wind climatological and energetical diagram for Budapest-Lőrinc station.

For every station, extrapolation has been carried out for the 10 m level. *Table 1* summarizes the extrapolated values for all measuring sites. Both the A and k parameters show relatively small variability. The A parameter has a minimum in Kisvárda ($A=2.24$), and its maximum value occurs in Kékestető ($A=4.55$). From the literature (*Troen* and *Petersen*, 1989), values of A can reach even 8–10 at special seashore stations. The k parameter shows even smaller variability, values are usually between 1.06 and 1.82 m s^{-1}. Consequently, values of the potential wind power are low as well.

Table 1. Weibull parameters and potential wind power. P_1 denotes potential wind power calculated by the cube of averages (Eq. (2)) at 10 m height. P_2 and P_3 are potential wind power values based on Weibull distribution (Eq. (4)) at 10 m and 50 m heights, respectively. The marked (*) value is based on measurements at 26 m height.

	Stations	k (m s^{-1})	c	P_1 (W m^{-2})	P_2 (W m^{-2})	P_3 (W m^{-2})
1.	Békéscsaba	1.48	2.93	32.1	29.3	85.3
2.	Budapest	1.72	3.32	41.0	32.9	97.9
3.	Debrecen	1.52	3.32	45.0	40.2	113.5
4.	Győr	1.41	3.21	39.7	42.0	116.0
5.	Kecskemét	1.65	2.71	20.5	18.4	59.2
6.	Kékes	1.61	4.55	167.4*	93.9	273.8
7.	Keszthely	1.33	2.81	34.9	32.1	90.6
8.	Kisvárda	1.06	2.24	27.6	30.8	82.5
9.	Nagykanizsa	1.17	2.26	24.4	23.2	66.5
10.	Pécs	1.82	3.71	49.3	42.6	123.2
11.	Siófok	1.13	3.34	78.2	82.9	169.7
12.	Szeged	1.60	3.70	60.2	50.9	140.5
13.	Szombathely	1.23	4.49	193.6	158.4	350.9

Potential available wind power values have been calculated using the two above described methods. However, we applied extrapolations not only for 10 m but also 50 m above the ground level in sight of the possible siting of the small and large wind energy conversation systems. Selected results can be found in Table 1. Potential wind power P_1 has been calculated for 10 m using the definition of available wind power as shown in Eq. (2). Power values P_2 and P_3 have been determined at 10 m and 50 m, respectively, based on the Weibull parameters (Eq. (4)). Actual values of P_1, P_2, and P_3 demonstrate well the spatial variability of estimated wind powers in different regions of the country. Furthermore, the difference between P_3 and P_2 is convincing about the importance of the rotor axis height.

3. *Wind measuring field experiments, analysis of possible error sources*

Field experiments carried out in the last five years provided more detailed information of local wind climate which is essential for siting and installing wind power stations. Selected results of two wind measuring field experiments will be discussed. Wind measurements started in Budapest (270 m above the sea level, Szabadság hill, July–August 1995) and in a Hungarian village, Perbál (310 m above the sea level, near the Pilis mountain, September–October 1995). The first site is located on the hilly western side of Budapest, in a residential area with average density of family houses, surrounded by green patches (gardens, parks). The measuring instruments were set on the flat roof of a building (12 m above the ground). The other site (8 m above the ground) had more rural surroundings: outskirts of a small village (24 km from Budapest) and a crop field. For the experimental measurements sonic anemometers (GILL research sonic anemometer) were used since they are suitable for estimating available wind power.

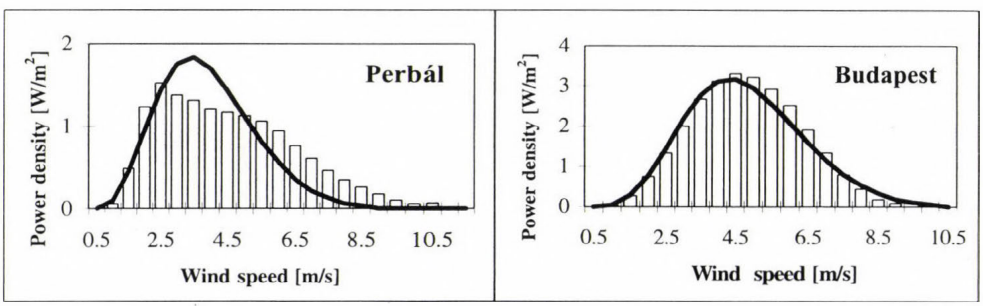

Fig. 4. Wind power density functions of field experiments. Bar values have been calculated using power density of empirical distribution, solid lines indicate estimation of power density based on Weibull distribution.

Wind density functions are good tools to analyze wind speed frequency distributions at a given site. *Fig. 4* compares wind power density functions for the two field experiments. Because of the different measuring conditions (agricultural fields/roof of a tall building), only distributions of wind speed frequencies could be analyzed and compared (*Vigh*, 1996), but not wind power values. Different measuring heights cause significant differences between power density values. In case of the residential area, the power density function has a sharp peak, and no significant differences appear between the estimated power density functions. In case of the rural region, which is a better

environment for steady wind energy production, the errors of the estimations are larger.

Important characteristics of wind generators are the "cut-in" and "cut-off" wind speeds. These characteristics strongly depend on the type and power of the wind energy station. *Fig. 5* compares those parameters for micro (300 W) and small (11 kW) wind turbines using available (Eq. (2)) and extractable (Eq. (3)) wind power terms. Only the area under the available wind energy curves shows the effective power. Although, the power represented by the area between the two curves is present over the geographical terrain, it is not extractable with any generator. The figure illustrates well the importance of siting and selection of the appropriate wind turbine type.

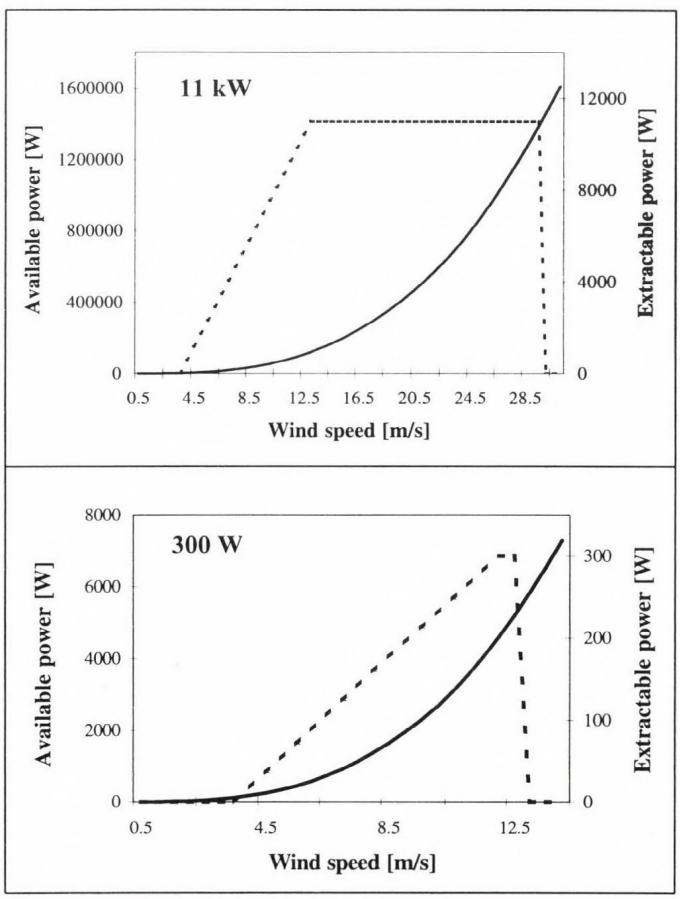

Fig. 5. Available (solid line) and extractable (dashed line) wind power curves for 11 kW and 300 W wind turbines, respectively.

Direct use of the measured wind speed data for wind resource calculations results in power estimations that are representative only for the actual position of the wind-measuring instruments. Characterization of available wind power of various sites of interest is via their average available wind power per unit area. Thus, an averaging process is included. The averaging period is a very important factor of determining the values of wind power (*Bartholy* and *Radics*, 1999). If only the mean speed is known and the mean available wind power is desired, then information about the *energy pattern factor* ($<V^3>/<V>^3$ ratio) is needed. *Fig. 6* gives information about this difference in case of Budapest and Perbál experiments. Note, that the stronger the wind the larger the error values. Therefore, to avoid very large estimation errors, the averaging period should be selected very carefully.

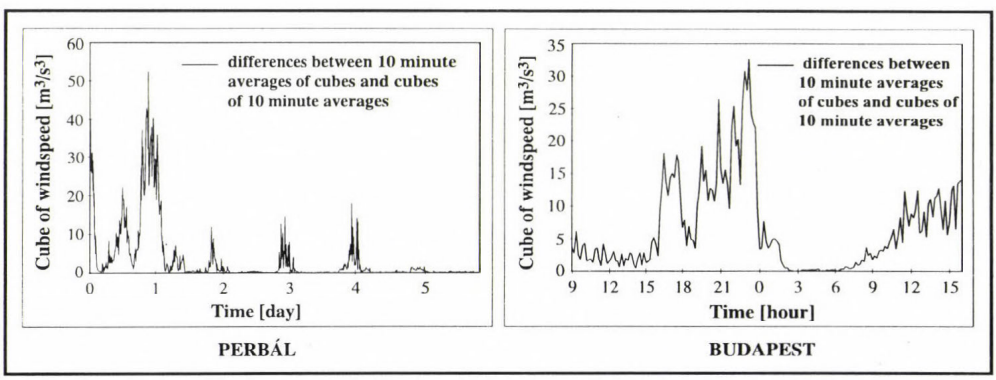

Fig. 6. Energy pattern factors of field experiments.

4. Wind field estimations with the WAsP model

In order to calculate and map the possibilities of potential wind energy usage in Hungary, several wind experiments and measured data series have been analyzed recently for selected subregions and the entire country (*Tar*, 1991; 2000). All of these studies used time series observed at the individual wind measuring stations. Before planning extractable wind power or siting wind power stations, it is necessary to know the spatially continuous wind fields, which can be obtained only by the use of wind models. Based on the recommendations of the European Wind Atlas (*Troen* and *Petersen*, 1989), among several appropriate models we chose the WAsP model (*Mortensen et al.*, 1993).

First we have analyzed the validity of the WAsP model over complex terrains. So, results of observations and model simulations have been compared in case of steep valley and hilly region. Wind data of the profile measurements in Hegyhátsál (Hungary) and from four Swedish stations (Suorva, Ritsem, Vietas, and Juobmotj kk) have been used to analyze and compare the wind climate of those different terrain types. For this purpose, WAsP model simulations have been run using different input data.

The WAsP model was developed at Ris National Laboratory, Roskilde, Denmark. It is a linear spectral model for near neutral boundary layer flow over complex terrain. The model can be used to analyze raw time series and to generate Wind Atlas data, which means that the wind observations have been cleaned from site specific conditions (roughness, shelter, topography). Also, it can be used to estimate the wind climate at any site using digitized topographical, roughness and shelter maps. Finally, it is possible to calculate total energy content of the mean wind, as well as the annual mean power production of a wind turbine, provided that the power curve of the turbine is available.

The WAsP model is based on the transformation of the frequency distributions of wind speed divided into twelve sectors (each of them represents 30 degrees). In order to clear the wind data from site-specific conditions, the model executes a so-called upward transformation, which calculates the geostrophic wind climate for a given region. Initially, three submodels (shelter model, orographic model, and roughness change model) are used to correct the sectorwise histograms of wind speed frequencies. The result is a corrected histogram that would be measured if the obstacles were taken away, the site was flat and the roughness values were low. After these calculations WAsP executes the so-called downward transformation. This process transforms the geostrophic wind distribution to a wind distribution at lower levels considering standard conditions.

The WAsP program allows to determine wind climate of any site during the measuring period if the site description and the Wind Atlas data set is available for the region. This application part of the model is an inverse of the analysis model, where input is the same as in case of calculating the Wind Atlas. In the application model the same submodels are used, however, the obstacle list, roughness description and orographic data are updated according to the new site.

4.1 WAsP simulations for mountainous terrain (case study for the valley of Lake Akkajaure)

First, we analyzed model simulation results for a mountainous terrain, for a steep valley. Since sufficiently long time series of any Hungarian site were not available, in the frame of the MOWIE project we run the model for a Swedish

site. In order to test WasP, one needs at least two simultaneous measurements of wind speed and wind direction from two different measuring stations. Wind data observed at one of the sites are used as input of the model and the corresponding wind field for the other site is calculated. Model output can be directly compared to the measurements. Mean wind speeds for twelve sectors were calculated using the model at Suorva and Ritsem (*Bartholy* and *Radics*, 2000). These stations located in the valley of Lake Akkajaure in the Sjöfallets National Park at northern part of Sweden (*Fig. 7*). Wind fields have been simulated using two different sets of input data measured at 10 m height. Since the main purpose of this analysis is the validation of the model, longer time series were not required (Ritsem: 1981–1995, Suorva: 1995–1996). Nevertheless, estimation of extractable wind power applies decadal timescale. First, input data from Ritsem have been used to simulate wind speed and direction at Suorva. This has been followed by using wind data from Suorva as input data to simulate wind climate at Ritsem station.

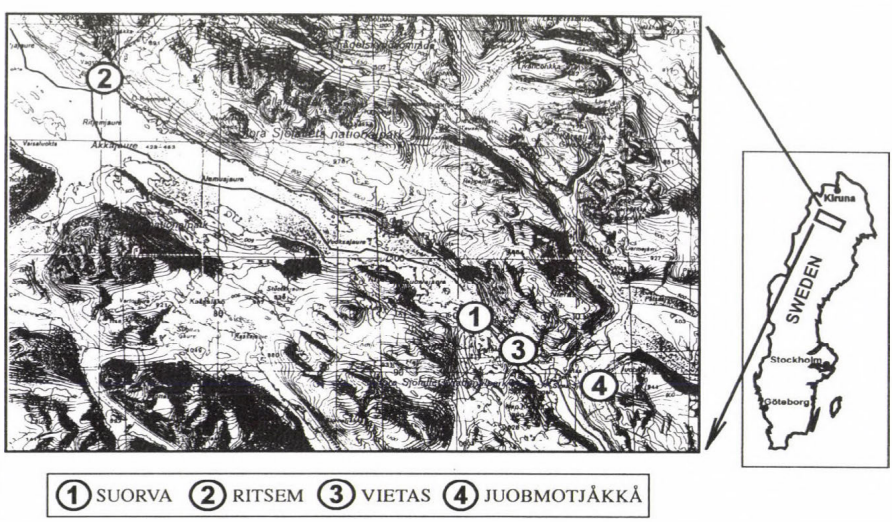

Fig. 7. Measurement stations in the valley of Lake Akkajaure in Sweden.

Topography has been included in WAsP as a height contour map using 100 m isolines. Because of model limitations, a 50 km × 50 km area has been used around the station. In this paper we selected the period between November 1 and May 30 every year assuming that the valley is covered by snow

during this time (geographical location of the stations are at 67°N). Roughness-change lines have been determined by a mathematical routine. Roughness length has been defined as 0.8 m, 0.2 m, and 0.1 m for forests, closed shrublands and open shrublands, respectively. In case of grasslands, barren or sparsely vegetated areas, water bodies, ice and snow covered regions roughness length of 0.001 m has been chosen. There were no obstacles nearby the stations. After calculating the wind atlas data set from the input data, wind field of the given site has been computed by the WAsP model. In the following part of this chapter, simulations will be described separately and then compared.

Measured wind data set of Ritsem has been applied to model wind climate at Suorva for twelve sectors. Simulated mean wind speeds are shown in *Fig. 8* and compared to measured values. The mean wind speed is plotted as a function of the wind direction of the individual sector (spanning over 30 degrees). Simulated mean wind speed is 3.96 m s^{-1}, while the mean wind speed calculated from the observations at Suorva is 6.31 m s^{-1}. So the model significantly underestimates (by 37%) the mean wind speed. In general, values of simulated mean wind speed are too low and differences are very large in the case of northerly, north-westerly and westerly winds. Neither the maximum nor the minimum of the simulated wind are in the same sector as those of the measured wind.

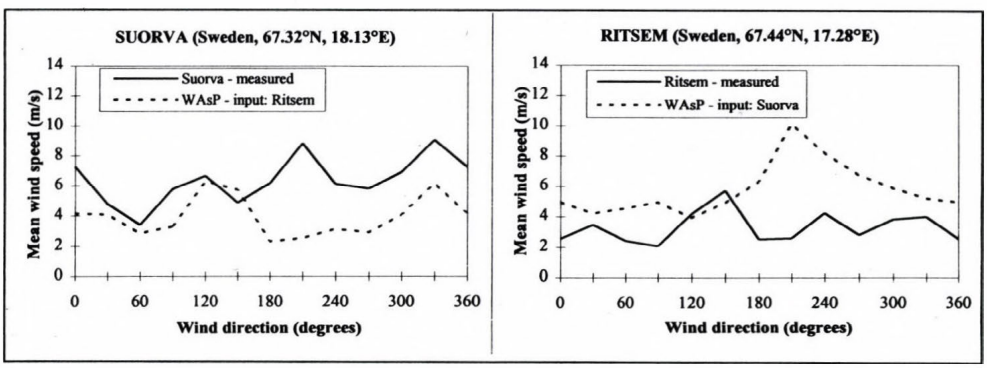

Fig. 8. Comparing measured and simulated wind speed values at Suorva and Ritsem stations.

For comparison, wind data measured at Suorva has been used to model the wind field at Ritsem. Simulated and observed values are compared in Fig. 8. The simulated mean wind speed is 5.83 m s^{-1} while the mean wind speed calculated from the observations at Ritsem is 3.36 m s^{-1}, which is a significant overestimation (with 74%). In this case the values of simulated mean wind

speed are much larger than the wind observed at Ritsem. Nevertheless, the largest differences occur at the same directions as before.

Suorva and Ritsem stations are located in a steep valley. In both cases, simulations fit measurements the best at south-easterly directions. Considering the orientation of the valley (315°–135°), it can be concluded that large errors originate from the steep terrain that surrounds the valley.

Testing the validity of WAsP simulations, data measured at Suorva have been applied to reconstruct wind field at the same site using two different sets of input data (*Sandström*, 1994). First, flat topography has been considered, then zero roughness-change line has been set in the model. The results are shown in *Fig. 9*.

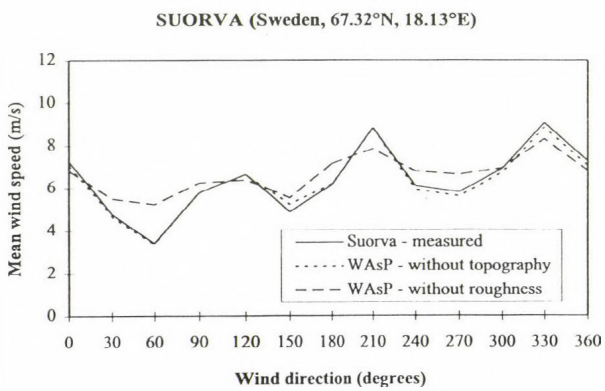

Fig. 9. Comparing measured and simulated wind speed values at Suorva station.

Considering flat topography, simulated mean wind speed is 6.26 m s^{-1}, while the mean measured wind speed is about the same, 6.31 m s^{-1}. The two curves do not differ very much and the courses are almost the same. Without the effect of the regional land use, the simulated mean wind speed is 6.63 m s^{-1}. The model overestimates the mean wind speed by only 5%, however, larger differences appear between the curves than in the previous case. Therefore, it is obvious that the topography is responsible for the large errors of WAsP simulations.

Because of large differences between model outputs and weather station time series, data sets of two other stations (Vietas and Juobmotj kk) of the valley have been included in the analysis. Since large errors have not disappeared in the simulations in spite of increasing the number of input stations, we do not present these other results in detail. After reconstructing wind fields for

all the four stations, it can be concluded that WAsP is not able to model correctly the topographical influences of the steep valley. Therefore, caution is needed when using WAsP in steep terrain.

4.2 WAsP simulations for hilly terrain (case study for Hegyhátsál)

Wind speed and wind direction are measured on a 117 m tall, free-standing TV and radio transmitter tower (*Haszpra et al.*, 2001) owned by Antenna Hungaria Corporation. As shown in *Fig. 10*, the lower part of the tower (56 m) is a 7.75 m diameter cylinder made of reinforced concrete, while the upper part (61 m) is a cylinder of 1.82 m diameter. The tower located in Hegyhátsál, which lays in a flat region of northwestern part of Hungary (46.96°N, 16.65°E), at an altitude of 248 m above sea level. Profile measurements of wind speed began at the end of September 1994 on 4 levels. The measuring station is surrounded by agricultural fields (mostly crops and fodder of annually changing types) and forest patches. Human settlements can be found within 10 km but only small villages with 100–400 inhabitants. The nearest villages are about 1 km to the northwest. The tower is also a NOAA/CMDL global air sampling network site (site code: HUN). In addition, carbon dioxide mixing ratios are continuously monitored at each level, and the atmosphere/surface exchange of CO_2 is measured by eddy covariance at 82 m height.

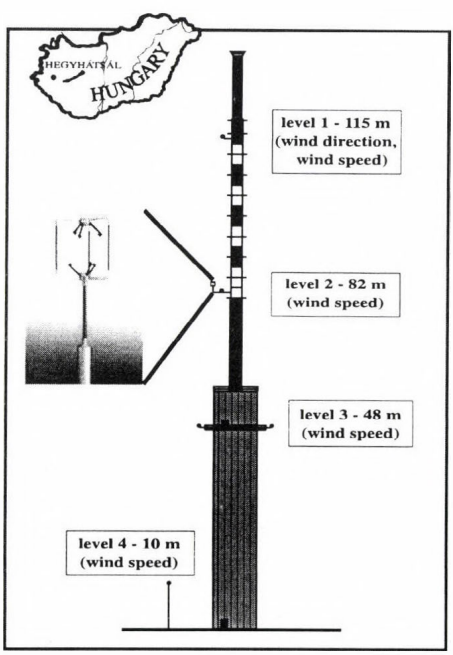

Fig. 10. Wind measuring station in Hegyhátsál.

In order to verify the adaptability of the WAsP model for Hungary, as in case of Suorva, input data measured at Hegyhátsál in 10 meter height have been used to regenerate the wind field at the same site over the hilly terrain. The topography has been included in WAsP as a height-contour map using 25 m isolines. The roughness-change lines have been determined by the same mathematic routine as before. Roughness length has been set to 1 m, 0.5 m, and 0.1 m for forests and cities, villages and orchards, and shrublands or grasslands, respectively. In case of water bodies, 0.001 m has been chosen. Effects of obstacles near the station have been taken into consideration. Results are shown in *Fig. 11*.

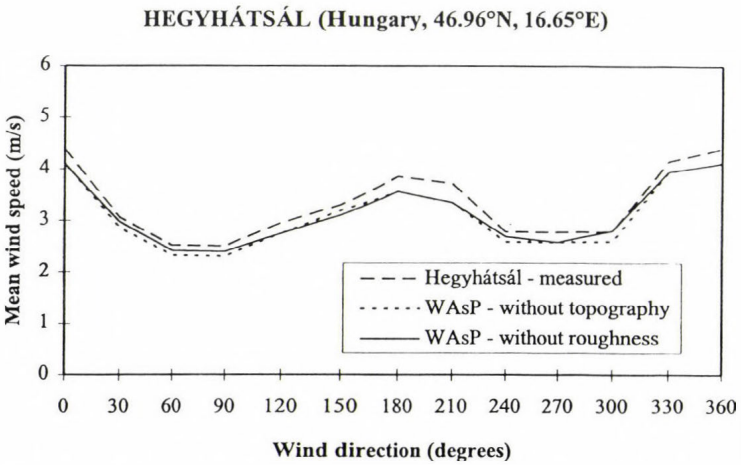

Fig. 11. Comparing measured and simulated wind speed values at Hegyhátsál station.

We did not find considerable differences between measured and simulated values; consequently, topography of flat terrain does not generate remarkable model errors. Therefore, it is possible to extrapolate wind data of Hegyhátsál in order to determine the wind field over the surroundings.

5. Conclusions

Wind climate and renewable energy resources of Hungary are analyzed, specially focusing on wind energy. A summary on recent wind climate research is presented for the Carpathian Basin.

Wind Climate Analysis – Wind Atlas: Field measured wind time series are compared to historical wind archive data. Using wind characteristics of 13 Hungarian climate stations, climatological and energetical diagrams are assembled according to the structure of the European Wind Atlas. On these charts, seasonality of the wind speed frequencies, annual distribution of wind duration and wind power, monthly wind speed anomalies and their cubic anomalies, relative frequencies of wind speeds in the least windy and the windiest month are presented.

Wind energetics: Temporary climate stations have been installed in the frame of field experiments for automated data collection and quality control. Vertical extrapolation of wind potential and calculation of the Weibull parameters were made to compare available and extractable wind power. Mean power outputs and errors of using different averaging times were estimated.

Modeling approaches: Using height and roughness parameters of the European Digital Terrain Model, a mesoscale wind model have been installed, adapted, and tested. Comparing complex and simple terrains, modeling errors are analyzed and the verification were done in the mountainous region of Lake Akkajaure (Sweden) and in a hilly part of western Hungary (Hegyhátsál). The WAsP model is not able to model the topographical influences of a steep valley (Sweden), while over a less complex hilly terrain (Hungary) the results are satisfactory.

Based on the five year results, it has been proved that Hungary has extractable wind power resources which was always used in the ancient times too. Results suggests that now and in the near future supporting energy supply systems can be one of the efficient forms of renewable (wind and solar) energy usage in Hungary.

A second part of this paper will appear soon, where concrete results of model experiments and estimation of local potential wind power will be discussed in order to define the different regions of Hungary on the basis of wind energy usage.

Acknowledgements—*G. Vigh* and *A. Kovács* is thanked for their contribution to the research in its initial phase.

The authors wish to thank the *MOWIE* project (Department of Earth Sciences – Meteorology, Uppsala University, Sweden, JOR3–CT98–0254) for the application of the WAsP model and the measured wind datasets. We thank *H. Bergström* for the helpful advises and comments.

We are very grateful to *L. Haszpra* (Hungarian Meteorological Service) for the wind profile data from Hegyhátsál, to *K. Tar* (University of Debrecen, Department of Meteorology) for the wind database and to *T. Weidinger* (Eötvös University of Budapest, Department of Meteorology) for the digital terrain model. The technical help provided by *Z. Barcza* and *R. Pongrácz* has been very constructive and is highly appreciated.

Research leading to this paper has been supported by the Hungarian National Science Research Foundation under grants T23811, T26629, T25803 and T15707, also, by the Hungarian Higher Education Support Program under grant FKFP-0193.

References

Bartholy, J. and *Radics, K.*, 1999: *Wind climate and wind energy usage in Hungary* (in Hungarian). OTKA (program T015707) Research Paper. ELTE, Budapest.

Bartholy, J. and *Radics, K.*, 2000: *Possibilities of wind energy usage in the Carpathian Basin* (in Hungarian). Egyetemi Meteorológiai Füzetek, No. 14. ELTE, Budapest.

Filep, A., 1981: Windmills (in Hungarian). In *Magyar Néprajzi Lexikon 4.*, Akadémiai Kiadó, Budapest.

Gipe, P., 1995: *Wind Energy Comes of Age*. John Wiley and Sons, Inc., New York.

Haszpra, L., Barcza, Z., Bakwin, P.S., Berger, B.W., Davis, K.J. and *Weidinger, T.*, 2001: Measuring system for the long-term monitoring of biosphere/atmosphere exchange of carbon dioxide. *J. Geophys. Res. 106,* No. D3, 3057-3070.

Heier, S. and *Kleinkauf, W.*, 2000: Wind energy usage in Germany. *Proc. of the Conference on Renewable Energy Resources of Hungary*, Budapest, 353-368.

Hills, R. L., 1994: *Power from Wind. A History of Windmill Technology*. Cambridge University Press.

Justus, C. G. and *Amir Mikhail*, 1976: Height variation of wind speed and wind distribution statistics. *Geophys. Res. Lett. 3*, 261-264.

Justus, C. G., 1985: Wind energy. In *Handbook of Applied Meteorology* (ed.: *D. Houghton*). John Wiley and Sons, New York, 915-944.

Justus, C. G., 1986: Introduction to wind energy. In *Physical Climatology for Solar and Wind Energy* (ed.: *R. Guzzi* and *C.G. Justus*). World Scientific, Singapore, 291-320.

Kovács, A., 1996: *Characteristics of Wind Climate in Hungary Considering Wind Energy Usage* (in Hungarian). Master Thesis, Eötvös Loránd University, Budapest.

Mezősi, M. and *Simon, A.*, 1981: The theory and practice of the meteorological wind measurements (in Hungarian). *Meteorológiai Tanulmányok,* No. 36. Orsz. Meteorológiai Szolg., Budapest.

Mortensen, N. G., Landberg, L., Troen, I. and *Petersen, E. L.*, 1993: *Wind Atlas Analysis and Application Program*. Ris National Laboratory, Roskilde.

Poje, D. and *Cividini, B.*, 1988: Assessment of wind energy potential in Croatia. *Solar Energy 41*, 543-554.

Sandström, S., 1994: WAsP - A comparison between model simulations and measurements. *Wind Energy Report*, WE 94:2, Uppsala University.

Tar, K., 1980: Statistical examination of temporal variability in wind directions (in Hungarian). *Időjárás 84*, 151-159.

Tar, K., 1983: Statistical examination of wind energy (in Hungarian). *Időjárás 87,* 29-37.

Tar, K., 1991: A *Complex Statistical Analysis of the Wind Climatology in Hungary* (in Hungarian). OMSZ Kisebb Kiadványai, No. 67. Orsz. Meteorológiai Szolgálat, Budapest.

Tar, K., 2000: Some statistical characteristics of the wind energy in Hungary in connection with climatic change. *III. European Conference on Applied Climatology*, Pisa, CD ROM.

Troen, I. and *Petersen, E. L.*, 1989: *European Wind Atlas*. Ris National Laboratory, Roskilde.

Vigh, G., 1996: *Possibilities of Wind Energy Usage* (in Hungarian). Master Thesis, Eötvös Loránd University, Budapest.

ZAMG, 1997: *Wind Atlas for the Central European Countries*. Österreichische Beiträge zu Meteorologie und Geophysik, Heft 16, Vienna, 105 p.

BOOK REVIEWS

Jacobson, M.C., Charlson, R.J., Rodhe, H. and *Orians, G.H.* (reds.), 2000: **Earth System Science for Biogeochemical Cycles to Global Changes.** Academic Press, A Harcourt Science and Technological Company, San Diego, San Francisco, New York, Boston, London, Sidney and Tokyo. 527 pages, a large quantity of tables, figures, references and a detailed index.

This book is a good symbol of the present evolution in natural sciences indicating that something is changing in our concept about our planet, Earth. The first point is that classical Earth sciences constitute one unit, thus, for example, it is impossible to understand the atmosphere without the knowledge of processes in other terrestrial spheres. Secondly, by discussing our planet we cannot separate biological and non-biological phenomena, since they are so interrelated that such a separation would make the subject not meaningful. This means that the quality of different environmental media is governed by biogeochemical cycles, by this huge material flow in Nature, controlled by the interaction of the biosphere and other geo-spheres. This material flow is modified in the time being by human activities which alter the surface of the continents and release into the air, soil and water a large quantity of waste materials.

There is still a debate whether *Earth system science* in its present form is an interdisciplinary science or this is a new science, a separate discipline. Even, its name is not clear, since in many countries it is called *environmental science*. Anyway, this new development in sciences indicate without doubt that a new approach is necessary if we want to study our planet and we want to solve global environmental problems mankind is facing. We have to recognize that the investigation of our planet cannot be realized on the basis of classical compartments of natural sciences.

The problem is how to write such a book since we were trained at the universities only for one special branch of sciences. We are geologists, meteorologists, biologists and chemists to mention only some examples. For this reason the chapters of this volume are written by such specialists (American or Swedish) of their own field who have recognized already that Earth system science is a uniform subject. This certainly makes the problems treated more appropriate, but, at the same time, makes the volume a bit less consistent. Each chapter is followed by a detailed literature list and eventually by questions and appendices.

The first part of the book consists of five chapters and it is entitled "*Basic concepts for Earth system science*". In this part the reader find the principles

of biogeochemical cycles as well as the bases of their numerical modeling. The origin and evolution of the planet and its biosphere are also presented together with equilibrium and rate of natural processes. The second part is devoted to the discussion of "*Properties of and transfers between the key reservoirs*". In this part the natural reservoirs (hydrosphere, atmosphere, soils and oceans) are discussed separately by taking into account their role in the control of natural material flows. In this respect the function of tectonic processes and erosion is presented in a separate chapter. The chapter on "*The Atmosphere*", prepared by *R.J. Charlson* from University of Washington, gives an excellent survey of relevant issues of atmospheric physics and chemistry.

The third part contain the most interesting chapters of the volume. It is entitled "*Biogeochemical cycles*". In this part good and up-to-date surveys are presented on the cycles of elements which play an important part in the control of the biosphere and other media of our planet. Thus, the cycles of carbon, nitrogen, sulfur and phosphorus are treated in details in separate chapters, while the cycles of trace metals are summarized in the last chapter of this part of the book. The cycle of metals is exemplified by mercury and copper. Finally, in the last part ("*Integration*") the chapters deal with such important problems as the acid-base and oxidation-reduction balances of the Earth, the coupling of biogeochemical cycles and climate, ice-records of climate changes as well as human modifications of the Earth system leading to global changes.

The present writer believes that even this short review makes it evident that this book is an important publication and its reading can be recommended for everybody who are interested in the evolution, state and function of our planet and its different media including the atmosphere.

E. Mészáros

Ernst, W.G. (ed.), 2000: **Earth Systems, Processes and Issues**. Cambridge University Press, Cambridge, United Kingdom. 566 pages, a large quantity of tables, figures, references and a detailed index.

This book, together with the previous one, indicate unambiguously that we are the witnesses of the birth of a new science. This means that the aim of the present volume is also to discuss our planet as a whole as well as its different spheres, including the biosphere. There is only a minor, but nevertheless important difference. In the book published by the Cambridge University Press plural is used concerning the word "system". Consequently, the expression of

Earth systems science is common in the volume. One can speculate, however, that the use of singular seems to be more appropriate if we want to emphasize the unity of the planet. It is interesting to note that the first part of the book is entitled correctly "*The Earth as a system*". The second difference with the book edited by the Academic Press is the fact that in the present volume no part is devoted to the biogeochemical cycles. Instead, the third (last) part deals with "*Societal and policy implications*" of Earth system(s) studies and engineering. On the other hand the similarity between the two books resides in the fact that even the chapters of the second volume were prepared by different authors specialized in their own respective field.

One of the most important feature of Earth system(s) science is outlined very clearly in the preface of the book. It is stated that the subject matter is based on an elementary course at Stanford University (California) entitled *Introduction to Earth systems* which integrates principle of physical sciences, engineering and economics as they pertain to the global environment. "The philosophy of the presentation is *problem-focused*, not discipline-focused". This aim suggests that we have to forget the classical division of natural sciences if we want to study processes governing our planet.

The second part of the book ("*Natural processes*") is devoted to the presentation of our knowledge (relevant to the subject) of the geosphere, hydrosphere, atmosphere and biosphere. The atmospheric section is written by *R. Chatfield* from NASA Ames Research Center and *S.H. Schneider* from Department of Biological Sciences at Stanford University (note that the latter world-famous atmospheric scientist works in a department of biology!). The atmospheric section consists of four chapters. One of the first two (written by Chatfield) discusses the atmospheric composition and mixing processes including the stratospheric ozone problem, while the other presents a brief summary of atmospheric motions and the greenhouse effect. Schneider's chapters are devoted to the forecasting of future climate (on the basis of past climate) as well as to the precision of the prediction of climate changes.

This is again a book which is recommended for libraries to buy it and for everybody to read it. As the previous volume, this book calls our attention to the fact that the understanding of the Earth's atmosphere is not easy without the knowledge of other parts of our planet.

E. Mészáros

ATMOSPHERIC ENVIRONMENT

an international journal

To promote the distribution of Atmospheric Environment *Időjárás* publishes regularly the contents of this important journal. For further information the interested reader is asked to contact *Prof. P. Brimblecombe*, School for Environmental Sciences, University of East Anglia, Norwich NR4 7TJ, U.K.; E-mail: atmos_env@uea.ac.uk

Volume 35 Number 3 2001

Volume 35 Number 4 2001

Volume 35 Number 5 2001

X. Querol, A. Alastuey, S. Rodriguez, F. Plana, E. Mantilla and *C.R. Ruiz:* Monitoring of PM10 and PM2.5 around primary particulate anthropogenic emission sources, 845-858.

L.D. Montoya and *L.M. Hildemann:* Evolution of the mass distribution of resuspended cat allergen (*Fel d* 1) indoors following a disturbance, 859-866.

C.A. Ross and *S.C. Jarvis:* Measurement of emission and deposition patterns of ammonia from urine in grass swards, 867-875.

U. Janicke and *L. Janicke:* A three-dimensional plume rise model for dry and wet plumes, 877-890.

S.R. Hanna, Z. Lu, H. Christopher Frey, N. Wheeler, J. Vukovich, S. Arunachalam, M. Fernau and *D. Alan Hansen:* Uncertainties in predicted ozone concentrations due to input uncertainties for the UAM-V photochemical grid model applied to the July 1995 OTAG domain, 891-903.

R.B. Ames and *W.C. Malm:* Comparison of sulfate and nitrate particle mass concentrations measured by IMPROVE and the CDN, 905-916.

C. Boissard, X.-L. Cao, C.-Y. Juan, C.N. Hewitt and *M. Gallagher:* Seasonal variations in VOC emission rates from gorse (*Ulex europaeus*), 917-927.

W.R. Stockwell, H. Geiger and *K.H. Becker:* Estimation of incremental reactivities for multiple day scenarios: an application to ethane and dimethyoxymethane, 929-939.

J. Gan, N.E. Megonnell and *S.R. Yates:* Adsorption and catalytic decomposition of methyl bromide and methyl iodide on activated carbons, 941-947.

J. Kukkonen, J. Harkonen, J. Walden, A. Karppinen and *K. Lusa:* Evaluation of the CAR-FMI model against measurements near a major road, 949-960.

P.A. Makar: The estimation of organic gas vapour pressure, 961-974.

D.P. Hereid and *R.K. Monson:* Nitrogen oxide fluxes between corn (*Zea mays L.*) leaves and the atmosphere, 975-983.

X. Li-Jones, D.L. Savoie and *J.M. Prospero:* HNO_3 losses within the cyclone inlet of a diffusion-denuder system under simulated marine environments, 985-993.

Volume 35 Number 6 2001

C.D. Idso, S.B. Idso and *R.C. Balling Jr.:* An intensive two-week study of an urban CO_2 dome in Phoenix, Arizona, USA, 995-1000.

C. Wiedinmyer, S. Friedfeld, W. Baugh, J. Greenberg, A. Guenther, M. Fraser and *D. Allen:* Measurement and analysis of atmospheric concentrations of isoprene and its reaction products in central Texas, 1001-1013.

T.J. Butler, G.E. Likens and *B.J.B. Stunder:* Regional-scale impacts of Phase I of the Clean Air Act Amendments, the USA: the relation between emissions and concentrations, both wet and dry, 1015-1028.

B.A. Schichtel and *R.B. Husar:* Eastern North American transport climatology during high- and low-ozone days, 1029-1038.

J.L. Bowen and *I. Valiela:* Historical changes in atmospheric nitrogen deposition to Cape Cod, Massachusetts, USA, 1039-1051.

B.B. Hicks, T.P. Meyers, R.P. Hosker and *R.S. Artz:* Climatological features of regional surface air quality from the Atmospheric Integrated Research Monitoring Network (AIRMoN) in the USA, 1053-1068.

S.A. Fruin, M.J.S. Denis, A.M. Winer, S.D. Colome and *F.W. Lurmann:* Reductions in human benzene exposure in the California South Coast Air Basin, 1069-1077.

C. Anastasio and *K.G. McGregor:* Chemistry of fog waters in California's Central Valley: 1. In situ photoformation of hydroxyl radical and singlet molecular oxygen, 1079-1089.

K.G. McGregor and *C. Anastasio:* Chemistry of fog waters in California's Central Valley: 2. Photochemical transformations of amino acids and alkyl amines, 1091-1104.

NOTES TO CONTRIBUTORS

The purpose of *Időjárás* is to publish papers in the field of theoretical and applied meteorology. These may be reports on new results of scientific investigations, critical review articles summarizing current problems in certain subject, or shorter contributions dealing with a specific question. Authors may be of any nationality but papers are published only in English.

Papers will be subjected to constructive criticism by unidentified referees.

* * *

The manuscript should meet the following formal requirements:

Title should contain the title of the paper, the names(s) of the author(s) with indication of the name and address of employment.

The title should be followed by an *abstract* containing the aim, method and conclusions of the scientific investigation. After the abstract, the *key-words* of the content of the paper must be given.

Three copies of the manuscript, typed with double space, should be sent to the Editor-in-Chief: *P.O. Box 39, H-1675 Budapest,* Hungary.

References: The text citation should contain the name(s) of the author(s) in Italic letter or underlined and the year of publication. In case of one author: *Miller* (1989), or if the name of the author cannot be fitted into the text: *(Miller,* 1989); in the case of two authors: *Gamov* and *Cleveland* (1973); if there are more than two authors: *Smith et al.* (1990). When referring to several papers published in the same year by the same author, the year of publication should be followed by letters a,b etc. At the end of the paper the list of references should be arranged alphabetically. For an article: the name(s) of author(s) in Italics or underlined, year, title of article, name of journal, volume number (the latter two in Italics or underlined) and pages. E.g. *Nathan, K. K.,* 1986: A note on the relationship between photosynthetically active radiation and cloud amount. *Időjárás 90,* 10-13. For a book: the name(s) of author(s), year, title of the book (all in Italics or underlined with except of the year), publisher and place of publication. E.g. *Junge, C. E.,* 1963: *Air Chemistry and Radioactivity.* Academic Press, New York and London.

Figures should be prepared entirely in black India ink upon transparent paper or copied by a good quality copier. A series of figures should be attached to each copy of the manuscript. The legends of figures should be given on a separate sheet. Photographs of good quality may be provided in black and white.

Tables should be marked by Arabic numbers and provided on separate sheets together with relevant captions. In one table the column number is maximum 13 if possible. One column should not contain more than five characters.

Mathematical formulas and *symbols:* non-Latin letters and hand-written marks should be explained by making marginal notes in pencil.

The final text should be submitted both in manuscript form and on *diskette.* Use standard 3.5" or 5.25" DOS formatted diskettes for this purpose. The following word processors are supported: WordPerfect 5.1, WordPerfect for Windows 5.1, Microsoft Word 5.5, Microsoft Word 6.0. In all other cases the preferred text format is ASCII.

* * *

Authors receive 30 *reprints* free of charge. Additional reprints may be ordered at the authors' expense when sending back the proofs to the Editorial Office.

Published by the Hungarian Meteorological Service

Budapest, Hungary

INDEX: 26 361

HU ISSN 0324-6329

IDŐJÁRÁS

QUARTERLY JOURNAL
OF THE HUNGARIAN METEOROLOGICAL SERVICE

CONTENTS

****

http://omsz.met.hu/firat/ido-e.html

VOL. 105 * NO. 3 * JULY–SEPTEMBER 2001

IDŐJÁRÁS

Quarterly Journal of the Hungarian Meteorological Service

Editorial Office: P.O. Box 39, H-1675 Budapest, Hungary or
Gilice tér 39, H-1181 Budapest, Hungary
E-mail: prager.t@met.hu or *antal.e@met.hu*
Fax: (36-1) 346-4809

Subscription by

mail: IDŐJÁRÁS, P.O. Box 39, H-1675 Budapest, Hungary
E-mail: prager.t@met.hu or *antal.e@met.hu*; *Fax: (36-1) 346-4809*

IDŐJÁRÁS

Quarterly Journal of the Hungarian Meteorological Service
Vol. 105, No. 3, July–September 2001, pp. 135–144

Model simulation on the transboundary contribution to the atmospheric sulfur concentration and deposition in Hungary

Ágnes Havasi[1], **László Bozó**[2] and **Zahari Zlatev**[3]

[1]*Department of Meteorology, Eötvös Loránd University,*
P.O. Box 32, H-1518 Budapest, Hungary; E-mail: hagi@nimbus.elte.hu

[2]*Hungarian Meteorological Service,*
P.O. Box 39, H-1675 Budapest, Hungary; E-mail: bozo.l@met.hu

[3]*National Environmental Research Institute of Denmark,*
P.O. Box 358, DK-4000 Roskilde, Denmark; E-mail: zz@dmu.dk

(Manuscript received August 13, 2001; in final form August 30, 2001)

Abstract—Reduction of sulfur emissions in Europe during the past decades have positively contributed to limit exposure to acidification. Based on long-range transport model computations by means of Danish Eulerian Model (DEM) as well as regional background concentration/deposition measurements, the transboundary contribution to the Hungarian sulfur concentration and deposition was estimated for the period of 1989–1998. It was found that despite the intense reduction of sulfur emission in Hungary during the period investigated, Hungary's own sources still significantly contribute to the sulfur deposition in the country. Measured versus modeled sulfur data for Hungary as well as ratios of transboundary and Hungary's own sulfur fluxes are presented and discussed in the paper.

Key-words: transboundary air pollution, Danish Eulerian Model, sulfur deposition.

1. Introduction

European countries of medium or smaller sizes are considerably exposed to the effects of transboundary air pollution. It is caused by the fact that the average atmospheric residence times of several pollutants (e.g., SO_2, sulfate particles) are in the range of a few days that makes possible to transport these species several hundred kilometers far away from their emitting sources. Due to the

deep economic changes during the past decade in the eastern part of Europe, their energy and industry structures were reorganized that resulted in significant decrease of sulfur emission. In the same time, other European countries reduced their sulfur emissions as well. Out-of-date industrial technologies in Hungary are being replaced by less energy consumer and more environment friendly ones. Equipping huge sulfur emitting lignite based thermal power plants with high efficiency sulfur and particle filters is in process at several power plants of Hungary. The rate of annual sulfur emission decreased from 550 kilotonnes (in sulfur) to 300 kilotonnes (S) between 1989 and 1998 (*EMEP,* 2000).

The main goal of present paper is to investigate how the transboundary sulfur flux and its contribution to the Hungarian regional background concentration and deposition rate changed between 1989 and 1998. Computations were based on the two-dimensional version of the European-scale Danish Eulerian Model (DEM) with 50 km × 50 km spatial resolution. Calculations presented in this paper are based on meteorological data obtained by use of EUROLAM, a version of HIRLAM developed at the Norwegian Meteorological Institute in Oslo. (A description of EUROLAM can be found e.g., in *HIRLAM,* 1996.) Regional background air pollution data gained from the EMEP network (including Hungarian monitoring sites) were used for the verification of the model.

2. Description of the Danish Eulerian Model and the model simulations

Part of the results presented in this paper were obtained by using the two-dimensional version of the Danish Eulerian Model. This model has been developed at the National Environmental Research Institute of Denmark for studying the long-range transport of air pollutants over the European region (*Zlatev*, 1995; *Zlatev et al.*, 1994, 1996).

The three-dimensional version of the model is based on the system of q partial differential equations:

$$\frac{\partial c_s}{\partial t} = -\frac{\partial (uc_s)}{\partial x} - \frac{\partial (vc_s)}{\partial y} - \frac{\partial (wc_s)}{\partial z}$$

$$+ \frac{\partial}{\partial x}\left(K_x \frac{\partial c_s}{\partial x} \right) + \frac{\partial}{\partial y}\left(K_y \frac{\partial c_s}{\partial y} \right) + \frac{\partial}{\partial z}\left(K_z \frac{\partial c_s}{\partial z} \right)$$

$$+ E_s - (\kappa_{1s} + \kappa_{2s}) c_s + Q_s(c_1, c_2, ..., c_q), \quad s = 1, ..., q. \qquad (1)$$

Here the unknown concentrations of the chemical species involved in the model are denoted by c_s, u, v and w are the wind velocities, K_x, K_y and K_z are the diffusion coefficients, the source term is denoted by E_s, κ_{1s} and κ_{2s} are the deposition coefficients (for dry and wet deposition, respectively) and the chemical reactions are described by $Q_s(c_1, \ldots, c_q)$. The chemical scheme used at present in the DEM contains $q = 35$ species, so 35 partial differential equations are solved.

It is difficult to treat the system (1) directly. This is the reason why some operator splitting procedure is applied during the numerical solution. A splitting technique, based on ideas proposed in *Marchuk* (1985) and *McRae et al.* (1984) leads, for $s = 1, 2, \ldots, q$, to five sub-models, representing the horizontal advection, the horizontal diffusion, the chemistry (together with the emission terms), the deposition and the vertical transport:

$$\frac{\partial c_s^{(1)}}{\partial t} = -\frac{\partial (u c_s^{(1)})}{\partial x} - \frac{\partial (v c_s^{(1)})}{\partial y},$$

$$\frac{\partial c_s^{(2)}}{\partial t} = \frac{\partial}{\partial x}\left(K_x \frac{\partial c_s^{(2)}}{\partial x} \right) + \frac{\partial}{\partial y}\left(K_y \frac{\partial c_s^{(2)}}{\partial y} \right),$$

$$\frac{\partial c_s^{(3)}}{\partial t} = E_s + Q_s(c_1^{(3)}, c_2^{(3)}, \ldots, c_q^{(3)}),$$

$$\frac{\partial c_s^{(4)}}{\partial t} = -(\kappa_{1s} + \kappa_{2s}) c_s^{(4)},$$

$$\frac{\partial c_s^{(5)}}{\partial t} = -\frac{\partial (w c_s^{(5)})}{\partial z} + \frac{\partial}{\partial z}\left(K_z \frac{\partial c_s^{(5)}}{\partial z} \right). \qquad (2)$$

The discretization of the spatial derivatives in the sub-models leads to the solution (successively at each time-step) of five systems ($i = 1, 2, 3, 4, 5$) of ordinary differential equations:

$$\frac{dg^{(i)}}{dt} = f^{(i)}(t, g^{(i)}), \quad g^{(i)} \in R^{N_x \times N_y \times N_z \times q}, \quad f^{(i)} \in R^{N_x \times N_y \times N_z \times q}, \qquad (3)$$

where N_x, N_y and N_z are the numbers of grid-points along the coordinate axes, the functions $f^{(i)}$, $i = 1, 2, 3, 4, 5$ depend on the particular discretization

methods used in the numerical treatment of the different sub-models, while the functions $g^{(i)}$, $i = 1, 2, 3, 4, 5$ contain approximations of the concentrations at the grid-points of the space domain. (More details about the splitting procedure and about the numerical treatment of the sub-models can be found, among others, in *Alexandrov et al.* (1997), *Hov et al.* (1988) and *Zlatev* (1995)).

The space domain of the model contains whole Europe together with parts of Asia, Africa and the Atlantic Ocean. In the basic version, which is also used in this study, the horizontal plane has been discretized by using a 96 × 96 grid, which means that the number of grid-cells is 9216 and the grid resolution is approximately 50 km × 50 km. (This is a sub-grid of the original 150 km × 150 km resolution EMEP grid.) In the vertical direction the grid is non-equidistant: the increments are smaller close to the surface and become larger towards the top boundary. Ten vertical layers are used at present.

The initial conditions for the system (1) are either available from a previous run of the model or obtained after a five-day start-up period. In the latter case the computations are started five days before the desired starting date with some background concentrations, and the concentrations found at the end of the fifth day are actually used as initial concentrations.

The lateral boundary conditions are represented in the DEM with typical background concentrations varied both diurnally and seasonally. The upper boundary condition is similar to that used in *Simpson* (1992) (see the curves in Fig. 2 in this reference).

The meteorological and emission input data have been prepared within the EMEP (*Vestreng* and *Støren*, 2000) and provided by the Norwegian Meteorological Institute.

The meteorological data contain horizontal wind velocity fields, vertical wind velocity fields (on the top of the boundary layer), precipitation fields, humidity fields, cloud covers, mixing heights and pressures. The resolution of the meteorological fields is coarser than the resolution used in the model: the time resolution for all fields except the mixing height fields is six hours (for the mixing height fields the resolution is 12 hours), while the spatial resolution is approximately 150 km × 150 km. Simple linear interpolation rules are used both in time and space to calculate the grid-point values for the finer grid of the DEM.

Emission of five chemical species are taken into consideration in the DEM: SO_2, NO_2, anthropogenic VOC, ammonia-ammonium and natural VOC emissions. The emission data in the first four fields are annual totals available on a 50 km × 50 km grid. Simple rules are used to get seasonal variations for the SO_2 emissions and the ammonia-ammonium emissions. Both seasonal variations and diurnal variations are simulated for the NO_x emissions and for the anthropogenic VOC emissions.

3. Results of the model computations

DEM model outputs for SO_2 concentrations in 1997 were compared with those of measured at 3 monitoring sites in Hungary. Results are plotted in *Fig. 1.*

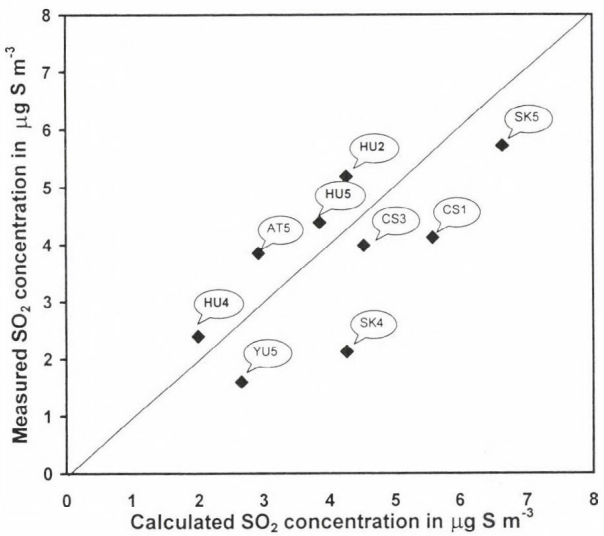

Fig. 1. Measured *vs* computed SO_2 concentrations (annual averages for 1997) at selected monitoring sites in central Europe.

Abbreviations of HU2, HU4 and HU5 represent K-puszta (central part of Hungary), Farkasfa (western part of Hungary) and Hortobágy (eastern part of Hungary), respectively. Results from a few other stations located in the Czech Republic (CS) , Austria (AT) , Slovakia (SK) and Yugoslavia (YU) are also plotted in the figure. It can be seen that model simulations slightly underestimate the annual average concentrations for all three Hungarian stations. The plots are, however, very close to the theoretical fitting line. Regarding the Hungarian monitoring sites, the lowest annual average concentrations in 1997 were simulated and measured for Farkasfa, while the highest ones for K-puszta. There is a factor of 2.2 between the annual average concentrations measured at K-puszta and Farkasfa. There is a four years long (1997–2000) simultaneous SO_2 measurement record from Farkasfa, K-puszta and Hortobágy. Sampling is based on 24 h exposure times at all the three stations. Annual averages are shown in *Fig. 2.* It can be concluded from the figure that each station recorded a decreasing concentration trend: lowest averages were calculated for Farkasfa while the highest ones for K-puszta during the entire

observation period. It can be stated that western part of the country is less exposed to atmospheric SO_2 pollution than central and eastern parts of Hungary.

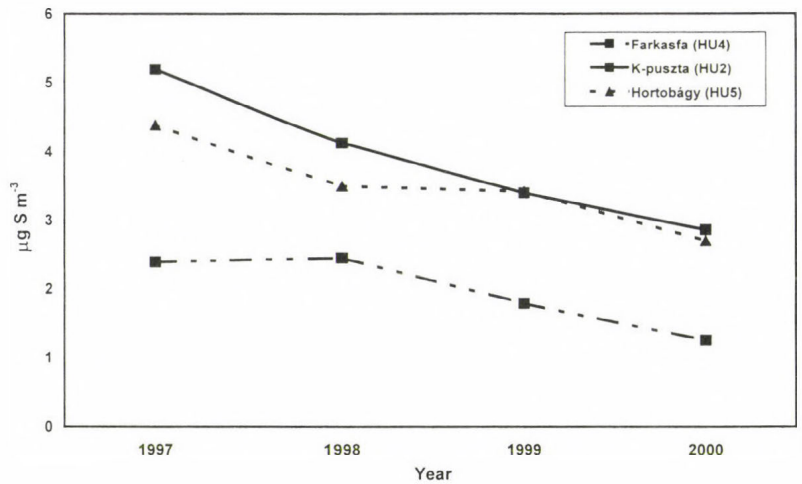

Fig. 2. Annual averages of SO_2 concentrations at three sites in Hungary, 1997–2000.

Model computations were performed with DEM to estimate annual average sulfur-dioxide concentrations in Hungary. Temporal variation of the modeled SO_2 concentration in Hungary during the period of 1989–1998 is shown in *Fig. 3.* Concentration values were averaged for the grids covering Hungary. It was estimated by means of model computations, to which extent the transboundary sources contributed to the sulfur-dioxide concentration over Hungary. Due to the model outputs, the percentage contributions of transboundary sulfur-dioxide emitters varied between 49% (in 1996) and 54% (in 1990 and 1992). Measured annual average sulfur-dioxide concentrations are also indicated in the figure: for the period of 1989–1992 only the data from K-puszta station were available, and between 1993–1995 even this sulfur-dioxide data record is incomplete and can not be used for evaluation. In 1996, however, two additional stations, Farkasfa and Hortobágy joined the regional background air pollution monitoring network in Hungary: the average of their annual sulfur-dioxide concentrations is plotted in the figure for the period of 1996-1998. It should be noted, that despite the continuous decrease in SO_2 emissions in all countries in the region during the second half of the 90's, a local annual maximum was detected in 1997 at all Hungarian stations as well as in the DEM model outputs. It might be explained by the variation of mete-

orological parameters (wind direction, precipitation amount, atmospheric stability, etc.) that requires further investigation in the future.

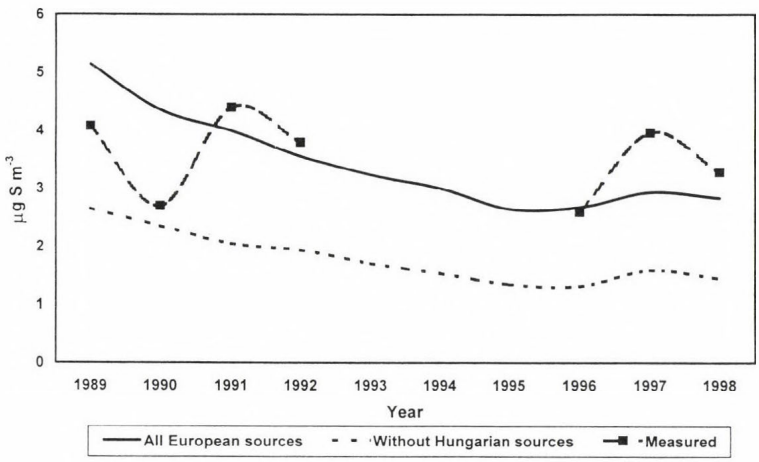

Fig. 3. Results of annual average SO_2 concentration simulations and measurements.

Temporal variations of measured and computed sulfate wet depositions are plotted in *Fig. 4.* Model computations were performed for two different cases:

(1) including all European sulfur sources and

(2) European sources without the input of Hungarian emitters.

It can be concluded from the model calculations that percentage contribution of transboundary sources to the wet sulfur depositions varied between 53% (1996) and 58% (1993) so Hungarian emitters are responsible for wet sulfur deposition at a rate of less than 50%. Wet deposition of sulfur is measured by means of wet only samplers at the regional background air pollution stations. Rate of wet sulfur deposition is calculated by multiplying the sulfate concentration by the amount of precipitation. Results of measurements are also plotted in the figure. It can be seen that rather good agreement between the modeled and observed (K-puszta) values was found for the period of 1993–1998. For the period of 1989–1992, model outputs significantly overestimate the rate of sulfate deposition measured. It should be noted, however, that measurements carried out at K-puszta station might not be representative for the whole country where the outputs of model computations refer to.

Wet deposition of sulfur-dioxide and sulfate can only been measured altogether as the sulfate content of precipitation. Based on DEM parameterization, the rain-out and wash-out processes for sulfur-dioxide and sulfate were separated. *Fig. 5.* shows the rate of wet sulfate deposition and the fraction of sulfate deposited over Hungary originates from sulfur-dioxide. It was estimated that SO_2 contributes at a rate of approximately 80% to the rate of wet sulfate deposition in Hungary.

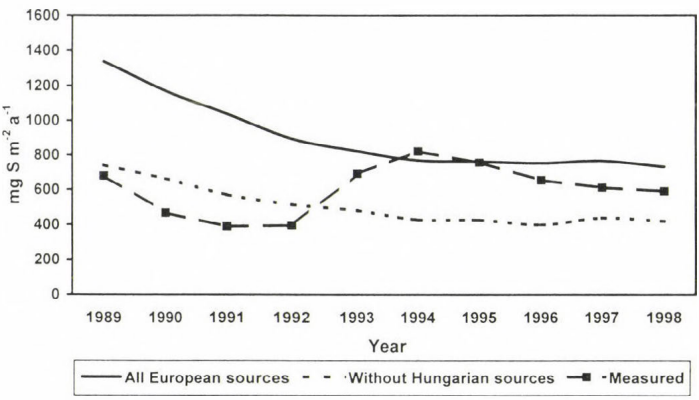

Fig. 4. Results of the simulations and measurements for the rate of wet sulfate deposition.

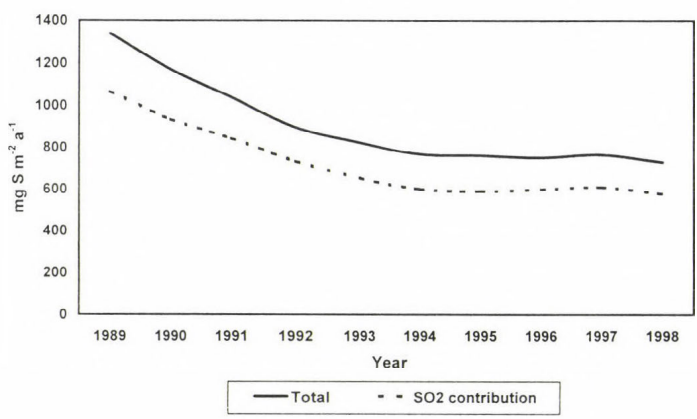

Fig. 5. Plot of SO_2 contribution to the rate of wet sulfate deposition in Hungary, simulated by DEM.

Transboundary contribution to the rate of sulfur deposition in Hungary was compared with the outputs for the same country computed by means of the EMEP Eulerian model (*EMEP,* 2000). Results of comparison is shown in *Fig. 6.*

Based on the EMEP model computations, 4.7 Mtonnes (S) of the 8.0 Mtonnes (S) deposited on EMEP area was originated from the transboundary exchange of pollution among these countries and neighboring areas. Figure also contains data on the percentage contribution of transboundary sources to nitrogen, lead and cadmium deposition: results for nitrogen were reported in *EMEP* (2000), while percentage contributions of lead were taken from *Bozó* (2000), whose computations were performed by means of a European scale Lagrangian-model (TRACE) developed for the investigation of the long-range atmospheric transport and deposition of trace metals. Data for cadmium were obtained from *Ilyin et al.* (2001). It can be concluded from the figure that there is a good agreement between the outputs of DEM and EMEP models for sulfur deposition. Rates of percentage transboundary contributions to lead and cadmium depositions are considerably higher than those of acidifying and eutrophying sulfur and nitrogen compounds.

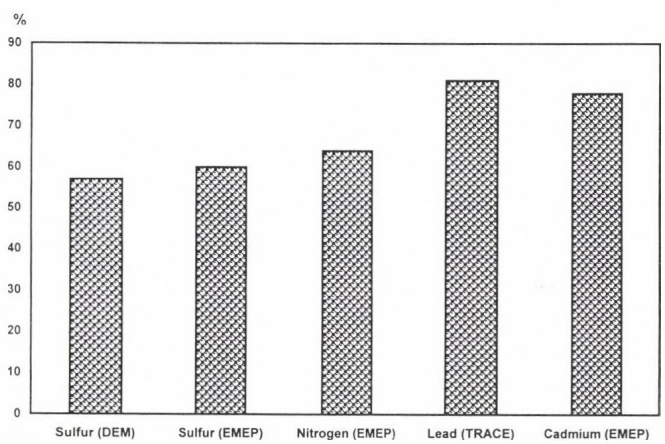

Fig. 6. Percentage contribution of transboundary sources to the total sulfur, nitrogen, lead and cadmium depositions in Hungary.

4. Conclusions

- Model simulations performed by DEM slightly underestimate the annual average concentrations for all the three Hungarian stations. There is little bias in annual averages for 1997.

- Each Hungarian regional background station reported a decreasing concentration trend of sulfur-dioxide between 1997–2000: lowest averages were calculated for Farkasfa (western part of Hungary), while the highest ones

for K-puszta (central part of Hungary) during the entire observation period. It can be stated that western part of the country is less exposed to atmospheric SO_2 pollution than central and eastern parts of Hungary.

- Model outputs show that the percentage contributions of transboundary sulfur-dioxide emitters to the ambient concentration level in Hungary varied between 49% (in 1996) and 54% (computed for 1990 and 1992).
- Percentage contribution of transboundary sources to the rate of wet sulfur depositions in Hungary varied between 53% (1996) and 58% (1993), so Hungarian emitters are responsible for wet sulfur deposition at a rate of less than 50%.
- It was estimated that SO_2 contributes at a rate of approximately 80% to the rate of wet sulfate deposition in Hungary.

Acknowledgements—This paper was partly supported by Hungarian Scientific Research Fund (OTKA T031997).

References

Alexandrov, V., Sameh, A., Siddique, Y. and *Zlatev, Z.*, 1997: Numerical integration of chemical ODE problems arising in air pollution models. *Environmental Modelling and Assessment 2,* 365-377.

Bozó, L., 2000: Estimation of historical atmospheric lead (Pb) deposition over Hungary. *Időjárás 104*, 161-172.

EMEP, 2000: Transboundary Acidification and Eutrophication in Europe. *EMEP Report 1/2000.* Norwegian Meteorological Institute, EMEP CCC and MSC- West.

HIRLAM, 1996: Documentation Manual, *HIRLAM PROJECT,* Research and Development Division, Norwegian Meteorological Institute, PB43, Blindern, 0313 Oslo, Norway.

Hov, Ø., Zlatev, Z., Berkowicz, R., Eliassen, A. and *Prahm, L. P.*, 1988: Comparison of numerical techniques for use in air pollution models with non-linear chemical reactions. *Atmospheric Environment 23,* 967-983.

Ilyin, I., Ryaboshapko, A., Afinogenova, O., Berg, T. and *Hjellbrekke, A.-G.* 2001: Evaluation of transboundary transport of heavy metals in 1999. Trend analysis. EMEP Report 3/2001. EMEP MSC - East.

Marchuk, G. I., 1985: Mathematical modelling for the problem of the environment. *Studies in Mathematics and Applications 16,* North-Holland, Amsterdam.

Simpson, D., 1992: Long-period modelling of photochemical oxidants in Europe. Model calculations for July. *Atmospheric Environment 26A,* 1609.

Vestreng, V. and *Støren, E.*, 2000: Analysis of UNECE/EMEP emission data, MSC-W Status Report 2000. *EMEP MSC-W Note 1/00, July 2000.* Meteorological Synthesizing Centre - West, Norwegian Meteorological Institute, P.O. Box 43 - Blindern, N-0313 Oslo 3, Norway.

Zlatev, Z., Dimov, I. and *Georgiev, K.*, 1994: Studying long-range transport of air pollutants. *Computational Science and Engineering 1*, 45-52.

Zlatev, Z., 1995: *Computer Treatment of Large Air Pollution Models.* Kluwer Academic Publishers.

Zlatev, Z., Dimov, I. and *Georgiev, K.*, 1996: Three-dimensional version of the Danish Eulerian Model. *Zeitschrift für Angewandte Mathematik und Mechanik 76*, 473-476.

IDŐJÁRÁS

Quarterly Journal of the Hungarian Meteorological Service
Vol. 105, No. 3, July–September 2001, pp. 145 –156

Characterization of atmospheric aerosol particles over Lake Balaton, Hungary, using X-ray emission methods

J. Osán[1†], B. Alföldy[1], S. Kurunczi[1], S. Török[1], L. Bozó[2], A. Worobiec[3], J. Injuk[3] and R. Van Grieken[3]

[1]*KFKI Atomic Energy Research Institute, P.O. Box 49, H-1525 Budapest, Hungary*
[2]*Hungarian Meteorological Service, P.O. Box 39, H-1675 Budapest, Hungary*
[3]*Department of Chemistry, University of Antwerp, Universiteitsplein 1, B-2610 Antwerpen, Belgium*

(Manuscript received May 24, 2001; in final form August 6, 2001)

Abstract—Aerosol samples were collected using Berner-type cascade impactor and stacked filter units at Siófok during four campaigns in 1999 and 2000. A total of 40 bulk samples were measured using X-ray fluorescence (XRF). The concentrations of light elements in individual particles were calculated using a reverse Monte Carlo method developed at the University of Antwerp. The particles were further classified using hierarchical and non-hierarchical cluster analyses. Around 25,000 individual particles were analyzed by computer-controlled electron probe microanalysis (EPMA). In order to determine the possible sources of the aerosol particles, the combined data set of the bulk XRF and single-particle EPMA results was subjected to principal component analysis. The obtained analytical results were compared to the air mass backward trajectories, showing good correlation for the sampling periods. The composition of the aerosol did not show characteristic seasonal variation, it was more correlated to the origin of the incoming air mass.

Key-words: aerosol deposition, single particle analysis, light element analysis, X-ray fluorescence.

1. Introduction

Lake Balaton is the largest lake in Central Europe (596 km^2). It has shallow water (average depth is 3 m, maximum depth is 11 m) and hence, because of its relatively low water volume, it is very vulnerable to pollution problems; indeed, dilution of pollutants is limited in Lake Balaton. On its northern part,

† Corresponding author; E-mail: osan@sunserv.kfki.hu

it is surrounded by picturesque hills and small villages. From May to September, many Hungarian tourists, and also millions of foreign visitors take their vacation there. The population around the Lake is several times higher in summer than in winter. A number of Government Decisions were issued during the last decade to improve the water and air quality in the region. They included the cleaning of the Zala river, which empties into Lake Balaton, the building up of the whole sewage water drain system around the Lake, etc. Environmental and human health concerns of atmospheric aerosol pollution in the region are three-fold:

- atmospheric deposition and accumulation of toxic metals and nutrients from urban and industrial emissions into the Lake with possible adverse effects on the ecology;
- air quality (inhalation); and
- visibility (controlled by sulfate particles).

So far, no extended environmental campaigns, with emphasis on the atmospheric heavy metal and nutrient inputs, have been carried out in the Lake region. It is suspected that the atmosphere could be an important source of environmental deterioration of the Lake, relative to the pollutant supply by rivers and direct discharges. Aerosol monitoring took place recently around the Lake, but the analyses included only concentration, fractionation and deposition of non-volatile heavy metals (*Hlavay et al.,* 2001). Only a preliminary paper appeared hitherto on the deposition of nitrogen and phosphorus into Lake Balaton (*Horváth et al.,* 1981). As such, we would like to pay attention to the following target compounds:

(i) particulate nitrogen and phosphorus compounds;

(ii) aluminum, silicon, manganese and iron which have also biological roles; and

(iii) heavy metals, which have been recognized as being toxic, i.e., chromium, nickel, copper, zinc, cadmium and lead.

On a global and regional scale, atmospheric inputs to the ocean environment are known to be an important source of nutrients like nitrogen and bioavailable trace elements, including silicon, manganese, iron, cobalt, nickel, copper and zinc, which play a key role in primary production and influence oceanic productivity. With respect to heavy metals, direct deposition from the atmosphere was recognized about fifteen years ago as a potentially major input for the North Sea (*Van Malderen et al.,* 1992). In this study, the findings for oceanic environments will be compared to the situation over a shallow lake.

Low-Z elemental analysis is mandatory when nutrient elements like nitrogen and phosphorus, have to be determined together with polluting metals. A recently developed method based on thin-window electron probe microanalysis (EPMA) enables the simultaneous determination of major low-Z and minor elements (*Osán et al.,* 2000), even at the single particle level, allowing chemical speciation on a micrometer scale. The full information provided by low-Z EPMA compared with air mass backward trajectories enables the identification of the sources of the particles without the need of combined measurements. In addition, the bulk trace element composition of the aerosol was studied using X-ray fluorescence (XRF) analysis.

2. Experimental

2.1 Samples

Aerosol samples were collected at the Siófok station of the Hungarian Meteorological Service during four campaigns in July 1999, February, June and September 2000. The meteorological station is located at the lakeshore, and can only be reached through a dead-end street with local traffic. The samplers were placed in the grassy backyard, at 2 m height, and around 10 m from the lake. A total of 29 TSP samples were taken on 0.4 μm pore-size Nuclepore filters, for bulk trace element analysis. 24-hour samples were collected daily during the campaigns. Stacked filter units were used for collection of coarse (2.5–10 μm) and fine (<2.5 μm) aerosol particles, for scanning electron microscope (SEM) visualization and single particle analysis. The coarse particles were collected on a 8.0 μm pore size Nuclepore filter, while the fine fraction was obtained on a 0.4 μm pore size Nuclepore filter. A total of 19 sets of size-fractionated samples were collected using a nine-stage Berner-type cascade impactor, on Al, Ag and Be foils as well as Si wafers. The aerodynamic cut-off diameters are 0.0625, 0.125, 0.25, 0.5, 1, 2, 4, 8 and 16 μm, for stages 1–9, respectively. The sampling time varied between 1 (for stage 3) and 240 (for stage 8) minutes, to obtain the best loading of particles in the impacted spots. Around 25,000 individual particles collected on stages 3–7 were analyzed using thin-window EPMA.

2.2 Methods

The bulk trace element analysis of the aerosol loaded Nuclepore filters was performed by an automated Tracor Spectrace 5000 EDXRF system (Tracor X-ray, CA, U.S.A.) coupled with a PC that controls the spectrometer and the

data acquisition. The Spectrace-5000 uses a lower power Rh-anode X-ray tube (17.5 W). In our measurements, the whole white spectrum generated by the tube was used for excitation of the samples under vacuum conditions. Emergent X-rays were detected at 90° relative to the incident X-ray beam by a Si(Li) detector. A standard operating procedure for the XRF analysis of aerosols on filters has been followed according to the guidelines of U.S. Environmental Protection Agency (US EPA). In the calibration procedure, a series of thin film reference standards (Micromatter, Seattle, WA, U.S.A.) were used. The acquired X-ray spectra were deconvoluted with a non-linear least-squares fitting procedure, using the AXIL software (*Vekemans et al.*, 1994). For quantitative analysis of the samples, the fundamental parameter method proposed by *Szalóki* (1991) was used. The accuracy of our measurement is on average 10% depending on the element and concentration, while the precision is around 4%.

The visualization and analysis of particles collected on Nuclepore filter was done using a JEOL 6300 (JEOL, Tokyo, Japan) scanning electron microscope (SEM) equipped with a PGT EDX detector. The detector has a 7.62 μm thick beryllium window, and its energy resolution is 150 eV at 5.9 keV. The conventional single-particle EPMA measurements were carried out at a typical accelerating voltage of 20 kV, and a beam current of 1 nA. The single particles were measured automatically, by scanning the electron beam over the whole projected area of the particles.

The low-*Z* EPMA measurements for the samples collected on metallic foils were carried out on a JEOL 733 electron probe micro-analyzer equipped with an OXFORD energy-dispersive X-ray detector with a super atmospheric thin window (SATW). The resolution of the detector was 133 eV for Mn-Kα X-rays. Measurements on individual particles were carried out automatically as well as manually in the point analysis mode. To achieve optimal experimental conditions, such as low background levels in the spectra and high sensitivity for light element analysis, a 10 kV accelerating voltage was chosen (*Ro et al.*, 1999). In order to minimize the damage of beam sensitive particles such as ammonium sulfate, the measurements were carried out using a liquid-nitrogen-cooled sample stage at a beam current of 1 nA.

Around 100–300 particles were measured in each sample. Morphological parameters such as diameter and shape factor were calculated by the image processing routine of the measuring program. The obtained characteristic X-ray spectra of the particles were evaluated using the AXIL code (*Vekemans et al.*, 1994). Semi-quantitative calculation of the particle composition, including light elements such as C, N and O, was performed by a recently developed approximation method (EP-PROC) (*Osán et al.*, 2000), for the particles collected on metallic foils. The iteration procedure is based on a reverse Monte

Carlo method: in each iteration step, the simulation program calculates the characteristic intensities and a new set of concentration values is determined. Using EP-PROC, the elemental composition of standard particles down to 0.3 μm can be calculated with good agreement between the expected and calculated concentrations (within 3–8% relative) (*Szalóki et al.*, 2000).

3. Results and discussion

3.1 Trace element concentrations

The average and maximum concentrations of trace elements obtained using XRF are shown in *Table 1*, in comparison with the limiting values according to the Hungarian Standard. The obtained concentrations are similar to those found in other areas of Hungary (*Borbély-Kiss et al.*, 1991; *Borbély-Kiss et al.*, 1999), and are in accordance with results obtained by wet chemical methods for the time period of 1995–1998 (*Hlavay et al.*, 2001). The average concentrations are far below the limiting values, and lead is the only element where the maximum concentration is close to the limiting value.

Table 1. Elemental concentrations of TSP samples compared to the limiting values in Hungary

Element	Concentration ($\mu g\ m^{-3}$)		
	Average	Maximum	Limiting value
Al	0.624	1.75	30
Si	1.65	4.96	23.3
P	0.0738	0.149	21.8
S	2.15	5.17	20
Cl	0.0736	0.27	30
K	0.419	1.12	22.6
Ca	1.2	3.38	21.4
Ti	0.042	0.124	n.a.
V	0.00179	0.00724	2
Cr	0.00442	0.0128	1.5
Mn	0.0113	0.0455	1
Fe	0.597	2.14	200
Ni	0.0023	0.00497	1
Cu	0.01	0.0436	2
Zn	0.0384	0.0886	50
Br	0.012	0.0193	10
Rb	0.00271	0.00589	n.a.
Sr	0.0058	0.0128	n.a.
Pb	0.0371	0.106	0.3

There are no large industrial point sources of air pollution near the lake. The nearest power plant, which burns coal, is about 30 km to the northwest. Local sources include motor vehicle emissions and dust suspended by vehicles on paved and unpaved roads or as the result of construction or by wind stress. Leaded gasoline was still widely used in 1995 in Eastern Europe. In Hungary, the lead content of leaded gasoline was decreased to 0.15 g L^{-1} and completely eliminated in April 1999. Some South European countries (e.g., Spain, Italy and Greece), however, asked derogation from the European Union, and they could sell leaded gasoline until the end of 2000. Other heavy metals shown in *Table 1* may originate from oil and coal fired power plants and from waste incinerators. In the former case these emissions are associated with emissions of SO_2, which can be oxidized to sulfate by atmospheric reactions.

3.2 Visualization of particles by SEM

Fig. 1 shows secondary electron images of four typical coarse and fine aerosol particles. By visualizing the samples with SEM, typical particles were found in the coarse fraction as biogenic particles (pollens, spores, algae, plant and insect fragments), crustal particles like aluminosilicates, calcium carbonate and calcium sulfate, as well as salt particles. In the fine fraction, however, irregularly shaped silicates and spherical silicates could be distinguished. The average composition of the particle types in the fine and coarse fractions obtained by single-particle analysis is shown in *Table 2*. A more quantitative description of the different particle types is shown below, in the discussion of the low-Z EPMA results.

3.3 Light element analysis of aerosol particles

In order to obtain information on the possible sources of the aerosol and the possible chemical interactions between gaseous and particulate pollutants, the particles were classified into representative groups using the chemical and morphological data obtained by thin-window EPMA. For comparison of the sample sets collected at different sites and times, all particles for each impactor stage (size fraction) were classified into twelve groups using the non-hierarchical clustering algorithm of Forgy (*Massart* and *Kaufmann*, 1983). The initial centroids for the method were obtained by two steps of hierarchical cluster analysis carried out for each sample using the multivariate statistical software package DPP (*Van Espen*, 1984).

As examples to indicate the differences between small and large particles over Lake Balaton, *Tables 3* and *4* show the classification results for stage 4 and 7, respectively. Particles having an aerodynamic diameter of 0.5–1 μm

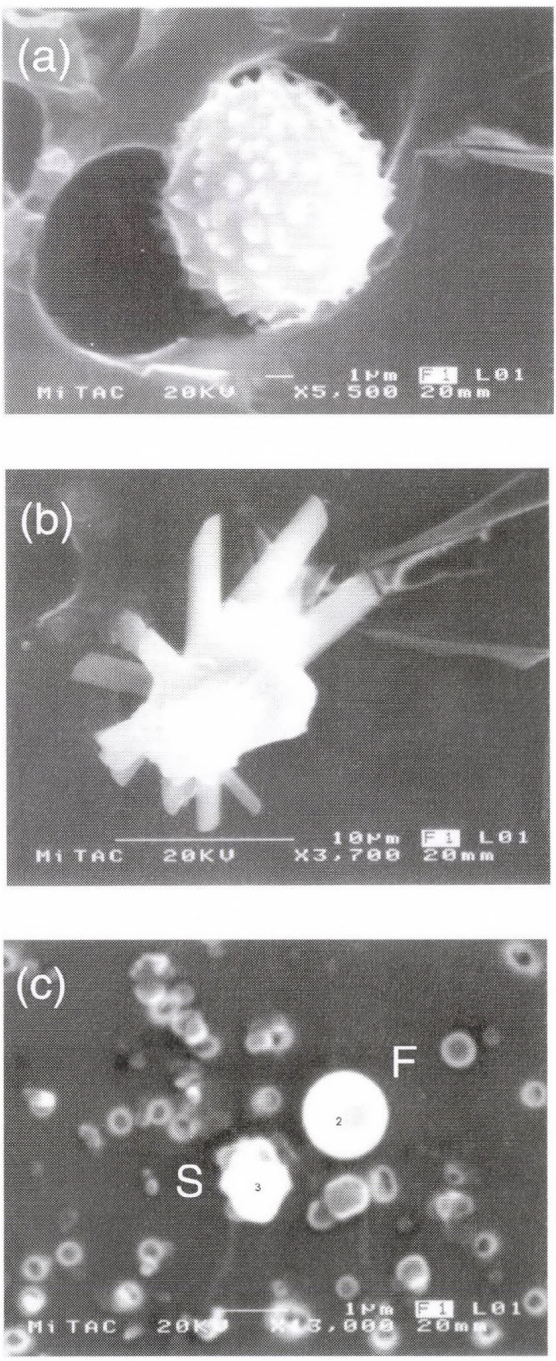

Fig. 1. Secondary electron images of typical aerosol particles collected at Siófok, *(a)* biogenic particle, (*b*) calcium sulfate particle, (*c*) fly-ash (marked as F) and S-rich silicate (marked as S) particle.

were collected on stage 4, while particles with diameters between 4 and 8 μm were collected on stage 7 of the Berner cascade impactor. The majority of the small particles collected on stage 4 are of organic, sulfate and nitrate types. As it can be seen in *Table 3*, the low-Z EPMA method is capable to distinguish different types of sulfur-rich particles, i.e., organic sulfur and ammonium sulfate. The abundance of aluminosilicates is low compared to the larger size fractions, being below 10%.

Table 2a. Average relative X-ray intensity and diameter for the particle types obtained for the stacked filter samples, fine fraction

	Abund.	Diam.	Average relative X-ray intensity (%)											
	(%)	(μm)	Na	Al	Si	S	Cl	K	Ca	Ti	Fe	Cu	Zn	Pb
S-rich	27.6	0.5	0.3	0.0	0.1	98.4	0.0	0.4	0.1	0.0	0.0	0.0	0.2	0.0
Aluminosilicates	19.9	1.1	0.0	20.0	50.1	9.5	0.1	5.5	4.9	0.6	8.2	0.0	0.3	0.0
Fe, S	10.0	0.7	0.0	0.4	3.2	10.9	0.1	0.6	1.4	0.1	79.3	0.2	1.6	0.1
K, S	8.8	0.5	0.6	0.3	2.8	63.8	0.9	20.3	0.7	0.2	4.2	0.6	2.4	0.0
Organic	8.7	0.6	0.1	0.4	0.4	1.3	0.7	0.4	0.3	0.0	0.5	2.0	0.5	0.1
Ca sulfate	7.3	0.7	0.1	0.9	5.6	46.5	0.3	2.0	41.2	0.1	1.9	0.1	0.2	0.0
Quartz	6.2	1.0	0.0	2.1	91.4	3.8	0.1	0.6	0.6	0.1	0.9	0.0	0.0	0.0
Ca-rich	3.7	1.3	0.0	1.2	7.7	6.8	0.8	0.4	76.3	0.0	1.4	0.0	0.1	0.1
K chloride, sulfate	2.5	0.6	0.2	0.0	1.0	12.4	11.4	64.7	1.6	0.2	0.3	0.3	0.4	6.3
Zn, S	1.8	0.5	0.1	0.3	0.5	24.1	0.3	0.2	0.6	0.0	2.8	1.4	62.3	6.8
Pb-rich	1.6	0.5	0.0	0.0	0.2	0.0	0.0	0.2	0.2	0.0	0.0	0.2	1.1	97.6
Cl-rich	1.4	0.5	0.9	0.0	0.9	7.4	74.7	9.9	2.2	0.0	0.0	0.4	0.0	1.9
Ti-rich	0.4	0.7	0.0	2.0	6.1	7.6	0.2	0.1	0.5	79.2	3.2	0.0	0.1	0.0
Na-rich	0.1	0.6	100.0	0.0	0.0	0.0	0.0	0.0	0.0	0.0	0.0	0.0	0.0	0.0

Table 2b. Average relative X-ray intensity and diameter for the particle types obtained for the stacked filter samples, coarse fraction

	Abund.	Diam.	Average relative X-ray intensity (%)											
	(%)	(μm)	Na	Mg	Al	Si	P	S	Cl	K	Ca	Fe	Zn	Pb
Aluminosilicates	31.3	2.9	0.2	0.8	17.6	48.6	0.3	5.6	0.4	6.8	10.7	8.4	0.0	0.0
Ca sulfate	14.2	1.9	0.7	0.7	0.9	4.6	0.6	44.1	1.4	1.5	44.2	1.2	0.1	0.0
Ca-rich	12.7	2.9	0.4	4.0	1.8	9.9	1.2	3.6	1.8	1.2	74.0	1.8	0.0	0.0
Quartz	8.5	2.7	0.2	0.3	3.9	88.0	0.0	1.9	0.1	1.2	2.3	1.9	0.0	0.0
Na, K sulfate	7.6	1.8	4.7	0.6	1.7	8.0	2.0	55.7	1.3	11.5	9.1	3.6	1.1	0.0
S-rich	7.2	1.5	1.7	0.2	0.0	0.6	0.3	92.5	0.0	3.3	0.8	0.3	0.2	0.0
Fe-rich	5.8	2.0	0.1	0.2	0.9	6.2	0.1	6.8	0.4	0.5	3.9	78.0	0.8	0.0
Organic	4.7	1.6	0.5	0.6	0.4	1.5	0.1	1.5	1.8	0.6	1.5	1.0	2.6	0.3
Biogenic	2.9	2.5	0.1	1.0	0.6	3.2	38.3	18.2	6.0	20.6	11.3	0.3	0.1	0.0
Salt	1.7	1.5	9.4	1.0	0.0	0.6	0.2	5.7	75.9	2.5	3.1	0.1	0.6	0.2
Na-rich	1.5	1.5	85.7	0.4	0.0	0.6	0.0	9.0	1.9	0.4	1.8	0.0	0.0	0.0
K-rich	1.1	2.0	0.3	0.4	0.1	2.2	3.9	8.3	4.3	74.2	2.7	0.3	0.3	2.6
Al-rich	0.6	2.2	0.1	0.3	89.6	3.3	0.1	2.6	0.9	0.2	1.5	1.0	0.0	0.0
Pb-rich	0.1	1.1	0.0	0.0	0.0	0.0	0.0	0.0	0.0	2.2	4.1	0.0	2.0	91.7

The time variation of the relative abundance of the particle types obtained is quite high. Although the low-Z EPMA measurements could provide only relative abundances, the significantly high abundance of lead-rich particles observed at the end of September is in agreement with the bulk XRF results showing the maximum lead concentration exactly at that time period. The composition of the "giant" particles collected at stage 7 is different from that of small particles. Crustal particles such as aluminosilicates and calcium carbonate are the most abundant types, followed by biogenic particles. Sulfates, nitrates and salt are less abundant. A high abundance of large ammonium sulfates was observed in September, while small ammonium sulfates were more frequent in the June samples. Sea-salt and aged sea-salt

Table 3a. Average concentration and diameter for the particle types obtained for the samples collected at stage 4 of the Berner impactor

	Abund.	Diam.	Average concentration (wt%)											
	(%)	(μm)	C	N	O	Na	Al	Si	S	K	Ca	Ti	Fe	Pb
Organic + sulfur	20.4	0.9	39.8	8.6	42.8	1.3	0.1	0.1	7.0	0.4	0.0	0.0	0.0	0.0
Organic	15.9	0.9	57.7	4.9	35.6	0.3	0.0	0.0	1.6	0.0	0.0	0.0	0.0	0.0
K sulfate, nitrate	15.1	1.3	8.3	10.6	53.4	0.9	0.0	0.0	14.5	12.2	0.0	0.0	0.0	0.0
Nitrates	9.8	0.6	6.0	10.3	59.3	0.2	0.0	0.2	1.4	0.0	0.0	0.0	22.5	0.0
Ammonium sulfate	9.6	1.0	1.4	6.7	70.2	0.0	0.0	0.0	21.4	0.3	0.0	0.0	0.0	0.0
Aluminosilicates	9.6	1.1	8.3	3.7	54.8	0.0	8.3	20.9	2.1	1.4	0.0	0.0	0.0	0.0
Na sulfate	7.3	0.7	13.2	3.0	52.6	20.3	0.0	0.0	7.3	2.2	0.0	0.0	1.4	0.0
Carbonaceous	4.5	0.9	83.2	0.7	15.8	0.2	0.0	0.0	0.2	0.0	0.0	0.0	0.0	0.0
Ca sulfate	4.2	1.2	10.1	4.4	58.1	0.0	0.6	1.0	5.1	0.0	19.5	0.0	0.0	0.0
Pb-rich	2.1	0.9	3.8	4.8	25.4	0.5	0.0	0.0	5.2	1.9	0.2	0.0	0.0	58.1

Table 3b. Relative abundances (in %) of the obtained particle types in the different samples collected at stage 4 of the Berner impactor

Date of sampling	19	20	16	20	22	23	07	09	11	13	15	20	22	24	25	26	28
	07	07	02	02	02	02	06	06	06	06	06	09	09	09	09	09	09
Origin of air mass			N-	W-		W-	N-	W-		W-				E-			
	n.a.	n.a.	NW	NW	NW	NW	NW	NW	SE	NW	NW	SW	NE	NE	E	E	E
Organic + sulfur	7	21	21	47	25	43	0	5	14	12	7	21	32	19	19	41	17
Organic	2	32	28	6	17	22	0	18	10	3	1	6	33	11	9	18	35
K sulfate, nitrate	3	5	3	21	22	9	9	17	9	6	37	43	10	17	27	16	16
Nitrates	64	6	15	14	16	13	0	3	2	14	1	3	9	0	6	1	4
Ammonium sulfate	11	1	0	2	4	0	81	0	35	2	32	1	1	1	0	1	0
Aluminosilicates	10	11	12	3	3	7	2	14	10	34	15	11	5	3	3	7	6
Na sulfate	0	12	13	3	8	1	0	6	1	10	1	10	2	43	10	3	5
Carbonaceous	1	3	0	1	1	0	1	28	7	3	0	2	4	4	4	9	6
Ca sulfate	2	7	8	3	1	5	0	7	4	11	1	2	3	1	1	0	8
Pb-rich	0	2	0	0	1	0	0	0	0	4	1	1	1	0	21	4	3

particles were observed in the February samples. The original chlorine anion in these particles was substituted by sulfate and/or nitrate through atmospheric reactions with gaseous pollutants (*Kerminen et al.*, 1998).

Table 4a. Average concentration and diameter for the particle types obtained for the samples collected at stage 7 of the Berner impactor

	Abund.	Diam.	Average concentration (wt%)											
	(%)	(μm)	C	N	O	Na	Mg	Al	Si	S	Cl	K	Ca	Fe
Aluminosilicates	26.0	4.6	4.4	3.7	52.0	0.3	2.0	9.3	24.9	0.0	0.0	1.0	2.4	0.0
Ca carbonate	19.2	4.4	5.7	8.1	58.3	0.0	2.3	1.5	2.8	0.1	0.0	0.0	21.1	0.0
Biogenic	13.5	5.6	28.6	11.0	40.3	0.0	0.7	0.0	0.3	0.6	0.0	0.6	17.4	0.0
Ca,Mg sulfate	13.0	4.5	6.8	6.2	62.0	0.9	3.9	0.6	1.4	8.7	0.0	0.0	9.5	0.0
Ammonium sulfate	9.9	5.9	8.7	21.1	54.2	0.1	0.6	0.1	0.0	15.2	0.0	0.0	0.0	0.0
Sodium nitrate	6.5	4.0	0.8	13.3	58.7	21.4	2.5	0.2	0.0	2.3	0.5	0.0	0.4	0.0
Carbonaceous	3.2	5.0	76.1	3.7	19.4	0.0	0.6	0.0	0.1	0.0	0.0	0.0	0.0	0.0
Iron oxide	1.4	3.1	1.1	1.7	33.3	0.0	0.4	0.4	1.0	0.2	0.0	0.0	0.0	61.9
Salt	0.4	2.1	1.7	6.8	24.0	21.0	0.8	0.4	0.4	0.0	44.9	0.0	0.0	0.0

Table 4b. Relative abundances (in %) of the obtained particle types in the different samples collected at stage 7 of the Berner impactor

Date of sampling	19 07	20 07	16 02	18 02	20 02	22 02	23 02	07 06	09 06	11 06	13 06	15 06	20 09	22 09	24 09	25 09	26 09	28 09
Origin of air mass			N-		W-		W-	N-	W-		W-				E-			
	n.a.	n.a.	NW	NW	NW	NW	NW	NW	NW	SE	NW	NW	SW	NE	NE	E	E	E
Aluminosilicates	32	41	40	15	25	32	39	12	59	57	54	17	18	28	4	15	21	38
Ca carbonate	39	34	28	12	32	31	23	26	27	28	34	31	15	9	1	3	7	33
Biogenic	12	14	12	13	8	5	5	15	9	6	6	13	24	11	16	18	24	17
Ca,Mg sulfate	9	7	1	7	7	19	12	12	2	4	3	30	15	40	8	27	12	4
Ammonium sulfate	1	0	0	3	7	3	4	2	0	0	0	0	2	4	66	23	31	0
Sodium nitrate	7	2	4	42	18	2	2	29	1	3	1	8	15	2	2	2	1	0
Carbonaceous	0	1	10	2	0	7	13	1	0	2	1	1	10	5	2	5	3	3
Iron oxide	0	1	3	2	0	1	2	1	2	0	1	0	0	0	0	6	1	4
Salt	0	0	2	4	3	0	0	2	0	0	0	0	0	0	0	0	0	0

3.4 Comparison with air mass backward trajectories

Isobaric trajectories have been compiled at the Hungarian Meteorological Service for the 850 hPa pressure level. It is expected that atmospheric long-range transport processes can be characterized by the wind conditions at that level. In order to determine the possible sources of the aerosol particles, the time variance of the bulk XRF and single-particle EPMA results was studied using principal component analysis. The obtained results were compared to the

850 hPa air mass backward trajectories. The incoming air mass sectors are indicated in *Tables 3* and *4*. During the February campaign, the major components as well as the trace element content did not show significant correlation with the origin of the air mass. For the June and September sampling campaigns, the origin of the air masses could be well explained by the abundance of the particle classes obtained by low-Z EPMA measurements. In June, small sulfate and nitrate particles dominated the samples for marine air masses, and crustal particles were characteristic for trajectories of more continental origin. In September, most of the trajectories crossed Eastern Europe. Large sulfate, nitrate and small lead-rich particles were characteristic for this sampling period. *Fig. 2* shows typical trajectories from June and September 2000.

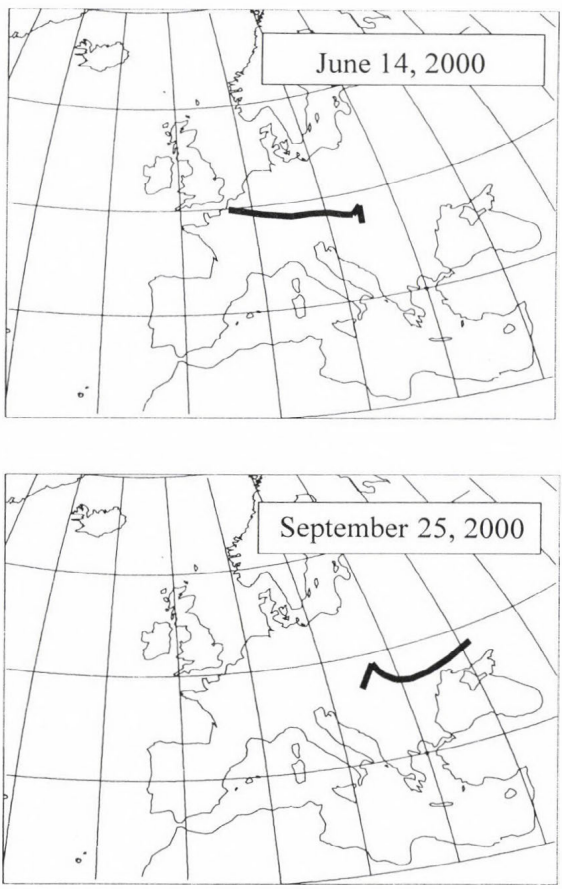

Fig. 2. Air mass backward trajectories calculated for Siófok at the 850 hPa level for 72 h.

4. Conclusions

The combination of bulk XRF and single-particle EPMA combined with cluster and principal component analysis is a powerful tool for characterizing the major, low-Z and trace element composition of atmospheric aerosols. Especially, the low-Z EPMA data were found to be useful for future nutrient deposition calculations for Lake Balaton. The comparison of the analytical data set with air mass backward trajectories yielded good correlation for the sampling periods. The composition of the aerosol did not show characteristic seasonal variation, it was more correlated to the origin of the incoming air mass.

Acknowledgements—The present work was partially supported by the Flemish and Hungarian governments through Joint Project No. B14/98, and by the Hungarian Scientific Research Fund through Project No. OTKA T034195.

References

Borbély-Kiss, I., Bozó, L., Koltay, E., Mészáros, E., Molnár, Á. and *Szabó, Gy.*, 1991: Elemental composition of aerosol particles under background conditions in Hungary. *Atmos. Environ. 25A*, 661-668.

Borbély-Kiss, I., Koltay, E., Szabó, Gy., Bozó, L. and *Tar, K.*, 1999: Composition and sources of urban and rural atmospheric aerosol in Eastern Hungary. *J. Aerosol Sci. 30,* 369-391.

Hlavay, J., Polyák, K. and *Weisz, M.*, 2001: Monitoring of the natural environment by chemical speciation of elements in aerosol and sediment samples. *J. Environ. Monit. 3,* 74-80.

Horváth, L., Mészáros, Á., Mészáros, E. and *Várhelyi, G.*, 1981: On the atmospheric deposition of nitrogen and phosphorus into Lake Balaton. *Időjárás 85,* 194-200.

Kerminen, V.-M., Teinilä, K., Hillamo, R. and *Pakkanen, T.*, 1998: Substitution of chloride in sea-salt particles by inorganic and organic anions. *J. Aerosol Sci. 29,* 929-942.

Massart, D. and *Kaufmann, L.*, 1983: *The Interpretation of Analytical Chemical Data by the Use of Cluster Analysis*. Wiley, New York.

Osán, J., Szalóki, I., Ro, C.-U. and *Van Grieken, R.*, 2000: Light element analysis of individual microparticles using thin-window EPMA. *Mikrochim. Acta 132,* 349-355.

Ro, C.-U., Osán, J. and *Van Grieken, R.*, 1999: Determination of low-Z elements in individual environmental particles using windowless EPMA. *Anal. Chem. 71,* 1521-1528.

Szalóki, I., 1991: Some application of the fundamental parameter method in energy-dispersive X-ray fluorescence analysis by isotope excitation. *X-Ray Spectrom. 20,* 297-303.

Szalóki, I., Osán, J., Ro, C.-U. and *Van Grieken, R.*, 2000: Quantitative characterisation of individual aerosol particles by thin-window EPMA combined with iterative simulation. *Spectrochim. Acta B55,* 1015-1028.

Van Espen, P., 1984: A program for the processing of analytical data (DPP). *Anal. Chim. Acta* 165, 31-49.

Van Malderen, H., Rojas, C. and *Van Grieken, R.*, 1992: Characterization of individual giant aerosol particles above the North Sea. *Environ. Sci. Technol. 26,* 750-756.

Vekemans, B., Janssens, K., Vincze, L., Adams, F. and *Van Espen, P.*, 1994: Analysis of X-ray spectra by iterative least squares (AXIL): New developments. *X-Ray Spectrom. 23,* 278-285.

IDŐJÁRÁS

Quarterly Journal of the Hungarian Meteorological Service
Vol. 105, No. 3, July–September 2001, pp. 157–164

Extreme temperature and precipitation years in Hungary during last century

István Matyasovszky

Department of Meteorology, Eötvös Loránd University,
P.O. Box 32, H-1518 Budapest, Hungary; E-mail: matya@ludens.elte.hu

(Manuscript received March 12, 2001; in final form June 26, 2001)

Abstract—A particular year is called extreme when the actual annual course of a climatic element differs substantially from the average annual course. This concept considers both the magnitude and length of departures from normal. A methodology to measure the difference between an actual and the average year is discussed. The procedure is applied to monthly mean temperatures and monthly precipitation amounts using ten locations in Hungary with homogeneous data sets from 1901 to 1999. Trends of above mentioned differences are analyzed. The chance for extreme years in overall decreases during last century, but there exists a slight tendency of more extreme years from the eighties. The most extreme temperature and precipitation years do not appear simultaneously.

Key-words: extreme year, temporal change, temperature, precipitation.

1. Introduction

Detection and estimation of climatic changes in observed data series have a long history. Data analysis is mainly based on variations of mean, i.e., much of these works applies particular versions of trend models (*Zheng* and *Basher*, 1999). However, several other statistical properties may vary during a changing climate. For instance, long-term change of extremes is an especially important issue for its socio-economic impacts.

The term extreme can be defined by several ways. A typical example is to estimate the probability distribution of the maximum of a climatic element during a given period. Here separate entire years are analyzed and a particular year is called extreme when the actual annual course differs substantially from the average annual course. This concept considers both the magnitude and length of departures from normal.

A methodology to measure the difference between an actual and the average year is discussed in Section 2. The procedure is applied to monthly mean temperatures and monthly precipitation amounts using ten locations in Hungary with homogeneous data sets from 1901 to 1999. Trends of above mentioned differences are analyzed with linear and non-parametric regression techniques in Section 3. Finally a brief section for conclusions is provided.

2. Methodology

A methodology for extremes of multivariate time series has been developed by *Szentimrey* (1999), the present technique is a specific version of his general procedure. The task is to define a quantity to measure the deviation of actual annual courses from the average annual course in the area considered. When this quantity is large, that year can be called extreme. Let $x(i,j)=(x_1(i,j),\ldots,x_K(i,j))^T$ be a vector representing monthly mean temperature or monthly precipitation amount at K locations for jth month in ith year where T denotes the transpose. In order to characterize the spatial distribution a principal component analysis is used. Only the first principal component is preserved, because it explains a large portion of the total variance of K variables due to the small area examined. This new variable is calculated as

$$y(i,j)=\mathbf{u}^T\,\mathbf{x}(i,j), \tag{1}$$

where $\mathbf{u}$ is the eigenvector corresponding to the largest eigenvalue of the matrix consisting of correlations among locations. To estimate these correlations a standardization

$$x_k^*(i,j)=\frac{x_k(i,j)-m_k(j)}{d_k(j)} \tag{2}$$

is introduced, because means and standard deviations change from month to month. Here $m_k(i,j)$ and $d_k(i,j)$ are means and standard deviations, respectively. Denoting the number of months by $J=12$ and having a data set which covers I years, the means and variances are replaced by their empirical values calculated as

$$\hat{m}_k(j)=\bar{x}_k(j)=\frac{1}{I}\sum_{i=1}^{I}x_k(i,j), \qquad \hat{d}_k^2(j)=\frac{1}{I-1}\sum_{i=1}^{I}(x_k(i,j)-\bar{x}_k(j))^2. \tag{3}$$

Since the covariance matrix of standardized variables is identical to the correlation matrix of original variables, the correlation r_{pq} between pth and qth locations is estimated by

$$r_{pq} = \frac{1}{IJ} \sum_{i=1}^{I} \sum_{j=1}^{J} x_p^*(i,j)\, x_q^*(i,j). \tag{4}$$

Note that temporal variation of these correlations within the year is assumed insignificant. Because the variable $y(i,j)$ has different variances in different months, larger deviations from mean can be expected in months having larger variances. Therefore, a further normalization is needed next. Taking empirical means $\bar{\mu}_j$ and standard deviations $\bar{\delta}_j$ of $y(i,j)$, an additional standardization is performed as

$$z(i,j) = \frac{y(i,j) - \bar{\mu}_j}{\delta_j}. \tag{5}$$

Finally, a norm $\|\mathbf{z}(i)\|^2$ should be introduced to quantify the deviation of actual annual courses from the average annual course, where $\mathbf{z}(i) = (z_1(i),..., z_J(i))^T$. Since components of the vectors $\mathbf{z}(i)$ are not statistically independent, a Euclidian norm is not very useful. Therefore, principal components of vectors $\mathbf{z}(i)$ are determined and the Euclidean squared norms

$$s(i) = \|\mathbf{w}(i)\|^2 = \mathbf{w}(i)^T \mathbf{w}(i) \tag{6}$$

with new uncorrelated variables are calculated, where

$$\mathbf{w}(i) = \Lambda^{-1/2}\, \mathbf{V}^T \mathbf{z}(i). \tag{7}$$

$\mathbf{\Lambda}$ is a diagonal matrix consisting of eigenvalues of the covariance matrix $\mathbf{C}$ of $\mathbf{z}(i)$ and columns of $\mathbf{V}$ includes eigenvectors corresponding to their eigenvalues. The (p,q)th element of $\mathbf{C}$ is estimated by

$$\hat{c}_{pq} = \frac{1}{I} \sum_{i=1}^{I} z_p(i)\, z_q(i). \tag{8}$$

3. Results

Monthly mean temperatures and monthly precipitation amounts are examined using data of ten stations, namely Budapest (KMI), Debrecen, Kecskemét, Miskolc, Mosonmagyaróvár, Nyíregyháza, Pécs, Sopron, Szeged and Szombathely. Data sets have been homogenized by *Szentimrey* (1999) and are available for the period from 1901 to 1999.

When applying a principal component analysis, the first principal component explains 94.5% of the total variance for temperature and 58.2% for precipitation. Using the procedure described in previous section, the first ten largest norms Eq. (6) were selected for both the temperature and precipitation. Also, a similar analysis was performed when the two elements were handled together, i.e., the dimension K is twice of locations according to temperature and precipitation of each station. Temporal distributions of these extreme years are shown in *Fig. 1*. In order to compare the magnitude of extremity the values are divided by two when both elements are considered together. An important conclusion is that extreme temperature and precipitation years take place separately, none of extreme years with respect to one element is extreme with respect to other element. In the joint case the source of large deviations from mean annual course is the temperature in four years (1902, 1929, 1940, 1946), while the precipitation is responsible in four other years (1914, 1922, 1936, 1947). Only two years with seventh and eighth largest norms are not extremes with respect to temperature or precipitation alone.

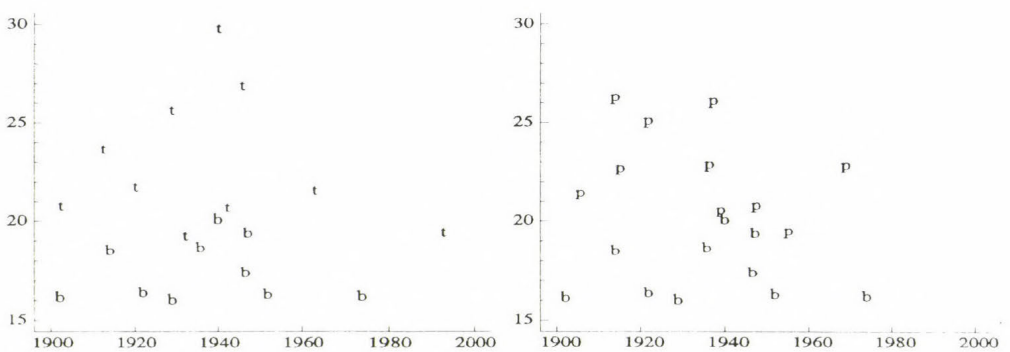

Fig. 1. Temporal distribution of extreme years: *t*- temperature, *p*- precipitation, *b*- both the temperature and precipitation. Vertical axis corresponds to squared norm Eq. (6).

An important question whether norms show temporal changes. Using a linear trend analysis for temperature a chance for decreasing deviations from mean annual course is detected, but the change is significant at only a

relatively weak 10% level. Allowing the trend to be not linear, a non-parametric technique discussed by *Matyasovszky* (1998) was also applied.

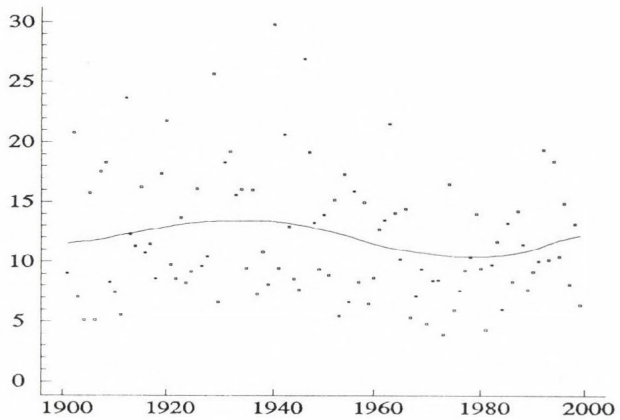

Fig. 2. Trend of squared norm Eq. (6) for temperature.

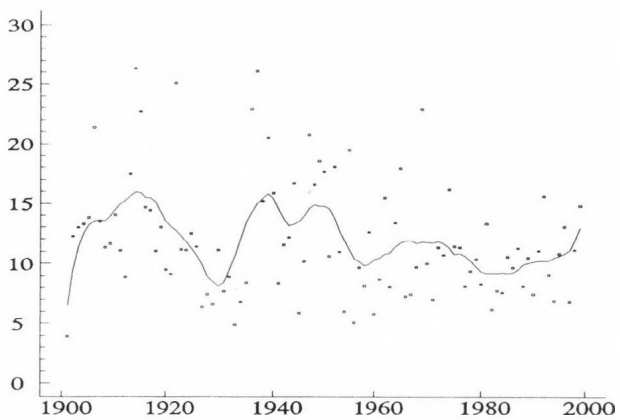

Fig. 3. Trend of squared norm Eq. (6) for precipitation.

Fig. 2 shows a decreasing tendency from forties to eighties and an increasing until forties and during the last two decades. Extremity of the annual course of precipitation is decreasing, because the linear trend is significant at a 2% level. The non-parametric technique results in a highly complicated form of trend showing that precipitation has no long term changes but fluctuates intensively on short time scales (*Fig. 3*). When analyzing the two elements together, a negative linear trend is significant at even a 0.4% level. The norm is essentially constant

until the end of forties but strongly decreases from these years. A slight increase of extremity can be observed in the last two decades (*Fig. 4*).

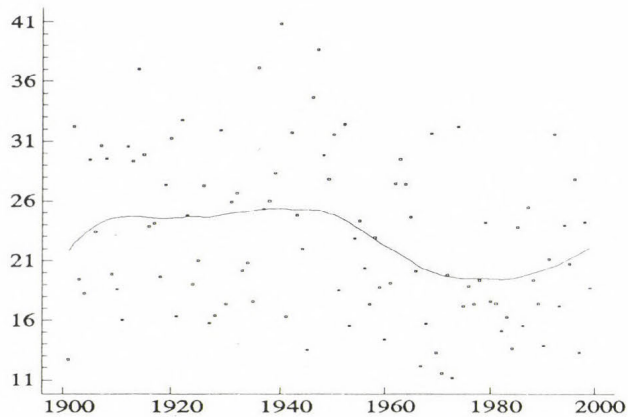

Fig. 4. Trend of squared norm Eq. (6) for temperature and precipitation together.

A natural way to describe the annual course is to use a discrete Fourier transform of data, i.e.,

$$z^*(i,j) = a_{i0} + \sum_{m=1}^{M} a_{im} \cos\left(\frac{2\pi mj}{J}\right) + \sum_{m=1}^{M-1} b_{im} \sin\left(\frac{2\pi mj}{J}\right), \tag{9}$$

where

$$z^*(i,j) = \frac{y(i,j) - \hat{\mu}_j}{\hat{\delta}_j} + \hat{\mu}_j, \tag{10}$$

$$a_{i0} = \frac{1}{J} \sum_{j=1}^{J} z(i,j), \tag{11}$$

$$a_{im} = \frac{2}{J} \sum_{j=1}^{J} z(i,j) \cos\left(\frac{2\pi mj}{J}\right), \qquad m = 1,\ldots,M, \tag{12}$$

$$b_{im} = \frac{2}{J} \sum_{j=1}^{J} z(i,j) \sin\left(\frac{2\pi mj}{J}\right), \qquad m = 1,\ldots,M-1, \tag{13}$$

and $M=J/2$. Temporal variations are mainly characterized by the annual cycle corresponding to $m=1$. Therefore, the amplitudes $\left(c_{i1}^2 = a_{i1}^2 + b_{i1}^2\right)^{1/2}$ are ana-

lyzed with linear and nonparametric regression techniques. For temperature, linear trend is not statistically significant at any reasonable level, but the nonparametric procedure results in considerable changes. The curve in *Fig. 5* is highly similar to the curve in *Fig. 2*. Smallest amplitudes in eighties correspond to warm winters and mild summers, while largest values in forties characterize principally cold winters. Note that two of the first ten largest norms take place during these years (*Fig. 1*). Extreme years are generally cold rather than warm especially during winters. To illustrate this fact *Fig. 6* shows the average annual course and the first four most extreme annual courses.

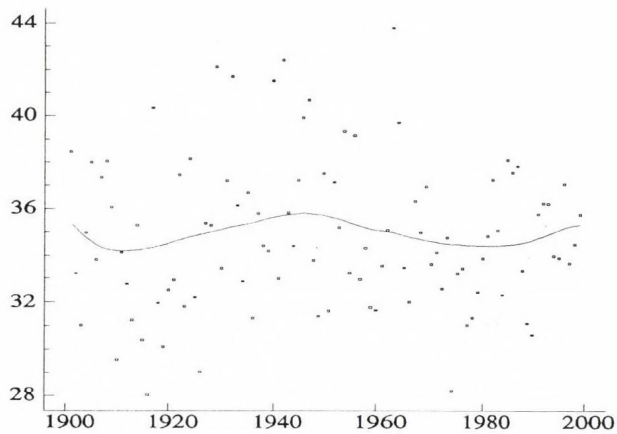

Fig. 5. Trend of annual cycle of the first principal component of monthly mean temperatures.

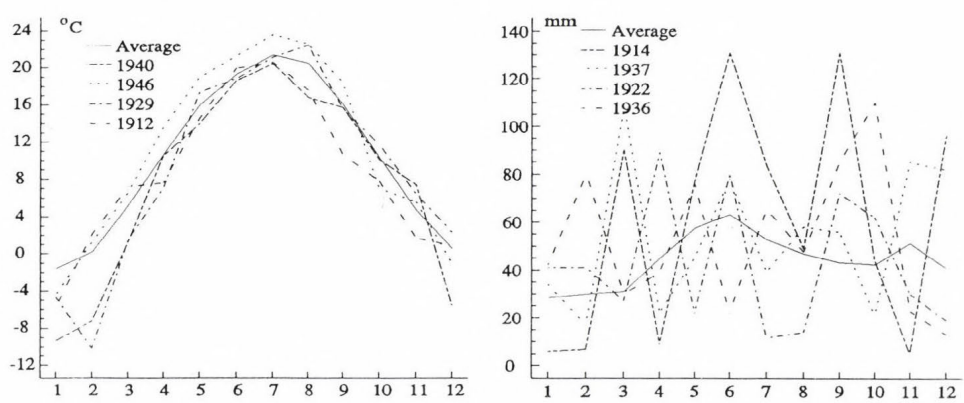

Fig. 6. First four most extreme temperature (*a*) and precipitation (*b*) years in Kecskemét.

Every curve is below the average in January and the cold period continues until middle of spring in two cases. The cold period is situated in the second half of summer and autumn in 1912. The year 1946 is, however, characterized by warm spring and summer. In case of precipitation no any trend of the annual cycle can be detected due to larger variability within the year. The most extreme years have a chance to suffer precipitation amounts considerably higher than normal, but the temporal distribution of excessive amounts or shortages appears quite irregular.

4. Conclusions

A norm was defined to measure departures of actual annual courses of monthly mean temperatures and monthly precipitation amounts from average annual courses. Large values of this quantity may identify extreme years. Main conclusions of the analysis of time series of the norm can be summarized as follows:

- Extremity of the annual course of both the temperature and precipitation is characterized by an overall decreasing tendency. A non-parametric regression technique shows a more complex form of trend functions especially for precipitation. The norms slightly increase from the eighties.
- Taking first ten largest norms, only one year follows after the sixties for temperature, while no any year of the last three decades belongs to first ten norms for precipitation.
- When analyzing the two elements together, a negative linear trend is very significant. The norm is essentially constant until the end of the forties but strongly decreases from these years. A slight increase of extremity can be observed in last two decades. Only two years with seventh and eighth largest norms are not extremes with respect to temperature or precipitation alone.

Acknowledgements—Research leading to this paper has been supported by grant from Hungarian Science Foundation OTKA T025803 and Bolyai János scholarship of Hungarian Academy of Sciences.

References

Matyasovszky, I., 1998: Non-parametric estimation of climatic trends. *Időjárás 102*, 149-158.

Szentimrey, T., 1999: Multiple Analysis of Series for Homogenization (MASH). *Proc. of the Second Seminar for Homogenization of Surface Climatological Data,* Budapest, Hungary. WMO, WCDMP-No. 41, 27-46.

Szentimrey, T., 1999: An analysis of extremes of multivariate time series. In *Weather and Climate Extremes* (in Hungarian). Meteorológiai Tudományos Napok 1999, Orsz. Meteorológiai Szolgálat, Budapest, 77-88.

Zheng, X. and *Basher, R.E.*, 1999: Structural time series models and trend detection in global and regional time series. *J. Climate 12*, 2347-2358.

IDŐJÁRÁS

Quarterly Journal of the Hungarian Meteorological Service
Vol. 105, No. 3, July–September 2001, pp. 165–182

The surface aerodynamic transfer parameterization method SAPA: description and performance analyses

Ferenc Ács and **Mihály Kovács**

[1]*Department of Meteorology, Eötvös Loránd University,*
P.O. Box 32, H-1518 Budapest, Hungary; E-mail: acs@caesar.elte.hu

[2]*Department of Applied Analysis, Eötvös Loránd University,*
Kecskeméti u. 10-12, H-1053 Budapest, Hungary

(Manuscript received December 4, 2000; in final form May 25, 2001)

Abstract—The **s**urface **a**erodynamic transfer **pa**rameterization method SAPA is presented. The method is based on the Monin-Obukhov similarity theory describing an implicit equation system of flux/profile relationships. The equation system is solved numerically using fixed-point method. This fixed-point method application is the unique and new feature of the scheme comparing to other schemes. We show that—though an iterative procedure is applied—the method seems to be reliable not only in the common but also in the extrem cases. This is demonstrated analysing the performance of the scheme in terms of both numerical and physical features. We tested also the goodness of the scheme on the Cabauw data set. The method considered can be applied in the land-surface parameterization schemes of weather and climate models.

Key-words: Monin-Obukhov similarity theory, fixed-point method, iterative solution, numerical and physical features of the scheme.

1. Introduction

A large number of surface aerodynamic transfer parameterization methods (SAPA) have been proposed and used in atmospheric modeling. All of these formulations are based on the Monin-Obukhov (M-O) similarity theory which defines an implicite equation system of flux/profile relationships. Such equation systems can be solved either analytically by reformulating the M-O theory in term of bulk Richardson number (*Deardorff*, 1972; *Louis*, 1979; *Byun*, 1990; *Lee*, 1997; *de Bruin et al.*, 2000) or numerically by applying a numeri-

cal procedure (*Schayes*, 1982; *Berkowicz* and *Prahm*, 1982; *Holtslag* and *van Ulden*, 1983; *Manju* and *Scharma*, 1987; *Mohan* and *Siddiqui*, 1998). Today both analytical and numerical approaches are common. Analytical approaches are described in more details. For unstable conditions they yield approximate solutions, that is, the solution can be treated as semi analytical. Description of the numerical approaches is poorer: commonly there are only short remarks concerning the numerical method applied and its performance in the procedure of solution (*Mohan* and *Siddiqui*, 1998).

In this study we present a SAPA method based on the numerical approach. The kernel of the numerical approach is the fix point method. Our basic intention is to show that the fix point method is a powerful numerical procedure for solving the implicitly defined equation system of flux/profile relationships. We analyzed its performance with more attention in terms as follows:

(1) Whether the number of iteration steps depends upon the meteorological conditions. How the equation system converges in both strong unstable and strong stable conditions.

(2) Whether the initial value of Monin-Obukhov's length determines the rate of the convergence.

We analyzed also the basic physical features of the the SAPA method. We estimated its performance on the Cabauw data (*Beljaars* and *Bosveld*, 1997) comparing the calculated and observed turbulent heat fluxes in the intensive observation period. We also analyzed the dependence of friction velocity, aerodynamic resistance and turbulent heat fluxes upon the main forcing factors: the surface-air temperature difference and the wind velocity. This study is a revised and updated text of the lecture presented as poster (*Kovács* and *Ács*, 2000) at the 25th General Assembly of the European Geophysical Society.

2. Method

The SAPA method is based on the Monin-Obukhov similarity theory considering an implicit equation system of flux/profile relationships. The equation system is solved by the fixed-point method. The method is used as turbulent heat flux parameterization module in the Psi1-PROGSURF model (*Ács* and *Hantel*, 1998). In the following both numerical procedure and physical background will be presented in detail.

2.1 *Basic equations*

2.1.1 *Turbulent heat fluxes*

The turbulent heat fluxes are calculated by aerodynamic formulae. The latent heat flux is parameterized as:

$$\lambda \cdot E^j = -\frac{\rho c_p}{\gamma} \frac{f^j \cdot e_S(T_{vg}) - e_r}{r_a^j + r^j}, \tag{1}$$

where ρ is the air density, c_p is the specific heat of air at constant pressure, γ is the psychrometric constant, $e_S(T_{vg})$ is the saturation vapor pressure at the vegetation-ground temperature T_{vg}, e_r is the vapor pressure at reference level, r_a is the aerodynamic resistance and r is the surface resistance. The superscript j refers to the domains of vegetation ($j = v$) and of bare soil ($j = b$). For vegetation we additionally distinguish between wet ($j = vw$) and dry ($j = vd$) vegetation surface. As a first approach in both cases we put

$$f^{vw} = f^{vd} = 1. \tag{2}$$

f^b represents the relative humidity on the bare soil surface. It is parameterized after *Noilhan* and *Planton* (1989) as

$$f^b = \begin{cases} 1 & if \quad \theta_{f1} \le \theta_1 \\ 0.5 \cdot \{1 - \cos(\theta_1 \cdot \pi / \theta_{f1})\} & if \quad \theta_{w1} \le \theta_1 < \theta_{f1} \\ 0 & if \quad \theta_1 \le \theta_{w1} \end{cases}, \tag{3}$$

where θ_1 represents actual soil moisture content. θ_{f1} and θ_{w1} is the field capacity and wilting point soil moisture content in the surface layer (m^3/m^3), respectively.

The sensible heat flux is parameterized as:

$$H^j = -\rho c_p \frac{T_{vg} - T_r}{r_a^j}, \tag{4}$$

where T_r is air temperature at the reference level.

2.1.2 Aerodynamic resistances

The aerodynamic resistance is divided into laminar and turbulent terms.

- Vegetation: $r_a^v = r_{al}^v + r_{at}^v$. (5)
- Bare soil: $r_a^b = r_{al}^b + r_{at}^b$. (6)

2.1.3 Laminar component

This term is generally not negligible and in many cases it is even larger than the turbulent aerodynamic resistance component.

Vegetation
Above vegetation, the aerodynamic resistance for heat transfer in the laminar layer is parameterized combining the expression of *Wetzel* and *Chang* (1988) and the so called excess resistance term:

$$r_{al}^v = \frac{5}{u_*} + 6 \cdot u_*^{-2/3}. \tag{7}$$

The first term characterizes the laminar layer resistance for momentum transfer, the second one expresses the deviation between the momentum and heat transfer mechanisms close to the vegetation surface. u_* is the friction velocity.

Bare soil
In the immediate vicinity of bare soil surface, there are no fundamental differences between the momentum and heat transfer mechanisms, therefore,

$$r_{al}^b = \frac{5}{u_*}. \tag{8}$$

2.1.4 Turbulent component

The turbulent component of aerodynamic resistance r_{at} is evaluated using Monin-Obukhov's similarity theory taking into account the atmospheric stability.

Parameterization of turbulent component will not be considered separately for vegetation and bare soil. The parameters which are different for vegetation and bare soil are as follows: D_{Stherm}, D_{Sdyn} and z_0. All three parameters are defined below (Eqs. (14), (17) and (15)).

- **Resistance**

The turbulent aerodynamic resistance is defined as follows:

Neutral stratification

$$r_{at} = \frac{0.74}{k \cdot u_*} \cdot \log\left(\frac{D_{Stherm}}{z_0}\right). \tag{9}$$

Stable stratification

$$r_{at} = \frac{1}{k \cdot u_*}\left[0.74 \cdot \log\left(\frac{D_{Stherm}}{z_0}\right) + 4.7 \cdot \chi \cdot (D_{Stherm} - z_0)\right]. \tag{10}$$

Unstable stratification

$$r_{at} = \frac{0.74}{k \cdot u_*} \cdot \log\left(\frac{1 - t_r}{1 - t_0} \cdot \frac{1 + t_0}{1 + t_r}\right), \tag{11}$$

with functions:

$$t_r = \left[1 - 9 \cdot D_{Stherm} \cdot \chi\right]^{-1/2}, \tag{12}$$

$$t_0 = \left[1 - 9 \cdot z_0 \cdot \chi\right]^{-1/2}. \tag{13}$$

k is von Kármán constant, $\chi = \frac{1}{L}$ and L is Monin-Obukhov length. Coefficient 0.74 appears in Businger's universal functions (*Ács et al.*, 2000). Thickness of layer D_{Stherm} differs above vegetation and bare soil, that is

$$D_{Stherm} = \begin{cases} z_{rtherm} & for\ bare\ soil \\ z_{rtherm} - d & for\ vegetation \end{cases}. \tag{14}$$

z_{rtherm} is the reference level for air temperature and humidity and d is the zero plane displacement height (m). d can be either estimated via vegetation morphological characteristics or prescribed as in this study. z_0 is the roughness length (m); it differs for vegetation and bare soil, that is

$$z_0 = \begin{cases} z_0^b & \textit{for bare soil} \\ z_0^v & \textit{for vegetation} \end{cases}. \tag{15}$$

χ is the stability wavenumber.

- **Friction velocity**

The friction velocity is defined by:

$$u_* = \frac{k \cdot U_r}{\log\left(\frac{D_{Sdyn}}{z_0}\right) - \Psi_m}, \tag{16}$$

where thickness of layer D_{Sdyn} is calculated by

$$D_{Sdyn} = \begin{cases} z_{rdyn} & \textit{for bare soil} \\ z_{rdyn} - d & \textit{for vegetation} \end{cases}. \tag{17}$$

Ψ_m is the stability function which depends upon $D_{Sdyn} \cdot \chi$; U_r is the wind speed at the wind's reference level z_{rdyn}.

- **Stability function**

Stability function depends upon stratification.

Neutral stratification

$$\Psi_m = 0. \tag{18}$$

We use two different entries for the argument of Ψ_m. When $D_{Sdyn} \cdot \chi \leq 0.5$ we enter the empirical expression of *Businger et al.* (1971):

$$\Psi_m = -4.7 \cdot D_{Sdyn} \cdot \chi. \tag{19}$$

For $D_{Sdyn} \cdot \chi > 0.5$ we use the formula of *Holtslag* and *de Bruin* (1988):

$$\Psi_m = -A \cdot D_{Sdyn} \cdot \chi - B \cdot \left(D_{Sdyn} \cdot \chi - \frac{C}{D} \cdot e^{-D \cdot D_{Sdyn} \cdot \chi} \right) - \frac{B \cdot C}{D} \tag{20}$$

with $A = 0.7$, $B = 0.75$, $C = 5$ and $D = 0.35$.

Unstable stratification

$$\Psi_m = 2 \cdot \log\left(\frac{1+x}{2} \right) + \log\left(\frac{1+x^2}{2} \right) - 2 \cdot \arctan(x) + \frac{\pi}{2}, \tag{21}$$

with the x function proposed by *Businger et al.*, (1971),

$$x = \left[1 - 16 \cdot D_{Sdyn} \cdot \chi \right]^{1/4}. \tag{22}$$

- **Stability wavenumber**

Stability wavenumber is defined by

$$\chi = \frac{1}{L}, \tag{23}$$

where L is the Monin-Obukhov length defined by

$$L = \frac{\rho \cdot T_r \cdot u_*^3}{g \cdot k \cdot \left(\frac{H}{c_p} + 0.61 \cdot T_r \cdot E \right)}, \tag{24}$$

where g is the acceleration of gravity (m s^{-2}) and E is the vapor flux (kg m^{-2} s^{-1}).

Neutral stratification is supposed for $|L| > 800$ m that is $\chi < 0.00125$ m^{-1}. If the stratification is not neutral, it is stable (L or $\chi > 0$) or unstable (L or $\chi < 0$).

2.2 Solving procedure

The stability wave number depends upon E, H and u_*, and vice versa. The chain of formulae involved is Eq. (23), Eq. (24) for χ and L; Eq. (1) for E; Eq. (4) for H; Eqs. (5) and (6) for r_a; Eq. (16) for u_*; Eqs. (18), (19) and (21) for Ψ_m which leads back to χ. Symbolically:

$$\chi = F\left\{E\left[r_a^j\left(u_*[\Psi_m(\chi)]\right)\right],\ H\left[r_a^j\left(u_*[\Psi_m(\chi)]\right)\right],\ u_*[\Psi_m(\chi)]\right\}. \tag{25}$$

Implementing all functional relationships and parameterizations with external conditions into Eq. (25) this reads:

$$\chi = F(\chi, bc)\,, \tag{26}$$

where

$$F(\chi,bc) = F\left\{E\left[r_a^j\left(u_*[\Psi_m(\chi),bc],bc\right),bc\right],H\left[r_a^j\left(u_*[\Psi_m(\chi),bc],bc\right),bc\right],u_*[\Psi_m(\chi),bc]\right\}. \tag{27}$$

bc represents external conditions involved in the various parameterizations (for example, the reference temperature or the wind speed). They are assumed constant. The implicit equation, Eq. (26) is solved by the fixed-point method. According to numerous tests the method always seems to be convergent. A short description of the method is presented in the Appendix. The χ and $F(\chi)$ functions for defined external conditions are presented in *Fig. 1*. As it can be seen, it yields exactly one χ^* solution (χ^* is the cross point of χ and $F(\chi,bc)$ functions) for the unstable, neutral and stable conditions. The χ^* solution is obtained iteratively fulfilling the $|\chi - F(\chi,bc)| \le 10^{-4}$ condition.

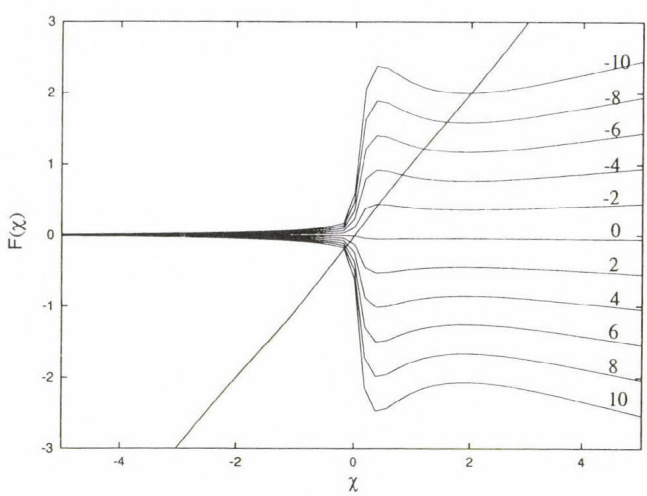

Fig. 1. The shape of $F(\chi)$ function obtained by SAPA. The curves refer to the following atmospheric forcing data: U_r = 2.0 m s^{-1}, relative humidity RH = 90 per cent, T_{vg} = 20°C and T_r varied from 10°C to 30°C in steps of 2°C. The numbers on the curves represent $T_{vg} - T_r$ values.

3. Results

First, the numerical features of the fixed-point method are investigated. Then we tested the scheme using Cabauw data set. Lastly, we analyzed the dependence of the friction velocity, aerodynamic resistance and the turbulent heat fluxes upon main forcing factors.

3.1 Numerical features

The results show that the number of the iteration steps N_i depends upon the meteorological conditions (*Fig. 2*). Usually N_i is less than 10 for both moderately stable and unstable conditions. But, in general, stable condition needs more iteration than the unstable one. N_i is determined by the wind velocity in the greatest extent. For strong unstable conditions, close to or at the boundary of free convection zone (extremely small wind and great surface/air temperature difference), there are cases when N_i is greater than 200. Similarly, for strong stable conditions with small winds (U_r is about or less than 1 m s^{-1}), N_i is about 100 or still greater. It is interesting to note that in these conditions the field of N_i shows maxima.

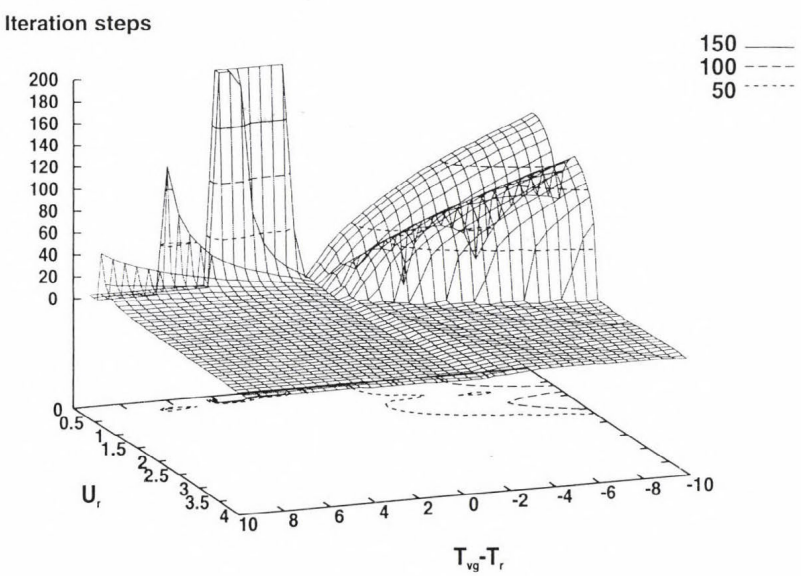

Fig. 2. The number of the iteration steps versus different wind velocity and temperature difference values $T_{vg} - T_r$ for small vegetation surface resistance (r^v = 60 s m^{-1}) and RH = 90 per cent.

The initial values of χ determine the rate of the convergence. This is shown with the aid of *Figs. 3* and *4*. *Fig. 3* refers to small winds ($U_r = 0.1$ m s^{-1}). Here in stable conditions there is such initial χ_0 value (about 2 m^{-1}), for which N_i would be considerably smaller. In spite of this, for average wind conditions ($U_r = 4$ m s^{-1}) there is no such initial χ_0 value. This is shown in *Fig. 4*.

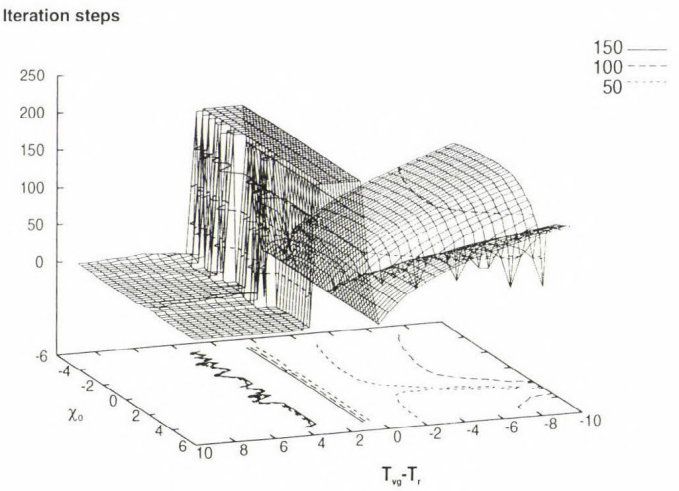

Fig. 3. The number of the iteration steps versus the initial values of χ and the temperature differences $T_{vg} - T_r$ for small vegetation surface resistance ($r^v = 60$ s m^{-1}) and $U_r = 0.1$ m s^{-1}.

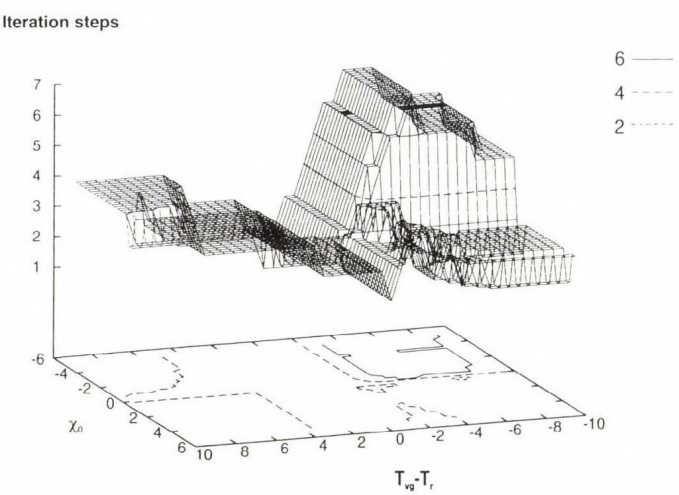

Fig. 4. As Fig. 3 but for $U_r = 4$ m s^{-1}.

3.2 Validation experiments

The scheme is tested by comparing simulated and observed turbulent heat fluxes. The well known 1987 data from Cabauw, The Netherlands, are used. Cabauw site has a humide, maritime climate. The soil texture in the root zone is silty clay. The plant cover is mainly short grass.

The data set contains also instantaneous values of turbulent heat fluxes measured in the intensive observation period between September 10–19, 1987. The comparison of simulated and observed latent and sensible heat fluxes is presented in *Figs. 5* and *6*. The results obtained are reliable. The agreement is somewhat better for λE than for H. The correlation coefficients obtained are 0.82 and 0.71, respectively. In these tests SAPA is used as submodule in the scope of Psil-PROGSURF (*Ács* and *Hantel*, 1998).

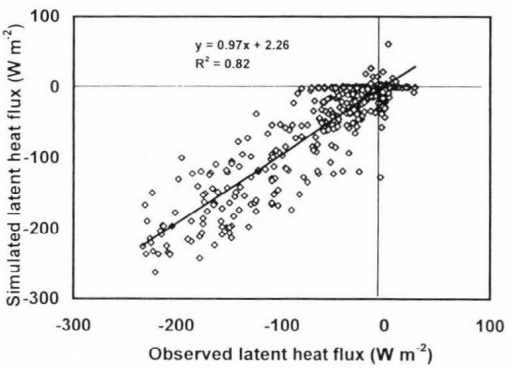

Fig. 5. SAPA-simulated versus observed latent heat flux in the intensive observation period (from day 253 to day 262). Thick line: regression.

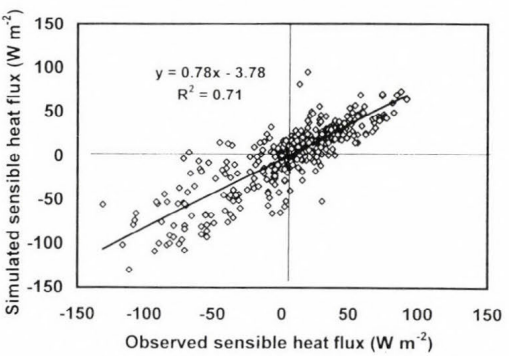

Fig. 6. SAPA-simulated versus observed sensible heat flux in the intensive observation period (from day 253 to day 262). Thick line: regression.

3.2 Physical features

The performance of SAPA is also briefly analyzed in terms of fields of $r_a(T_{vg} - T_r, U_r)$, $u_*(T_{vg} - T_r, U_r)$, $\lambda \cdot E(T_{vg} - T_r, U_r)$ and $H(T_{vg} - T_r, U_r)$. Vegetation surface is choosen. The vegetation surface resistance is small, that is $r^v = 60$ s m^{-1}. The vegetation type is short grass. Note, that these surface conditions are very similar to the conditions on the Cabauw site. The atmospheric boundary conditions are as follows: The $T_{vg} - T_r$ temperature difference is changed between -10 and $+10$°C. This is achieved by $T_{vg} = 20$°C and changing T_r from 10°C to 30°C in steps of 0.5°C. U_r is varied from 0.1 to 4.0 m s^{-1} in steps of 0.1 m s^{-1}. The relative humidity of air RH is constant. In the so called "wet case" RH is 90 per cent, in the "dry case" RH is 30 per cent. It has to be noted that in the simulations the moisture state of the surface (represented by r^v) and the surface/air temperature difference (represented by $T_{vg} - T_r$) are independent from each other.

The fields of r_a^v, u_*, $\lambda \cdot E$ and H are presented in *Figs. 7, 8, 9* and *10*, respectively. The "wet" and "dry" case are distinguished by notation a and b, respectively. The basic characteristics of the fields are as follows:

(1) In all cases three stability regimes can be recognized: the stable stratification, the unstable stratification and the free convection zone. Note that the free convection zone (region of small winds and great positive surface/air temperature differences) can be recognized though the universal functions for unstable stratification (Eqs. (12), (13) and (22)) are used.

(2) There is no qualitative difference between the fields of r_a^v, u_*, $\lambda \cdot E$ and H for "wet" ($RH = 90$ per cent) and "dry" ($RH = 30$ per cent) cases. The deviation between the "wet" and "dry" case seems to be more pronounced for $\lambda \cdot E$ field. In "dry" case the change of $\lambda \cdot E$ versus $T_{vg} - T_r$ is more pronounced than in the "wet" case.

(3) The fields of u_*, $\lambda \cdot E$ and H are basically similar. It can be said that the form of u_* field governs in great extent the form of $\lambda \cdot E$ and H fields. The form of r_a^v field does not follow the form of u_* field. r_a^v can be treated as an opposite of u_*. In the regions where u_* has a minimum, r_a^v appears with the maximum and vice versa.

Let us inspect each figure separately in more details. We will describe the fields of "dry" case.

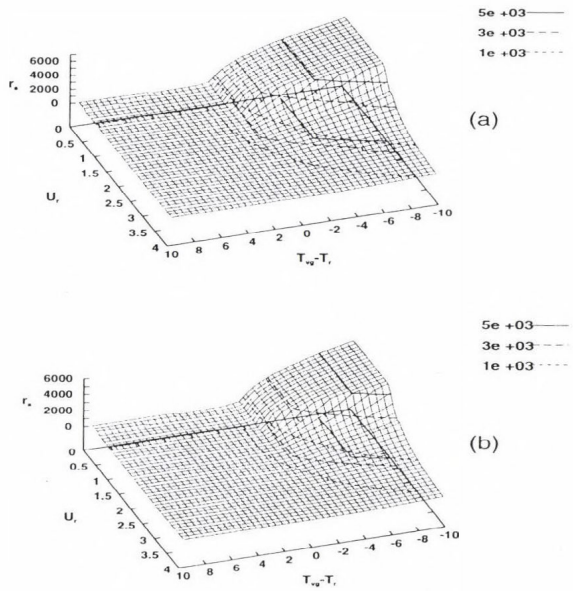

Fig. 7. The aerodynamic resistance versus the surface/air temperature difference $T_{vg} - T_r$ and the wind velocity for (*a*) $RH = 90$ per cent ("wet" case) and (*b*) $RH = 30$ per cent ("dry" case).

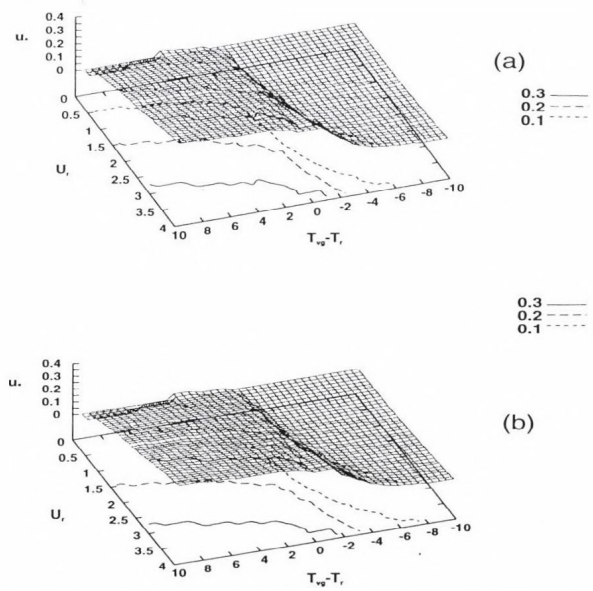

Fig. 8. The friction velocity versus the surface/air temperature difference $T_{vg} - T_r$ and the wind velocity for (*a*) $RH = 90$ per cent ("wet" case) and (*b*) $RH = 30$ per cent ("dry" case).

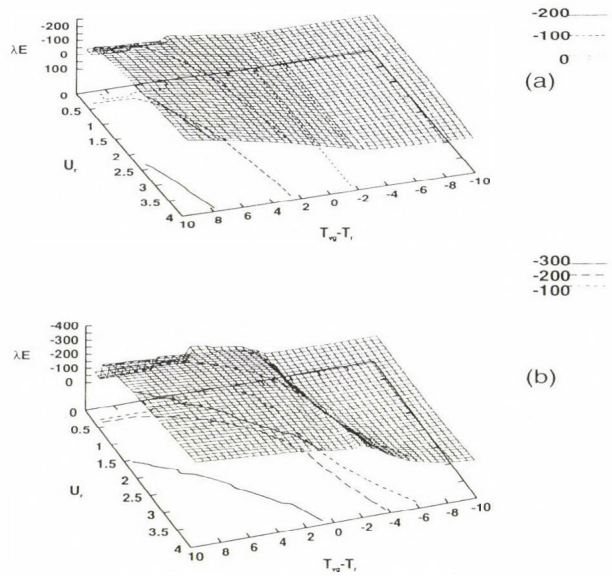

Fig. 9. The latent heat flux versus the surface/air temperature difference $T_{vg} - T_r$ and the wind velocity for (*a*) $RH = 90$ per cent ("wet" case) and (*b*) $RH = 30$ per cent ("dry" case).

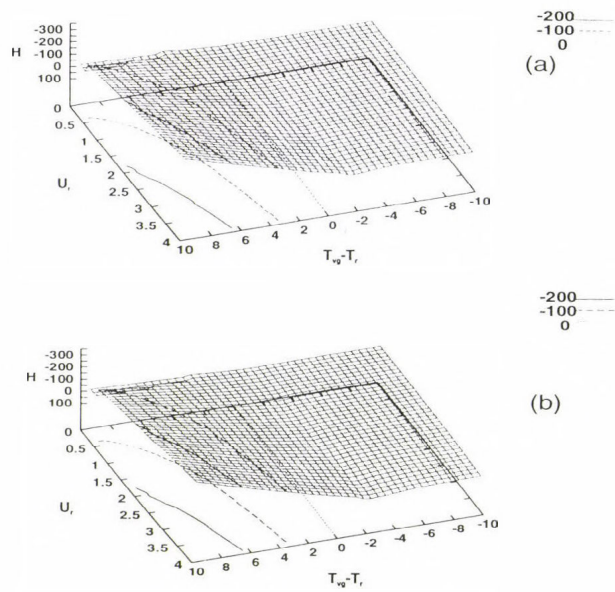

Fig. 10. The sensible heat flux versus the surface/air temperature difference $T_{vg} - T_r$ and the wind velocity for (*a*) $RH = 90$ per cent ("wet" case) and (*b*) $RH = 30$ per cent ("dry" case).

- r_a^v and u_*

In strong unstable conditions (great positive surface/air temperature difference and strong wind), $r_a(T_{vg}-T_r,U_r)$, is about 40 s m^{-1}, so for example r_a^v(9.5°C, 3.9 m s^{-1})=37 s m^{-1}. In strong stable conditions (great negative surface/air temperature difference and small wind) r_a^v values are about 5000 s m^{-1}. In the left (great positive surface/air temperature difference and small wind) and right (great negative surface/air temperature difference and strong wind) corners of the field r_a^v is about the same of 360 s m^{-1}.

The greatest u_* values are between 0.3 and 0.4 in the strong unstable stratification. The $u_*(T_{vg}-T_r,U_r)$ field decreases towards decreasing surface/air temperature difference and wind. For small winds —independently from the temperature difference forcing— the u_* values are extremely small. In the simulations the lower limit of u_* values is taken as 0.02 m s^{-1}. Two facts can also be observed: the relative sharp boundary between the unstable and stable stratifications and that u_* values decrease with decreasing wind in both stratifications. Since u_* (–10°C, 3.9 m s^{-1})=0.09 m s^{-1} this decrease is obviously greater in the unstable stratification than in the stable one.

- $\lambda \cdot E$ and H

According to our convention, $\lambda \cdot E$ is negative in unstable and positive in stable stratification. The $\lambda \cdot E$ field is very similar to u_* field. Its characteristics agree with u_* field characteristics: in strong unstable stratification the $\lambda \cdot E$ values are between –300 and –400 W m^{-2} and decrease towards decreasing surface/air temperature difference and wind. In the left corner of the field (free convection zone) $\lambda \cdot E$ values are about –100 W m^{-2}. In spite of this the $\lambda \cdot E$ values are about –50 W m^{-2} in the right corner of the field (stable stratification with moderate wind), that is they are about two times smaller than in the state of free convection. In the strong stable stratification (great negative surface/air temperature difference and extremely weak wind) $\lambda \cdot E$ is very close to zero but still positive.

The H field is also similar to the field of u_* and $\lambda \cdot E$ but there is a basic deviation: the minimum of H is not in the region of small winds and great negative surface/air temperature differences (H (–10°C, 0.1 m s^{-1})=2 W m^{-2}) but in the region of stable stratification with moderate winds (H (–10°C, 3.9 m s^{-1})= 32 W m^{-2}). In the free convection zone H is not great (H (9.5°C, 0.1 m s^{-1})= –32 W m^{-2}). In spite of this in strong unstable conditions H can reach –300 W m^{-2}.

4. Conclusions

The surface aerodynamic transfer parameterization method SAPA is described, tested and analyzed in terms of its numerical and physical features. The physics of the scheme is based on the M-O similarity theory. It differs from similar M-O based schemes in the application of the numerical procedure for solving the implicitly defined equation system (Eqs. from (1) to (24)). The fixed-point method (Eq. (27)) is applied. We demonstrated that—though an iterative procedure is used—the method seems to be reliable not only in the common but also in the extreme cases. We have also proved the performance of the scheme on the Cabauw data set. According to these results, the scheme seems to be quite reliable. Analyzing the dependence of the scheme upon the main forcing factors (the surface-air temperature difference and the wind velocity), we observed some new and interesting features. Among others:

- In general the number of iteration steps N_i is greater in stable stratification than in unstable one. N_i is determined by the wind velocity in the greatest extent.
- The initial values of $\chi = \frac{1}{L}$ determine the rate of the convergence. So N_i has a minimum in stable stratification for small winds at $\chi \approx 2$ m^{-1}.
- The fields of u_*, $\lambda \cdot E$ and H are quite similar. The similarity is more pronounced in "dry" than in "wet" case.

In the simulations, the surface resistance—a very important factor—is used as constant. Further we assumed that the surface resistance and the surface/air temperature difference are independent from each other. Presently, these assumptions are used because of the simplicity. By modeling both the surface resistance and its relation to the surface/air temperature difference, it would be possible to get a somewhat more sophisticated scheme with necessary key ingredients to do near surface climate diagnostics. This is a task for the future.

Acknowledgements—This study is financially supported by both the Österreichische Akademie der Wissenschaften within the National Austrian Committee for the IGBP and the Hungarian Ministry for Culture and Education via OTKA Foundation, project number T-029358. The authors wish to thank to *Professor Michael Hantel* for his motivation, ideas and helpful discussions. Further we especially appreciate *Mr. Zoltán Barcza*'s help transforming the text from Latex to Winword.

Appendix

The fixed-point method application

Let χ_0 be an arbitrary real number and let us define the following iteration procedure:

$$\chi_{n+1} = F(\chi_n). \tag{A.1}$$

If the iteration (A.1) is convergent, i.e., there exists $\lim_{n\to\infty} \chi_n = \chi^*$ then by (A.1)

$$\lim_{n\to\infty} \chi_n = \lim_{n\to\infty} F(\chi_n). \tag{A.2}$$

Since $F(\chi)$ is continuous function, $\lim_{n\to\infty} F(\chi_n) = F(\lim_{n\to\infty} \chi_n) = F(\chi^*)$. So Eq. (A.2) can be rewritten as

$$\chi^* = F(\chi^*). \tag{A.3}$$

Lastly according to Eq. (A.3), χ^* is the solution of the equation $\chi = F(\chi)$.

References

Ács, F. and *Hantel, M.*, 1998: The Land-Surface Flux Model PROGSURF. *Global Planet Change, 19*, 19-34.

Ács, F., Hantel, M. and *Unegg, J.W.*, 2000: Climate diagnostics with The Budapest-Vienna Land-Surface Model SURFMOD. *Austrian Contributions to the Global Change Program.* Austrian Academy of Sciences, Vol. 3, 116 pp.

Beljaars, A.C.M. and *Bosveld, F.C.*, 1997: Cabauw data for the validation of land surface parameterization schemes. *J. Climate 10*, 1172-1194.

Berkowicz, R. and *Prahm, L.P.*, 1982: Evaluation of the profile method for estimation of surface fluxes of momentum and heat. *Atmos. Environ. 16*, 2809-2819.

Businger, J., Wyngaard, J., Izumi, Y. and *Bradley, E.*, 1971: Flux-profile relationships in the atmospheric surface layer. *J. Atmos. Sci. 28*, 181-189.

Byun, D., 1990: On the analytical solutions of flux-profile relationships for the atmospheric surface layer. *J. Appl. Meteorol. 29*, 652-657

Deardorff, J.W., 1972: Numerical investigation of neutral and unstable planetary boundary layers. *J. Atmos. Sci. 29*, 91-115.

de Bruin, H.A.R., Ronda, R.J. and *Van De Wiel, B.J.H.*, 2000: Approximate solutions for the Obukhov length and the surface fluxes in terms of bulk Richardson Numbers. *Boundary-Layer Meteorol. 95*, 145-157.

Holtslag, A.A.M. and *van Ulden, A.P.*, 1983: A simple scheme for daytime estimates of the surface fluxes from routine weather data. *J. Climate Appl. Meteorol. 22*, 517-529.

Holtslag, A.A.M. and *de Bruin, H.A.R.*, 1988: Applied modelling of the nighttime surface energy balance over land. *J. Appl. Meteorol. 27*, 689-704.

Kovács, M. and *Ács, F.*, 2000: A Surface Aerodynamic Transfer Parameterization Method: Numerical Studies For Different Stability Regimes. CD rom of the EGS 25th General Assembly, Geophysical Research Abstracts, ISSN: 1029-7006, 2, Nice, 24-29 April.

Lee, H.N., 1997: Improvement of surface flux calculations in the atmospheric surface layer. *J. Appl. Meteorol 36*, 1416-1423

Louis, J.-F., 1979: A parametric model of vertical eddy fluxes in the atmosphere. *Bound.-Layer Meteorol. 17*, 187-202

Manju, K. and *Sharma, O.P.*, 1987: Estimation of turbulence parameters for application in air pollution modelling. *Mausam 38*, 303-308.

Mohan, M. and *Siddiqui, T.A.*, 1998: Applied modeling of surface fluxes under different stability regimes. *J. Appl. Meteorol. 37*, 1055-1067.

Noilhan, J. and *Planton, S.*, 1989: A simple parameterization of land surface processes for meteorological models. *Mon. Wea. Rev. 117*, 536-549.

Schayes, G., 1982: Direct determination of diffusivity profiles from synoptic reports. *J. Atm. Sci. 27*, 1122-1137.

Wetzel, P.J. and *Chang, Y. T.*, 1988: Evapotranspiration from nonuniform durfaces: A first approach for short term numerical weather prediction. *Mon. Wea. Rev. 116*, 600-621.

BOOK REVIEW

Ruddiman, W. F., 2001: **Earth's Climate—Past and Future.** W. H. Freeman and Company, New York. 465 pages, over four hundred four color illustrations, extended glossary and index.

The author is a geologist, professor of the Department of Environmental Sciences at the University of Virginia, USA. This fact largely determines the key value of the book for meteorologists and other scientists, trained in climatology of relatively short time scales. The issue depicts interactions within Earth's climate system at all scales, indexes of climate change, evidence of the past climate changes, and projections of possible future changes.

The author recommends the volume "To five colleagues who headed the effort to make the study of Earth's climate a science: *John Imbrie, John Kutzbach, Wally Broecker, Nick Shackleton* and *Murray Mitchell.*" These names, as the most affecting banner, demonstrate the widest geophysical scope that promises special value among the numerous volumes, already written about the topic.

The book moves step-by-step through logically developed summaries of the major lessons learned from 550 million years of climate changes, including the impact on and by humans. The five parts of the book are: "Framework of Climate Science"; "Tectonic-Scale Climate Change"; "Orbital-Scale Tectonic-Scale Climate Change"; "Deglacial and Millennial Climate Change"; and "Historical and Future Climate Change". After a balanced and fairly informative introduction to the climate system, this classification is motivated by the peculiarities of climate represent separation climate. The second part represents the recent 10% of the Eath's age, an interval during which mammals evolved from primitive to more distinctive forms. Part Three looks at the last 3 million years, a time span when our species was rapidly evolving towards its present form. Part Four explores changes over the last 50,000 years, an interval during which humans initially lived a primitive hunting-and-gathering life. Then developed and practiced agriculture and created the first recorded human civilizations. The final Part describes how changes in Earth's climate may have influenced the biological and cultural development of the human species. Its last chapter also makes predictions about "Climate Change in the Next 100 to 1000 years".

The features and recurring themes, that link together sections of the text, include glaciations, intensity of monsoons, flow of deep water in the ocean, the

role of carbon as it moves through the Earth system, and other factors that contribute to icehouse (!) or greenhouse worlds.

Summarizing, the reader meets an excellent introductory volume into the climate science, with clear qualitative explanation of the processes at all scales, driven by any branch of natural sciences. The additional Glossary, itself, counts eight A4 pages, where many definitions apply specifically to their use in climatic studies. The text is accompanied by a large number of colored figures that are clear and well explained in their captions.

J. Mika

ATMOSPHERIC ENVIRONMENT

an international journal

To promote the distribution of Atmospheric Environment *Időjárás* publishes regularly the contents of this important journal. For further information the interested reader is asked to contact *Prof. P. Brimblecombe*, School for Environmental Sciences, University of East Anglia, Norwich NR4 7TJ, U.K.; E-mail: atmos_env@uea.ac.uk

Volume 35 Number 7 2001

Short communication

S.G. Yeatman, L.J. Spokes, P.F. Dennis and *T.D. Jickells:* Can the study of nitrogen isotopic composition in size-segregated aerosol nitrate and ammonium be used to investigate atmospheric processing mechanisms? 1337-1345.

Volume 35 Number 8 2001

J. Kuebler, H. van den Bergh and *A.G. Russel:* Long-term trends of primary and secondary pollutant concentrations in Switzerland and their response to emission controls and economic changes, 1351-1364.

C.A. Pio, C.A. Alves and *A.C. Duarte:* Identification, abundance and origing of atmospheric organic particulate matter in a Portuguese rural area, 1365-1376.

A. Ezcurra, I. Ortiz de Zárate, P.V. Dhin and *J.P. Lacaux:* Cereal waste burning pollution observed in the town of Vitoria (northern Spain), 1377-1386.

A. Charron, P. Coddeville, S. Sauvage, J.-C. Galloo and *R. Guillermo*: Possible source areas and influential factors for sulphur compounds in Morvan, Fance, 1387-1394.

M. Sofiev, G. Petersen, O. Krüger, B. Schneider, M. Hongisto and *K. Jylha:* Model simulations of the atmospheric trace metals concentrations and depositions over the Baltic Sea, 1395-1410.

R.D. Edwards and *M.J. Jantunen:* Benzene exposure in Helsinki, Finland, 1411-1420.

S. Huang, R. Arimoto and *K.A. Rahn:* Sources and source variations for aerosol at Mace Head, Ireland, 1421-1438.

L. Brown, S.A. Brown, S.C. Jarvis, B. Syed, K.W.T. Goulding, V.R. Philips, R.W. Sneath and *B.F. Pain*: An inventory of nitrous oxide emissions from agriculture in the UK using the IPCC methodology: emission estimate, uncertainty and sensitivity analysis, 1439-1450.

J.R. Stedman, J.W.L. Goodwin, K. King, T.P. Murrells and *T.J. Bush:* An empirical model for predicting urban roadside nitrogen dioxide concentrations in the UK, 1451-1464.

I.K. Koponen, A. Asmi, P. Keronen, K. Puhto and *M. Kulmala:* Indoor air measurement campaign in Helsinki, Finland 1999 – the effect of outdoor air pollutinon on indoor air, 1465-1478.

C.I. Beattie, J.W.S. Longhurst and *N.K. Woodfield:* Air quality management: evolution of policy and practice in the UK as exemplified by the experience of English local government, 1479-1490.

Volume 35 Number 9 2001

R.N. Colvile, E.J. Hutchinson, J.S. Mindell and *R.F. Warren:* The transport sector as a source of air pollution, 1537-1565.

J.G. Watson, J.C. Chow and *E.M. Fujita:* Review of volatile organic compound source apportionment by chemical mass balance, 1567-1584.

C.Y.H. Chao and *T.C. Tung:* An empirical model for outdoor contaminant transmission into residential buildings and experimental verification, 1585-1596.

S. Du: A heuristic Lagrangian stochastic particle model of relative diffusion: model formulation and preliminary results, 1597-1607.

R. De Winter-Sorkina: Impact of ozone layer depletion I: ozone depletion climatology, 1609-1614.

R. De Winter-Sorkina: Impact of ozone layer depletion II: changes in photodissociation rates and tropospheric composition, 1615-1625.

Volume 35 Number 10 2001

NOTES TO CONTRIBUTORS

The purpose of *Időjárás* is to publish papers in the field of theoretical and applied meteorology. These may be reports on new results of scientific investigations, critical review articles summarizing current problems in certain subject, or shorter contributions dealing with a specific question. Authors may be of any nationality but papers are published only in English.

Papers will be subjected to constructive criticism by unidentified referees.

* * *

The manuscript should meet the following formal requirements:

Title should contain the title of the paper, the names(s) of the author(s) with indication of the name and address of employment.

The title should be followed by an *abstract* containing the aim, method and conclusions of the scientific investigation. After the abstract, the *key-words* of the content of the paper must be given.

Three copies of the manuscript, typed with double space, should be sent to the Editor-in-Chief: *P.O. Box 39, H-1675 Budapest,* Hungary.

References: The text citation should contain the name(s) of the author(s) in Italic letter or underlined and the year of publication. In case of one author: *Miller* (1989), or if the name of the author cannot be fitted into the text: *(Miller,* 1989); in the case of two authors: *Gamov* and *Cleveland* (1973); if there are more than two authors: *Smith et al.* (1990). When referring to several papers published in the same year by the same author, the year of publication should be followed by letters a,b etc. At the end of the paper the list of references should be arranged alphabetically. For an article: the name(s) of author(s) in Italics or underlined, year, title of article, name of journal, volume number (the latter two in Italics or underlined) and pages. E.g. *Nathan, K. K.,* 1986: A note on the relationship between photosynthetically active radiation and cloud amount. *Időjárás 90,* 10-13. For a book: the name(s) of author(s), year, title of the book (all in Italics or underlined with except of the year), publisher and place of publication. E.g. *Junge, C. E.,* 1963: *Air Chemistry and Radioactivity.* Academic Press, New York and London.

Figures should be prepared entirely in black India ink upon transparent paper or copied by a good quality copier. A series of figures should be attached to each copy of the manuscript. The legends of figures should be given on a separate sheet. Photographs of good quality may be provided in black and white.

Tables should be marked by Arabic numbers and provided on separate sheets together with relevant captions. In one table the column number is maximum 13 if possible. One column should not contain more than five characters.

Mathematical formulas and *symbols:* non-Latin letters and hand-written marks should be explained by making marginal notes in pencil.

The final text should be submitted both in manuscript form and on *diskette.* Use standard 3.5" or 5.25" DOS formatted diskettes for this purpose. The following word processors are supported: WordPerfect 5.1, WordPerfect for Windows 5.1, Microsoft Word 5.5, Microsoft Word 6.0. In all other cases the preferred text format is ASCII.

* * *

Authors receive 30 *reprints* free of charge. Additional reprints may be ordered at the authors' expense when sending back the proofs to the Editorial Office.

Published by the Hungarian Meteorological Service

Budapest, Hungary

INDEX: 26 361

HU ISSN 0324-6329

IDŐJÁRÁS

VOLUME 105 * 2001

BUDAPEST, HUNGARY

AUTHOR INDEX

TABLE OF CONTENTS

I. Papers

II. Book review

III. Contents of journal Atmospheric Environment, 2001

IV. SUBJECT INDEX

The asterisk denotes book reviews

T

W

X

GUIDE FOR AUTHORS OF *IDŐJÁRÁS*

The purpose of the journal is to publish papers in any field of meteorology and atmosphere related scientific areas. These may be

- research papers on new results of scientific investigations,
- critical review articles summarizing the current state of art of a certain topic,
- short contributions dealing with a particular question.

Some issues contain "News" and "Book review", therefore, such contributions are also welcome. The papers must be in American English and should be checked by a native speaker if necessary.

Authors are requested to send their manuscripts to

Editor-in Chief of IDŐJÁRÁS

P.O. Box 39, H-1675 Budapest, Hungary

in three identical printed copies including all illustrations. Papers will then be reviewed normally by two independent referees, who remain unidentified for the author(s). The Editor-in-Chief will inform the author(s) whether or not the paper is acceptable for publication, and what modifications, if any, are necessary.

Please, follow the order given below when typing manuscripts.

Title part: should consist of the title, the name(s) of the author(s), their affiliation(s) including full postal and E-mail address(es). In case of more than one author, the corresponding author must be identified.

Abstract: should contain the purpose, the applied data and methods as well as the basic conclusion(s) of the paper.

Key-words: must be included (from 5 to 10) to help to classify the topic.

Text: has to be typed in double spacing with wide margins on one side of an A4 size white paper. Use of S.I. units are expected, and the use of negative exponent is preferred to fractional sign. Mathematical formulae are expected to be as simple as possible and numbered in parentheses at the right margin.

All publications cited in the text should be presented in a *list of references*, arranged in alphabetical order. For an article: name(s) of author(s) in Italics, year, title of article, name of journal, volume, number (the latter two in Italics) and pages. E.g., *Nathan, K.K.,* 1986: A note on the relationship between photo-synthetically active radiation and cloud amount. *Időjárás 90,* 10-13. For a book: name(s) of author(s), year, title of the book (all in Italics except the year), publisher and place of publication. E.g., *Junge, C. E.,* 1963: *Air Chemistry and Radioactivity*. Academic Press, New York and London. Reference in the text should contain the name(s) of the author(s) in Italics and year of publication. E.g., in the case of one author: *Miller* (1989); in the case of two authors: *Gamov* and *Cleveland* (1973); and if there are more than two authors: *Smith et al.* (1990). If the name of the author cannot be fitted into the text: *(Miller,* 1989); etc. When referring papers published in the same year by the same author, letters a, b, c, etc. should follow the year of publication.

Tables should be marked by Arabic numbers and printed in separate sheets with their numbers and legends given below them. Avoid too lengthy or complicated tables, or tables duplicating results given in other form in the manuscript (e.g., graphs)

Figures should also be marked with Arabic numbers and printed in black and white in camera-ready form in separate sheets with their numbers and captions given below them. Good quality laser printings are preferred.

The text should be submitted both in manuscript and in electronic form, the latter on diskette or in E-mail. Use standard 3.5" MS-DOS formatted diskette or CD for this purpose. MS Word format is preferred.

Reprints: authors receive 30 reprints free of charge. Additional reprints may be ordered at the authors' expense when sending back the proofs to the Editorial Office.

More information for authors is available: antal.e@met.hu

Information on the last issues: http://omsz.met.hu/irodalom/firat_ido/ido_hu.html

Published by the Hungarian Meteorological Service

Budapest, Hungary

INDEX: 26 361

HU ISSN 0324-6329